EXPLORING A SYMMETRY BASED LOGIC FOR PALAU'AMINE SYNTHESIS

APPROVED BY SUPERVISORY COMMITTEE

_____

_____

_____

_____

To my grandparents.

ACKNOWLEDGEMENTS

I would like to thank my advisor Dr. Patrick G. Harran. His passion for science and his incredible creativity was inspiring through the years. He always emphasized the importance of novelty and invention in organic synthesis. I also deeply appreciate his support, guidance and patience during my graduate study.

I also want to thank my committee members, Professor Jef De Brabander, Professor Joseph Ready and Professor Chuo Chen, for their support and helpful suggestions with my project and my dissertation.

Dr. Hugo Garrido and Dr. Masa Nakakai were the pioneers of our palau'amine project. I not only benefited from the foundation they laid for the project but learned a great deal of chemistry from them. My life in the lab was very enjoyable thanks to my friendships with Dr. Qi Wei, Dr. Hugo Garrido, Dr. Kendra Carter, Patricia Harmon, and Lidet Negash.

Outside the lab, I want to acknowledgement my friends: Alethia Villasenor, Youn-Kyoung Lee, Tong Chao, Zoltan Metlagel, Andrei Marconescu and Francis Yoshimoto. Thank you guys for so many good times and also for helping me go through some tough times.

My parents always emphasized the importance of education for a person. They are the reason I pursued a Ph.D. The love and support from my grandparents are my motivation to go after my dreams.

EXPLORING A SYMMETRY BASED LOGIC FOR PALAU'AMINE SYNTHESIS

by

QINGYI LI

DISSERTATION

Presented to the Faculty of the Graduate School of Biomedical Sciences

The University of Texas Southwestern Medical Center at Dallas

In Partial Fulfillment of the Requirements

For the Degree of

DOCTOR OF PHILOSOPHY

The University of Texas Southwestern Medical Center at Dallas

Dallas, Texas

March, 2008

Copyright

by

QINGYI LI, 2008

All Rights Reserved

EXPLORING A SYMMETRY BASED LOGIC FOR PALAU'AMINE SYNTHESIS

Qingyi Li, Ph.D.
The University of Texas Southwestern Medical Center at Dallas, 2008

Patrick. G. Harran, Ph.D.

Palau'amine is a natural product originally isolated in 1993 from the marine sponge *Stylotella aurantium*. It is reported to posess impressive biological activities, including: antifungal, antibacterial, and antineoplastic characters.. Moreover, it is a strong immunosuppressant (IC_{50}<18ng/mL, allogenic lymphocyte reaction). The molecule has a complex polycyclic structure having a contiguous array of eight stereogenic centers. It is unusually rich in heteroatoms. A recent revision of its relating stereochemistry has brought further attention to this fascinating molecule. The current strategy of our group features a chlorination initiated cascade process on a symmetric precursor that assembles the skeleton of palau'amine with in a single operation. A symmetric bisalkylidene precursor for this process was synthesized. During the process,

two new methodologies were developed: a titanocene dichloride mediated regioselective and stereoselective dimerization of heterocyclic dineolates; and a chemoselective Rh(I) carbene complexes catalyzed conjugation hydrosilylation of enamides. Our core idea was subsequently validated by the formation of the spirocyclopentane motif in palau'amine by an electrophilic halogen induced desymmetrization.

TABLE OF CONTENTS

PRIOR PUBLICATIONS

- M. Shanmugasundaram, I. Garcia-Martinez, **Q. Li**, A. Estrada, N. E. Martinez, L. E.Martinez. Microwave-assisted Solid-phase Dötz Benzannulation Reaction: a FacileSynthesis of 2,3-disubstituted-1,4-naphthpquinones, *Tetrahedron Letters,*(**2005)**, *46*, 75457548.

- W. G. Burgett, **Q. Li,** Q, Wei, P. G. Harran. A Concise and Flexible Total Synthesis of (–)-Diazonamide A, *Angewandte Chemie International Edition,* (**2003)**, *42*, 4961-4966.

- H. Garrido-Hernandez, M. Nakadai, M. Vimolratana, **Q. Li**, T. Doundoulakis, P. G.Harran. Spirocycloisomerization of Tethered Alkylidene Glycocyamidines: Synthesisof a Base Template Common to the Palau'amine Family of Alkaloids, *AngewandteChemie International Edition,* (**2005)**, *44*, 765-769.

- **Q. Li**, P. Hurley, P. G. Harran. Exploring Symmetry-Based Logic for a Synthesis of Palau'amine, *J. Am. Chem. Soc.* (**2008**), Submitted April 3.

LIST OF FIGURES

LIST OF SCHEMES

LIST OF APPENDICES

LIST OF ABBREVIATIONS

AAPE – 3-amino-1-(2-aminoimidazolyl)prop-1-ene

AcOH – acetic acid

aq – aqueous

BF_3•Et_2O – boron trifloride diethyl etherate

Boc – *tert*-butyloxycarbonyl

Bn –benzyl

t-Bu – *ter*- butyl

calc'd – calculated

m-CPBA – *meta*-chloroperoxybenzoic acid

COD – 1,5-cyclooctadiene

DBU – 1,8-diazabiocyclo[5.4.0]undec-7-ene

DIPEA – diisopropyl ethylamine

DMAP – 4-dimethylaminopyridine

DMDO – dimethyldioxirane

DME – dimethoxyethane

DMF – dimethylformamide

DMSO – dimethylsulfoxide

EDTA – ethylenediamine tetraacetic acid

EtOAc – Ethyl acetate

Hex – Hexane

hυ – Light

i-Pr – Isopropyl

IR – Infrared

KHMDS – Potassium Hexamethyldisilazide

min – Minute

NCS – *N*-chlorosuccinimide

NHC – N-heterocyclic carbene

Ph – Phenyl

pH – hydrogen ion concentration

ppm – parts per million

p-TsOH – para-toluenesulfonic acid

Pyr – Pyridine

SEM – 2-(trimethylsilyl)ethoxymethyl

TEA – triethyl amine

THF – tetrahydrofuran

TBTU – 2-(1H-Benzotriazole-1-yl)-1,1,3,3-tetramethyluronium tetrafluoroborate

CHAPTER ONE

INTRODUCTION

Marine sponges have become the new rich sources for discovery of natural products with unprecedented structures. The discovery of palau'amine **1** is a good example. Palau'amine **1** was isolated in 1993 by the Kinnel and Sheuer groups from marine sponge *Stylotella aurantium*. It contains a unique polycyclic structure and two guanidine motifs. It is identified as a strong immunosuppressant, however its structure is very different from the known immunosuppresants, such as cyclpsporin A, FK506 and rapamycin (Figure 1.1). This indicates it is very possible that palau'amine **1** functions via a new mechanism. Palau'amine belongs to the imidazole-pyrrole group of alkaloids.

Figure 1.1

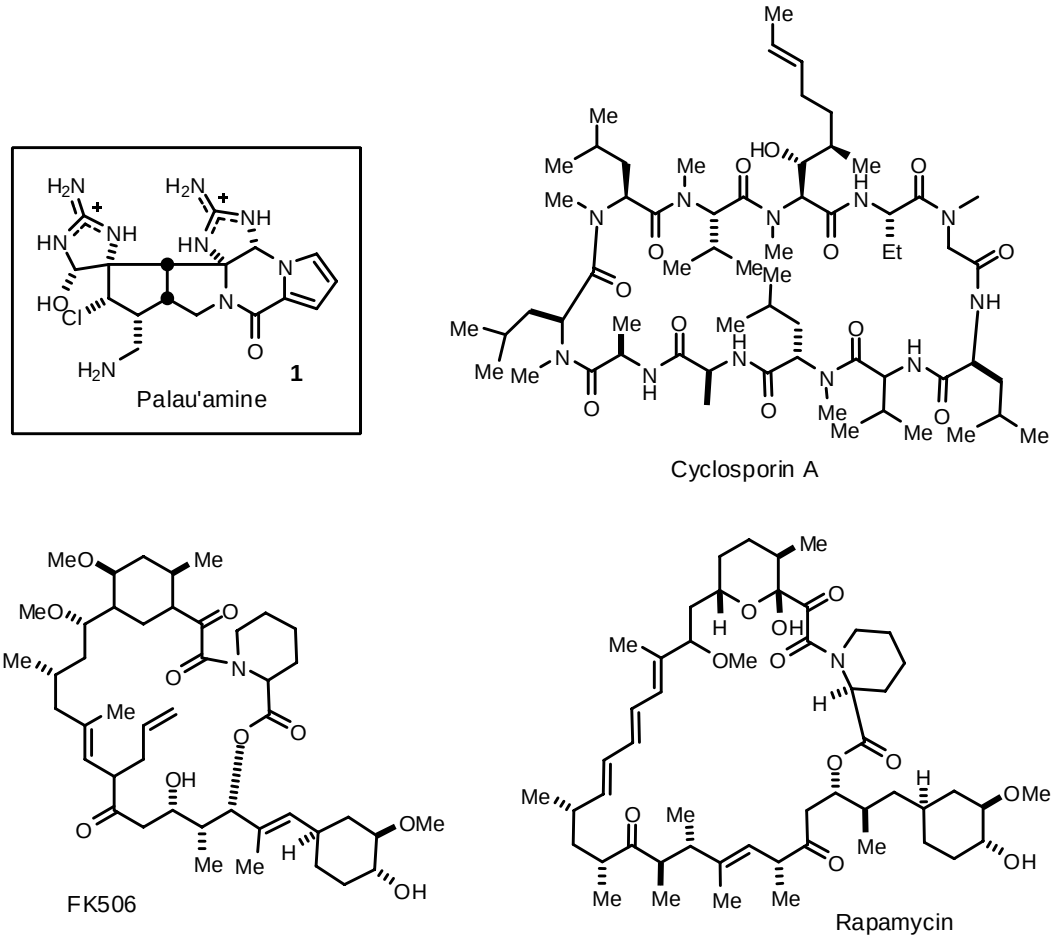

1.1 Pyrrole-Imidazole Alkaloids

Pyrrole-imidazole group alkaloids have been isolated from the following families of marine sponges: *Agelasidae*, *Axinellidae* and *Halichondridae*[1]. More than one hundred members have been discovered. Oroidin **2** and dispacamide **3** are the simpliest members of this group (Figure 1.2). All the other members can be traced back to these two molecules. No direct evidence of supporting either

one of them to be the biosynthetic precursor has been found (Section 1.2). To simplify the discussion, the oroidin **2** is used as the basic building block to categorize the group of alkaloids.

Figure 1.2

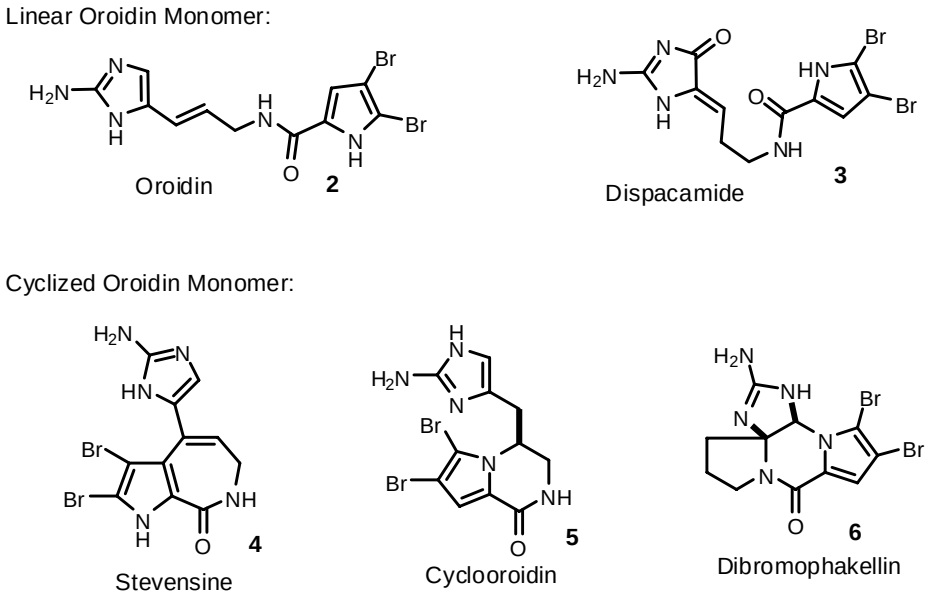

Dispacamide **3** is the oxidized form of oroidin **2**. Recent studies have suggested that dispacamide **3** could also be the biosynthetic precursor of this family of alkaloids (section 1.2.2). The tetracyclic Dibromophakellin **6** was discovered in 1971 by the Sharma group[3]. It represents the most complex structure of the members derived from one molecule of oroidin **2** (Figure 1.2).

The alkaloid derived from two oroidin **2** molecules can be further categorized into three sub-groups (Figure 1.3). One C-C bond formation between two oroidin moieties affords a group of noncyclized dimers. Two C-C bonds

between two oroidin moieties result in a new ring formation, such as: sceptrin[4] **9**, ageliferin[5] **10** and nagelamide[6] **11**. If three or more bonds form between two oroidin moieties, then more complex ring systems result, such as: palau'amine[7] **11**, axinellamine[8] **12** and massadine[9] **13**.

Figure 1.3

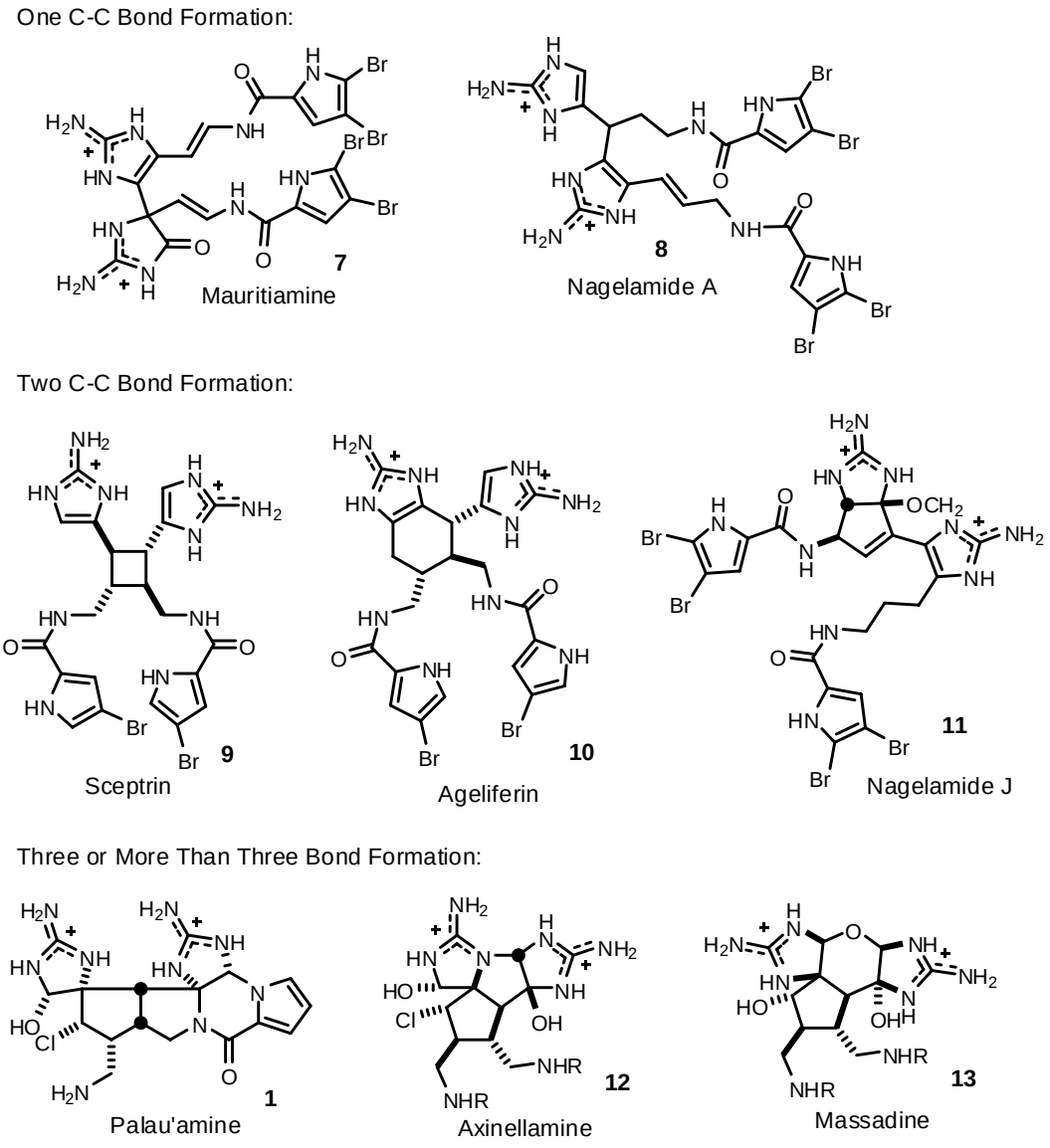

1.2 The Biosynthetic Origin

1.2.1 Kerr's Biosynthetic Studies of Stevensin 3

Due to the difficulty of culturing marine organisms in the laboratory environment, reports on biosynthetic studies of marine-sponge derived alkaloids are very limited. For pyrrole-imidazole group alkaloids, there is only one biosynthetic study, which was conducted by the Kerr group in 1999[10] (Figure 1.4). Their study shows that ^{14}C-labeled histidine, ornithine and proline were involved in the biosynthesis of stevensine[11] **14**. The experiments were done with a cell culture of marine sponge *Teichaxinella morchella*.

Figure 1.4

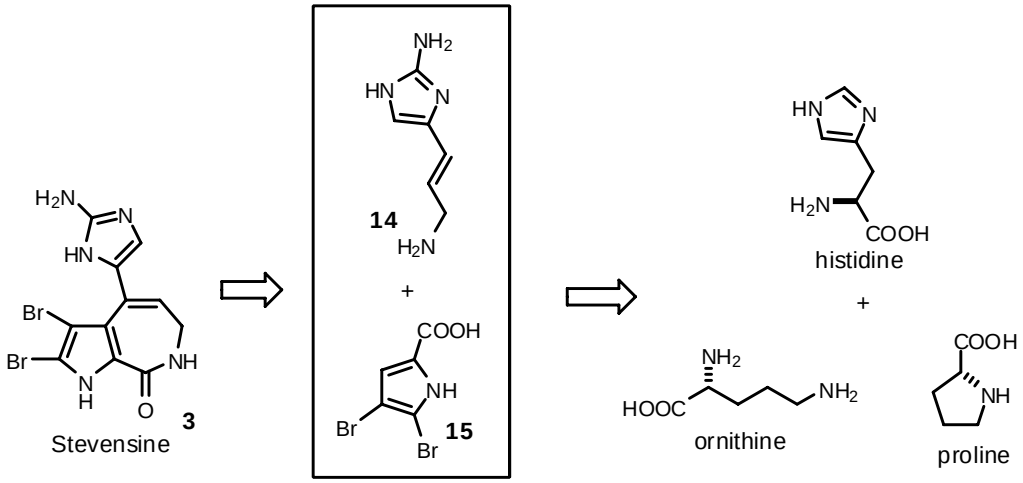

1.2.2 Al-Mourabit's Proposal of Dispacamide 3 as Biosynthetic Forerunner of Oroidin.

In an interesting study[12] done by the Al-Mourabit group in France, dispacamide **3** was synthesized from three simple units: proline **17**, pyrrole-2-

carboxylic acid **16** and guanidine **19** (Scheme 1.1). Diketopiperazine **18** was obtained from condensation of **16** and **17**. When it was exposed to air and guanidine **19**, compound **21** was generated directly through dioxetanone **20** as the intermediate. After dehydration and bromination, dispacamide **2** was synthesized in good yield.

Scheme 1.1[12]

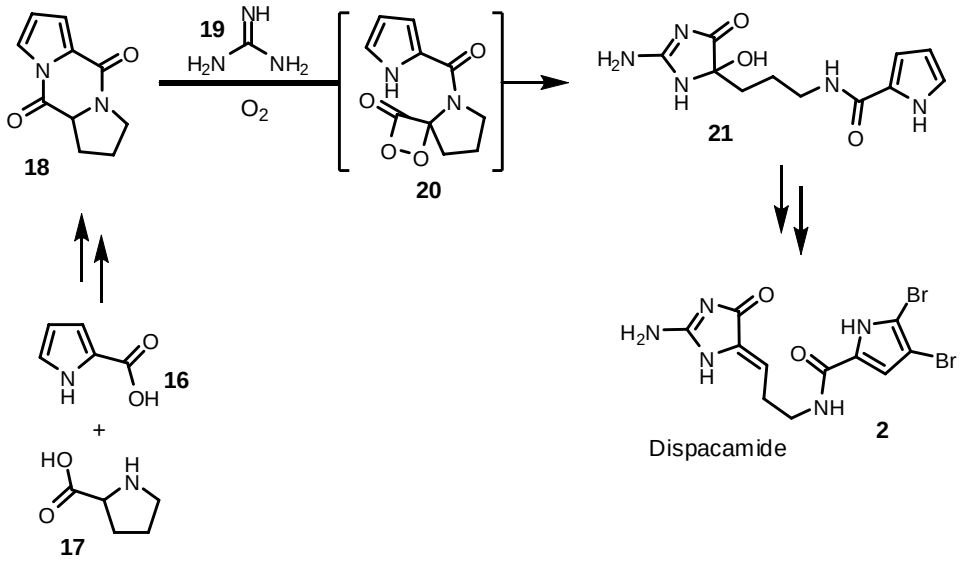

Based on this biomimetic synthesis, they proposed that oroidin **2** was the reduced product of dispacamide **3** biosynthetically. The hypothesis of dispacamide **3** being biosynthetic forerunner of oroidine **2** was also supported by the successful isolation of verpacamides A-D[13] (Figure 1.5). Verpacamide A **22** can be seen as the condensation product of amino acids proline and arginine. Verpacamide B-D (**23**-**25**) can be viewed as the products of subsequent oxidation

of verpacamide A **22**. The authors also proposed that dispacamide **3** could be generated from compound **20** through a dioxetanone intermediate **26**.

Figure 1.5[13]

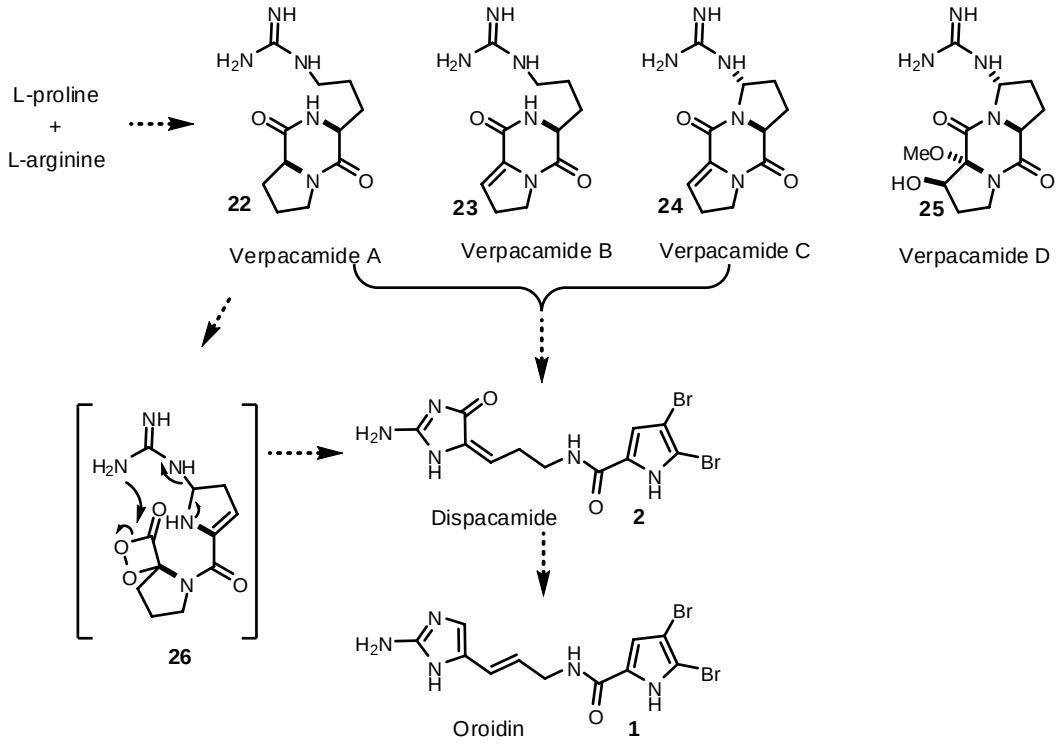

1.2.3 Kinnel and Sheuer's Biosynthetic Proposal of Palau'amine 1

For the biosynthesis of palau'amine, Kinnel and Scheuer[7] proposed a Diels-Alder reaction between 3-amino-1-(2-aminoimidazolyl)prop-1-ene (AAPE) **14** and 11,12-dehydrophakellin **27** to afford intermediate **28** (Scheme 1.2). After chlorination and bond migration, the resulting iminium ion **29** was trapped with one molecule of water to produce palau'amine **1**. This hypothesis has gained

considerable attention from the synthetic community. The Romo[14] and Lovely[15] groups have been pursuing synthetic pathways along this approach.

Scheme 1.2

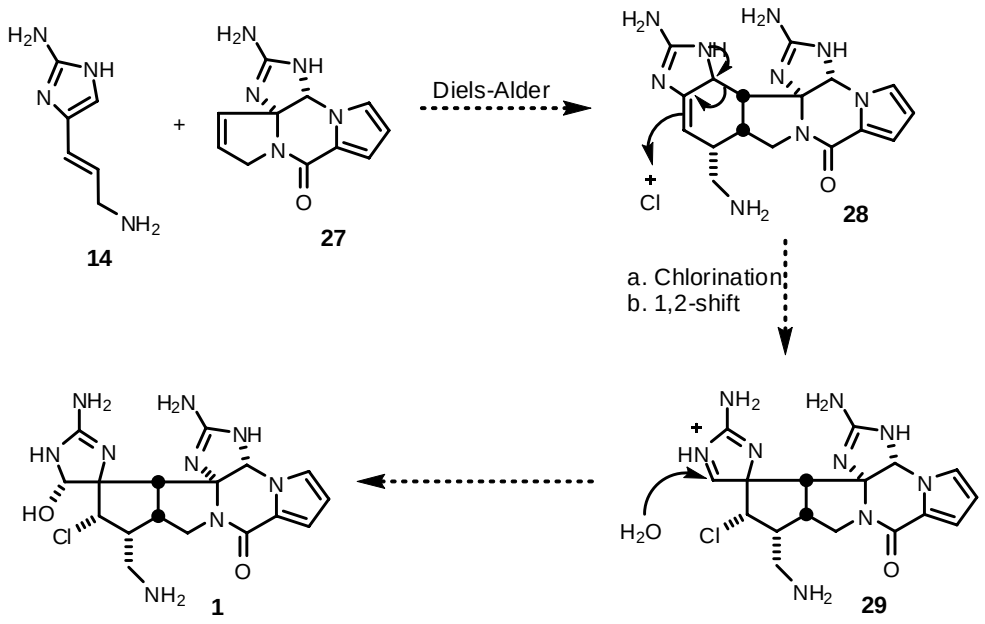

1.2.4 A Universal Chemical Pathway to Pyrrole-Imidazole Family Alkaloids Proposed by Al Mourabit.

In 2001, Potier and Al Mourabit[16] proposed biogenetic pathways that can explain the formation of almost all members of this group. They ingeniously recognized that the same carbon center, in the molecule of AAPE **14**, can be either electrophilic or nucleophilic depending on its tautomeric form (see Figure 1.6). They proposed that the host enzyme could control the tautomeric forms by exchanging protons with its substrate, thus resulting in the amazing diversity observed in these alkaloids.

Figure 1.6

TheTautomerism and Ambivalent Reactivity of AAPE **14**

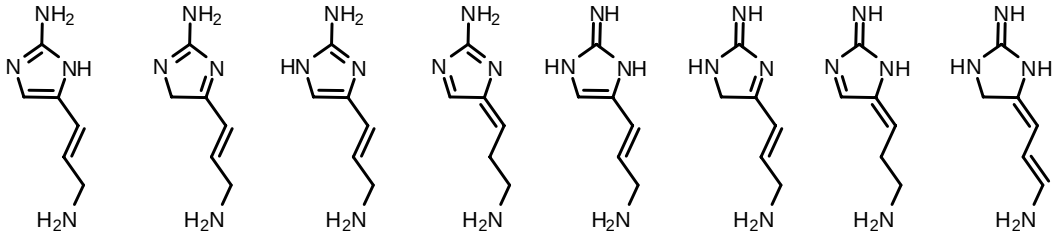

With respect to the palau'amine family of alkaloids, they proposed that the AAPE **14** and oroidin **2** dimerized at the C7 position to produce intermediate **30** (Scheme 1.3). Intermediate **30** could then go through "chlorohydroxylation" to give intermediate **31**. Different cyclization modes (Scheme 1.2) can lead to the formation of palau'amine **1** styloguanidine **33**, or axinellamine **12** skeletons.

Scheme 1.3

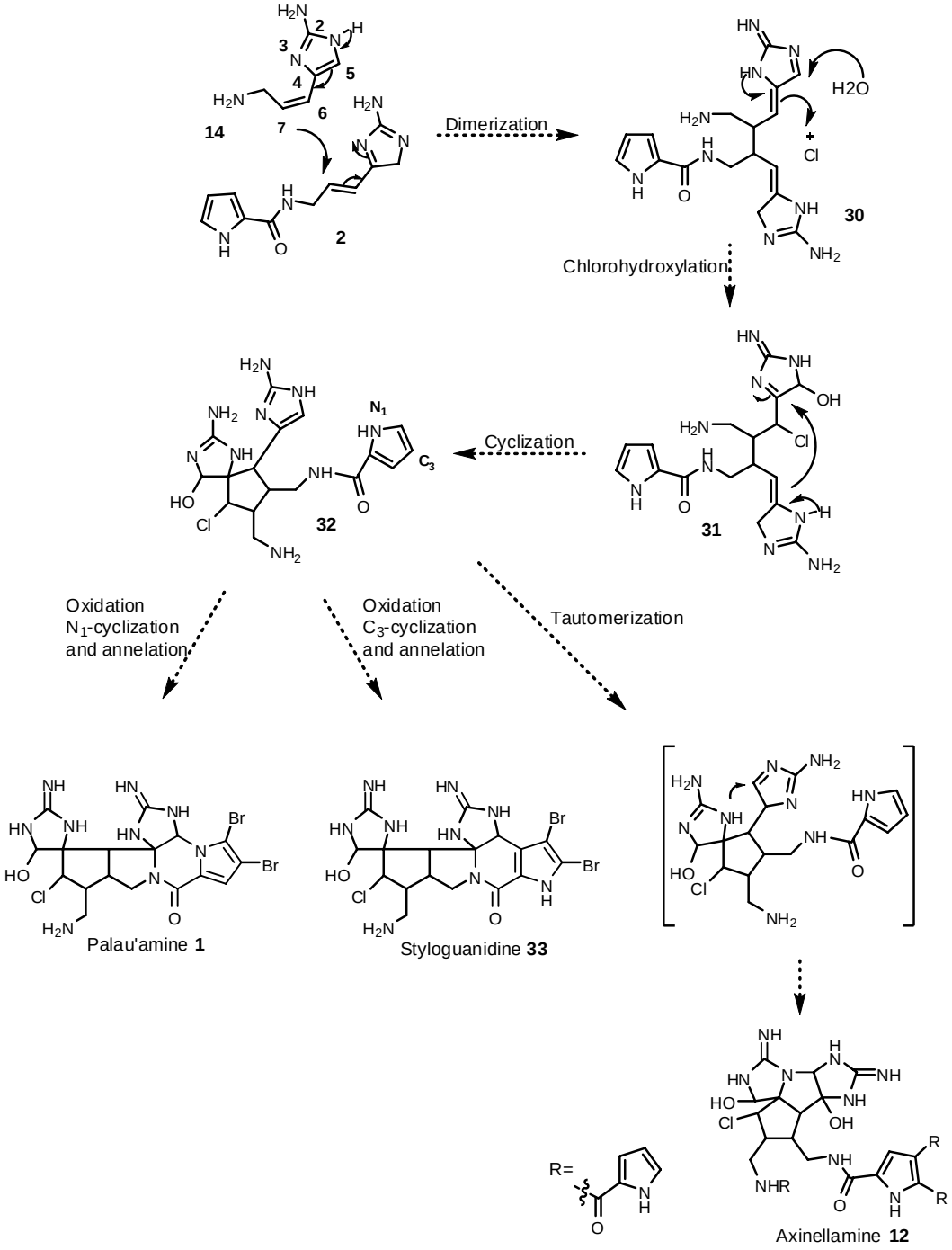
Dimerization
H2O
Chlorohydroxylation
Cyclization
Oxidation
N1-cyclization
and annelation
Oxidation
C3-cyclization
and annelation
Tautomerization
Palau'amine 1
Styloguanidine 33
Axinellamine 12
R=

1.3 The Revisions of Palau'amine's Stereochemisty

Early in 2007, the Köck group in Germany[17], the Quinn group in Australia[18] and the Matsunaga group in Japan[19] independently questioned the original assignment of palau'amine relative stereochemistry. In their revised version **34**, the relative stereochemistries of chlorinated carbon C17 and of C12 at the junction of the azabicyclo[3,3,0]- octane were reversed (Figure 1.7).

In the original assignment[7], Kinnel and Scheuer observed that the coupling constant between H11 and H12 was 14.1 Hz. Despite this large coupling constant and the absence of correlation between H11 and H12 in a ROESY spectrum, they made the assumption that the bicyclo[3,3,0]-azaoctane "has to be *cis* fused", perhaps based on the well-accepted theory that the *cis* fused 5,5-bicycle is much more thermodynamically stable than the *trans*[20].

Figure 1.7

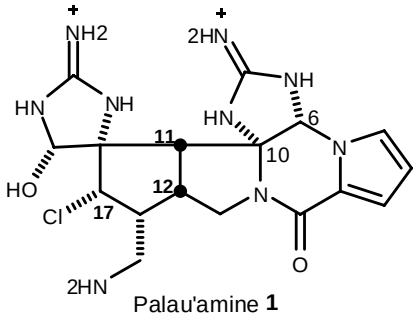

Palau'amine **1**

Kinnel and Scheuer:
J. Am. Chem. Soc. 1993, 115, 3376
J. Org. Chem. 1998, 63, 3281

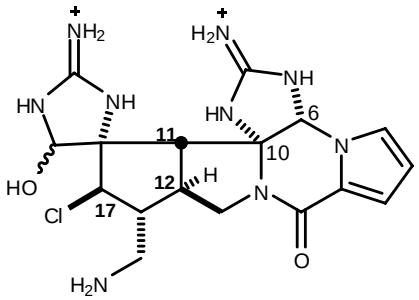

Revised Palau'amine **34**

Matsunaga:
Tetrahedron lett. 2007, 48, 2127

Quinn:
J. Org. Chem, 2007, 72, 2309

Kock:
Angew. Chem. Int. Ed. 2007, 46, 2320

Characterization of newly discovered relatives, along with re-interpretation of spectroscopic data collected on palau'amine itself[18b] made the other three groups conclude that the 5,5-bicycle contained a *trans* fusion. The change of the stereochemistry of C12 called for the alternation of the stereochemistry of C17 as well, based on the NOESY spectrum. The stereochemistry revisions also applied to palau'amine's constitutional isomer styloguanidine **33**. Their revisions not only explained the existing NMR data, but were supported by computational studies combined with 2D-NMR studies performed by the Köck group[17]. The distances between protons were obtained from the quantitative ROESY analysis. The distance geometry (DG)[20] and distance-bounds-driven dynamics (DDD)[21]computational methods were used to find the best fit relative stereochemistry of the eight stereogenic centers.

With the revised structure **34**, palau'amine now has the same relative stereochemistry as massadine **13** and axinellamine **12** around the central cyclopentane ring. The revised structure **34** is more feasible from a biosynthetic point of view. In Baran and Köck's biosynthetic proposal in 2007[22] (Scheme 1.4), which is parallel to Al Mourabit and Potier's in 2001[21] (section 1.2.4). Two intermediates were named pre-axinellamine **35-36**. From these intermediates and through different cyclization modes, palau'amine **1**, axinellamine **12** and massadine chloride **37** could derive. Massadine **13** is proposed to be generated from massadine chloride **37** through an aziridine intermediate **38**[23]. This

hypothesis was supported by a experiments performed done by Köck and Baran[24], in which massadine chloride **37** was in fact isolated from a Caribbean sponge *Stylissa caribica*. Compound **37** was smoothly converted to **13** in a warm aqueous DMSO solution. The revised stereochemistry of palau'amine **34** is also supported by the NMR data of palau'amine congeners **46-47** synthesized by the Overman laboratory (section 1.4.1)

Scheme 1.4

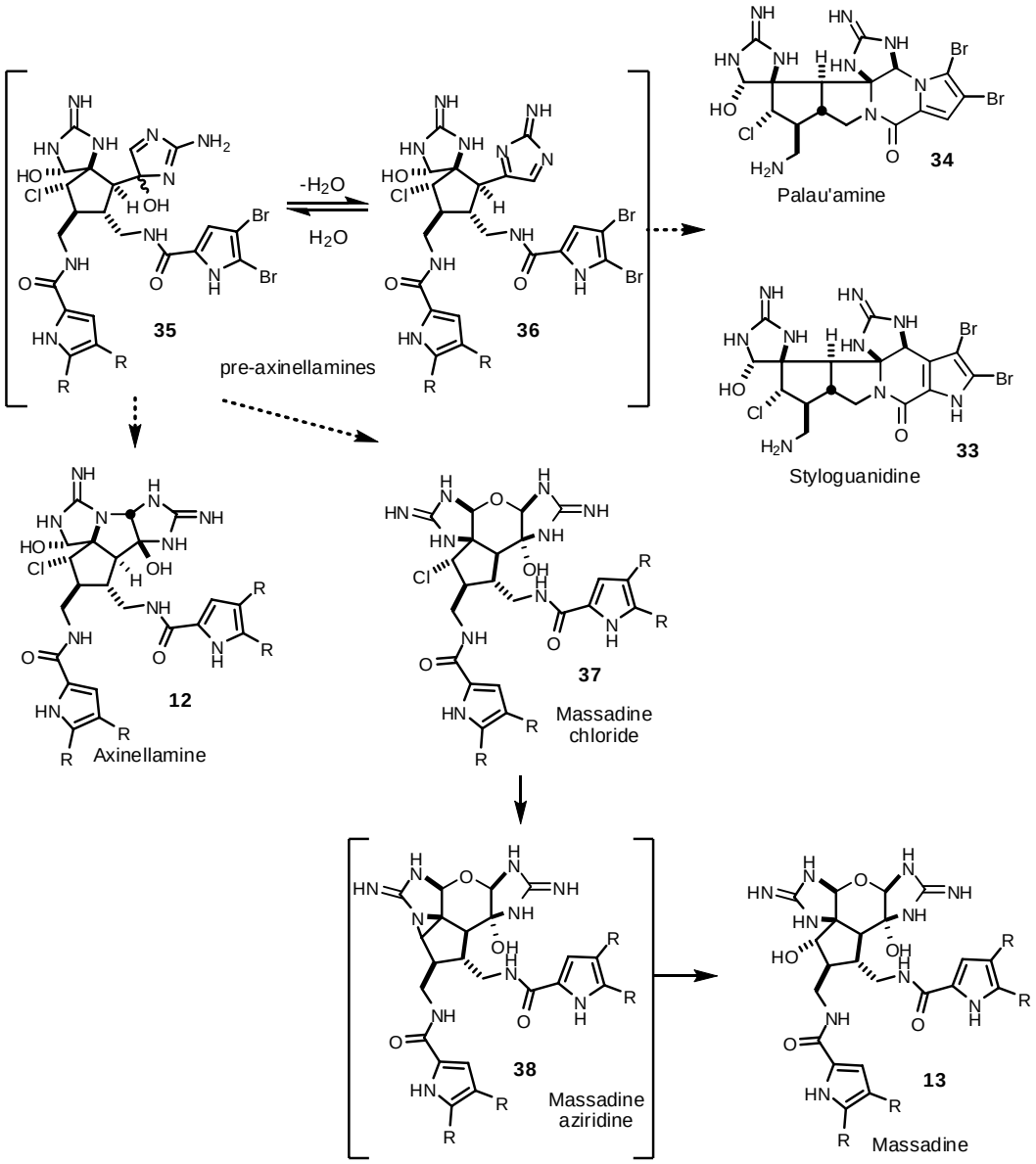

Based on all of the present data, the revised palau'amine stereochemistry **34** is more supported. Since there is no crystallographic data, the synthesis of either structure will be meaningful in the final structure elucidation.

1.4 Palau'amine and Its Biological Activities

Palau'amine was isolated from the marine sponge *Stylotella aurantiuem* in 1993[7a]. It is a potent immunosuppressant (IC_{50} < 35nM in allogenic lymphocyte reaction). Other biological activities[25] include: anti-bacterial (*S. saureus, B. subtillis* – 10 μg/disk), anti-fungal (*Pencillium notatium* – 24 mm zone at 50 μg/disk) and anti-tumor (P-388, IC_{50} = 0.1 μg/mL and A-549, IC_{50} = 0.2μg/mL).

In addition to its impressive biological activities, the hexacyclic ring structure represents unique synthetic challenges. It contains eight contiguous stereogenic centers. In the original *cis* bicyclo[3,3,0]-azaoctane structure **1**, the chlorine containing cyclopentane ring has "all-syn" relative stereochemistry of their tertiary substituents. To construct this extremely congested ring is a difficult task. In the case of the revised structure **34**, to synthesize the unusual *trans* bicyclo[3,3,0]-azaoctane is not a trivial problem either. The computational studies show that the revised structure **34** is energetically less stable[26] than the *cis* one **1** by 27.3 KJ/mol^{-1}. Interestingly, palau'amine starts to decompose once the pH>6[7b]. This brings more limitations into the last stage of the synthesis. Therefore, the synthesis of palau'amine challenges the current capacity of synthetic chemisty with its high density of functionality and stereochemistry, highly polar nature due to the bisguanidine motif and high hetero-atom content.

1.5 Recent Progress Towards the Total Synthesis of Palau'amine Family Alkaloids

Palau'amine has become one of the most attractive synthetic targets to the synthetic community[1b]. Even though the total synthesis has not yet been achieved after thirteen years, extensive efforts invested by a number of research groups have led to some creative chemisty.

1.5.1 Büchi's Biomimetic Synthesis of Dibromophakellin

The biomimetic synthesis of the tetracyclic dibromophakellin **4** was achieved by Foley and Büchi[27] in 1982 (Scheme 1.5). Dihydrooroidin **39** was treated with bromine to generate intermediate **40**, followed by treatment with base to generate dibromophakellin **4** in quantitive yield**.** Because of the structural similarity between dibromophakellin **6** and palau'amine, this synthesis has a major influence on the current pursuits of palau'amine's synthesis.

Scheme 1.5

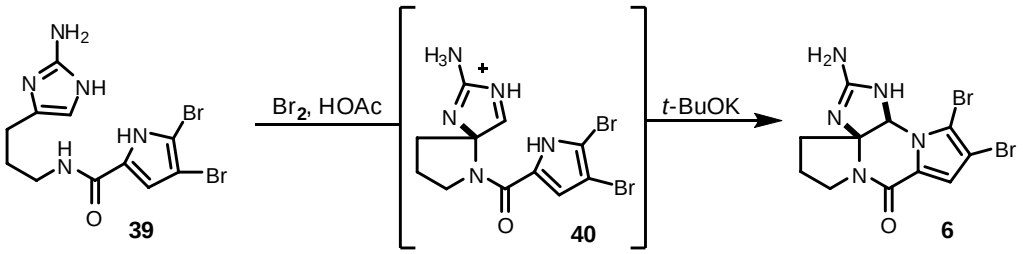

1.5.2 Cycloaddition Approaches

Overman's group has been actively pursuing the synthesis of palau'amine ever since its structure was disclosed[28]. Their approach focuses on constructing

the *cis*-3-azobicycle[3,3,0]octane using an intramolecular [3+2] cycloaddition of azomethine imine **43** to afford triazatriquinane **44** (Scheme 1.6). Intermediate **44** eventually rendered palau'amine congeners **46-47**[29].

Scheme 1.6

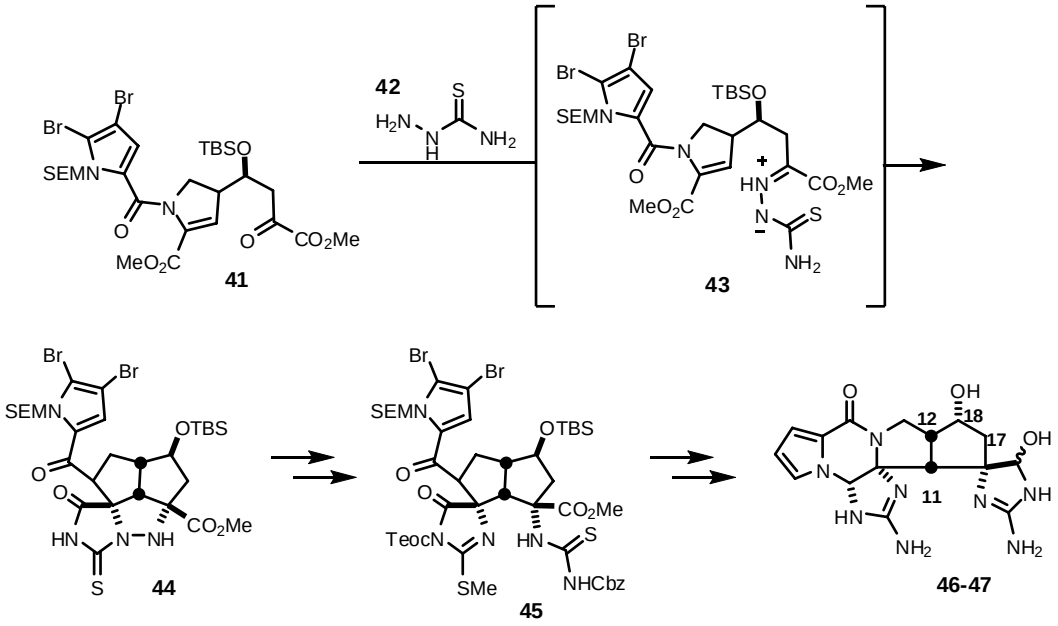

The hexacyclic **46** and **47** differ from the originally assigned palau'amine structure **11** by lacking the chlorine at C17 position and different substituents at C18 (Scheme 1.6). Based on this synthetic achievement, they were able to directly compare the NMR data of **46-47** to palau'amine's. The coupling constants between H11 and H12 in **46** and **47** are 12.0 and 10.7 Hz respectively. In comparison palau'amine's coupling constant value is over 14 Hz. Unlike palau'amine, a strong correlation between H11 and H12 was observed in the NOESY spectrum of compounds **46** and **47**. Combined with computational

studies[17], they concluded that the relative stereochemistries of C12 and C11 in the derivatives are the opposite of the natural product itself. Thus their data support the *trans* relation of the azobicycle[3,3,0]octane newly proposed by Köck[17], Quinn[18], Matsunaga[19] groups.

The Romo[14] and Lovely[15] groups pursued the Diels-Alder reaction followed by ring contraction to construct the core of palau'amine. In Romo's synthesis (Scheme 1.7), the Diels-Alder product **50** was treated with DMDO to afford allylic alcohol **51**. The fully functionalized cyclopentane **52** was formed by an intermolecular chlorination and a ring contraction of compound **48**. Even though it was not mentioned in their publications, the revised palau'amine stereochemistry **34** could be obtained by a simple epimerization of compound **53.**

Scheme 1.7

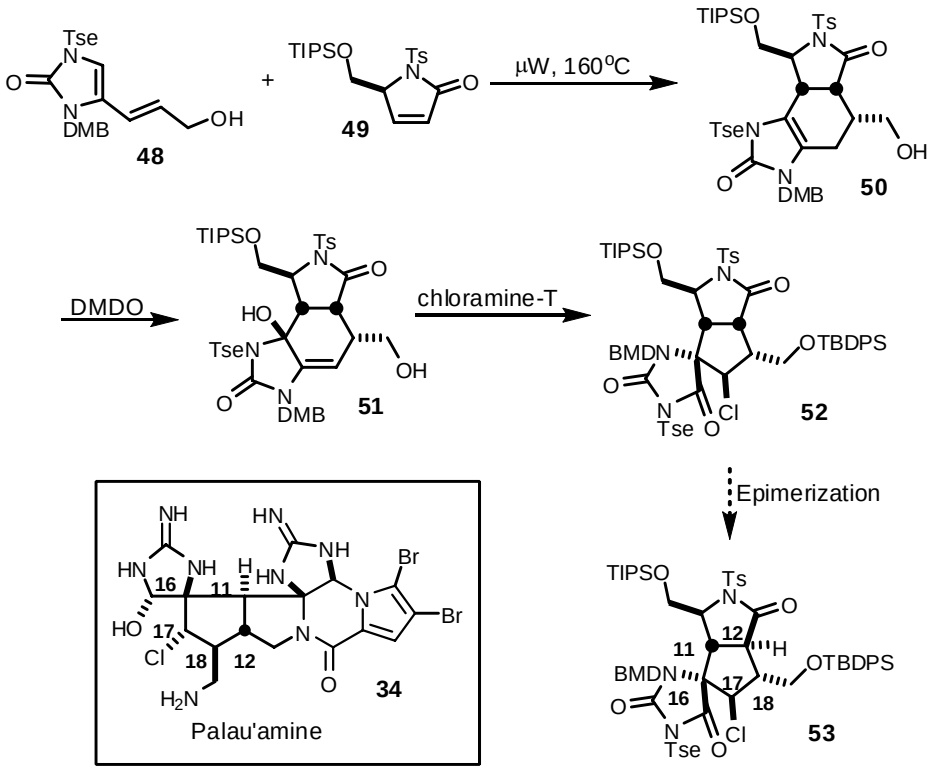

1.5.3 Baran Group's Progress in Palau'amine Family Synthesis

The Baran group is interested in using sceptrin **9** or ageliferin **10** as the starting material to perform either a ring expansion or ring contraction to directly synthesize the palau'amine family of alkaloid[30].

In 2004, the Baran group published the total synthesis of sceptrin[31] **8** and ageliferin[32] **10** (Scheme 1.8). The *trans, trans, trans*-cyclobutane core of sceptrin **8** was quickly assembled by the rearrangement of 3-oxaquadricyclane **56** under acidic conditions. Ageliferin **9** was synthesized in one step from sceptrin **9** though

an aqueous microwave reaction. The Baran group later achieved enantioselective syntheses of sceptrin **9** and ageliferin **10** based on the above work.

Scheme 1.8

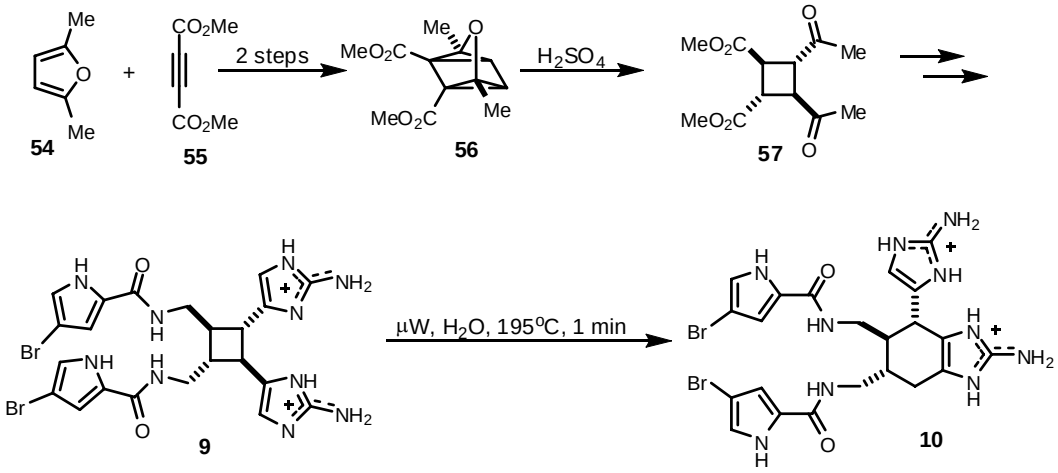

1.5.4 Chen Group's Strategy Towards Palau'amine Family Alkaloids

Chen's group is interested in a Mn (III) mediated free radical reaction to synthesize the core structures of the palau'amine family alkaloids[33] (Scheme 1.9). Mn(III) treatment on (E)-allylic-β-ketone ester **58** afforded cyclic compound **59** and another diastereomer. In this impressive oxidation, two C-C bonds and three stereogenic centers were generated. The ageliferin core in **59** was rearranged to the massadine **13** core and the original palau'amine core **1** via an *m*CPBA oxidation[14,15].

Scheme 1.9

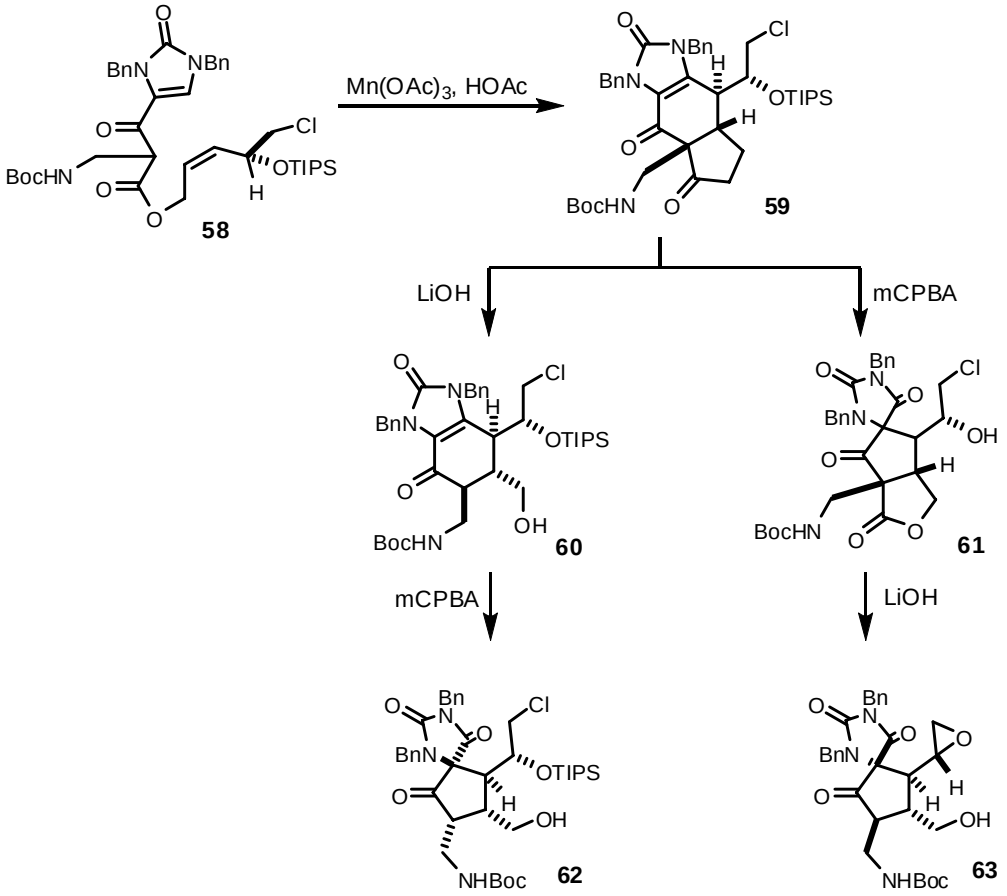

1.6 Our Approach- Symmetry Based Strategy

As mentioned previously (section 1.1), the palau'amine family of alkaloids (**1**, **12-13**) can be seen as dimeric structures formed from two oroidin motifs (Figure 1.8). They all share the common cyclopentane ring, which is formed by two carbon-carbon bonds between the 7→7' and 5→6' positions[34]. As for the original assignment of palau'amine **1**, axinellamine **12** and massadine **13** are the epimers at the C12 and C17 centers. However, based on the revised

stereochemistry **34**, this family of alkaloids shares the same stereochemistry around the central ring.

Figure 1.8

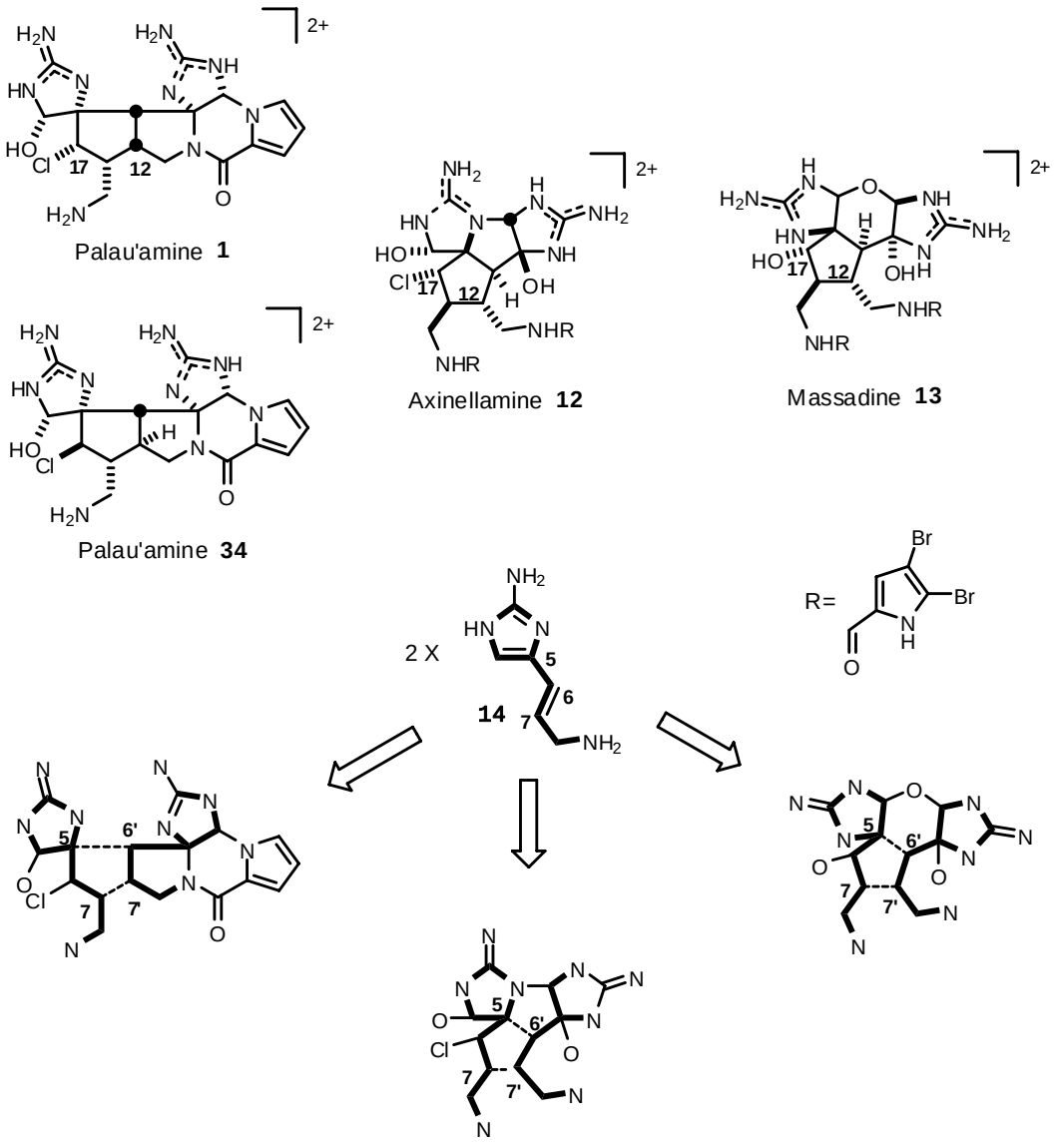

Our strategy[34] to target this family of alkaloids is to design a route to form the central cyclopentane ring with selected stereochemistry (Scheme 1.10). Particularly in the case of the palau'amine **1**, the natural product can be potentially obtained from its higher oxidation form **64**. The diaminoketal on the right hand part of **64** is reminiscent of the intermediate **40** proposed in the oxidative synthesis of dibromophakellin from dihydrooroidin by Buchi[27] (section 1.4.1). Analogously, this portion of the structure could arise from an internal trapping of a C-acyl iminium ion **65** with the adjacent amide nitrogen. The intermediate **65** could be in equilibrium with the fragmented species **66**, another C-acyl iminium ion. The latter could be formed by the addition of a chloronium ion on the pseudosymmetric *meso*-bisalkylidene **67**. If this were possible, then hypohalite oxidation of **67** could initiate the formation of two rings and four new stereocenters in a single operation.

Scheme 1.10

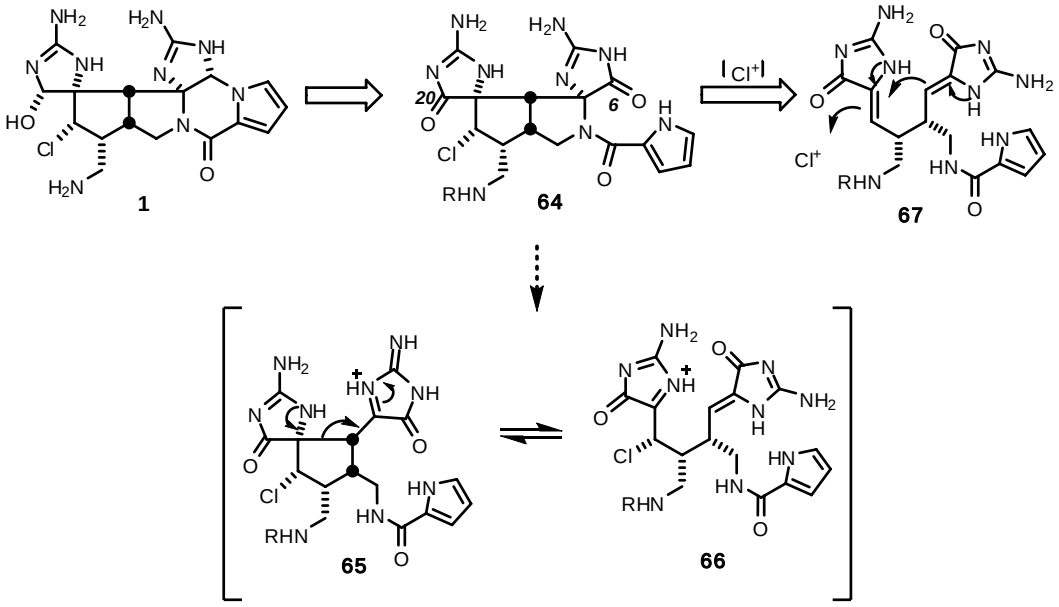

We believe our strategy could be biologically relevant. The intermediate **67** could be viewed as two dispacamide molecules joined at their 7 positions (Figure 1.9). New evidences (section 1.2.2) show dispacamide[35] **3**- the oxidized form of oroidin, could potentially be the biogenetic forerunner for this group.

Figure 1.9

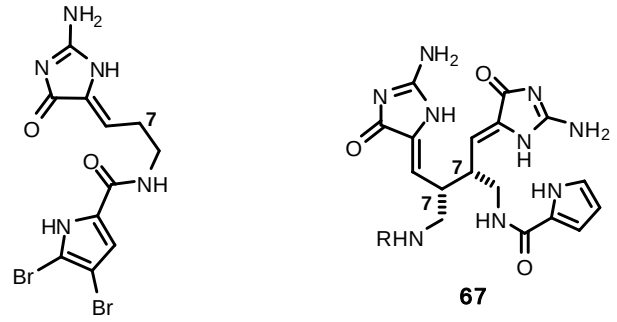

Another important advantage of our approach is that it can target both the proposed stereochemistries of palau'amine, **1** and **34**. By starting with the C_2-bisalkylidene **68**, a similar strategy can be applied to the synthesis of revised palau'amine stereochemistry **34**, axinellamine **12** and massadine **13** (Scheme 1.11).

Scheme 1.11

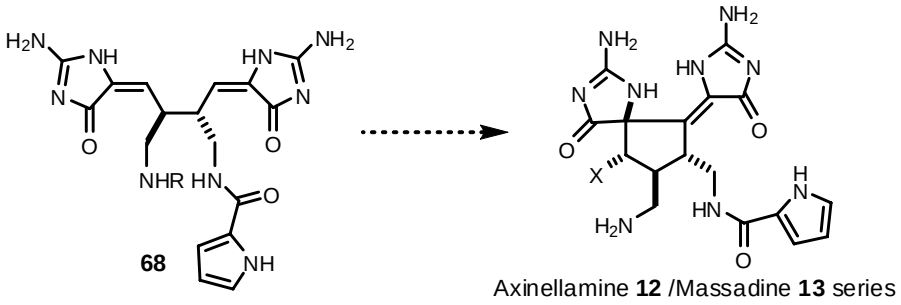

1.6 Notes and References

(1) (a) Hoffmann, H.; Lindel, T. *Synthesis*, **2003**, 12 1753-1783. (b) Jacquot, D. E. N.; Lindel, T. *Current Organic Chemistry*, **2005**, 9, 1551-1565.

(2) (a) Forenza, S.; Minale, L.; Riccio, R.; Fattorusso, E. J. *J. Chem. Soc. Chem. Commun*. **1971**, 1129-1130. (b) Garcia, E. E.; Benjamin, L. E.; Fryer, R. I. *J. Chem. Soc. Chem. Commun*. **1973**, 78-79.

(3) Sharma, G.; Magdoff-Fairchild, B. *J. Org. Chem*. **1977**, 42, 4118-4124.

(4) Walker, R. P.; Faulkner, D. J. *J. Am. Chem. Soc*. **1981**, 103, 6772-6773.

(5) Ishibashi, M.; Iwamura, Michiko. *Tetrahedron.* **1990**, 46, 5579-5586.

(6) Araki, A.; Tsuda, M.; Kubota, T.; Mikami, Y.; Fromont, J.; Kobayashi, J. *Org. Lett.* **2007**, 9, 2369-2371.

(7) (a) Kinnel, R. B.; Gehrken, H-P.; Scheuer, P. J. *J. Am. Chem. Soc.* **1993**, 115, 3376-3377. (b) Kinnel, R. B.; Gehrken, H-P.; Swali, R.; Skoropowshi, G.; Scheuer, P. J. *J. Org. Chem*. **1998**, 63, 3281-3286.

(8) Urban, S.; Leone, P. A.; Carroll, A. R.; Fechner, G. A.; Smith, J.; Hooper, J. N. A.; Quinn, R. J. *J. Org. Chem*. **1999**, 64, 731-735.

(9) Nishimura, S.; Matsunaga, S.; Shibazaki, M.; Suzuki, K.; Furihata, Soest, R. W. M.; Fusetani, N. *Org. Lett.* **2003**, 5, 2255-2257.

(10) Andrade, P.; Willoughby, R.; Pomponi, S. A.; Kerr, R. G.; *Tetrahedron Lett*, **1999**, 40, 4775-4778.

(11) Albizati, K. F.; Faulkner, D. *J. J. Org. Chem*. **1985**, 50, 4163-4164.

(12) Travert, N.; Al-Mourabit, A.; *J. Am. Chem. Soc*. **2004**, 126, 10252-10253.

(13) Vergne, C. V.; Boury-Esnault, N.; Perez, T.; Martin, M-Y.; Adeline, M-T.; Dau, E. T. H.; Al-Mourabit, A. *Org. Lett.* **2006**, 8, 2421-2424.

(14) Dransfield, P. J.; Dilley, A. S.; Wang, S.; Romo, D. *Tetrahedron*, **2006**, 62, 5223-5247

(15) Du, H.; He, Yong, Sivappa, R.; Lovely, C. J. *Synlett*, **2006**, 965-992.

(16) Al Mourabit, A.; Potier, P. *Eur. J. Org. Chem.* **2001**, 237-243.

(17) Köck, M.; Grube, A.; Seiple, I. B.; Baran, P. S. *Angew. Chem. Int. Ed*. **2007**, 46, 6586-6594.

(18) (a) Buchanan, M. S.; Carroll, A. R.; Addepalli, R.; Avery, V. M.; Hooper, J. N. A.; Quinn, R. J. *J. Org. Chem.* **200**7, 2309-2317. (b) Buchanan, M. S.; Carroll, A. R.; Quinn, R. J. *Tetrahedron Lett*. **2007**, 48, 4573-4574.

(19) Kobayashi, H.; Kitamura, K.; Nagai, K.; Nakao, Y.; Fusetani, N.; Soest, R. W. M.; Matsunaga, S. *Tetrahedron Lett*. **2007**, 48, 2127-2129

(20) Havel, T. F.; Kuntz, I. D.; Crippen,G. M. *Bull. Math. Biol.* **1983**, 45, 665 – 720.

(21) Kaptein, R.; Boelens, R.; Scheek, R. M. Van Gunsteren, W. F. *Biochemistry*, **1988**, 27, 5389-5395.

(22) Köck, M.; Grube, A.; Seiple, I. B.; Baran, P. S. *Angew. Chem. Int. Ed*. **2007**, 46, 6586-6594.

(23) The same hypothesis was also proposed by Romo group, see: Wang, S.; Dilley, A. S.; Poullennec, K. G. Romo, D. *Tetrahedron*, **2006**, 62, 7155-7161.

(24) Grube, A.; Immel, S.; Baran, P. S.; Köck, M. *Angew. Chem. Int. Ed*. **2007**, 46, 6721-6724.

(25) Kinnel, R. B.; Gehrken, H-P.; Scheuer, P. J.; Bravalos, D. G.; Faircloth, G. T. *Eur. Pat. Appl.* **1994**, 94302770.

(26) Köck, M.; Grube, A.; Seiple, I. B.; Baran, P. S. *Angew. Chem. Int. Ed*. **2007**, 46, 6586-6594.

(27) Büchi, G.; Foley, L. H.; *J. Am. Chem. Soc*. **1982**, 104, 1776-1777.

(28) Overman, L. E.; Rogers, B. N.; Tellew, J. E. Trenkle, W. C. *J. Am. Chem. Soc.* **1997**, 119, 7159-7160.

(29) (a) Katz, J. D.; Overman, L. E. *Tetrahedron*, **2004**, 60, 9559-9568. (b) Lanman, B. A.; Overman, L. E.; Paulini, R.; White, N. S. *J. Am. Chem. Soc*. **2007**, 129, 12896-12900.

(30) O'Malley, D. P.; Li, K.; Maue, M.; Zografos, A. L.; Baran, P. S. *J. Am, Chem, Soc.* **2007**, 129, 4762-4775.

(31) Baran, P. S.; Zografos, A. L.; O'Malley, D. P. *J. Am. Chem. Soc,* **2004**, 126, 3726-3727.

(32) Baran, P. S.; O'Malley, D. P.; Zografos, A. L. *Ange., Chem. Int. Ed*, **2004**, 43, 2674-2677.

(33) Tan, X.; Chen, C. *Angew. Chem. Int,. Ed.* **2006**, 45, 4345-4348.

(34) Garrido-Hernandez, H.; Nakadai, M.; Vimolratana, M.; Li, Q.;Doundoulaskis, T. *Angew. Chem. Intl. Ed.* **2005**, 117, 775-779

(35) Cafieri, F.; Fattorusso, E.; Mangoni, A.; Taglialatela-Scafati, O. *Tetrahedron Lett*, **1996**, 37, 3587-3590.

CHAPTER TWO

THE INITIAL REACTIVITY STUDY

2.1 Model Study I

In our ambitious retrosynthetic analysis, we are planning on building two rings and four stereocenters in a single step (Scheme 2.1). The primary requirement for such a cascade reaction to occur is that the two glycocyamidine rings have to pack in parallel which forces both the external electrophile and internal nucleophile[1] to approach from trajectories peripheral to this self-assembled unit. In other words, the stereochemical outcome will depend on the reactive conformer of the bisalkylidene structure **67**, given that the reaction is performed under kinetic conditions.

Scheme 2.1

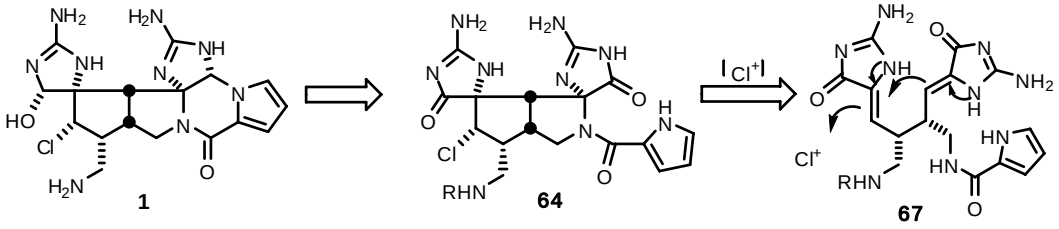

We first needed to assess the behavior of an isolated alkylidene glycocyamidine toward an electrophilic halogen. This work was performed by previous post-doctoral scholar Masakazu Nakadai. Heterocycle[2] **69** was condensed with isobutyraldehyde in the presence of catalytic *N, N*-dimethylethylene diamine monotosylate to afford alkylidene **70**[3] (Scheme 2.2).

When this material was treated with *t*-BuOCl in glacial AcOH, epimeric vicinal chloroacetoxylation products **71** were produced efficiently. Angular acetates **71** are unstable, methanolysis affords isolable congener **72**. These results confirm a desired "enamine" type reactivity of alkylidene in **70** towards hypohalite[4].

Scheme 2.2

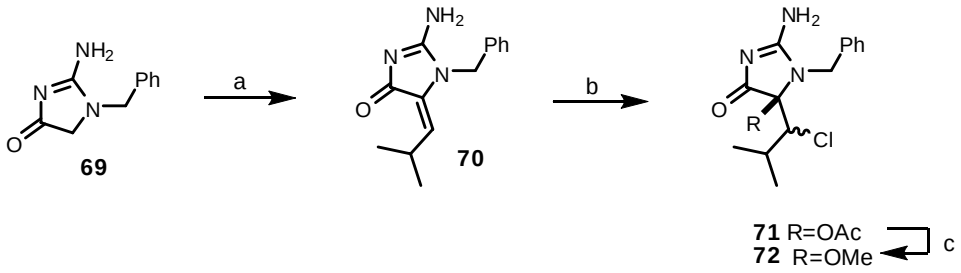

Conditions: a). isobutyraldehyde (1.2 eq),N,N-dimethylethylene diamine (30 mol%), *p*TsOH (30 mol%), DMF, μW (150 °C), 50 min (41%, *E*/*Z*=5:1); b). *t*-BuOCl (1.1 eq, neat), glacial AcOH, rt, 1 h (> 80%, ^{1}H NMR); c). silica gel, MeOH, rt, 6 h (95 %).

2.2 Model Study II

After the "enamine" type acitivity was demonstrated in an isolated alkylidene glycocyamidine, we then examined if similar chemistry executed on a dimeric substrate would result in spirocyclization (Figure 2.1).

The original plan was to retain the substitution pattern of **69** in this dimer. As the condensation of **69** with dialdehyde **75** was unproductive, we decided to install the bisalkylidene motif using SeO_2[5] from the bisglycocyamidine **76**.

Figure 2.1

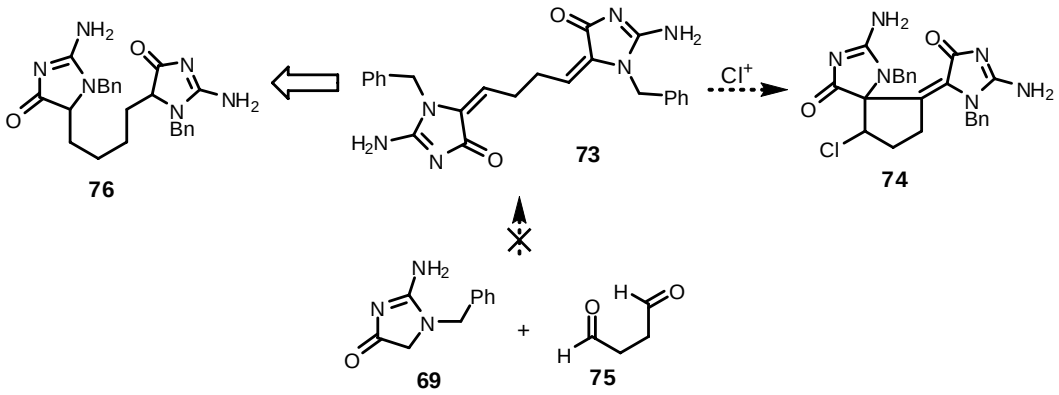

A synthesis of **76** was developed that began with 1,4-dibromo-2-butyne **77** and elaborated symmetrically in two directions (Scheme 2.3). This part of the work was performed by post-doctoral researcher Hugo Garrido-Hernandez. Interestingly, with **76** in hand, its properties were apparently not those intended. The substance readily formed insoluble aggregates. Under conditions in which dehydrogenation to **73** was possible, both the starting material **76** and the product **73** were almost completely insoluble.

Scheme 2.3

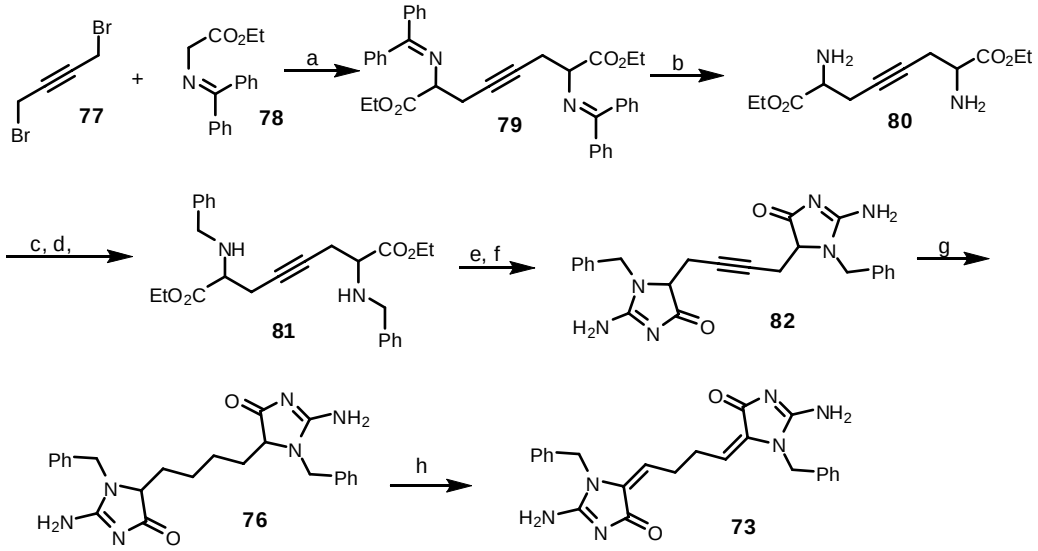

Conditions: a). NaH (1.06 eq), 85 °C, 1.5 h, rt, 20 h; b). HCl (1N), rt, 14h; c) PhCHO (4.5 eq), TEA (2 eq), $MgSO_4$, THF, rt, 14 h; d). $NaBH_4$ (3 eq), MeOH, 0 °C, 15 min, rt, 0.5 h; e). BrCN (1.1 eq), $NaHCO_3$, $CHCl_3$, rt, 14 h; f) NH_3, rt, 24 h; g). H_2, 10%w/w Pd/C, rt, 2 h; h). SeO_2 (4 eq), *t*-BuOH, 80 °C, 5 h.

Compound **73** has all of the functionality to test our key idea. However it is proved to be a poor model because of its poor solubility. The unit cell of its crystal structure contains four molecules of **73**, each in extended conformation with their glycocyamidine rings interacting bimolecularly through multiple H bonds (Figure 2.2).

Figure 2.2

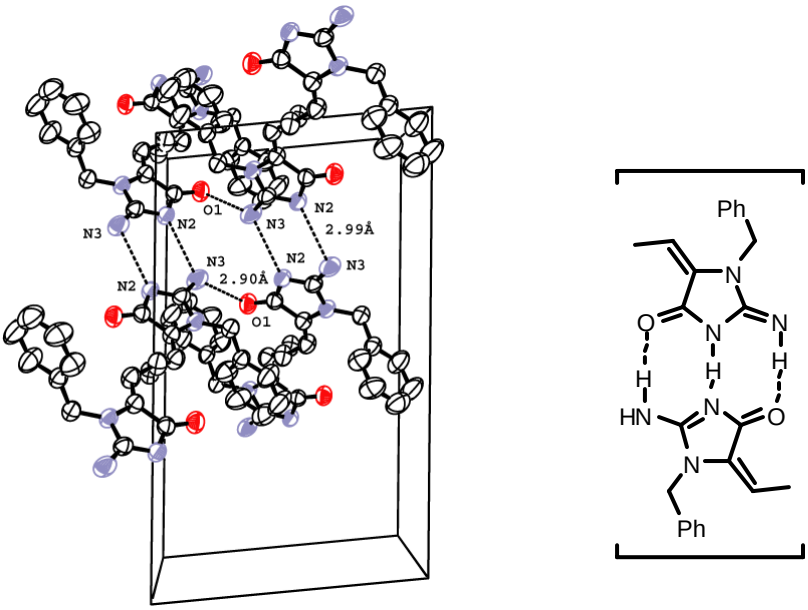

As a means to disrupt the multiple bimolecular hydrogen bonding observed in compound **73**, we considered repositioning the N1 benzyl unit on each heterocycle to N2. Alone, the change was synthetically awkward, but the incorporation of both N2 and N3 into a 2,4-benzodiazepine appeared workable (Figure 2.3). Compound **83** became the target. After the unsuccessful attempts of using SeO_2 and Br_2 methodologies to install the exo-cyclic double bond from compound **84**, we eventually adopted the approach based on basic degradation[6]of sulfonamides **86** (Scheme 2.4)**.**

Figure 2.3

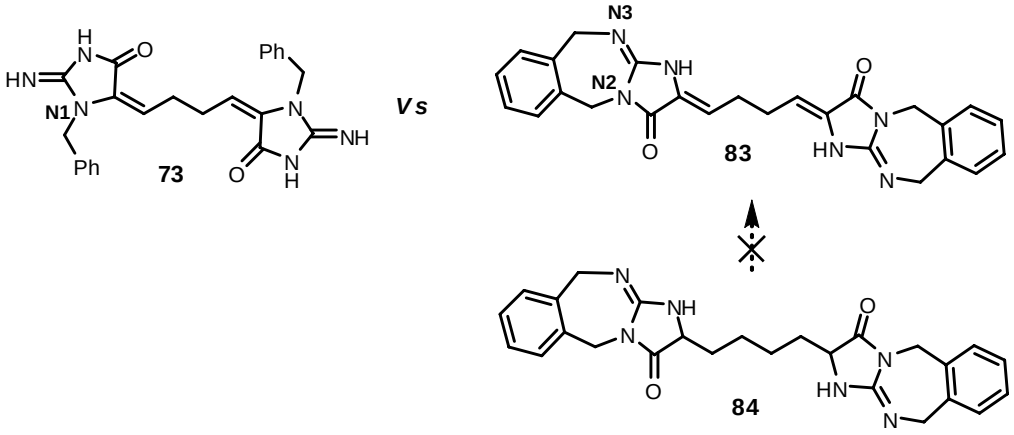

Condensing compound **85** with a twofold excess of *o*-xylyldiamine-derived methylisothiourea **77**[7] provided **86** directly. The *seco* amides presumably formed transiently in the reaction and cyclized spontaneously, with the ejection of methanethiol at each end of the molecule (Scheme 2.4).

With **86** available, we examined its response to base. Exposure to KHMDS caused degradation. However, when the compound was treated with DBU in DMF, monoalkylidene **87** formed rapidly. This material was isolated without incident. When **87** was re-exposed to DBU, two new products emerged in high yield. Surprisingly, neither was found to be bisalkylidene **83**. Rather, they proved to be geometric isomers of spirocycloisomerization product **88-89**.

Scheme 2.4

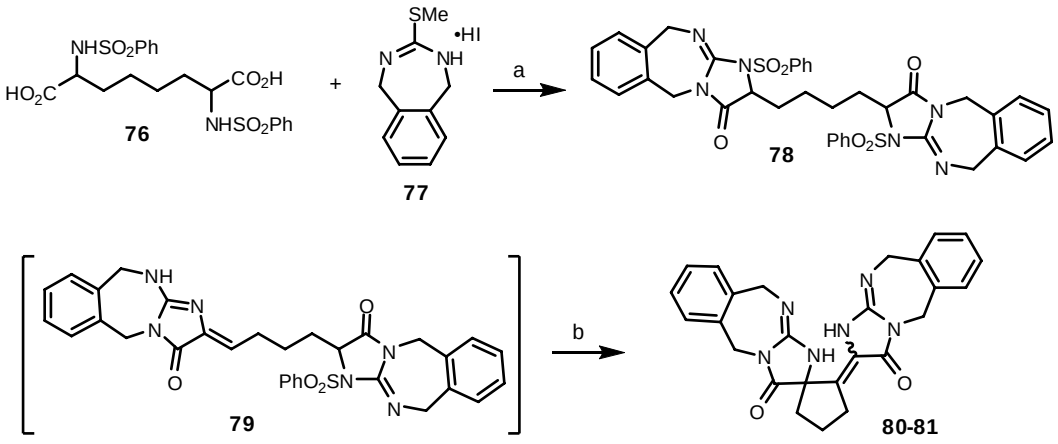

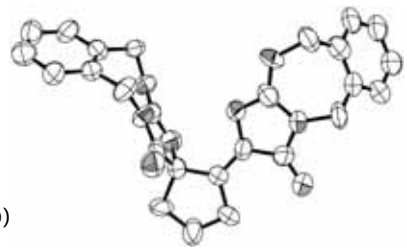

Conditions: a). TBTU, DIPEA, **77** (2.2 eq), CH_2Cl_2, rt (35 %); b)

This is precisely the behavior we wanted to see. Whereas **83** was designed to participate in a spirocyclization initiated by hypohalite, this molecule is apparently so well-poised for the reaction that a proton is sufficient provocation. Nevertheless, this outcome validated the central tenet of our approach to **1** and **12-13**.

2.3 The Design of Substrate that Leads to the Synthesis of Palau'amine 1.

We are facing a much more complicated stereochemistry problem for the chlorination reactons on the substrates that can potentially lead to the synthesis of palau'amine **1**. If the cyclization process does happen as planned, the

stereochemistry of the four newly-established chiral centers should highly depend on the reactive conformers of the substrate given the reaction is under kinetic control.

Computational calculations[8] were employed to study the conformations of potential starting materials. Starting with a *Z*,*Z* C12/C18-anti configured **90**, the calculations suggest the two heterocycles stack in parallel in the low energy conformers (Figure 2.5). The chain connecting the two glycocyamidines readily adopt either boat **92** or chair like **91** orientation to minimize $A^{1,3}$ strain[9] by eclipsing the C18-H to C16-N bond.

Based on the seminal work of the Beak group on the mechanistic studies on the electrophilic chlorination reactions[10], a trigonal bipyramidal transition structure with a 180° bond angle between the nucleophile and the leaving group is required for the chlorine atom transfer (Figure 2.4). With the stereochemistry of palau'amine **11** in mind, it is very possiblethe kinetically controlled cyclization initiated by chlorination would expectedly lead to products having trans stereochemistry between C17 and C18 (**93**/**94**), which is the unnatural relative stereochemistry, from the stable conformers.

Figure 2.4

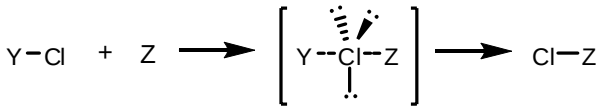

Figure 2.5

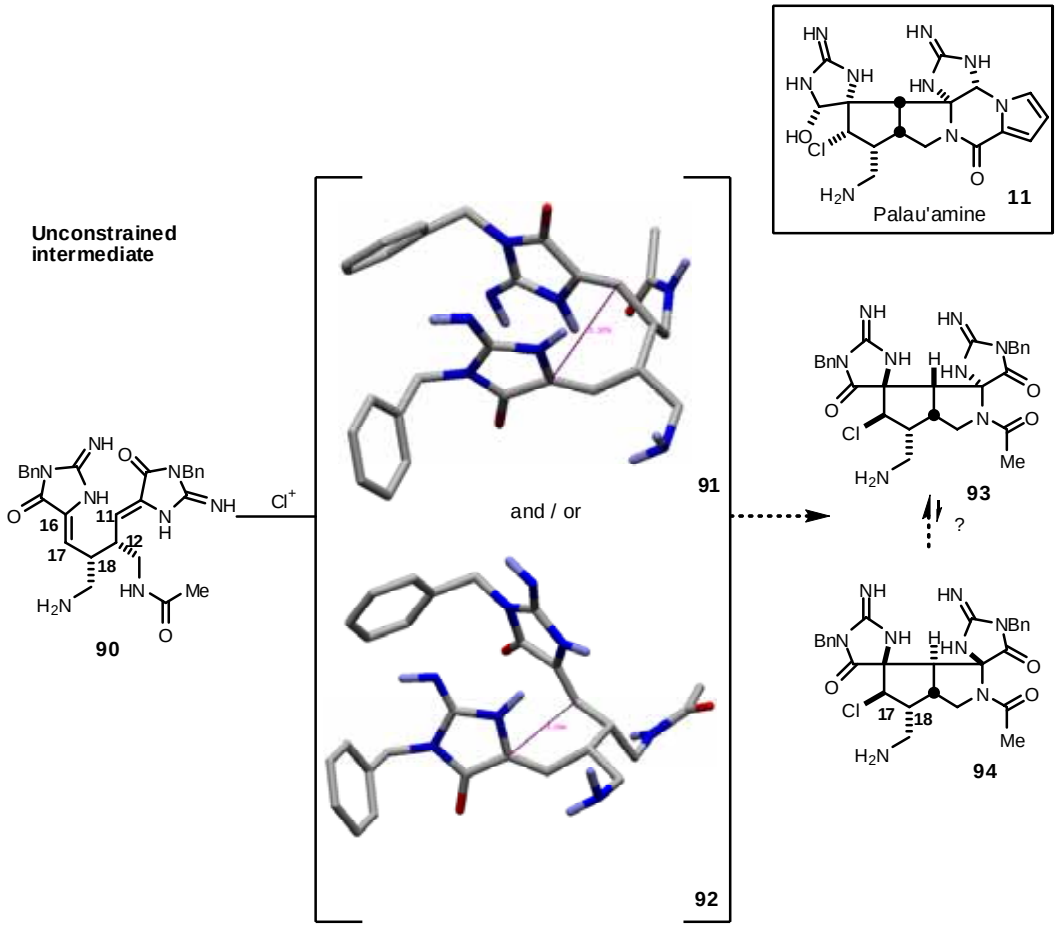

A way to achieve natural stereochemical outcome is by using the constrained starting material. For example, the operation of tethering the primary amine to the N1 nitrogen of the same side glycocyamidine ring will lead to a hydrazine complex **95** (Figure 2.6). In complex **95**, not only is C16/C17 *Z*-alkene geometry assured but the rotational orientation of the C18/C19 bond is fixed. Oxidative spiroannulation executed on this material should initiate at the more

electron rich and sterically accessible olefin (the vinyl hydrazine) and precede through conformers **96** and /or **97** to afford pentacyclic products **98**/**99**. It is difficult to predict which precise pathway will predominate, although the *trans* C11/C12 ring fusion in **98** is strained and this material might not form at all. The important point from this analysis is that the all-syn relationship between substituents at C16, C17, and C18 can be established beginning with **95**.

Figure 2.6

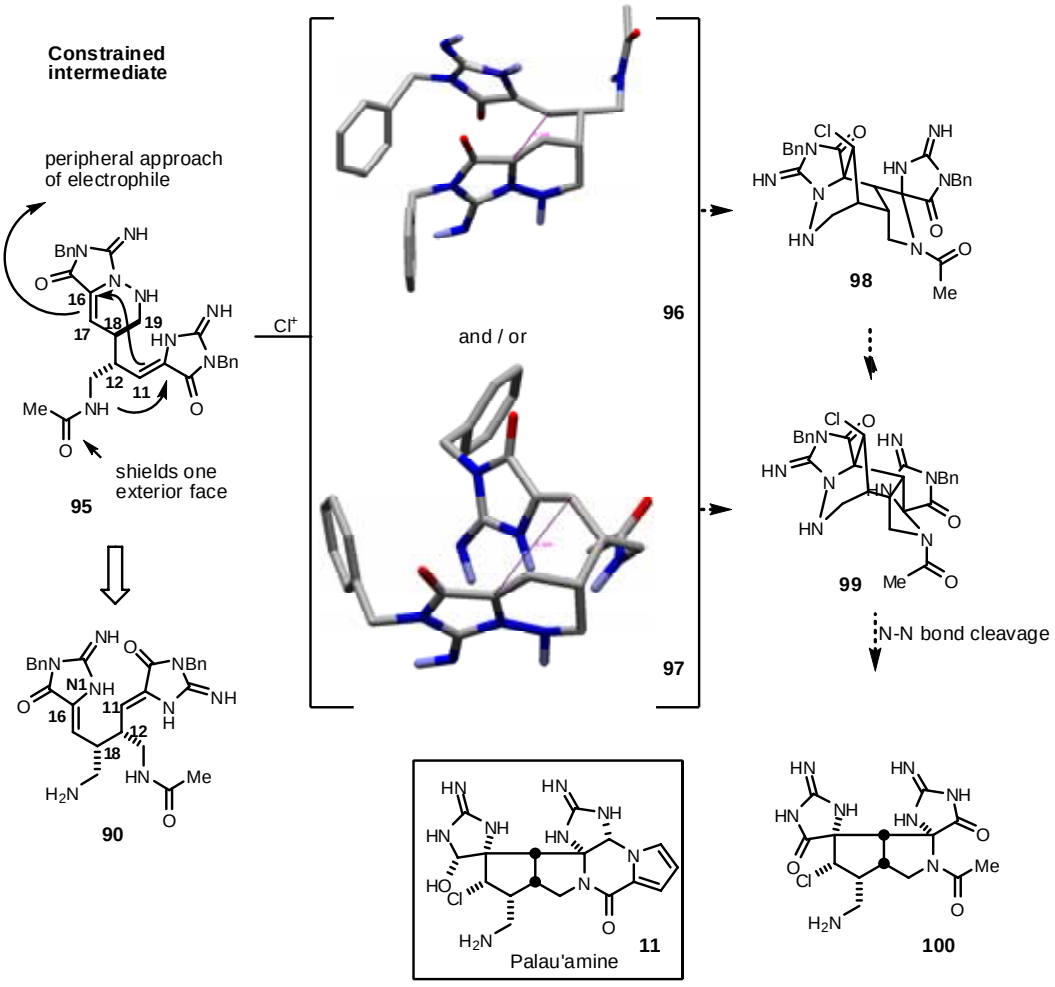

2.4 Notes and References

(1) Knűppel, S.; Wang, C.; Kehr, G.; Fröhlich, R.; Erker, G. *J. Organomet. Chem.* **2005**, 690, 14-32.

(2) Kienzle, F.; Kaiser, A.; Chodnekar, M. S. *Eur. J. Med. Chem.* **1982**, 17, 547-556.

(3) Saito, S.; Nakadai, M.; Yamamoto, H. *Synlett* **2001**, 1245-1248.

(4) (a) Waegell, B.; Heumann, A.; Lacrampe, J.; Esposito, G.; Tadayoni, R.; Furstoss, R. *Can. J. Chem.* **1976**, 54, 3569-3579. (b) Padwa, A.; Lee, H. I.; Rashatasakhon, P.; Rose, M. *J. Org. Chem*. **2004**, 69, 8209-8218.

(5) Nicolaou, K. C.; Petasis, N. A. *Selenium in Natural Products Synthesis*, CIS, Philadephia, **1984**. Chap. 3.

(6) Trenkle, W. C. Ph.D. Thesis, University of California, Irvine, **2000**, UMI no. 9950654.

(7) Elslager, E.; Worth, D. F.; Haley, N. F.; Perricone, S. C. *J. Heterocycl. Chem.* **1968**, 5, 609-613.

(8) Five thousand structures were randomly generated within the Monte Carlo subroutine of Macromodel®v6.5. 1020 unique conformers were found and minimized (Amber force field, water solvation) to convergence using a maximum of 3000 iterations of truncated Newton conjugate gradient minimization. Calculated structures shown in Figure 2.2 and Figure 2.3 are representative of lowest-energy conformers. In each case, they are at or within 1.0 kcal/mol of the calculated 'global' minimum.

(9) Hoffmann, R. W. *Chem. Rev*. **1989**, 89, 1841-1860.

(10) Lee, S. J.; Terrazas, M. S.; Pippel, D. J.; Beak, P. *J. Am. Chem. Soc.* **2003**, 125, 7307-7312.

CHAPTER THREE

SYNTHESES AND DIMERIZATION STUDIES OF MONOMERS

In order to achieve the stereochemistry in palau'amine **1**, we decided to perform the electrophilic chlorination on substrates like **95** (Scheme 3.1). The next question is how to synthesize a compound of **95** types. The 2, 4-benzodiazepine protecting group strategy will still be adopted in the real system. This makes **101** the target compound (Scheme 3.1). It can be potentially obtained from *meso* compound **102** via N-N bond cleavage. Due to the dimeric nature of compound **102**, the most direct way to generate it is from the monomeric form **103**. Among possible means to dimerize **103**, we chose a radical manifold **106** available via one-electron oxidation of a carbanion of **103**. The heterocyclic ring system of **103** is not known in the literature, but it can be quickly traced back to three simpler components, 2,5-dihydro-3-(methylthio)-1H-2,4-benzodiazepine **77**, hydrazine **104**, and 5-bromo-2-oxopentanoic acid **105**.

Scheme 3.1

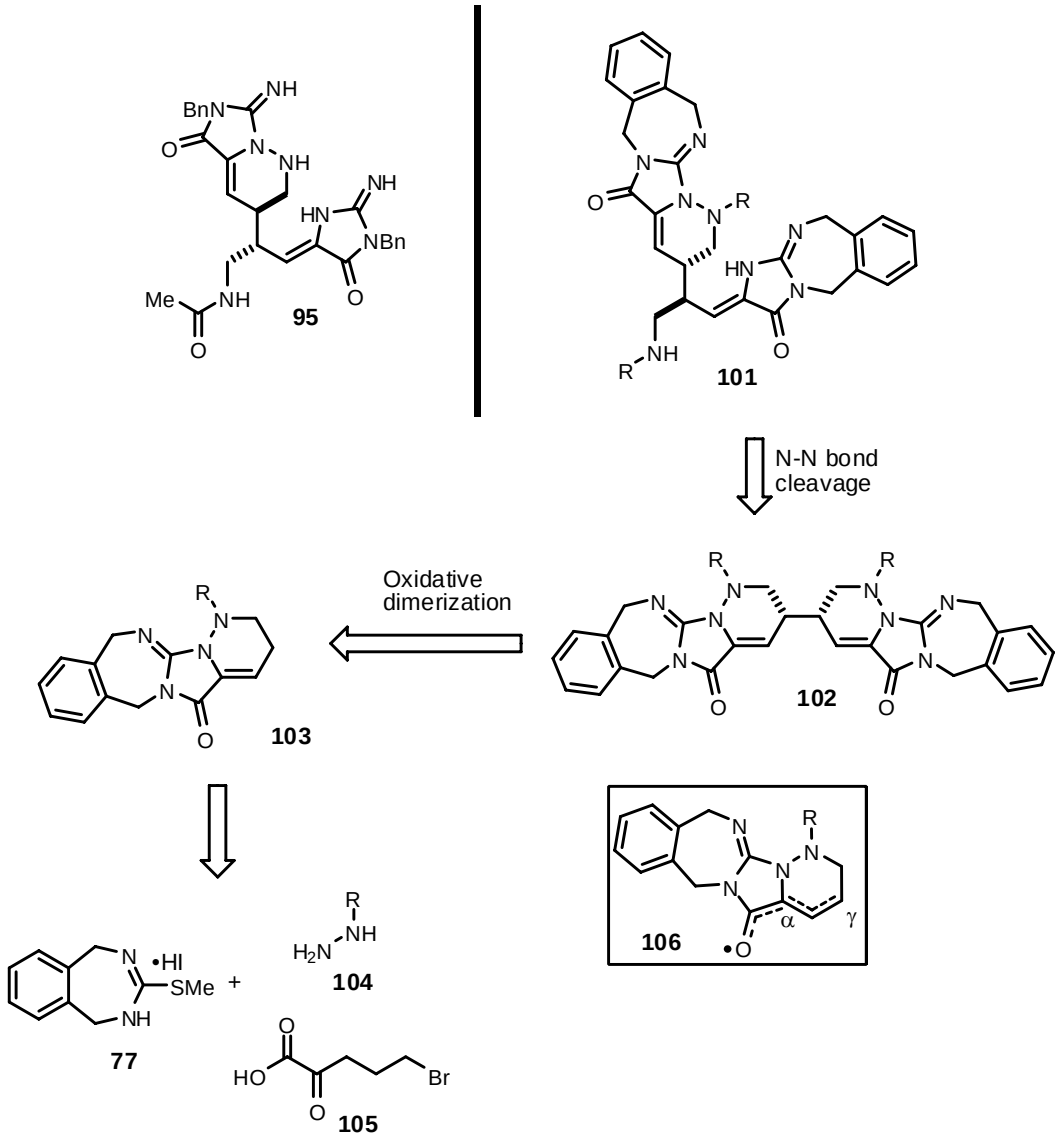

3.1 Boc-Monomer Synthesis

2,5-dihydro-3-(methylthio)-1H-2,4-benzodiazepine **110** is a known compound[1]. Started with dibromide **106**, compound **110** can be synthesized after seven steps with overall 70% yield (Scheme 3.2). As the free base form **110** can

be obtained via base treatment of the HI salt **77**, the methyl group migration from N to S occurred even under the condition of being stored as solid at −12 °C in a freezer. Due to this instability, the HI salt form **77** was used directly for the reactions.

Scheme 3.2

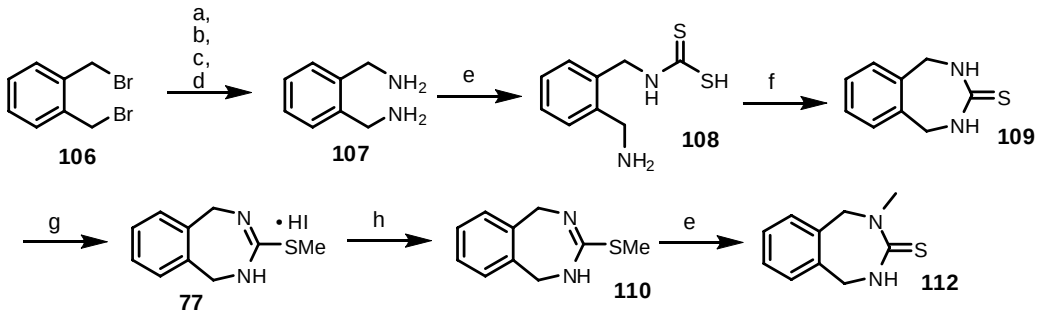

Conditions: a) NaN_3 (2.18 eq),THF/EtOH/H_2O, 110 °C, 1 h, b). PPh_3 (2.5 eq), 110 °C, 1 h; c) HCl (35% aq), reflux, 2 h; d) NaOH; e) CS_2 (2 eq), EtOH, rt, overnight; f) 2-methoxyethanol, 130 °C, 1 h; g) CH_3I (1.2 eq), MeOH, 70 °C, 4 h (70% from **96**), ; h) NaOH; e). solid state, -12 °C, 1 month (30% conversion).

The Claisen condensation product of γ-butyrolactone **103** and $(CO_2Et)_2$ **114** was degraded with HBr/AcOH and the crude reaction mixture was treated with MeOH with a catalytic amount of concentrated H_2SO_4 to afford α-keto ester **116**[2] (Scheme 3.3). This material was exposed to hydrazine to generate a tetrahydropyridine carboxylate **117**[3].

Scheme 3.3

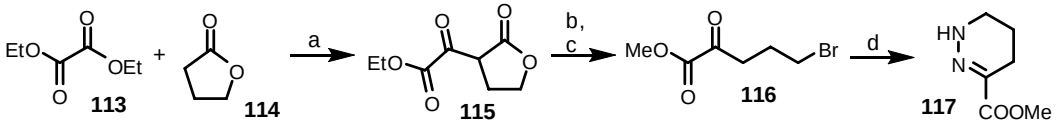

Conditions: a) Na (1.1 eq), EtOH, rt, overnight (100% conversion by ^{1}H NMR); b) HBr/HOAc (35%), 120 °C, 3h; c) H_2SO_4, MeOH (85%); d) NH_2NH_2, (1 eq), AcOH (10 eq), MeOH/H_2O, rt to 62 °C (>95%).

Initially we chose the easy removal Boc protecting group. Compound **117** was protected and hydrolyzed to afford acid **119** (Scheme 3.4). The acid was coupled with **77** and was subsequently treated with $HgCl_2$ to afford Boc-monomer **122**[4].

Scheme 3.4

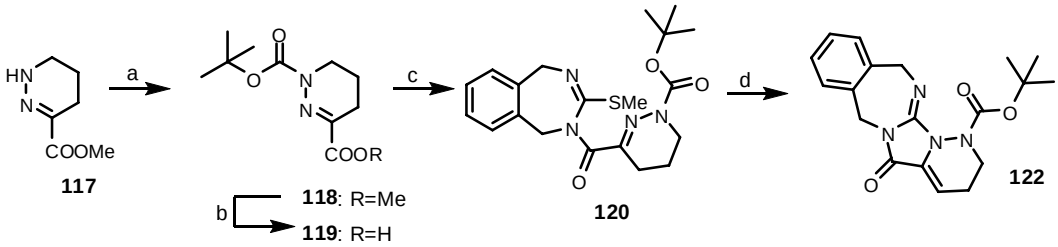

Conditions: a) $(Boc)_2O$ (1.1 eq), Pyr (1.15 eq), DMAP (0.1 eq), THF, rt, overnight (92%); b) LiOH (1.05 eq), THF/H_2O (> 95%); c) **77** (1.1 eq), TBTU (1 eq), DIPEA (2.1 eq), (85%); d) $HgCl_2$(1.1 eq), Pyr (2 eq), 120 °C, 2h (75%).

3.2 Oxidative Dimerization of Boc Monomer 122

With the successful synthesis of Boc monomer **122**, the next question is now to generate the dimer directly from the monomer moiety. Conventional oxidative enolates dimerization appeared to be an attractive means to achieve this transformation.

Oxidative enolate dimerization methodology has a long history. Its first report appeared in 1934, where the magnesium enolate of phenylacetate was oxidized by molecular bromine and afforded the dimer in 22% yield[5]. Up to today, there are numerous literature articles in this field. Its substrate scope has been expanded to ketones[6], esters[7], carboxylic acids[8], silyl enol ethers[9], and titanocene enolates[10]. A wide range of oxidants have been utilized. Electrochemistry[11] had been successfully utilized as the oxidation method too. Even with the extensive study in this field, little is known about its detailed mechanism[12] and the results of the reaction depend on the substrates and conditions employed.

There are relatively few reports about regioselectivity of the oxidation of dienolates. Even in the existing ones, they are mainly observations of what happened instead of solutions on how to achieve the desired regioselectivity. In the study conducted by the Saegusa group[13], the oxidative coupling of enolates of vinylogous ester **123** produced γ,γ-coupling dimer **124** and α, γ-coupling dimer **125** as major products and no α,α region-isomer was found (Scheme 3.5).

Scheme 3.5

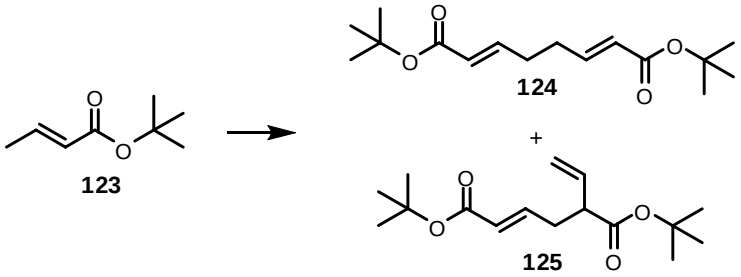

Conditions: LDA, $CuCl_2$, –78 °C, **124** (33%), **125** (33%).

The Paquette group[14] reported an interesting correlation between regioselectivity and the oxidants employed in the reactions. When $CuCl_2$ was utilized as an oxidant for the oxidative coupling of (1*R*)-(+)-verbenone **126**, the γ,γ regio-isomer **127** was obtained as the major product (Scheme 3.6). However when Fe(III) was used as the oxidant, the selectivity for γ,γ regio-isomer **127** was largely diminished.

Scheme 3.6

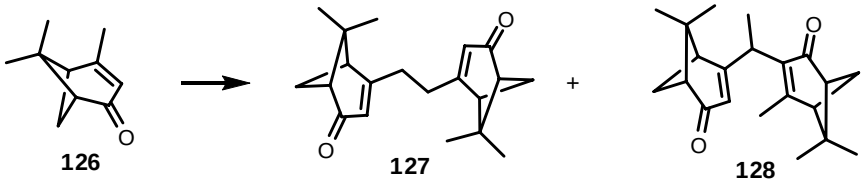

Oxidants	Yield
$CuCl_2$	**127**: 44% **128**: <5%
$FeCl_3$	**127**: 19% **128**: 13%

Conditions: LDA, oxidants, THF/HMPA, -78 °C

For the transformation we wanted to achieve, oxidative dimerization of compound **122** to product the γ,γ-coupling dimer, we were facing several challenges. In addition to the regioselectivity metioned above, we also needed to achieve the diastereo-selectivity since two new chiral centers were going to be created in the process.

Bearing in mind the above concerns the oxidative dimerization of **122** was attempted. The THF solution of **122** at −78 °C was treated with freshly prepared LDA, the dark brown solution was stirred at −78 °C for 30 minutes before adding a DMF solution of $CuCl_2$. No dimers or any identifiable products were isolated from the reaction. Then the stability of the lithium dienolate was tested. Instead of adding oxidants, acetic acid was added to quench the reaction after the LDA treatment. No starting material was recovered from the reaction; only decomposition was observed.

This instability could be due to the electron-withdrawing nature of the Boc protecting group. As shown in Scheme 3.7, there are two potential pathways. Further reactions among these products (**129-131**) are very likely, such as: cycloaddition or polymerization. This presumption is also supported by the similar behavior of Teoc-monomer and SEM-pyrrole monomer **150** for the KHMDS treatment. In SEM-pyrrole monomer **150** case, a small percentage of compound **132** was isolated.

Scheme 3.7

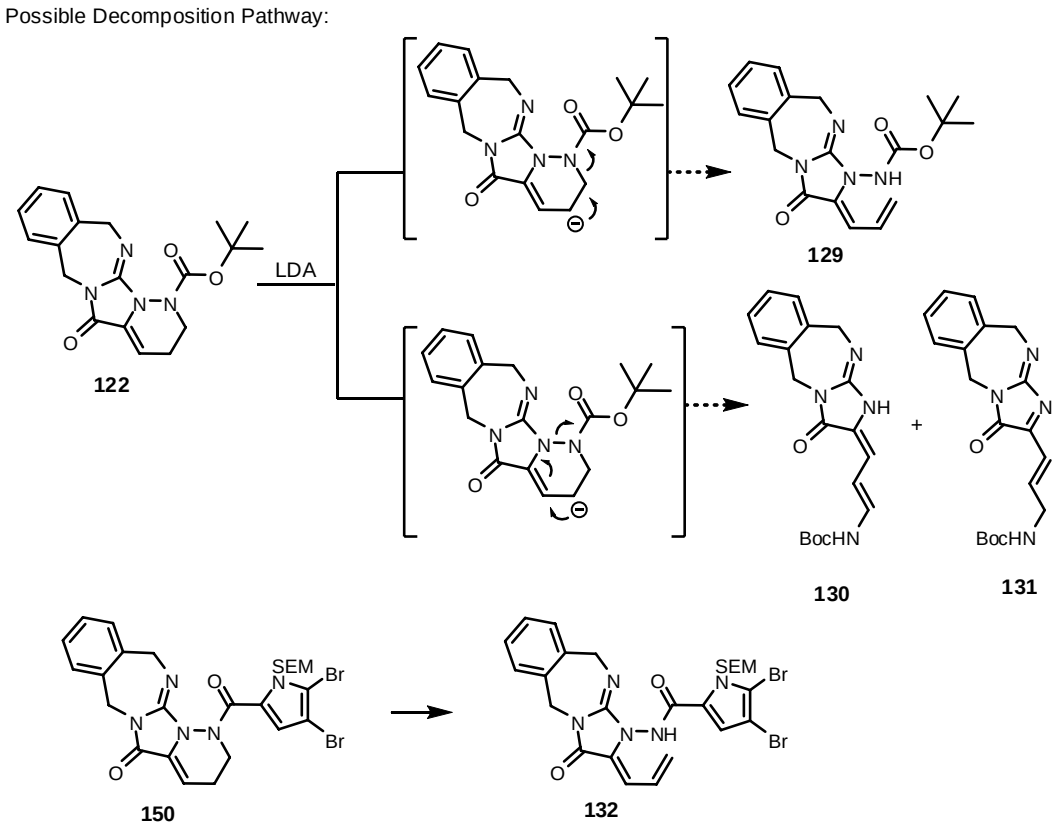

3.3 Allyl-Monomer Synthesis

We next turned our attention to electron-donating protecting groups on the nitrogen. The allyl- protecting group was eventually chosen. We intended to take advantage of Noyori's asymmetric isomerization of allylic amines[15] to achieve an enantioselective synthesis of the natural product (Scheme 3.8).

Scheme 3.8

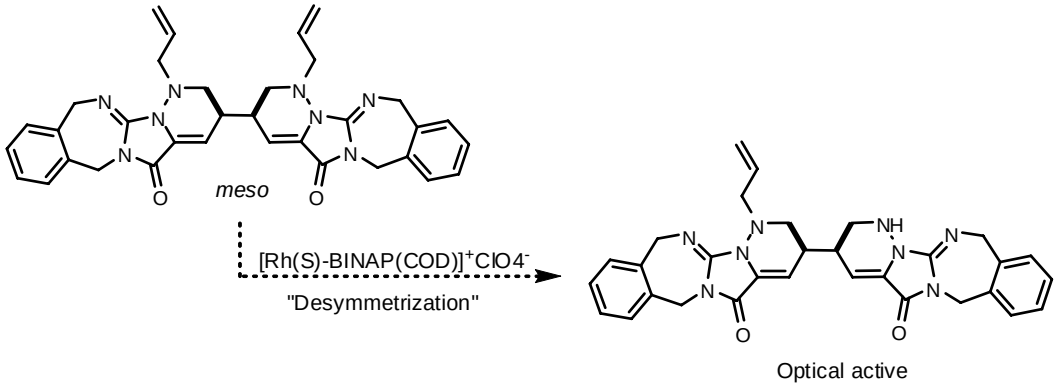

The synthesis of the allyl monomer **135** started with allylation of compound **117** with allyl bromide (Scheme 3.9). The resultant ester was saponified and condensed with **77**. Unlike the Boc monomer synthesis, the adduct **134** could be induced to cyclize in situ by concentrating the reaction mixture at 70 °C under vacuum, without isolating isothiourea **134** and the mercuric salt treatment. The target N-amino glycocyamidine **135** was generated via net extrusion of methyl mercaptan.

Scheme 3.9

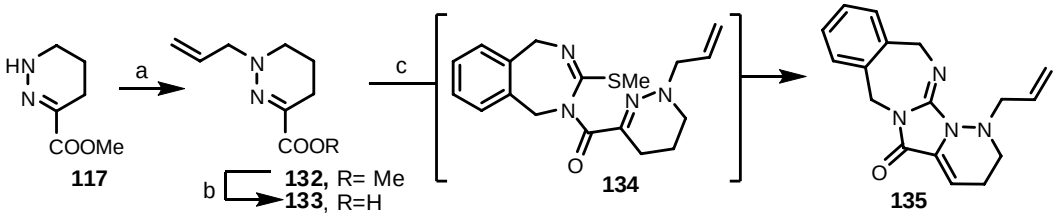

Conditions: a) KHMDS (1.1 eq), allyl bromide (1.2 eq), THF,–35 °C, (90%); b) LiOH (1.5 eq), THF/MeOH/H_2O (2:1:1); aq citric acid (> 95%); c) **77** (1.1 eq), TBTU (1 eq), DIPEA (3 eq), DMF, then concentrate in vacuo at 70 °C (72%).

3.4 Allyl-Monomer's Potassium Enolate Dimerization Study

With **135** in hand, the conventional enolate oxidation chemistry was reexamined. First, its stability toward the basic conditions was tested. The KHMDS solution was added to the THF solution of **135** at −78 °C. The resultant red brown solution was stirred at −78 °C for half an hour and then quenched with deuterated acetic acid. The starting material was recovered from the reaction in good yield and deuterium was incorporated at the γ position.

Encouraged by the stability of the dienolate, its behaviors toward different oxidants were studied next. Iodine was tested first. Under strict deoxygenated and anhydrous conditions, the stock solution of half equivalent iodine in THF was added to the dienolate solution at −78 °C. The yellow solution was continually stirred at −78 °C for another hour. The reaction afforded two regio-isomers (Scheme 3.10, entry 1). The α,α regio-isomer **137** was isolated in 50% yield as a single *d.l* diastereoisomer, which was established by X-ray crystallography (Figure 3.1). The α,γ regio-isomers **136** were isolated in 24% yield. A single crystal of one of the diastereoisomers was also obtained from a dilute acetonitrile solution (Figure 3.1).

Figure 3.1

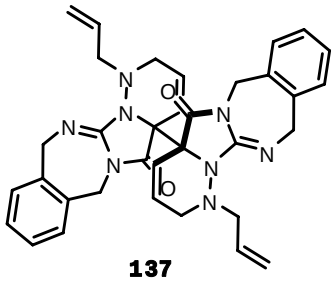

137

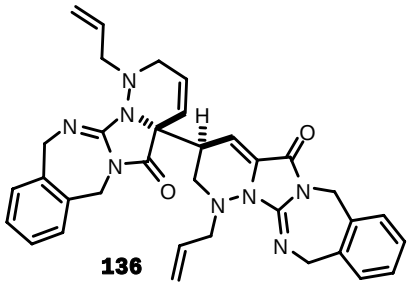

136

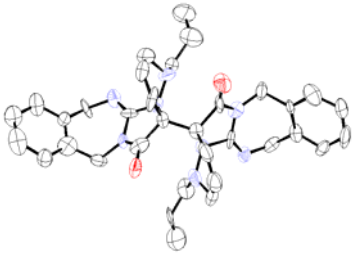

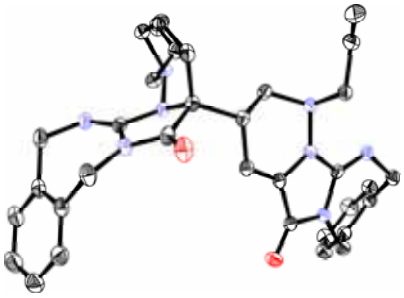

Unfortunately, no desired γ, γ regio-isomer **138** was detected from the reaction. It was rationalized that the reactive intermediates in this reaction have more carbon centered radical character[16]. The α position was stabilized by a neighboring heteroatom, an electron-withdrawing carbonyl group and a double bond. Under kinetic conditions[17], the most sterically hindered α,α regio-isomer **127** was formed quickly and isolated as major product. Since the reaction was not in equilibrium, the thermodynamic product γ,γ regio-isomer **138** was not observed from the reaction.

Next, I turned my attention to the Fe (III) oxidants. The DMF complex of ferric chloride was employed. Compared to normal Fe (III) salts, the DMF complex of ferric chloride has the advantages of being non-hygroscopic, and good solubilities in organic solvents, such as: DMF or THF[18]. The oxidative dimerization reaction was executed under similar conditions as in the I_2 case. And under these conditions, the reaction favored the formation of the α,γ regio-isomer **136**. It was isolated in 55%, together with the α,α regio-isomer **137** in 11% and γ,γ **138** in 11% (Scheme 3.10, entry 2).

The next oxidant screened was copper triflate. It was added to the reaction as a fine suspension in THF. And in this case, the α,α regio-isomer **137** was isolated in 24%, α, γ regio-isomer **136** in 37% and γ, γ regio-isomer **138** in 25%. Even though the regio-selectivity for the γ,γ dimers **138** is the best compared to the results of the other oxidants, it is still not synthetically useful because of the low yield. A lot other oxidants were screened also, including: silver nitrate[19], [Cu(*S*,*S*)-tert-butylbis(oxazolinyl)]Cl_2[20], ferrocenium hexafluorophosphate[21], Copper (II) benzylacetonate and tris(4-bromophenyl)aminium hexachloroantimonate, however none of them provided better selectivity than copper triflate.

Scheme 3.10

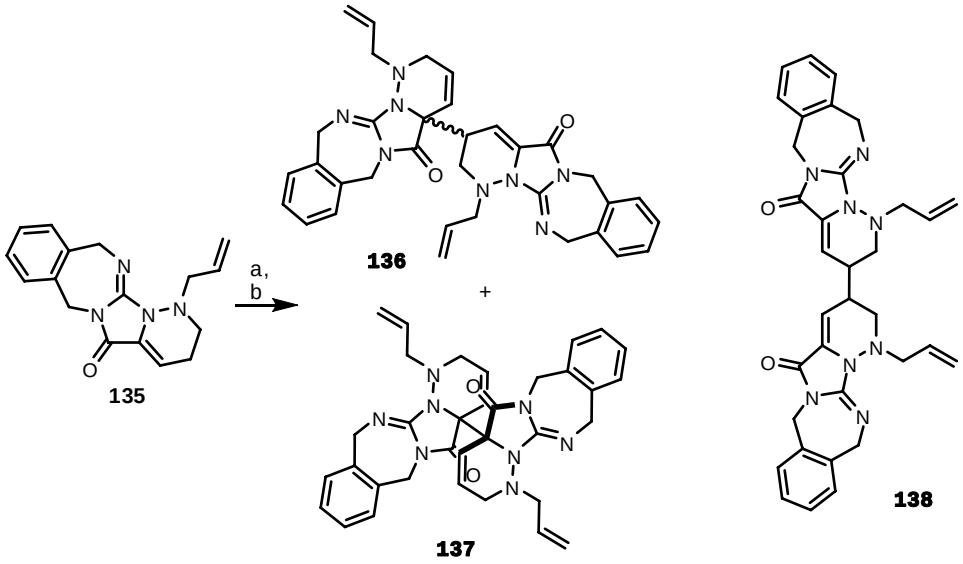

Conditions: a) KHMDS (1.05 eq), degassed THF, –78 °C, 0.5 h; b) oxidants (see table below), 1 h, –78 °C.

entry	oxidants	αυ : αα : γγ	combined yield(%)
1	I_2	1.0 : 2.0 : --	71
2	$[Fe(DMF)_3Cl_2][FeCl_4]$	5.4 : 1.0 : 1.0	77
3	$Cu(OTf)_2$	1.5 : 1.0 : 1.0	86

3.5 The Thermal and Photolytic Properties of the Allyl-Dimers

I next explored the possibility of regenerating the radical intermediate from the "wrong" regio-isomer **136** and **137**. Theoretically, the reaction should afford the most stable products **138** under thermodynamic conditions.

I first investigated the thermal properties of the two regio-isomers. When the α,α isomer **137** was heated in toluene at 95 °C, it converted to the α,γ isomers **136** in 2.5 hours, however no γ,γ regio-isomer **138** was detected from the reaction. Since none of the desired regioisomer **138** was detected, the α,γ regioisomer was

further resubjected to thermal conditions to see if there would be a second net [1,3] sigmatropic rearrangement to yield the γ,γ regioisomer. Unfortunately major decompositions occurred, when the isomers of **136** were heated up in various solvents. In several cases, very small amounts of monomer were recovered from the reaction.

Then photolytic conditions were examined. The acetonitrile solution of the α,γ isomers **136** was proven inert at 300 nm and 350 nm even after prolonged irradiation. The α,γ isomers **136** decomposed when they were exposed to 250 nm. However the α,α isomer **137** rearranged to the α,γ regio-isomers **136** and γ,γ isomers **138** at 250 nm (Scheme 3.11). As a control experiment, one reaction was wrapped with aluminum-foil and set up under the identical reaction conditions as others. After exposure to UV light for the same amount time, the starting material of the control experiment was left intact while the starting material of other reactions was consumed completely. This indicated that the reaction was initiated by light and not heat.

Under optimal reaction conditions, 0.01 M solution of α,α dimer **137** in benzene was deoxygenated via freeze-pump-thaw method (Scheme 3.11). It was irradiated at 250 nm for two hours before the reaction went to completion. At the end of the reaction, **136** was isolated in 36% yield and the desired isomer **138** was isolated in 20%. Even though the results are interesting, the chemistry is not synthetically useful to generate compound **138**.

Scheme 3.11

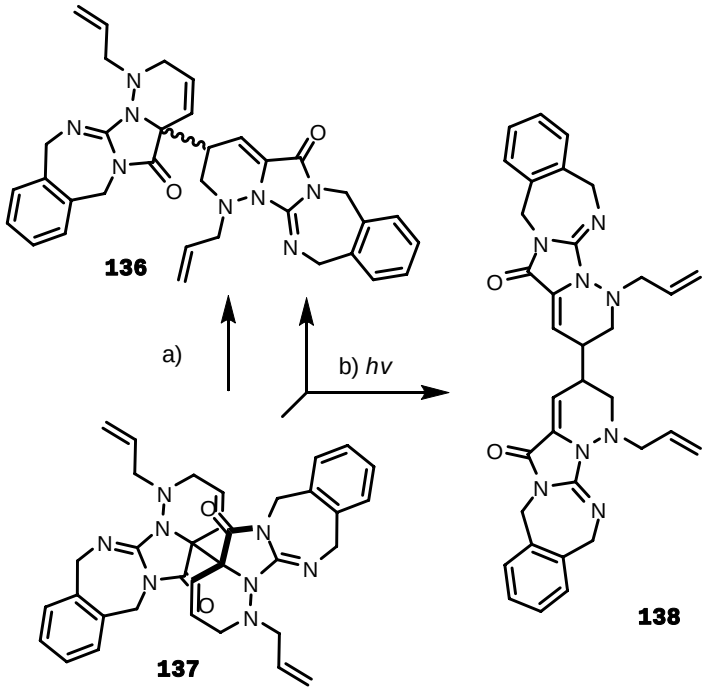

a) deoxygenated toluene (0.02 M), 95 °C, 1 h (81%). b) *hv* (Rayonet-254 nm bulb set), in deoxygenated PhH (0.01 M), 2 h (36% **136**, 20% **138**)

3.6 Allyl-Monomer's Titanocene Enolate Dimerization Study

In many cases, the counter-ions of the corresponding enolates play a big role for the outcomes of the chemistry[20]. In our case, we were especially interested in the generation of the monomer's titanocene dienolate. It should be readily generated from the potassium enolate by transmetallation due to the high oxophilicity of Ti (IV). The bulkiness of titanocene would make the α position of the dienolate sterically hindered. If the carbon-carbon bond formation occurred before the breakage of the titanium oxygen bond[23], the desired regiochemistry could be achieved.

The yield of the desired regioisomers **138** was largely improved to 40% when the potassium dienolate was treated with an equivalent of Cp_2TiCl_2 prior to oxidation (Scheme 3.12). When $[i\text{-PrCp}]_2TiCl_2$ was used, the selectivity for **138** is essentially complete – region-iosmers **136** or **137** could no longer be detected in the crude reaction mixture. Further increase in the size of the substituents of cyclopentadiene, from the *i*-Pr to *t*-Bu, did not improve the results further but rather afforded lower selectivity for **138**, possibly due to the inefficient transmetallation step.

Scheme 3.12

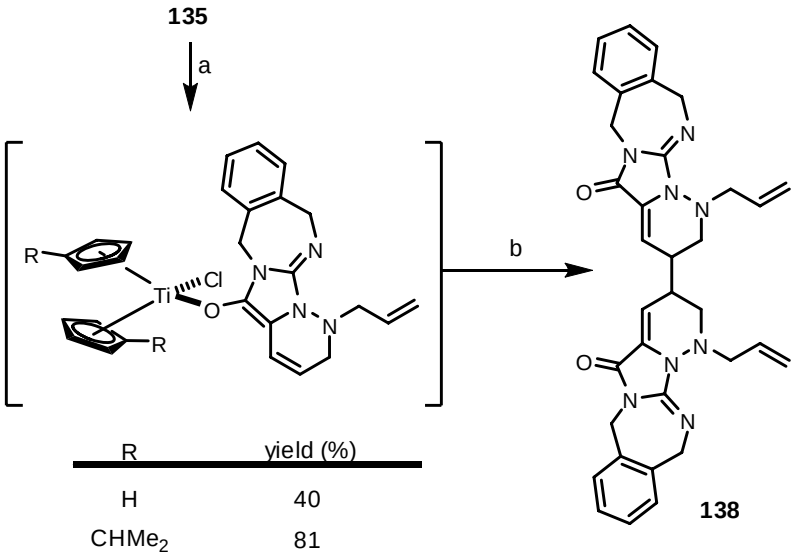

R	yield (%)
H	40
$CHMe_2$	81

Conditions: a). KHMDS (1.1 eq), THF, –78 °C, 30 min; $[R\text{-Cp}]_2TiCl_2$ (1.15 eq), –78 °C, 3 h; $Cu(OTf)_2$ (1.6 eq), –78 °C, 3.5 h.

3.7 The Determination of Diastereoisomers Ratio of 138

The regioisomers **138** were isolated as a diastereoisomeric mixture. Many solvent systems were used in an effort to separate them by chromatographic means, but without success. The *Chiralcel*® OD-H column from Chiral Technologies Inc was employed to separate the stereoisomeric the mixture of the γ, γ regioisomers **138**. Using *i*-propanol and hexanes as eluents, there were three peaks (Scheme 3.13). Presumably, the two similar size peaks belong to the two enantiomers of C_2.

By studying the ^{1}H NMR of **138** regioisomers obtained from the oxidative dimerization mediated by [*i*-PrCp]$_2$TiCl$_2$, there are two apparent singlets at 5.5 and 5.4 ppm with an integration ratio of 2:1 which were identified as the vinyl protons (Scheme 3.13). Combining the assumption that the two diastereoisomers have the same absorption coefficient at the wavelength used in the HPLC analysis and the integration data of the ^{1}H NMR, it is reasonable to determine the ratio between the *meso* and C_2 diastereoismer to be 2:1. Using the same method, the diastereoisomeric ratio was determined to be 1:1 in the potassium dienolate oxidation (Scheme 3.10, entry 3).

Scheme 3.13

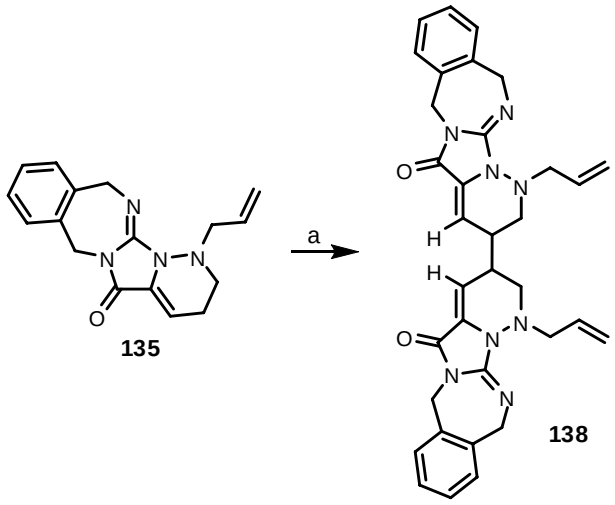

Conditions: a). KHMDS (1.1 eq), THF, –78 °C, 30 min; $[i\text{-Pr-Cp}]_2TiCl_2$ (1.15 eq), –78 °C, 3 h; $Cu(OTf)_2$ (1.6 eq), –78 °C, 3.5 h (81%).

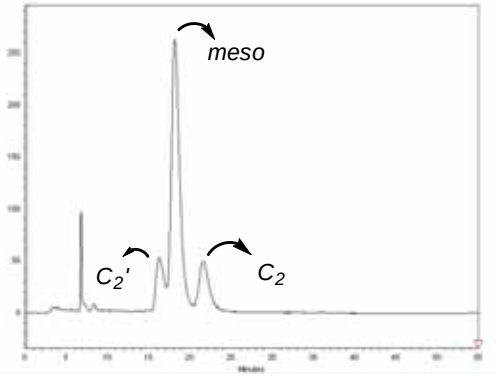

HPLC graph of γ, γ regioisomers using *Chiralcel* OD-H column

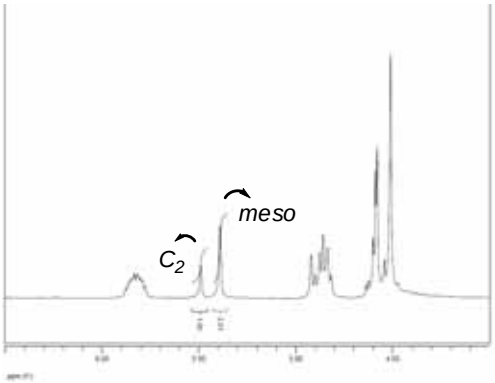

^{1}HNMR spectrum (4.0-6.5 ppm) of γ, γ regioisomers

3.8 The Synthesis of SEM Pyrrole Monomer 150

Previous studies showed that the potassium enolate of the monomers with an electron-withdrawing protecting group are not stable under the oxidative dimerization reaction conditions (Scheme 3.7). We solved this instablility issue by

switching to the monomer with an allyl protection group. Even though the dimerization of the allyl monomer was efficient, the desired regioselectivity was poor. And so, to our satisfaction, the regioselectivity problem was solved by the use of the allyl monomer's titanocene enolate.

Inspired by the efficient and regioselective dimerization of the allyl monomer's titanocene enolate, we thought that the titanocene enolates of the monomers with an electron-withdrawing group could be stable, unlike the potassium forms, considering the high bond energy between titanium and oxygen[24]. Moreover, as the acyl pyrrole motif was found in the natural product itself, direct dimerization of compound **150** is highly desired (Figure 3.2).

Figure 3.2

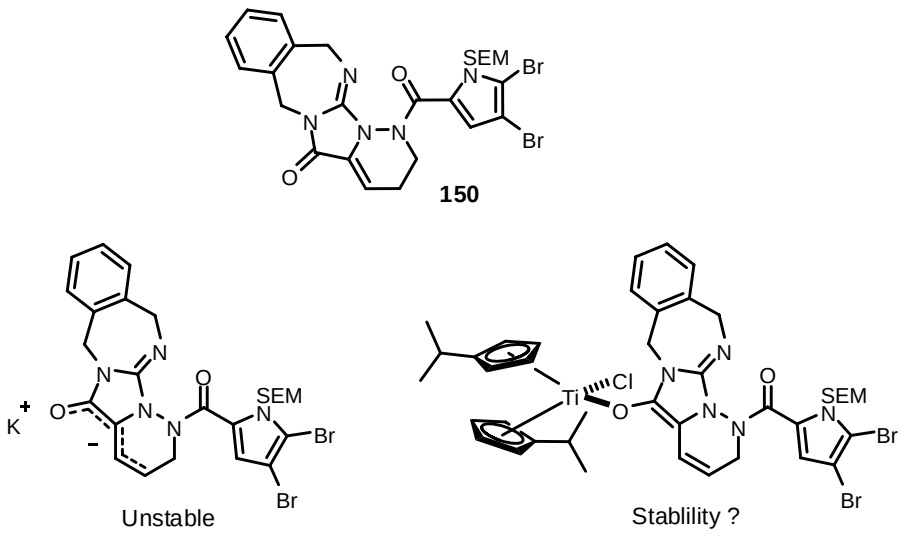

Nucleophilic substitution of ketone **139** with NaOEt affords ester (Scheme 3.14). The compound 140 was obtained after bromination and SEM protection. It was subsequently hydrolyzed to provide acid **142**.

Scheme 3.14

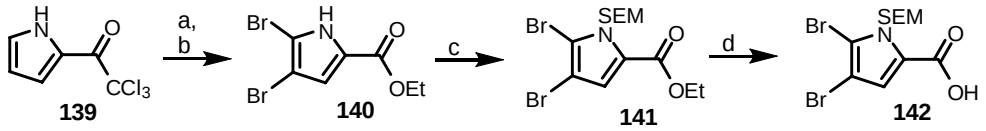

Conditions: a). NaOEt (12%), EtOH, rt, 10 min, (>95%); b). Br_2 (2 eq), AcOH, rt, 2 h, (>95%); c). Et_3N (1.1 eq), SEM-Cl (1.05 eq), THF, r t, 2h, (>95%); d). NaOH (2 eq), THF/H_2O/MeOH, 65 °C, 4 h, (>95%).

Compound **117** was acylated with acyl chloride **145**, which was generate by treating acid **142** with oxalyl chloride and catalytic DMF (Scheme 3.15). The ester was carefully hydrolyzed with LiOH at 0 °C to afford acid **147** in quantitative yield.

Scheme 3.15

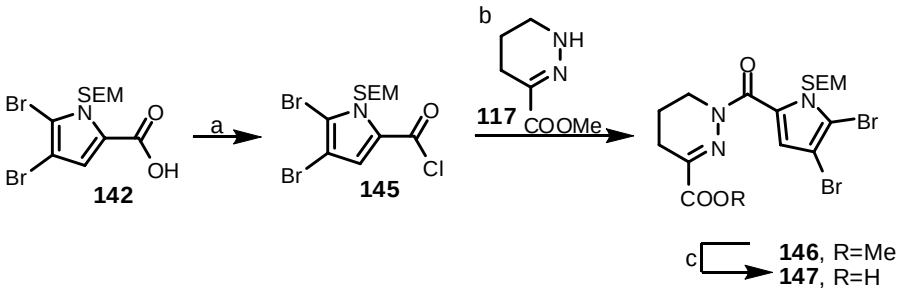

Conditions: a). $(COCl)_2$ (2 eq), DMF (0.1 ml), CH_2Cl_2, rt, 3 h, (> 95%); b). Pyr (2 eq), **117** (1.05 eq), DMAP (0.1 eq), CH_3CN, rt, 3 h, (> 95%). c), LiOH (1.1 eq), THF/H_2O, 0 °C, 2.5 h, (> 95%).

Then acid **147** was coupled with the HI salt of methylisothiourea **77**. The coupled product **148** was treated with $HgCl_2$ (Scheme 3.16). The reaction mixture

was heated in refluxing CH_3CN and the desired cyclized compound was obtained in 52% yield together with the side product **149**. When **149** was resubjected to the same $HgCl_2$ conditions, it smoothly converted to **150**. Thus the yield of this step was improved to 70% simply by increasing the amount of $HgCl_2$ utilized in the reaction.

One thing worthy of mentioning is that during the whole monomer synthesis, the yield of each step before the mercury chloride treatment is quantitative and no purification is needed. More impressively, the yield does not diminish when the reaction sequence is scaled up to over a hundred grams.

Scheme 3.16

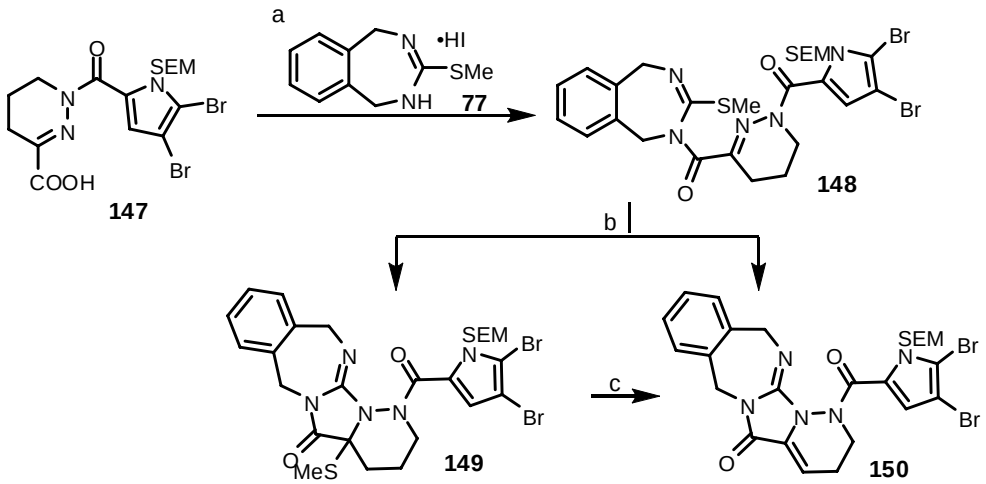

Conditions: a). **77** (1.05 eq), TBTU (1.1 eq), DIPEA (3 eq), DMF, rt, 3 h, (>95%); b). $HgCl_2$ (1 eq), Pyr (3 eq), CH_3CN, 85 °C, 3 h, **150** (52%), **149** (20%); c). indentical as b , **150** (72%)

3.9 The Dimerization Study of SEM Pyrrole Monomer 150

With an efficient monomer synthesis in hand, the oxidative dimerization was pursued promptly. Unlike in the case of the allyl monomer **135**, the

potassium enolate of **150** was not stable even at low temperature, so the transmetallation step was avoided. Instead, the titanocene enolate of **150** was directly generated from the reaction by premixing [*i*-PrCp]$_2$TiCl$_2$ and **150** before the KHMDS addition. After the oxidation step, the desired regioisomers were produced efficiently.

Fortunately, the diastereoisomers **151** and **152** can be separated from each other by column chromatography. Their stereochemistries were established based on the X-ray crystallography of a single crystal of *meso* form **151** (Figure 3.3).

Figure 3.3

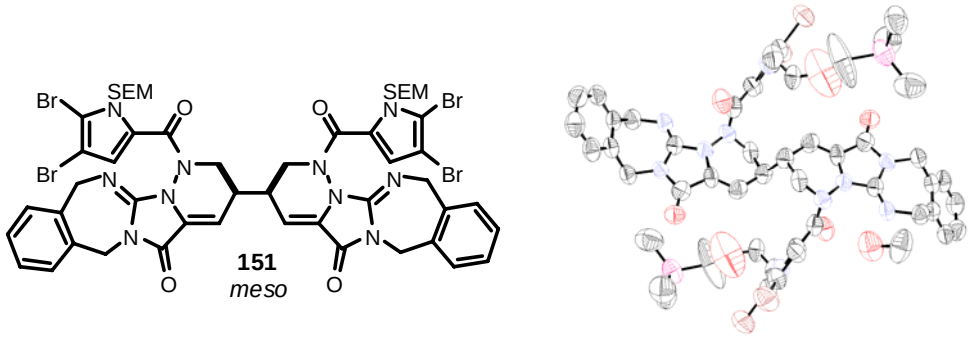

The diastereoselectivity was achieved by employing different oxidizing reagents. The oxidation reaction using Cu(OTf)$_2$ as an oxidant is selective for the *meso* isomer **151**, while the one using [Fe(DMF)$_3$Cl$_2$][FeCl$_4$] is selective for C_2 isomer **152** with a better ratio (Scheme 3.17). The ability to attain the selectivity at this step is very important for our ultimate goal, which is not only to achieve the synthesis of palau'amine **11** but also the syntheses of styloguanidine **33**,

axinellamine **12** and massadine **13**. Also considering the recent revisions of palau'amine's stereochemisty, it offers a good opportunity to access both proposed structures. The slightly diminished yield of this dimerization is due to the competitive formation of α,γ dimers. In each case, the α,γ dimers were isolated in 13-15% and the structure was verified via X-ray crystallography (Scheme 3.17).

Scheme 3.17

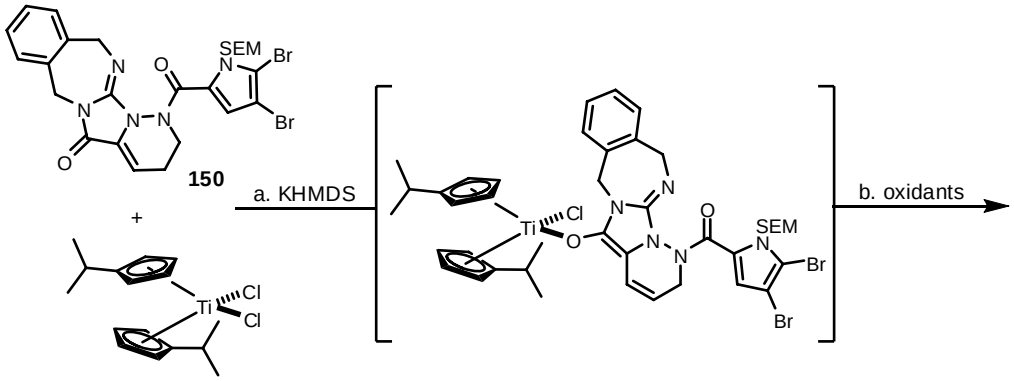

entry	oxidant	**151** : **152**	combined yield (%)
1	$Cu(OTf)_2$	3.3:1	70%
2	$[Fe(DMF)_3Cl_2][FeCl_4]$	1:5	60%

Conditions: a). [*i*-PrCp]$_2$TiCl$_2$ (1.05 eq), KHMDS (1.1 eq), THF, –78 °C, 1.5h. b). oxidants (1.5 eq), –78 °C, 3h, **153** (13-15% in each case)

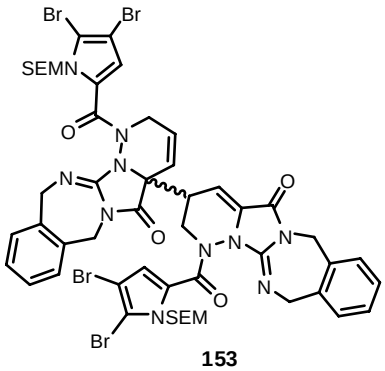

153

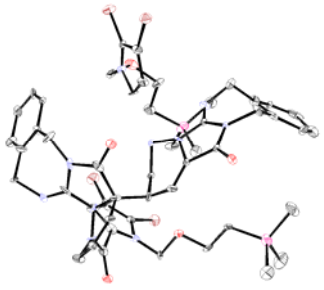

3.10 Experimental Section

3.10.1 Materials and Methods

Unless stated otherwise, reactions were performed under an argon atmosphere in flame-dried glassware. Tetrahydrofuran (THF), dichloromethane (CH_2Cl_2), diethyl ether (Et_2O), toluene (C_7H_8), benzene (C_6H_6) and acetonitrile (CH_3CN) were passed through Glass Contour solvent drying systems prior to use. Fine chemical reagents were obtained from commercial sources and used without further purification. Column chromatography was performed on E. Merck silica gel 60 (240-400 mesh). Thin layer chromatography and preparative layer chromatography utilized pre-coated plates from E. Merck (silica gel 60 PF254, 0.25mm or 0.5mm). Nuclear Magnetic Resonance (NMR) spectra were recorded on either a Varian Inova-600, Inova-400 or Mercury-300 magnetic resonance spectrometer. ^1H NMR chemical shifts are given in parts per million (δ) relative to a residual solvent signal. Infrared spectra were recorded on a Perkin-Elmer FT-IR spectrum 1000 using samples prepared as thin films between salt plates. Electrospray-ionization mass spectra (LRMS) were measured on a Shimadzu LCMS-2010 single quadrupole.

3.10.2 Preparative Procedures

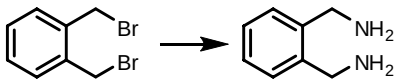

106 **107**

***o*-Xylylene diamine (107).** To a solution of *o*-xylylene dibromide (Aldrich – 100 g, 378 mmol) in THF (1.3 L), EtOH (1 L) and H2O (0.33 L) was added NaN_3 (53.7 g, 826 mmol) in H2O (0.33 L). The solution was heated at reflux for 1 h. After cooling to rt, PPh_3 (248 g, 947 mmol) was added in small portions. When the evolution of N_2 (g) ceased, the solution was heated at reflux for 2h. Upon cooling to rt and standing overnight, needle shaped crystals had formed, which partially dissolved with the addition of 100 mL H_2O. Solid NaOH was added to the aqueous solution until a pink oily layer appeared. The organic layer was separated and the aqueous layer was extracted with Et_2O (2 × 50 mL). The combined organic layers were dried over Na_2SO4, filtered and concentrated *in vacuo*. The slightly pink oil obtained was used without further purification.

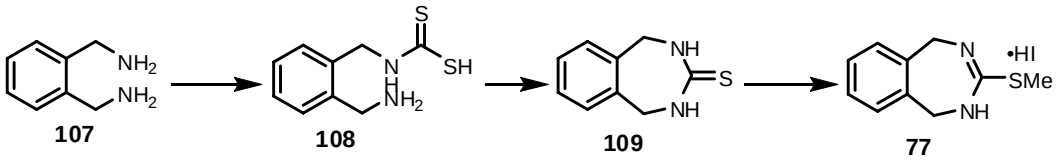

107 108 109 77

2, 5-Dihydro-3-(methylthio)-1*H*-2,4-benzodiazepine Hydroiodide (77). The compound was synthesis as the procedure in Ref 1.

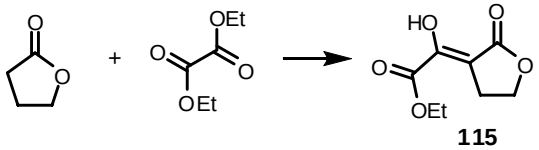

115

α-Ethoxalybutyrolactone (115). EtOH used in this reation was refluxed and distilled from magnesium turnings. The compound was synthesized as the procedure in Ref 2 (b), without modification.

Methyl 5-bromo-2-oxopentanoate (116). A solution of lactone **115** in 30% HBr/AcOH (150 mL) was heated at 110°C for 2h. An additional 100 mL of 30% HBr/HOAc was added and the reaction maintained at 110°C for 14h. The mixture was concentrated *in vacuo* to afford a brown oil that was dissolved in 250 mL MeOH. Concentrated aqueous H_2SO_4 (0.5 mL) was added and the solution stirred at rt for 14h. The reaction was concentrated and the incipient residue dissolved in Et_2O. Saturated aqueous $NaHCO_3$ was carefully added until gas evolution ceased. The organic layer was separated and washed with H2O and dried over Na_2SO_4. Concentration *in vacuo* provided a brown oil that was used without further purification.

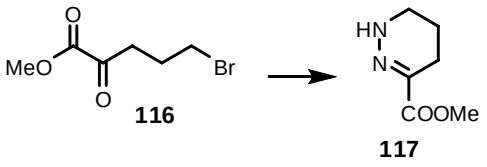

Methyl-1,4,5,6-tetrahydro-3-pyridazinecarboxylate (117). Hydrazine hydrate (20.4 g, 398 mmol) was dissolved in a mixture of MeOH (300 mL) and water

(37.5 mL). Glacial AcOH (7 mL) was added and the solution cooled in an ice-bath. A solution of crude **116** in MeOH (50 mL) was added over 30 min wherein a white precipitate formed. The ice-bath was removed wherein the solids dissolved. The pH of the mixture was maintained between 4 and 7 with 3M aq K2CO3. After the pH had stabilized at rt, the reaction was immersed into an oil-bath pre-heated to 60 °C and 3M aq K_2CO_3 was used to adjust the pH to ~5. The reaction was heated at 60 °C for 1 h at which time the pH was 6. After removing MeOH *in vacuo*, the residue was dissolved in a minimum amount of water and extracted with EtOAc. The organic layer was dried over Na_2SO_4, filtered and concentrated to afford a solid that was recrystallized from EtOAc to afford **117** (42.5 g, 81%).

117: colorless crystals [m.p. 72 °C]; Rf = 0.5 (2:3 EtOAc/CH_2Cl_2); IR (film): 3200, 2957, 1694, 1588, 1442, 1303, 1237, 1190, 115, 972, 743 cm-1; 1H NMR (400 MHz, $CDCl_3$): δ 5.1-5.9 (bs, 1H), 3.78 (s, 3H), 3.23 (t, 2H, *J* = 5.2 Hz), 2.45 (t, 2H, *J* = 6.8 Hz,), 1.90 (m, 2H); 13C NMR (75 MHz, CDCl3): δ 165.8, 132.0, 52.1, 41.9, 21.2, 17.6. MS (positive electrospray) calc'd for $(C6H10N2O2+H)^+$: 143.07, found: 143.06.

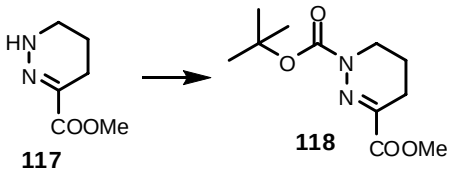

1-tert-butyl 3-methyl 5,6-dihydropyridazine-1,3(4H)-dicarboxylate (118). A solution of Methyl ester **117** (5 g, 35.2 mmol) in THF (80 mL) was cooled to 0 °C. Pyridine (3.2 mL, 40 mmol) and DMAP (0.86 g, 7 mmol) were added, followed by $(Boc)_2O$ (1M, 38.7 mL). The resulting solution was stirred at room temperature overnight. Volatiles were removed in vacuo and the residue dissolved in EtOAc, washed with water and brine, dried over Na_2SO_4. Concentration in vacuo followed by flash chromatography on silica gel (EtOAc/Hexanes, 3:7) afford **118** (7.88 g, 92%) as white solid.

118: colorless solid; R_f = 0.8 ($EtOAc/CH_2Cl_2$ = 2:3); IR (film, cm^{-1}): 2358, 2088, 1698, 1644, 1446, 1367, 1280, 1149, 1069, 971; ^1H NMR (300 MHz, $CDCl_3$): δ 3.80 (s, 3H), 3.67 (m, 2H), 2.46 (t, 2H, *J* = 6.5 Hz), 1.87 (m, 2H), 1.52 (s, 9H); ^{13}C NMR (75 MHz, $CDCl_3$): δ165.0, 139.8, 82.9, 52.7, 41.7, 28.3, 21.8, 17.1; MS (positive electrospray) calcd for $(C_{11}H_{18}N_2O_4+H)^+$: 243.13, found: 243.30.

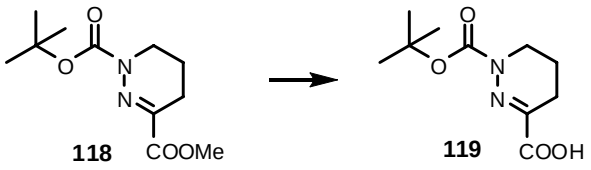

1-(tert-butoxycarbonyl)-1,4,5,6-tetrahydropyridazine-3-carboxylic acid (119). Aqueous solution (12 mL) of LiOH (1.43 g, 34.17 mmol) was added to solution of **118** (7.88 g, 32.54 mmol) in THF (100 mL). The resultant solution was stirred at rt for 0.5 hour. The reaction was quenched by citric acid. The organic solvent

was removed. The residue was taken up in ethyl acetate and washed with water and brine, died over Na_2SO_4. The solvent was removed and the resultant oil was used directly for the next step.

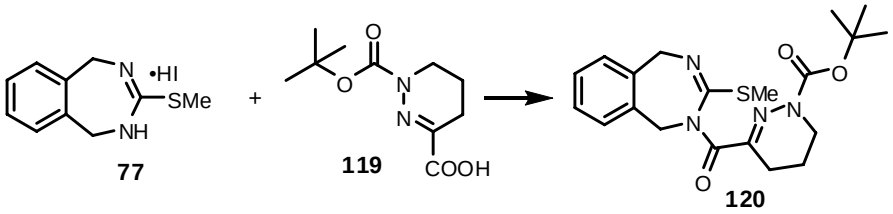

(E)-tert-butyl 3-(3-(methylthio)-2,5-dihydro-1H-benzo[e][1,3]diazepine-2-carbonyl)-5,6-dihydropyridazine-1(4H)-carboxylate (120). HI salt **77** (0.677 g, 3.52 mmol) was added to the DMF (16.8 mL) solution of acid **119** (0.77 g, 3.36 mmol) cooling in ice-bath, followed by HATU (1.4 g, 3.7 mmol). DIPEA (0.70 mL, 4.03 mmol) was added slowly to the above yellow solution. The reaction was stirred at rt for 3 hours before the TLC indicating the completion of the reaction. The reaction mixture was diluted with EtOAc and washed with sat. NH_4Cl, water, brine and dried over Na_2SO_4. The solvent was removed and the residue was purified by the second silica gel column chromatography (EtOAc:Hex = 2:8) (1 g, 74%)

120: white foam; R_f = 0.8 (EtOAc/hex, 1:1); IR (film, cm^{-1})1645, 1416, 1333, 1241, 1127; ^1H NMR (400 MHz, CD_3CN): δ 7.01-7.38 (m, 4H), 4.93 (s, 2H), 4.87 (s, 2H), 3.68 (m, 2H), 2.51 (m, 2H), 1.90 (m, 2H), 1.56 (s, 9H), ^{13}C NMR (75 MHz, CD_3CN): δ 134.8, 134.5, 129.5, 128.0, 127.6, 127.1, , 81.6, 55.2, 45.5,

41.4, 27.8, 22.4, 17.1, 14.6; MS (positive electrospray) calcd for $(C_{20}H_{26}N_4O_3S+H)^+$: 403.17, found: 403.40.

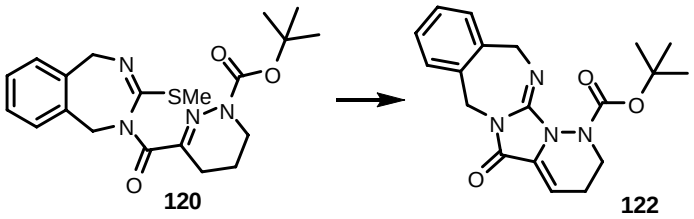

Boc-Monomer (122). The reaction mixture of **120** (3.52 g, 8.74 mmol) and $HgCl_2$ (2.61 g, 9.62 mmol) in pyridine (43 mL) was heated to 120 °C for 3 hours. The white solid was filtered and the solvent was removed in vacuo. The reaction mixture was taken up in EtOAc. The organic layer was washed with 1N NaOH solution, water, brine and dried over $NaSO_4$. After the solvent removal in vacuo the residue was purified by silica gel column chromatography (CH_3CN:$CHCl_3$ = 1:19) to afford white foam (2.3 g, 75%).

122: white foam; R_f = 0.2 (ETOAC/hex, 1:1); IR (film, cm^{-1}): 2978, 1691, 1454, 1402, 1309, 1246, 1155, 1015, 845, 734; ^1H NMR (400 MHz, CD_3CN): δ 6.93-7.78 (m, 4H), 5.70 (t, 2H, *J* = 4.6 Hz), 4.95 (s, 2H), 4.69 (appr s, 2H), 4.21 (appr s, 1H), 2.88 (appr s, 1H), 2.23 (appr s, 2H), 1.30 (s, 9H); ^{13}C NMR (75 MHz, CD_3CN): δ 160.0, 156.7, 142.4, 135.6, 129.8, 129.5, 129.4, 129.0, 103.9, 83.3, 49.8, 43.9, 28.2, 22.6; MS (positive electrospray) calcd for $(C_{19}H_{22}N_4O_3+H)^+$: 355.17, found: 355.30.

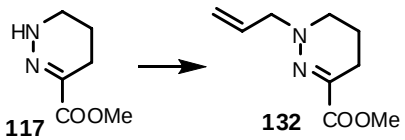

A solution of **117** (5.2 g, 35.9 mmol) in THF (180 mL) was cooled to −30 °C. KHMDS (0.5 M in toluene, 73.3 mL) was added over 5 min. The reaction was stirred for 10 min before adding allyl bromide (3.8 mL, 43.2 mmol). The reaction was stirred at −25 °C for 1h, quenched with MeOH, warmed to rt, and filtered through a pad of Celite. Concentration *in vacuo* followed by flash chromatography on silica gel (3:7 EtOAc/hexanes) afforded **132** (5.88 g, 90%) as colorless solid.

132: R_f= 0.5 (1:1 EtOAc/Hexanes); IR (film): 3079, 2925, 2844, 1700, 1562, 1439, 1261, 1108, 983, 744 cm-1; 1H NMR (400 MHz, CDCl3): δ 5.84 (m, 1H), 5.21 (tdd, 2H, *J* = 6.2, 10.1, 16.5 Hz), 4.99 (m, 2H), 3.78 (s, 3H), 3.06 (m, 2H), 2.39 (t, 2H, *J* = 6.7 Hz), 1.89 (m, 2H); 13C NMR (75 MHz, CDCl3): δ 132.5, 117.2, 60.3, 43.6, 19.3, 16.6. MS (positive electrospray) calcd for $(C9H14N2O2+H)^+$: 183.11, found: 183.11.

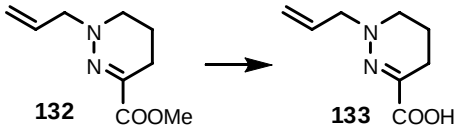

1-Allyl-1,4,5,6-tetrahydro-3-pyridazinecarboxylic acid (133). Solid LiOH (0.78 g, 32.7 mmol) was added to a solution of ester **132** (5.4 g, 29.7 mmol) in THF/MeOH/H2O (40 mL/15 mL/20 mL). The resultant solution was stirred at rt for 3h and then neutralized with 10% aq citric acid. The solvents were removed *in vacuo* and the residue dissolved in EtOAc. The solution was washed with H_2O and brine, dried over Na_2SO_4, filtered and concentrated. The crude acid was used in the next step without purification.

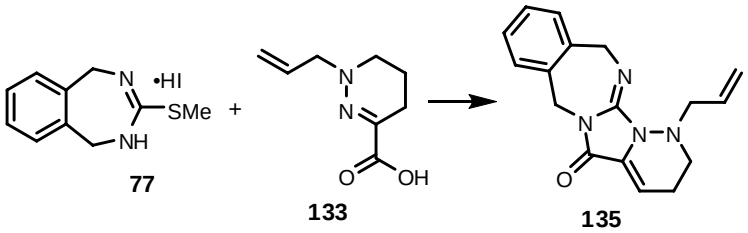

TBTU (0.27 g, 0.84 mmol) was added to a solution of **133** (0.14 g, 0.94 mmol) and **77** (0.3 g, 0.94mmol) in DMF (4.5 mL). DIPEA(0.44 mL, 2.51 mmol) was added and the resultant yellow solution stirred at rt for 2 h. The mixture was placed under house vacuum and heated at 70 °C overnight. The residue was dissolved in 20 mL EtOAc and washed with saturated $NaHCO_3$, water and brine. The organic layer was dried over Na2SO4, filtered and concentrated *in vacuo*. Purification by silica gel chromatography (4:1 EtOAc/hexanes) provided **135** (0.173 g, 71%) as a light brown solid.

135: Rf = 0.45 (2:3 EtOAc/CH_2Cl_2); IR (film): 3411, 2947, 1734, 1620, 1451, 1409, 1180, 1013, 761, 667 cm-1; ^{1}H NMR (500 MHz, DMSO-*d6*): δ 7.25-7.40 (4H, m), 5.87 (tdd, 1H, *J* = 6.7, 10.2, 17 Hz), 5.7 (t, 1H, *J* = 4.6Hz), 5.20 (d, 1H, *J* = 17.2Hz), 5.11 (d, 1H, *J* = 10.1Hz), 4.94, (s, 2H), 4.65 (s, 2H), 3.33 (d, 2H, *J* = 6.6Hz), 2.92 (t, 2H, *J* = 5.5Hz), 2.21 (dd, 2H, *J* = 5.3, 10.3Hz); ^{13}C NMR (125 MHz, DMSO*d6*):δ 158.8, 141.0, 140.1, 134.2, 133.6, 128.3, 128.0, 127.9, 127.5, 127.1, 118.7, 101.7, 56.0, 48.2, 44.8, 42.2, 16.2. MS (positive electrospray) calcd for $(C17H18N4O+H)^+$: 295.15, found: 295.10.

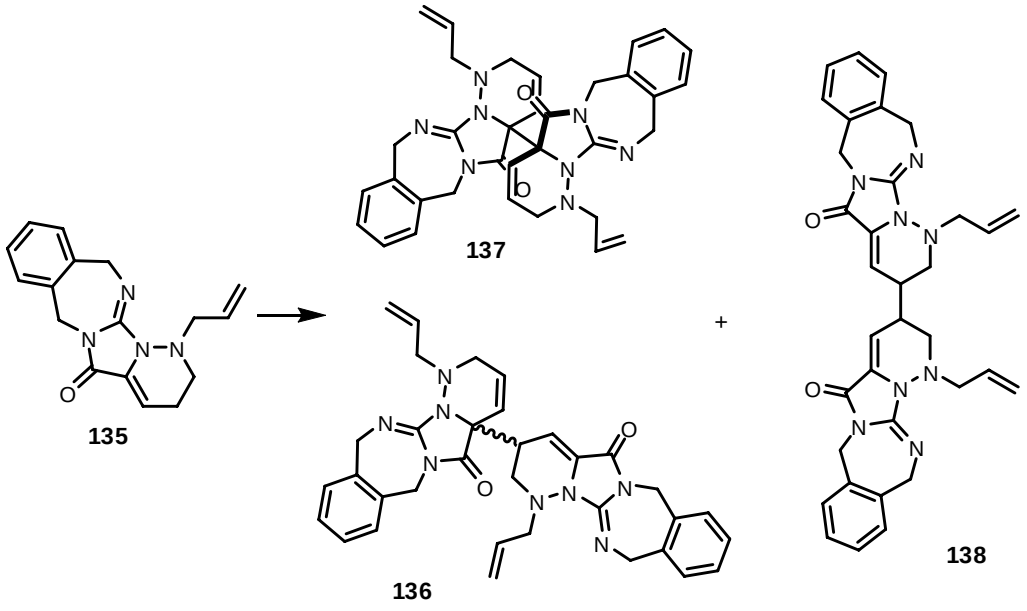

The dimerization reactions of allyl monomer (135)

Procedure A. I2 as oxidant

The THF used in this reaction was degassed via the freeze-pump-thaw method prior to use. Monomer **135** (1.03 g, 3.51 mmol) was dissolved in THF (10 mL) and cooled to −78 °C. This solution was added via cannulating needle to a flask containing KHMDS (7.38 mL, 0.5M in toluene) at −78 °C and the resulting dark red mixture was stirred at −78 °C for 30 minutes. A solution of I_2 (0.445 g, 1.76 mmol) in THF (0.5 mL) was then added and the reaction was stirred at −78 °C for 3 h. The solvent was removed *in vacuo* and the residue purified by silica gel chromatography (4:1 EtOAc/hexanes) to afford 485 mg

(47%) of α,α dimer **137** and 250 mg (24%) of α,γ dimers **136**.

137: light pink solid; R_f= 0.75 (EtOAc); IR (film): 3412, 1743, 1671, 1394, 1371, 1287, 1154, 1064, 968, 741, 667 cm-1; 1H NMR (400 MHz, DMSO-*d6*) δ 7.29 (m, 8H), 5.97 (dd, 2H, *J* = 4.0, 9.9Hz), 5.79 (d, 2H, *J* = 9.9Hz), 5.62 (tdd, 2H, *J* = 6.2, 10.3, 12.3 Hz), 5.07 (d, 2H, *J* =17.2Hz), 4.92 (d, 2H, *J* = 10.3Hz), 4.67 (m, 8H), 3.80 (d, 4H, *J* = 5.8Hz), 3.50 (d, 2H, *J* = 16.8Hz), 2.87 (ddd, 2H, *J* = 1.3, 5, 16.6Hz). MS (Positive electrospray) for (C34H34N8O2+H)+ calcd: 587.28, found: 587.25.

α,γ dimers **136**: yellow solid; Rf = 0.3 (EtOAc). Two diastereomers of this material were separated by preparative thin layer chromatography (1:19 MeOH/PhH).

Diastereomer 1: yellow crystals, Rf = 0.65 (1:19 MeOH/PhH), IR (film): 3640, 2980, 1739, 1675, 1413, 1150, 820, 740. 558 cm-1; 1H NMR (400 MHz,CD_3CN):

δ 7.22-7.40 (m, 8H), 6.05 (ddd, 1H, *J* =1.4, 5.2, 9.9 Hz), 5.85 (m, 2H), 5.68 (dddd, 1H, *J* = 5.5, 7.2, 10.2, 17.4 Hz), 5.42 (t, 1H, *J* = 1.7Hz), 5.13 (m, 3H), 4.91 (s, 2H), 4.88 (m, 1H), 4.81 (s, 2H), 4.61 (m, 4H), 3.99 (tdd, 1H, *J* = 1.5, 5.3, 13.8 Hz), 3.78 (dd, 1H, *J* = 7.2, 13.8Hz), 3.63 (m, 1H), 3.48 (dd, 1H, *J* = 5.0, 13.2Hz), 3.25 (m, 3H), 3.11 (ddd, 1H, *J* = 2.4, 5.0, 10.5Hz), 2.92 (m, 2H), 2.26 (m, 1H); MS (positive electrospray) for $(C34H34N8O2+H)^+$ calc'd:587.28, found: 587.25. Crystals of this material suitable for X-ray diffraction were grown from a mixture of CH_2Cl_2 and CH_3CN (slow evaporation).

Diastereomer 2. yellow solid, Rf = 0.60 (1:19 MeOH/PhH), IR (film): 3640, 2980, 1739, 1675, 1413, 1150, 820, 740. 558 cm-1; 1H NMR (400 MHz, CD3CN): δ 7.2-7.4 (m, 8H), 6.08 (ddd, 1H, *J* = 1.5, 5.2, 9.9Hz), 5.85 (m, 2H), 5.66 (m, 2H), 5.11 (m, 4H), 4.91 (s, 2H), 4.81 (m, 2H), 4.62 (m, 4H), 4.00 (m, 1H), 3.67 (ddd, 1H, *J* =1.7, 4.9, 13.5 Hz), 3.48 (m, 1H), 3.25 (m, 1H), 3.12 (m, 1H), 2.97 (m, 1H), 2.27 (m, 1H). MS (positive electrospray) for $(C34H34N8O2+H)^+$: calcd: 587.28, found: 587.25.

Procedure B. $FeCl_2(DMF)_3FeCl_4$ as oxidant

The THF used in this reaction was degassed via the freeze-pump-thaw method prior to use. Monomer **135** (0.150 g, 0.51 mmol) in THF (2.6 mL) was cooled to −78 °C and added via cannulating needle to a flask containing KHMDS (1.12 mL, 0.5M in toluene) at −78°C. After stirring the resulting dark red mixture at −78 °C for 30 minutes, a solution of $[FeCl_2(DMF)_3][FeCl_4]$ (0.141 g, 0.26 mmol) in THF

(0.4 mL) was added via syringe. The reaction was stirred at −78 °C for 3 hours. The reaction was quenched with pH 8.0 EDTA (3 mL). The majority of the solvent was removed *in vacuo* and the residue

diluted in CH_2Cl_2. The solution was washed with pH 8.0 EDTA (0.35M, 3 x10 mL), water and brine. The organic layer was dried over Na_2SO_4, filtered and concentrated *in vacuo*. Purification by silica gel chromatography (progression from 4:1 EtOAc/hexanes → EtOAc → 99:1 EtOAc/MeOH) to afford

α,α dimer **137** (16 mg, 11%), α,γ dimers **136** (87 mg, 55%) and γ,γ dimers **128** as an orange solid (16mg, 11%) .

128; Rf = 0.2 (3:7 CH_3CN:$CHCl_3$); IR (film): 3400, 1669, 1456, 1404, 1181, 1066 cm-1;

1H NMR (400 MHz, CDCl3): δ 7.25-7.35 (m, 4H), 5.97 (m, 1H), 5.57 (s, 0.32H), 5.55 (s, 0.63H), 5.15 (m, 2H), 4.95 (m, 2H), 4.73 (m, 2H), 3.58 (m, 1H), 3.26 (m, 2H), 2.64 (m, 2H). 13C NMR (75MHz, $CDCl_3$): δ 159.7, 141.2, 140.9, 134.0, 133.2, 133.2, 129.1, 128.9, 128.8, 128.7, 120.0, 119.9, 102.4, 101.8, 58.2, 58.1, 49.7, 49.3, 48.4, 29.2, 28.5. MS (positive electrospray) for $(C34H34N8O2+H)^+$: calcd: 587.28, found: 587.25.

Procedure C. $Cu(OTf)_2$ as oxidant.

The THF used in this reaction was degassed via the freeze-pump-thaw method prior to use. Monomer **135** (0.20 g, 0.68 mmol) was dissolved in THF (3.4 mL) and cooled to −78 °C. This solution was added via cannulating needle to a flask

containing KHMDS (1.23 mL, 0.5M in toluene) at −78 °C. After stirring the resulting dark red mixture at −78 °C for 30 min, a solution of $Cu(OTf)_2$ (0.177 g, 0.7 mmol) in THF (0.7 mL) was added via syringe. The reaction was stirred at −78 °C for 3 h and quenched with aq pH 8.0 EDTA (0.35M) solution (3 mL). The mixture was concentrated *in vacuo* and diluted in

CH_2Cl_2. The solution was washed with aqueous pH 8.0 EDTA solution (3 x 10 mL), water and brine. The organic layer was dried over Na_2SO_4, filtered and concentrated *in vacuo*. The residue was purified by silica gel chromatography (progression from 4:1 EtOAc/Hexanes → EtOAc → 99:1 EtOAc/MeOH) to afford α,α dimer **137** (47 mg, 24%), α,γ dimers **136** (73 mg, 37%) and γ,γ dimers **138** as an orange solid (50 mg, 25%) .

Procedure D. Using [*i*-PrCp]$_2$TiCl$_2$ additive and Cu(OTf)$_2$ as oxidant.

The THF used in this reaction was degassed via the freeze-pump-thaw method prior to use. KHMDS (7.3 mL, 0.5 M in toluene) was added dropwise to a solution of **135** (0.98 g, 3.33 mmol) in THF (18 mL)

at −78°C. After stirring at −78°C for 30 min, the reaction mixture was added to a solution of [*i*-PrCp]$_2$TiCl$_2$ (1.2 g, 3.53 mmol) in THF (24 mL). The reaction mixture was stirred at −78 °C for 3 h before being added to a solution of $Cu(OTf)_2$ (1.97 g, 5.39 mmol) in THF (26.7 mL) at −78 °C. The resulting mixture was stirred at −78 °C for an additional 3.75 hours and quenched with aq pH 8.0 EDTA

(0.35M) solution (20 mL). The reaction mixture was concentrated *in vacuo* and diluted in CH_2Cl_2. The solution was washed with aqueous pH 8.0 EDTA solution (3 x 50 mL), water, brine and dried over Na_2SO_4. After removal of solvent *in vacuo*, the residue was purified by silica gel chromatography (gradient from EtOAc to 99:1 EtOAc/MeOH) to afford **138** as an orange solid (0.78 g, 80%).

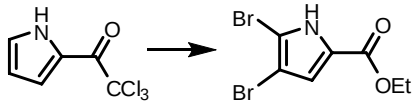

139 **140**

4,5-dibromo-1H-pyrrole-2-carboxylate Ethyl ester (140). Sodium (0.66 g, 28.7 mmol) was dissolved in dry 180 mL EtOH. 2-(trichloroacetyl) pyrrole **139** (50 g, 235 mmol) was added to the NaOEt solution over 10 minutes. The resultant dark red solution was stirred at rt for 40 min. The solvent was removed *in vacuo* and the residue diluted in Et2O. The ether solution was washed with 3N HCl. The black cotton-like solid was removed by filtration. The acidic aqueous washings were extracted with ether. The combined organic layers were washed the saturated $NaHCO_3$, dried over $MgSO_4$, filtered and concentrated *in vacuo* to give a light brown solid (32.1 g, 98%) that was used without further purification. The crude ester from the previous step was dissolved in glacial AcOH (1275 mL). A solution of bromine (23.7 mL, 462 mmol) in AcOH (272 mL) was added via addition funnel over 2 h. The resultant solution was stirred at rt for 3 h. Removal

of acetic acid *in vacuo* provided a pink solid (67.6 g, 99%). That was used without further purification

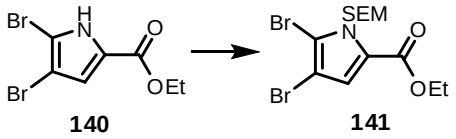

140 **141**

4,5-dibromo-1-((2-(trimethylsilyl)ethoxy)methyl)-1H-pyrrole-2-carboxylate Ethyl Ester (141). Et_3N (38.4 mL, 274 mmol) was slowly added to a solution of **140** (67.6 g, 228 mmol) in THF (900 mL). The reaction was stirred at rt for 10 minutes and treated with SEM-Cl (38.34 g, 230 mmol). The reaction was stirred at rt for 2 h. The mixture was concentrated and the residue was taken up in CH2Cl2. The resulting solution was washed with water and brine, dried over Na_2SO_4, filtered and concentrated *in vacuo* to afford **141** as a brown oil (94.4 g, 97%). This material was used without further purification.

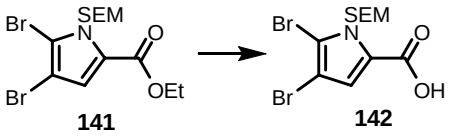

141 **142**

4,5-dibromo-1-((2-(trimethylsilyl)ethoxy)methyl)-1H-pyrrole-2-carboxylic acid (142). A solution of NaOH (17.6 g, 439 mmol) in H2O (218 mL) was added to a solution of **141** (94.4 g, 221 mmol) in THF/MeOH (1000 mL / 70 mL). The resulting solution was stirred at 65 °C for 5 hours. The reaction was quenched

with 10% aq citric acid. The solvents were removed *in vacuo* and the residue taken up in CH_2Cl_2. The solution was washed with saturated NH4Cl, water and brine. The organic layer was dried over Na_2SO_4, filtered and concentrated *in vacuo* to give **142** as an off white solid (86.5g, 98%). This material was used without further purification.

142: IR (film): 3400, 1652, 1635, 1338, 1250, 1148, 667 cm-1; ^{1}H NMR (400 MHz, CDCl3): δ 7.21 (s, 1H), 5.81 (s, 2H), 3.60 (t, 2H, *J* = 8.4Hz), 0.91 (t, 2H, *J* = 8.4Hz), 0.02 (s, 9H). ^{13}C NMR (75MHz, CDCl3): δ 164.3, 123.2, 122.7, 115.3, 101.1, 75.5, 66.3, 17.8, -1.5. MS (positive electrospray) for $(C11H17Br2NO3Si+H)^+$ calcd: 399.93, found: 400.10.

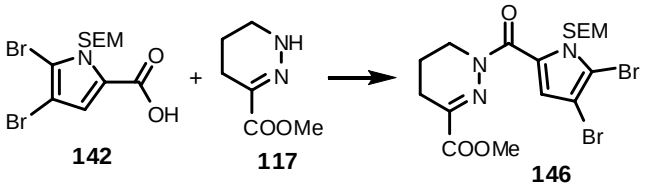

methyl 1-(4,5-dibromo-1-((2-(trimethylsilyl)ethoxy)methyl)-1H-pyrrole-2-carbonyl)-1,4,5,6-tetrahydropyridazine-3-carboxylate (146). Oxalyl chloride (20.3 mL, 236 mmol) was added to a solution of acid **142** (47.1 g, 118 mmol) in CH_2Cl_2 (400 mL). DMF (0.5 mL) was added and the resulting mixture was stirred at rt for 1 hour. The solvent was removed *in vacuo* to give a brown oily residue that was dissolved in CH_3CN (370 mL). To this solution was added **117** (16.8 g, 118 mmol), pyridine (19 mL, 236 mmol) and DMAP (50 mg) and the resulting

mixture was stirred at rt overnight. The solvent was removed *in vacuo* and the residue taken up in CH_2Cl_2. The solution was washed with water and brine. The organic layer was dried over

Na_2SO4, filtered and concentrated *in vacuo*. Purification by silica gel chromatography (10→20% EtOAc/hexanes) provided **146** (58 g, 94%) as a white solid.

146: Rf = 0.3 (1:4 EtOAc/CH2Cl2); IR (film): 1711, 1648, 1413, 1337, 1267, 1239, 1090, 973, 834 cm-1; ^{1}H NMR (400 MHz, CDCl3): δ 7.50 (s, 1H), 5.84 (s, 2H), 3.88, (s, 3H), 3.86 (m, 2H), 3.56 (t, 2H, *J* = 8Hz), 2.56 (t, 2H, *J* = 6.4Hz), 1.96 (td, 2H, *J* = 6.3, 12.4Hz), 0.89 (t, 2H, *J* = 8Hz), 0.04 (s, 9H); ^{13}C NMR (75MHz, CDCl3): δ 164.5, 160.0, 139.3, 125.2, 124.1, 113.2, 100.3, 76.0, 66.0, 52.5, 39.6, 21.8, 17.8, 16.6, -1.5. MS (positive electrospray) for $(C17H25Br2N3O4Si+H)^+$ calcd: 524.00, found: 524.10.

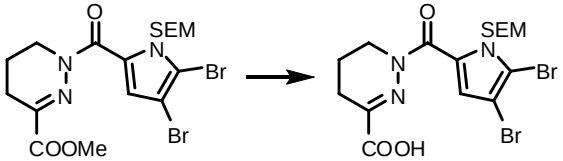

146 **147**

1-(4,5-dibromo-1-((2-(trimethylsilyl)ethoxy)methyl)-1H-pyrrole-2-carbonyl)-1,4,5,6-tetrahydropyridazine-3-carboxylic acid (147). A solution of ester **146** (66 g, 126 mmol) in THF/H2O (520 mL / 250 mL) was stirred for 30 min in an ice-water bath. A solution of LiOH (30 mL. aq 0.5M) was added and the resulting

mixture stirred at 4 °C for 1 h. The reaction was quenched with 10% aq citric acid and concentrated *in vacuo*. The residue was taken up in EtOAc and washed with saturated NH_4Cl, water and brine. The organic layer was dried over Na2SO4, filtered and concentrated *in vacuo*. The resulting white solid (62.2 g, 97%) was used without further purification.

147: IR (film): 3203, 2951, 1715, 1652, 1422, 1240, 1179, 1096, 1096, 969, 860. 742, 684, 612 cm-1; ^{1}H NMR (400 MHz, CDCl3): δ 7.36 (s, 1H), 6.95 (bs, 1H) 5.74 (s, 2H), 3.86 (t, 2H, *J* = 5.6Hz), 3.55 (t, 2H, *J* = 8Hz), 2.61 (t, 2H, *J* = 6.4Hz), 2.01 (td, 2H, *J* = 6.3, 12.3Hz), 0.88 (t, 2H, *J* = 8Hz), 0.06 (s, 9H). ^{13}C NMR (75MHz, CDCl3): δ 163.8, 160.5, 139.8, 128.3, 125.2, 121.5, 113.0, 100.4, 75.8, 66.4, 40.0, 21.0, 17.7, 16.4, -1.5. MS (positive electrospray) for $(C16H23Br2N3O4Si+H)^{+}$ calcd: 509.98, found: 510.05.

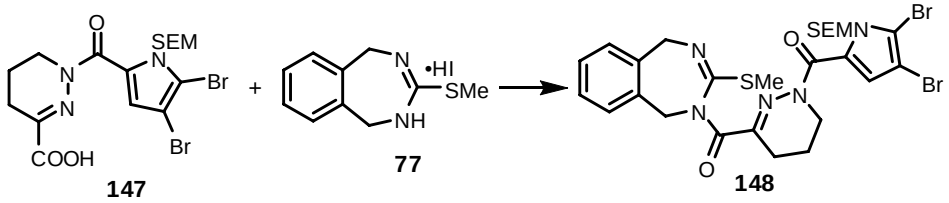

(4,5-dibromo-1-((2-(trimethylsilyl)ethoxy)methyl)-1H-pyrrol-2-yl)(3-(3-(methylthio)-2,5-dihydro-1H-benzo[e][1,3]diazepine-2-carbonyl)-5,6-dihydropyridazin-1(4H)-yl)methanone (148). HI salt **77** (9.2 g, 28.9 mmol) was added to a solution of **147** (14 g, 27.5 mmol) in DMF (183 mL) at 0 °C. TBTU (9.7 g, 30.3 mmol) was added, followed by the slow addition of DIPEA (14.4 mL,

82.5 mmol). The resulting mixture was stirred at rt for 3 h. The reaction mixture was diluted with 1L EtOAc and washed with sat. NH_4Cl (2 x 200 mL), water (8 x 200 mL) and brine (200 mL). The organic layer was dried over Na_2SO_4, filtered and concentrated *in vacuo* to afford **148** as a slightly pink foam (18.5 g, 99%). This material was used without further purification.

148: R_f = 0.9 (1:9 CH3CN/CHCl3); IR (film): 3420, 1645, 1430, 1340, 1241, 1130, 835, 750, 697 cm-1; ^{1}H NMR (400 MHz, CDCl3): δ 7.15 (m, 4H), 6.68 (s, 1H), 5.65 (s, 2H), 4.90 (s, 2H), 4.44 (s, 2H), 3.84 (t, 2H, *J* = 5.6Hz), 3.46(t, 2H, *J* = 8Hz), 2.63 (t, 2H, *J* = 5.6Hz), 2.31 (s, 3H), 2.02 (m, 2H), 0.86 (t, 2H, *J* = 8Hz), -0.07 (s, 9H). ^{13}C NMR (75 MHz, CDCl3): δ 165.7, 161.8, 157.4, 146.6, 134.02, 133.8, 129.7, 127.9, 127.7, 127.2, 126.1, 120.9, 111.3, 99.9, 75.8, 66.2, 54.8, 45.9, 40.4, 23.9, 17.9, 17.3, 15.3, -1.2. MS (positive electrospray) for $(C26H33Br2N5O3SSi+H)^+$ calcd: 684.04, found: 683.90.

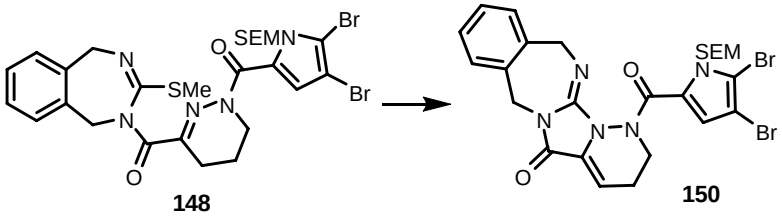

SEM Monomer (150). A mixture of **148** (34 g, 50 mmol), $HgCl_2$ (19 g, 67 mmol) and pyridine (12.1 mL, 150 mmol) in CH_3CN (250 mL) was heated at reflux for 3 h. A second portion of $HgCl_2$ (2.7 g, 13.4 mmol) was added and reflux continued

for 1 h. Upon cooling to rt, a white solid was removed by filtration and the solvent evaporated *in vacuo*. The reaction mixture was taken up in EtOAc and undissolved solids were removed by filtration. The organic layer was washed with 1N NaOH whereupon a white precipitate formed. The precipitate was filtered and the NaOH wash / filtration sequence continued until no further solid formed (6-7 x). The organic layer was then washed with water and brine and dried over Na_2SO_4. Concentration *in vacuo* and purification by silica gel chromatography (1:3 EtOAc/hexanes) afforded **150** as a white foam (15.0 g). Mixed fractions were purified on a second silica gel column (1:9 EtOAc/CH2Cl2) to provide a further 5.0 g of **150** (total yield = 70%).

150: R_f = 0.7 (1:9 CH3CN:CHCl3); IR (film): 2951, 1741, 1635, 1402, 1093, 859, 758, 793 cm-1. ^{1}H NMR (400 MHz, CD3CN): δ 7.28-7.38 (m, 4H), 6.81 (s, 1H), 5.82 (t, 1H, *J* = 4.7Hz), 4.89 (s, 2H), 4.66 (s, 2H), 3.80 (m, 2H), 3.57 (t, 2H, *J* = 12Hz), 2.33 (dd, 2H, *J* = 5.3, 10.4Hz), 0.883 (t, 2H, *J* =12Hz), 0.0 (s, 9H). ^{13}C NMR (75 MHz, CD3CN): δ 163.8, 159.3, 141.6, 141.4, 134.9, 129.5, 129.2, 129.1, 129.0, 126.3, 118.7, 118.0, 112.6, 104.2, 100.2, 76.1, 66.7, 49.5, 45.7, 43.6, 23.5, 18.2, -1.3. MS (positive electrospray) for $(C25H29Br2N5O3Si+H)^+$ calcd: 636.04, found: 636.10.

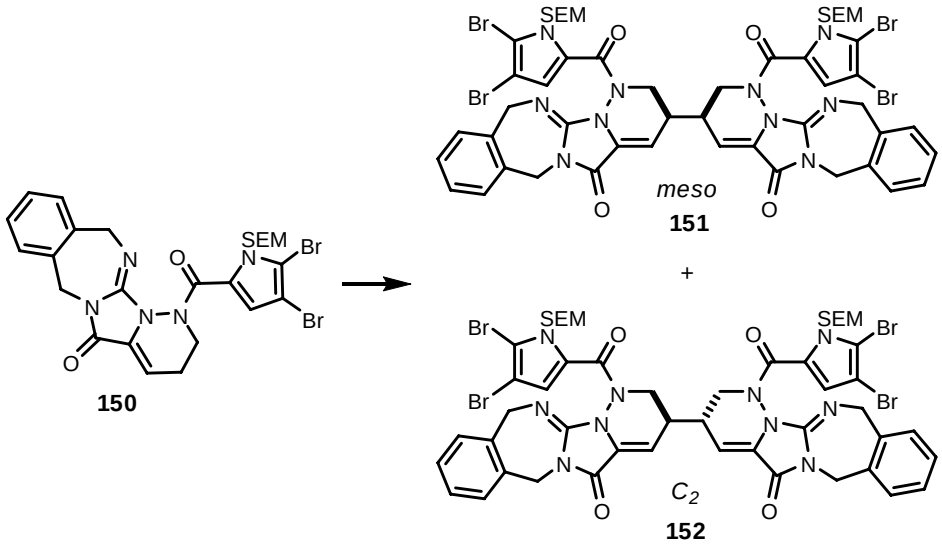

SEM Dimers (151 and **152).** Monomer **150** (311 mg, 0.49 mmol) and solid [*i*-PrCp]$_2$TiCl$_2$ (190 mg, 0.57 mmol) were dissolved in 2.5 mL anhydrous THF. The brandy colored solution was degassed via consecutive freeze-pump-thaw cycles (3x) and cooled to −78 °C. KHMDS (1.08 mL, 0.5M toluene) was added dropwise and the resultant dark green slurry was stirred at −78°C for 1.5 hours. A fine suspension of Cu(OTf)$_2$ (260 mg, 0.74 mmol) in dry, degassed THF was added over 15 minutes and the dark red/brown slurry stirred at −78 °C for 3h and then at rt for 1.5 h. The reaction was treated with 5 mL pH 8.0 aq EDTA (0.35M) and the volatiles were removed *in vacuo*. The residue was diluted in EtOAc, washed with additional pH 8.0 EDTA solution (until blue color no longer observed), H_2O and brine. The organics were dried over Na_2SO_4, filtered and concentrated. Purification by column chromatography on silica gel (1% $CH_3CN/CHCl_3$) afforded **151** *meso* (150 mg, 49%) and **152** *C*$_2$ (45 mg, 15%).

151 *meso*: light yellow solid; R_f = 0.35 (10% $CH_3CN/CHCl_3$); IR (film): 1745, 1745, 1698, 1447, 1396, 1093, 934, 836 cm-1; ^{1}H NMR (400 MHz, CD_3CN, 70 °C): δ 7.40-7.20 (m, 8H), 6.71 (s,2H), 5.66-5.48 (m, 6H), 4.95 (s, 4H), 4.62 (s, 4H), 3.77 (bs, 2H), 3.57 (t, *J* = 8Hz, 4H), 2.49 (s, 2H), 0.86 (t, *J* = 8Hz, 4H), 0.01 (s, 18H); ^{13}C NMR (75 MHz, CDCl3, 55 °C): δ 163.0, 158.4, 140.7, 140.2, 133.6, 130.3, 129.3, 128.8, 128.7, 128.5, 125.3, 118.0, 112.4, 104.0, 100.2, 75.6, 66.5, 49.6, 45.6, 43.6, 36.5, 18.2, −1.2; MS (positive electrospray) calc'd for $(C50H56Br4N10O6Si2+H)^+$: 1269.06, found 1268.80. Crystals of **151** *meso* suitable for X-ray diffraction were grown from MeOH (slow evaporation).

152 C_2: light yellow solid; R_f = 0.2 (10% $CH_3CN/CHCl_3$); IR (film): 1745, 1698, 1448, 1397, 1093, 934, 836 cm-1; ^{1}H NMR (400 MHz, CD3CN, 70 °C): δ 7.40-7.20 (m, 8H), 6.72 (s, 2H), 5.72 (s, 2H), 5.51(s, 4H), 4.95 (s, 4H), 4.61(S, 4H), 3.87 (bs, 2H), 3.58 (t, *J* = 8Hz, 4H), 2.49 (s, 2H), 0.86 (t, *J* = 8Hz, 4H), 0.01 (s, 18H); ^{13}C NMR (75 MHz, CDCl3, 55 °C): δ 163.0, 158.5, 140.7, 140.2, 133.6, 130.2, 129.3, 128.8, 128.8, 128.5, 125.0, 118.1, 112.5, 103.7, 100.2, 75.6, 66.6, 49.6, 46.4, 43.6, 36.7, 18.2, -1.2; MS (positive electrospray) calc'd for $(C50H56Br4N10O6Si2+H)^+$: 1269.06, found 1268.94.

3.11 Notes and References

(1) Elslager, E.; Worth, D. F.; Haley, N. F.; Perricone, S. C. *J. Heterocycl. Chem.* **1968**, 5, 609-613.

(2) (a) Öhler, E.; Schmidt, U. *Chem. Ber.* **1975**, 2907-2916. (b) Mark Cushman, D. Y., Stefan Gerhardt, Robert Huber, Markus Fischer, Klaus Kis, and Adelbert Bacher *J. Org. Chem* **2002**, *67*, 5807 -5816.

(3) Broger, E. M.; Crameri, Y.; Imfeld, M., Montavon, F.; Widmer, R. *Eur. Pat. Appl.* **1993**, EP 570764 A2 19931124.

(4) Levallet, C.; Lerpiniere, J.; Ko, S. Y. *Tetrahedron* **1997**, 53,5291-5304

(5) Ivanoff, D.; Spassoff, A. *Bull. Soc. Chim. Fr., Mem*. **1935**, *2*, 76-78.

(6) Kobayashi, Y.; Taguchi, T.; Tokuno, E. *Tetrahedron lett*. **1977**, 42, 3741-3742.

(7) Rathke, M. W.; Lindert, A. *J. Am. Chem. Soc*. **1971**, 93, 4605-4606.

(8) Renaud, P.; Fox, M. A. *J. Org. Chem.* **1988**, *53*, 3745-3752.

(9) Hirai, K.; Ojima, I. *Tetrehedron Le*t. **1983**, 24, 785-788.

(10) Schmittel, M.; Burghart, A.; Malisch, W.; Reising, J.; Söllner. *J. Org. Chem.* **1998**, 63, 396-400.

(11) VandenBorn, H. W.; Evans, D. H. *J. Am. Chem. Soc.* 1974, 96, 4296-4301.

(12) (a) Schmittel, M.; Haeuseler, A. *J. Organomet. Chem*. **2002**, 661, 169-179. (b) Schmittel, M. *Top. Curr. Chem* **1994**, 183-230.

(13) Ito, Y.; Konoike, T.; Harada, T.; Seagusa, Y. *J. Am. Chem. Soc.* **1977**, 99, 1487-1493.

(14) Paquette, L. A.; Bzowej, E. I.; Branan, B. M.; Stanton, K. J. *J. Org. Chem*. **1995**, 60, 7277-7283.

(15) Inoue, S. I.; Takaya, H.; Tani, K.; Otsuka, S.; Sato, T.; Noyori, R. *J. Am. Chem. Soc.* **1990**, 112, 4897-4905.

(16) Carey, F. A.; Sunberg, R. J. *Advanced Organic Chemistry.* 4th ed. New York, Kluwer Academic/Plenum Publishers, **2000,** Chap. 12.

(17) Hammond, G. S. *J. Am. Chem. Soc.* 1955, 77, 334-338.

(18) Tobinaga, S.; Kotani, E. *J. Am. Chem. Soc*. **1972**, 94, 309-310.

(19) Aurell, M. J.; Gill, S.; Tortajada, A.; Mestres, R. *Tetrahedron Lett*, **1988**, 29, 6181-6182.

(20) Baran, P. S.; Richter, J. M. *J. Am. Chem. Soc.* **2004**, 126, 7450-7451.

(21) Jahn, U. *J. Org. Chem.* **1998**, 63, 7130-7131.

(22) Jahn, U.; Hartmann, P. *J. Chem. Soc., Perkin Trans.1*, **2001**, 2277-2282.

(23) Schmittel, M.; Burghart, A.; Werner, H.; Laubender, M.; Söllner, R. *J. Org. Chem.* **1999**, 64, 3077-3085.

(24) Lehnert, W. *Tetrahedron Lett*, **1970**, 54, 4723-4724.

APPENDIX A
Spectra of Compounds Appearing In Chapter 3

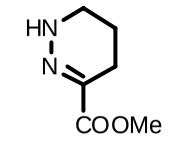

117

Solvent: $CDCl_3$
Temp: 25 °C, 400MHz

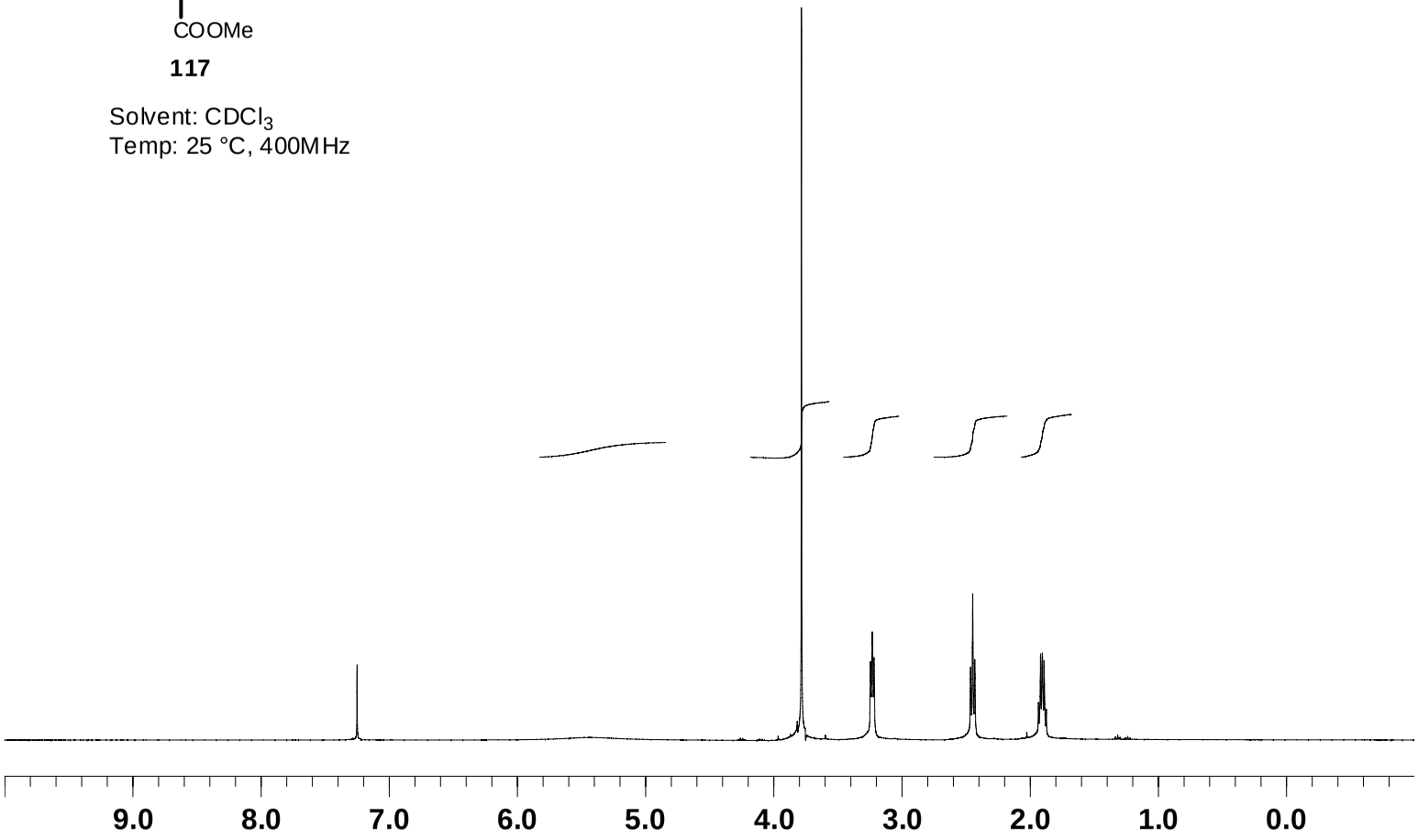

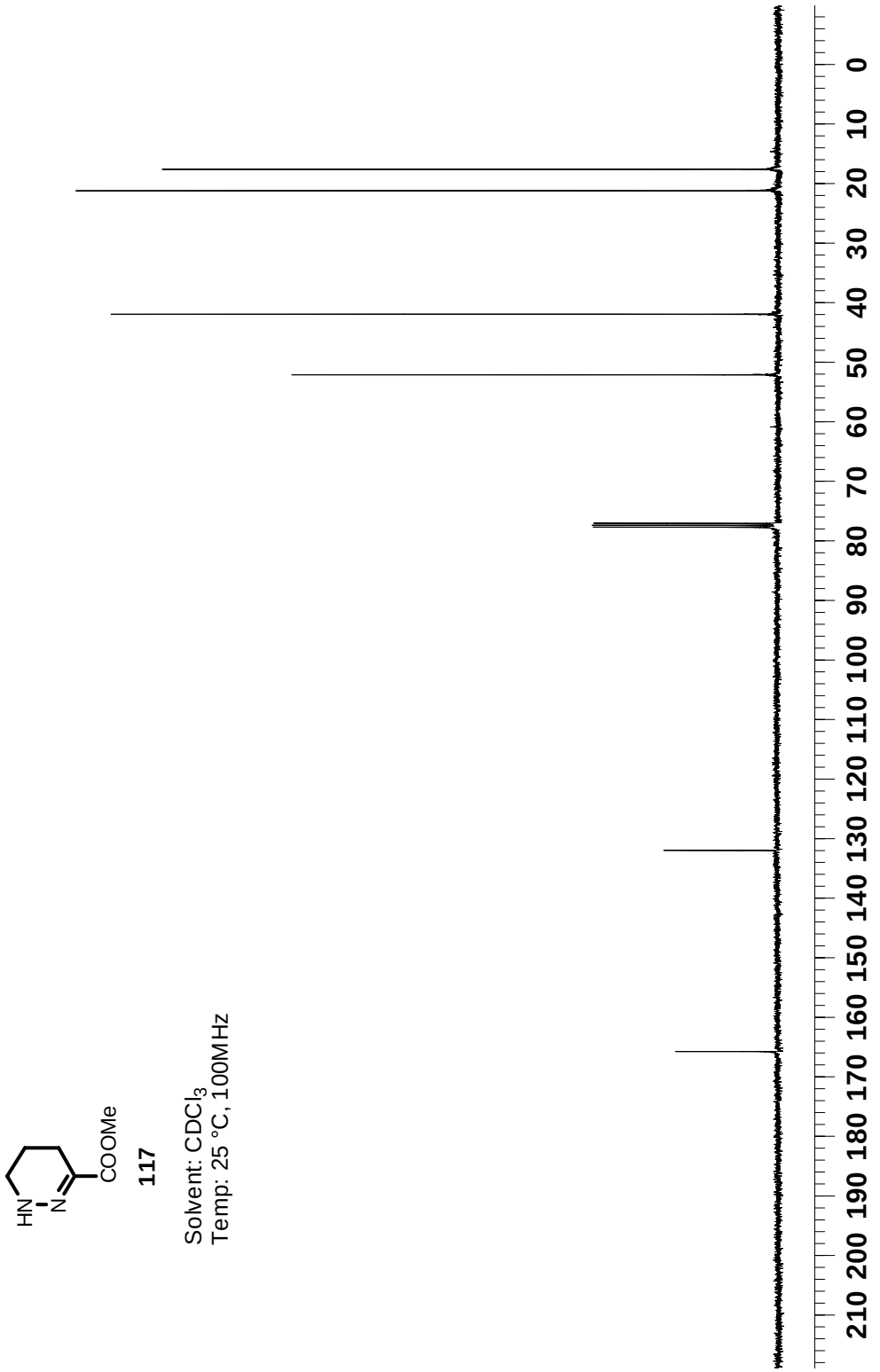
HN
N
COOMe
117
Solvent: CDCl3
Temp: 25 °C, 100MHz
210 200 190 180 170 160 150 140 130 120 110 100 90 80 70 60 50 40 30 20 10 0

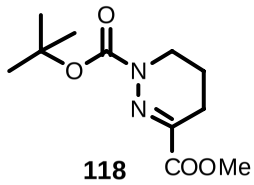

118

Solvent: $CDCl_3$
Temp: 25 °C, 300MHz

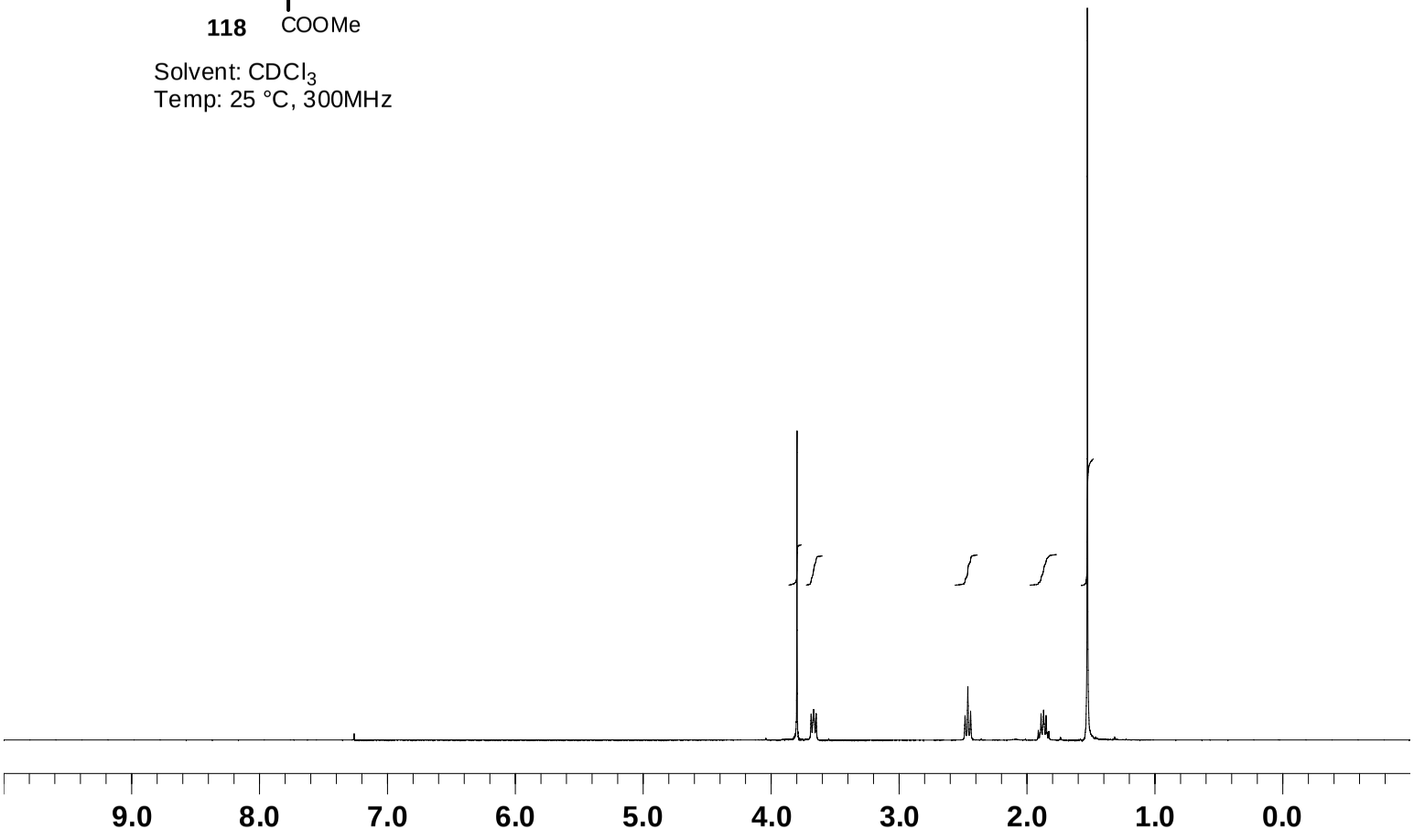

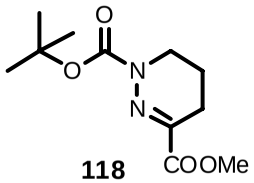

118

Solvent: $CDCl_3$
Temp: 25 °C, 75MHz

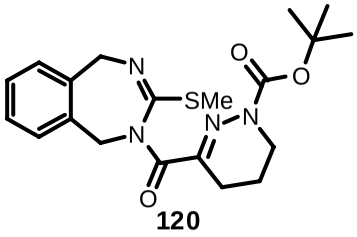

120

Solvent: $CDCl_3$
Temp: 25 °C, 400MHz

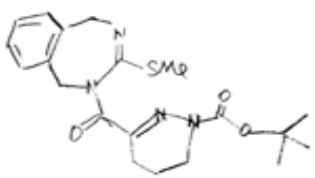

^{13}C-APT

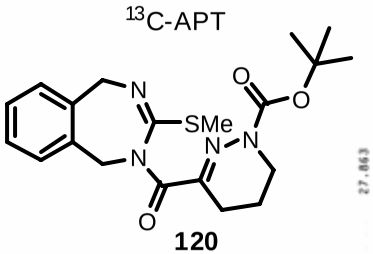

120

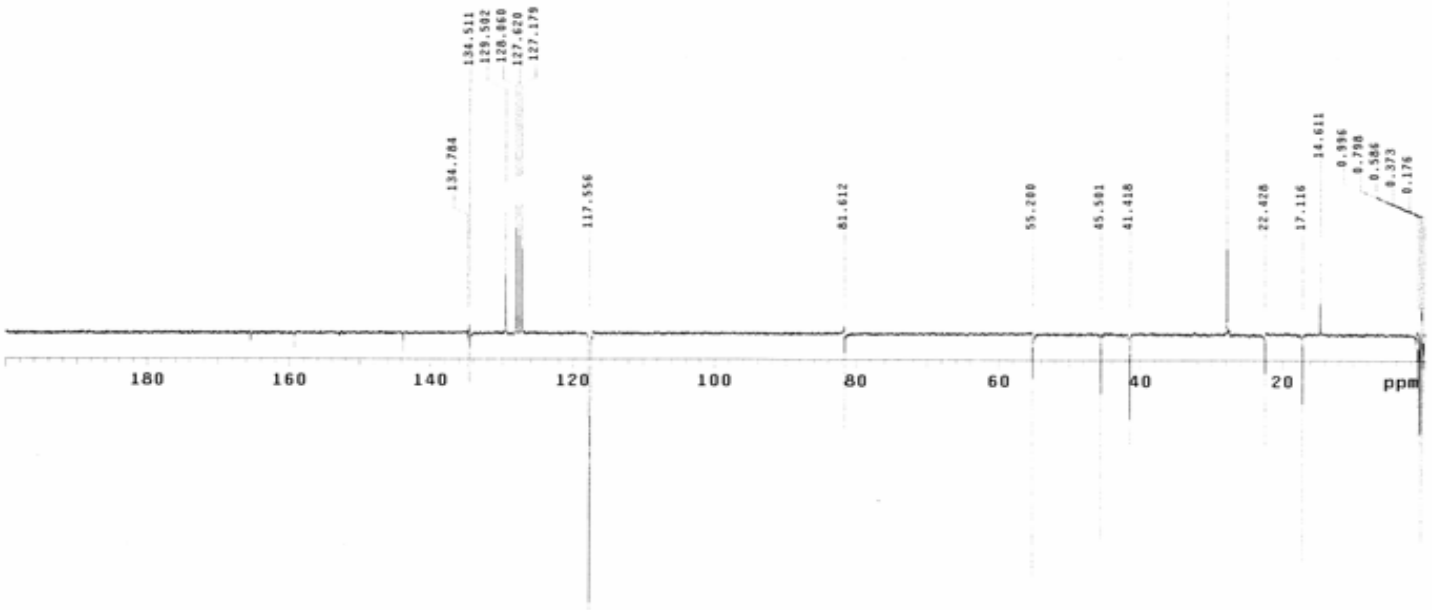
134.784
134.511
129.592
128.860
127.620
127.179
117.556
81.612
55.280
45.581
41.418
27.863
22.428
17.116
14.611
0.996
0.798
0.586
0.373
0.176
180
160
140
120
100
80
60
40
20
ppm

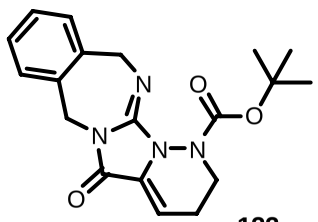

122

Solvent: CD_3CN
Temp: 50 °C, 400MHz

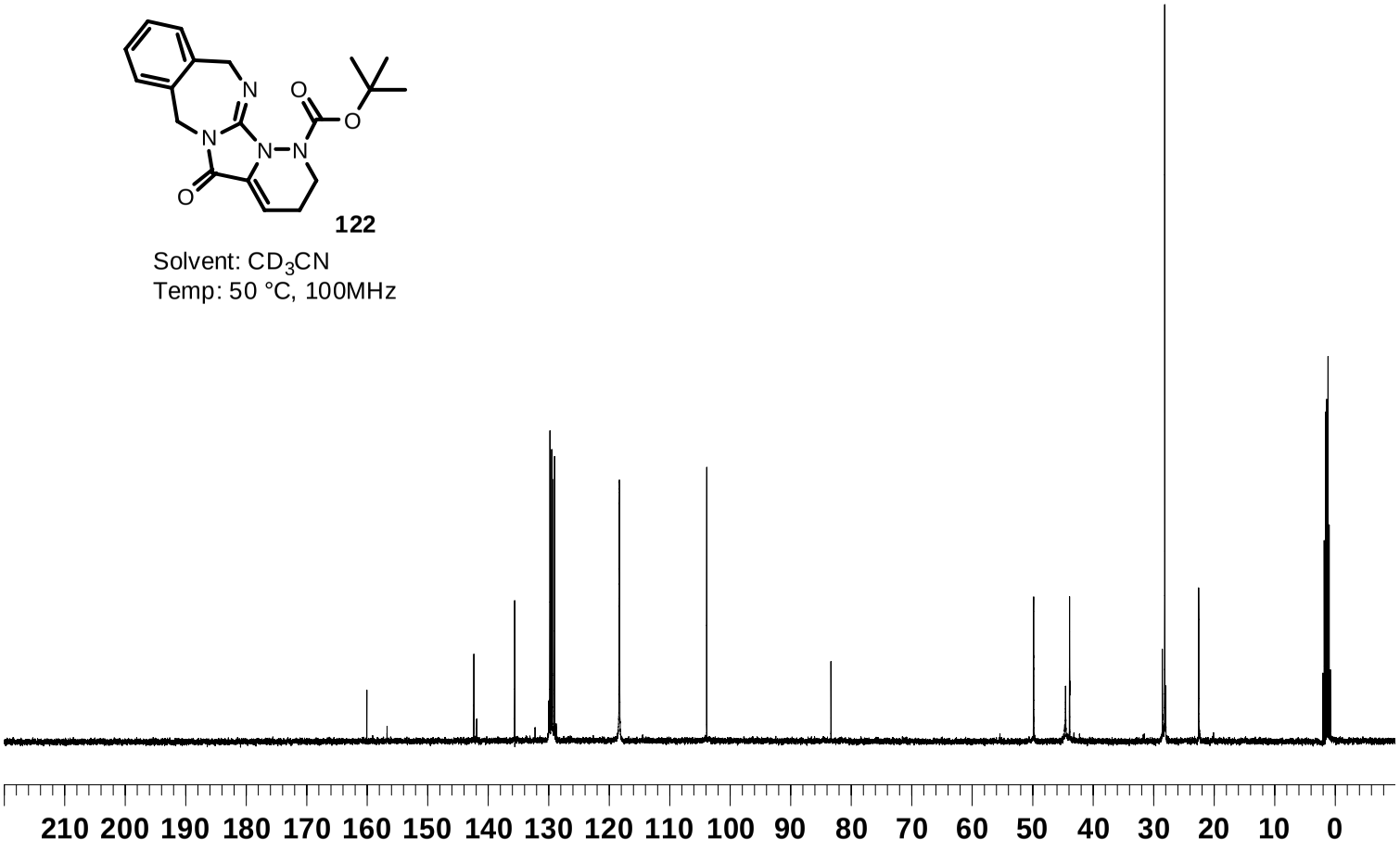
N
O
O
N
N–N
O
122
Solvent: CD3CN
Temp: 50 °C, 100MHz
210 200 190 180 170 160 150 140 130 120 110 100 90 80 70 60 50 40 30 20 10 0

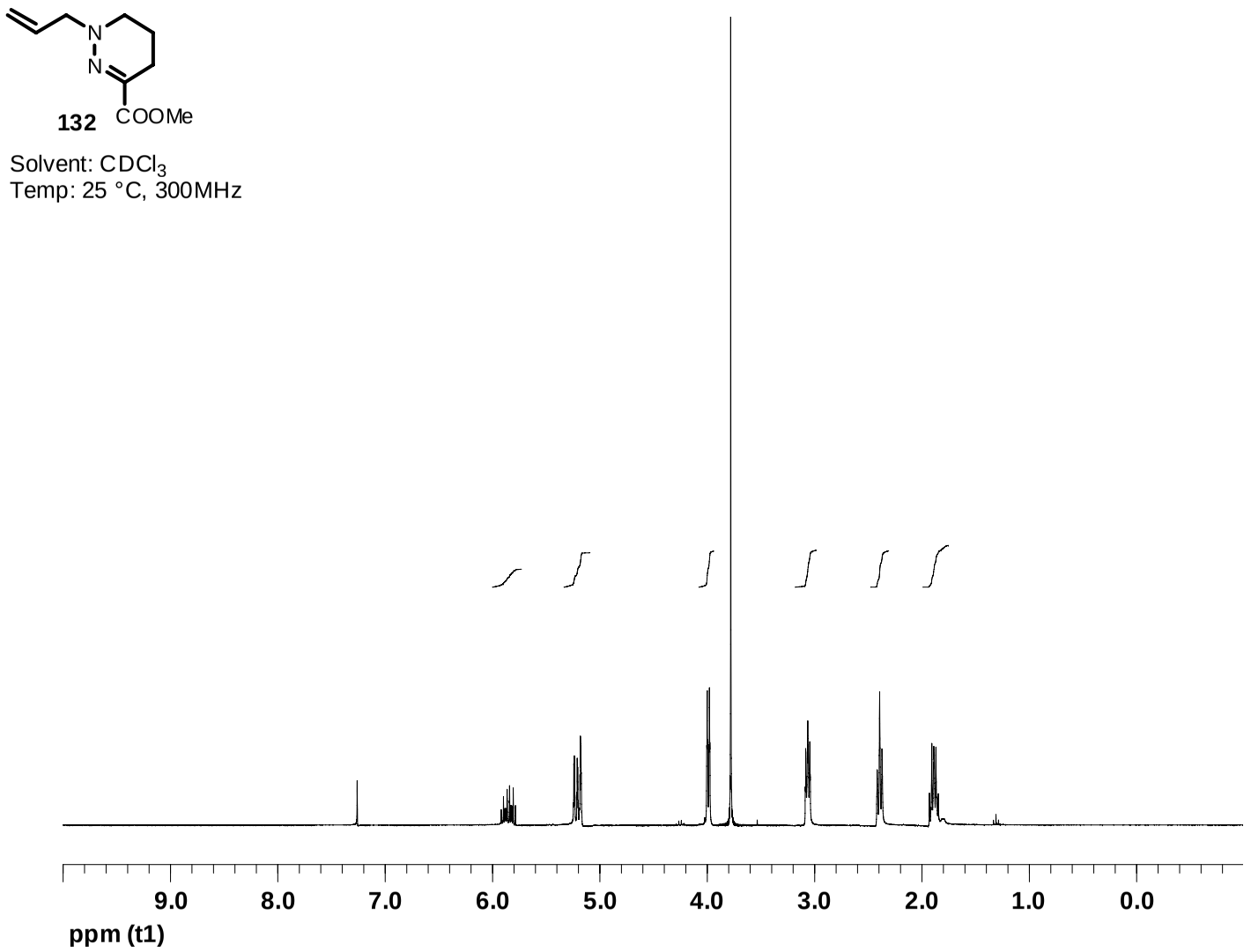
N
N
COOMe
132
Solvent: CDCl3
Temp: 25 °C, 300MHz
9.0
8.0
7.0
6.0
5.0
4.0
3.0
2.0
1.0
0.0
ppm (t1)

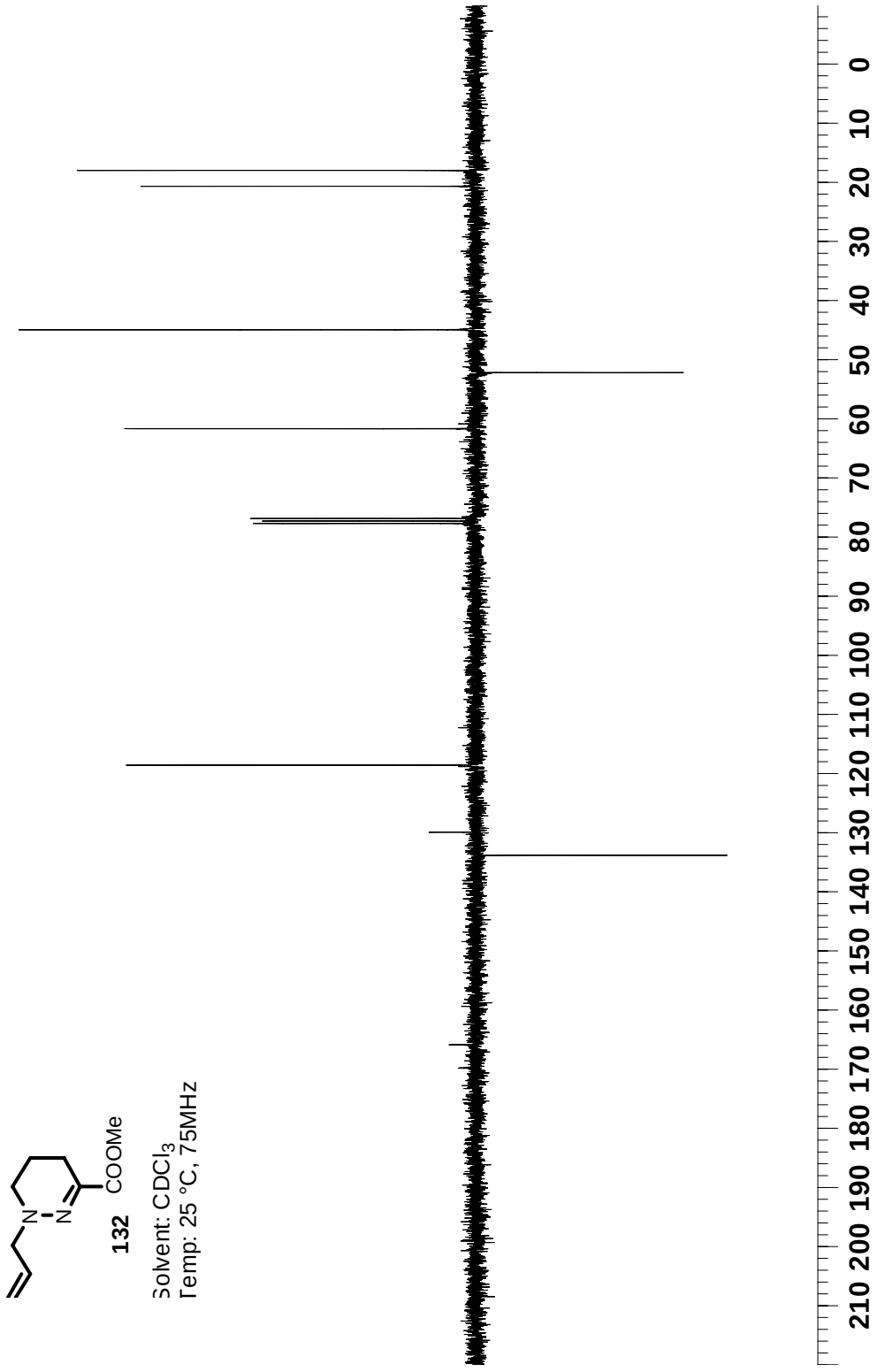
COOMe
132
Solvent: CDCl3
Temp: 25 °C, 75MHz
210 200 190 180 170 160 150 140 130 120 110 100 90 80 70 60 50 40 30 20 10 0

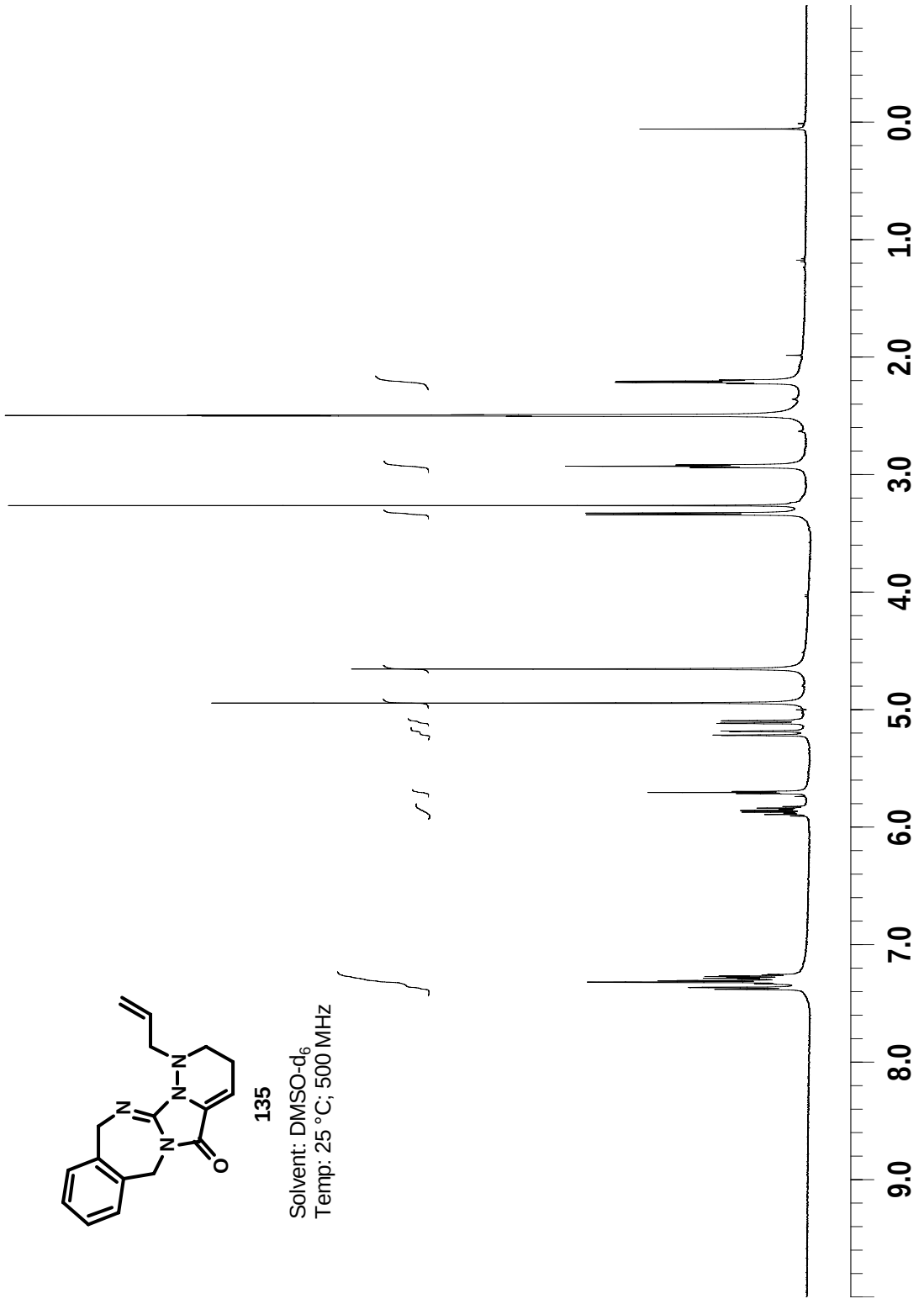
135
Solvent: DMSO-d6
Temp: 25 °C; 500 MHz
9.0
8.0
7.0
6.0
5.0
4.0
3.0
2.0
1.0
0.0

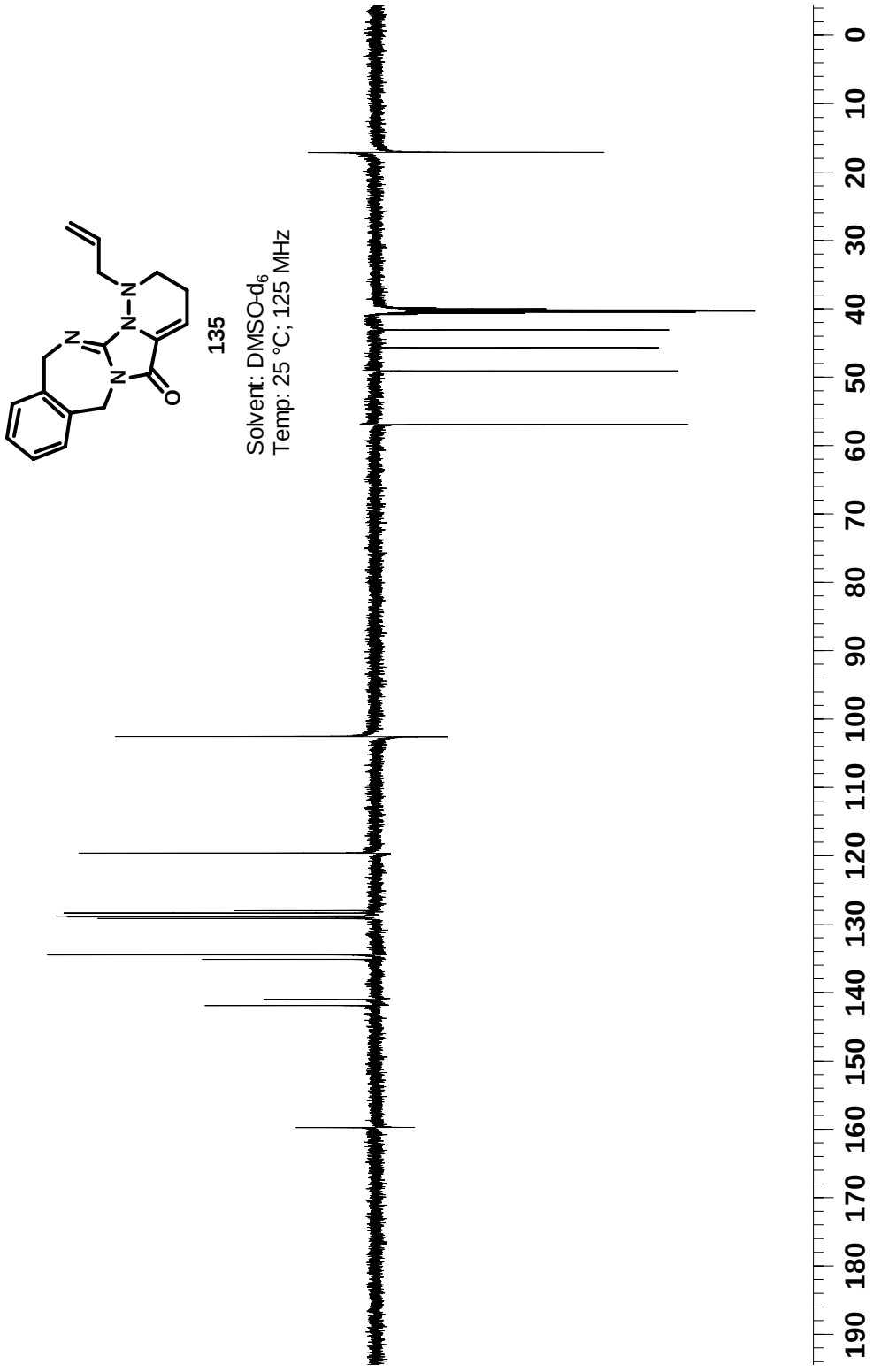
135
Solvent: DMSO-d6
Temp: 25 °C; 125 MHz
0
10
20
30
40
50
60
70
80
90
100
110
120
130
140
150
160
170
180
190

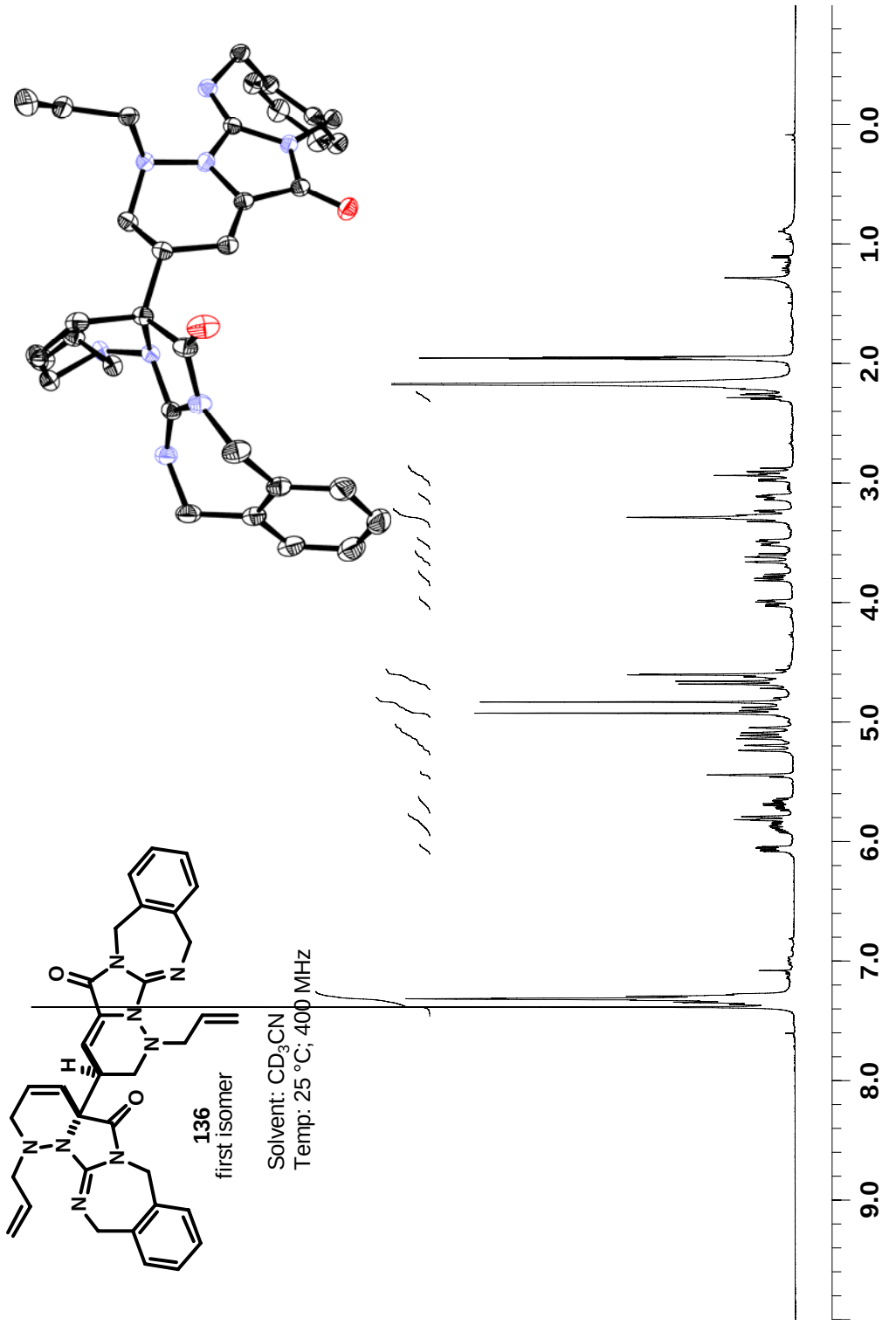
136
first isomer
Solvent: CD3CN
Temp: 25 °C; 400 MHz
9.0
8.0
7.0
6.0
5.0
4.0
3.0
2.0
1.0
0.0

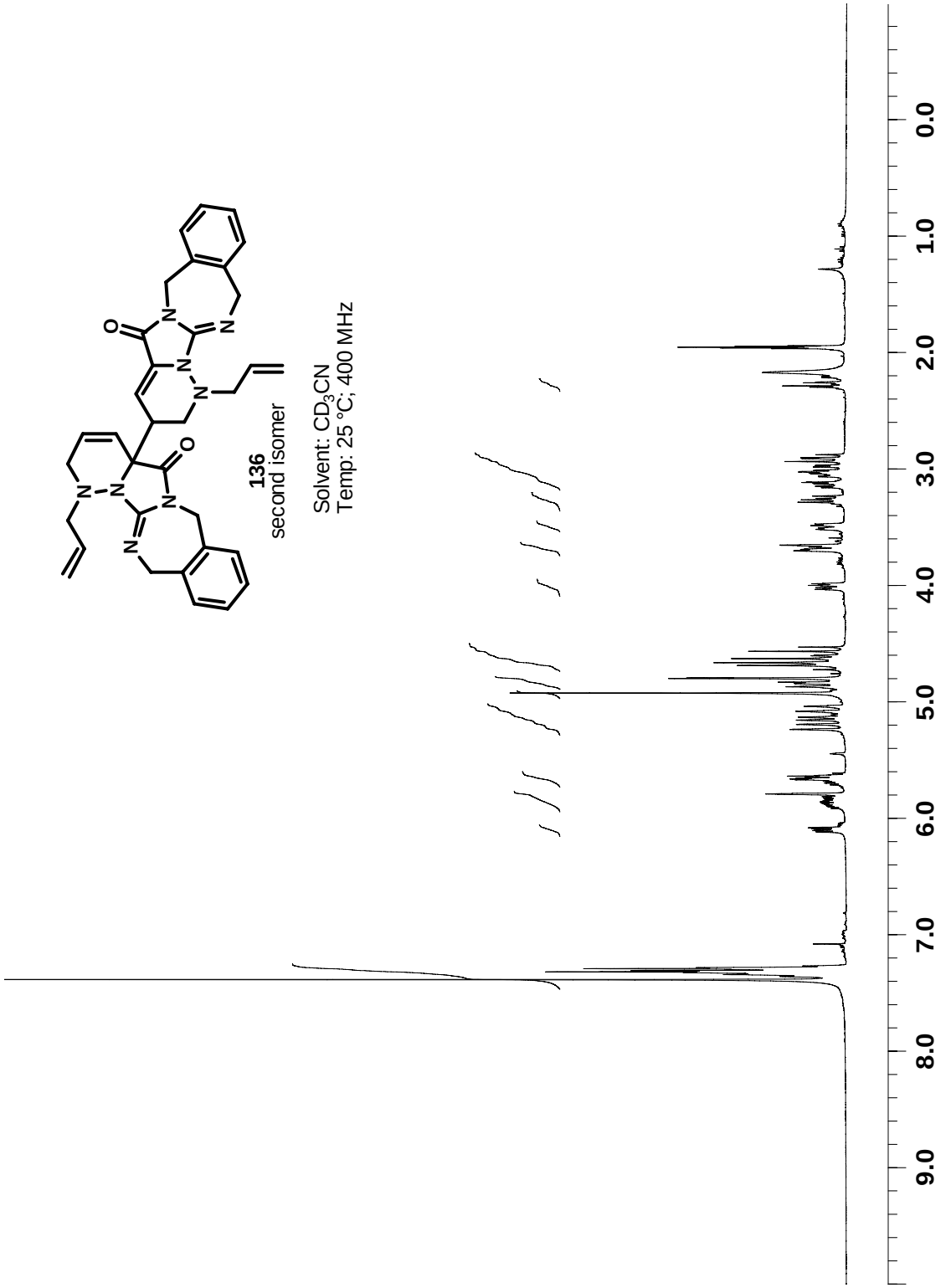
136
second isomer
Solvent: CD3CN
Temp: 25 °C; 400 MHz
9.0
8.0
7.0
6.0
5.0
4.0
3.0
2.0
1.0
0.0

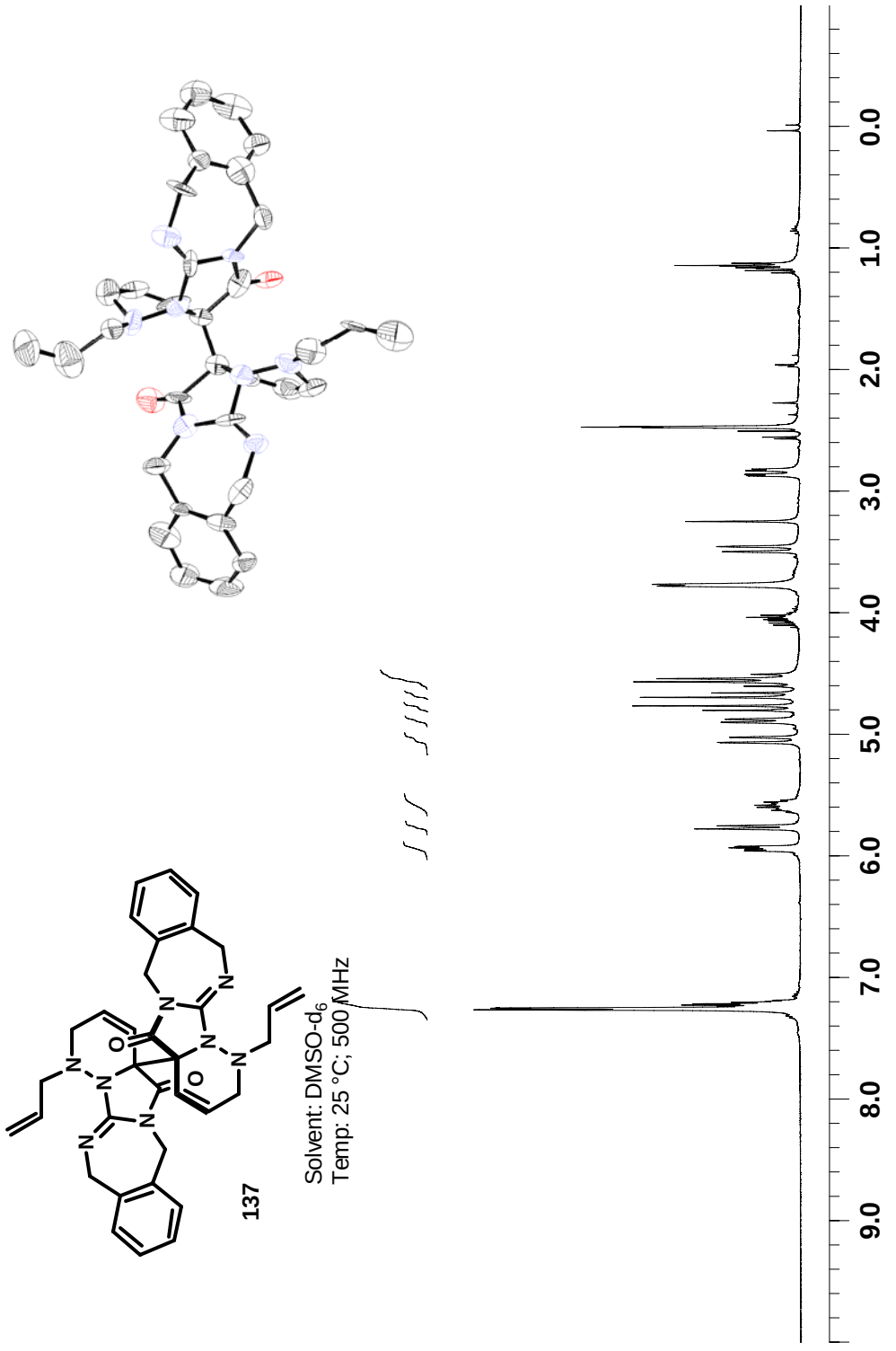
137
Solvent: DMSO-d6
Temp: 25 °C; 500 MHz
9.0
8.0
7.0
6.0
5.0
4.0
3.0
2.0
1.0
0.0

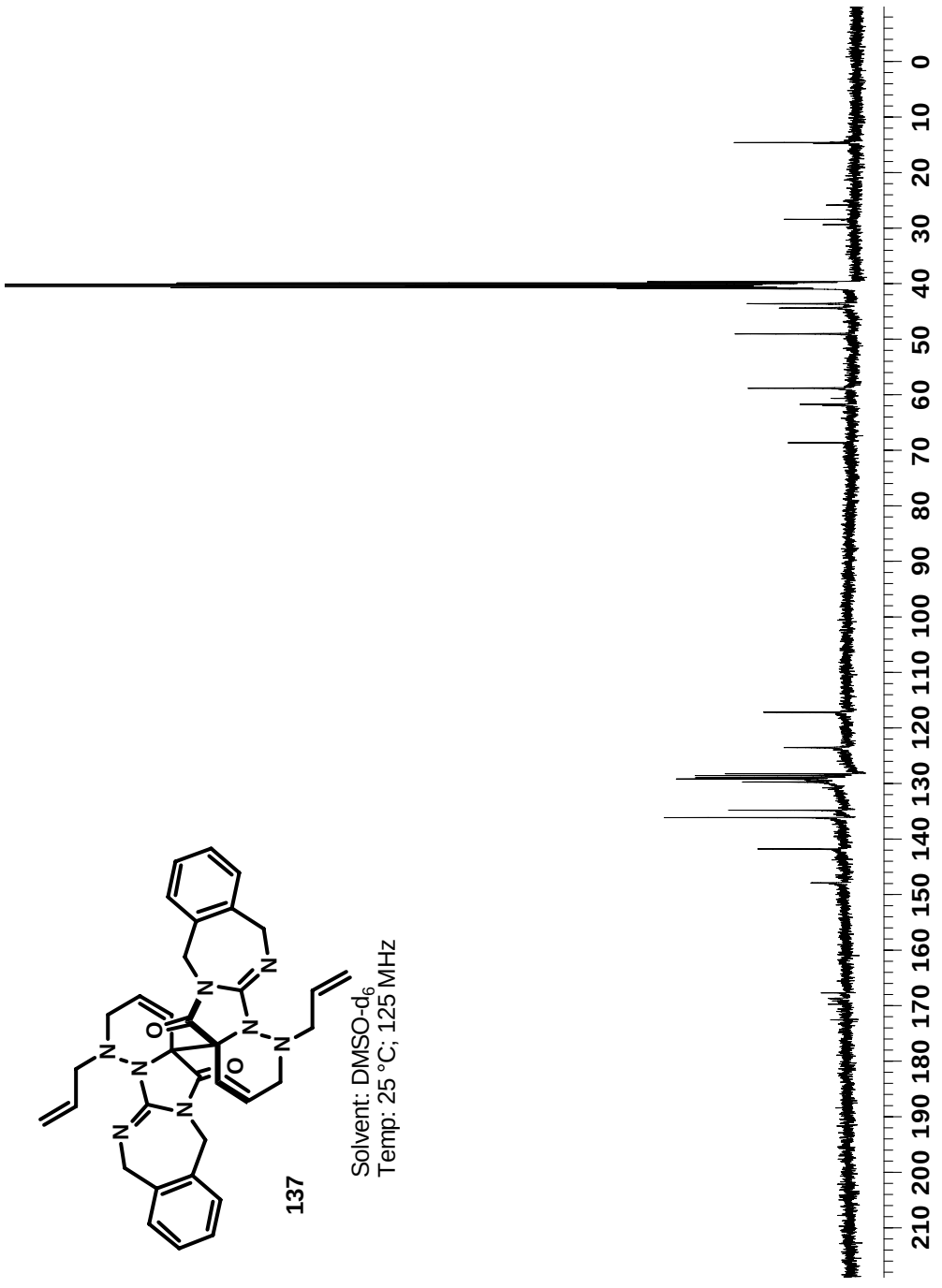
137
Solvent: DMSO-d6
Temp: 25 °C; 125 MHz
210 200 190 180 170 160 150 140 130 120 110 100 90 80 70 60 50 40 30 20 10 0

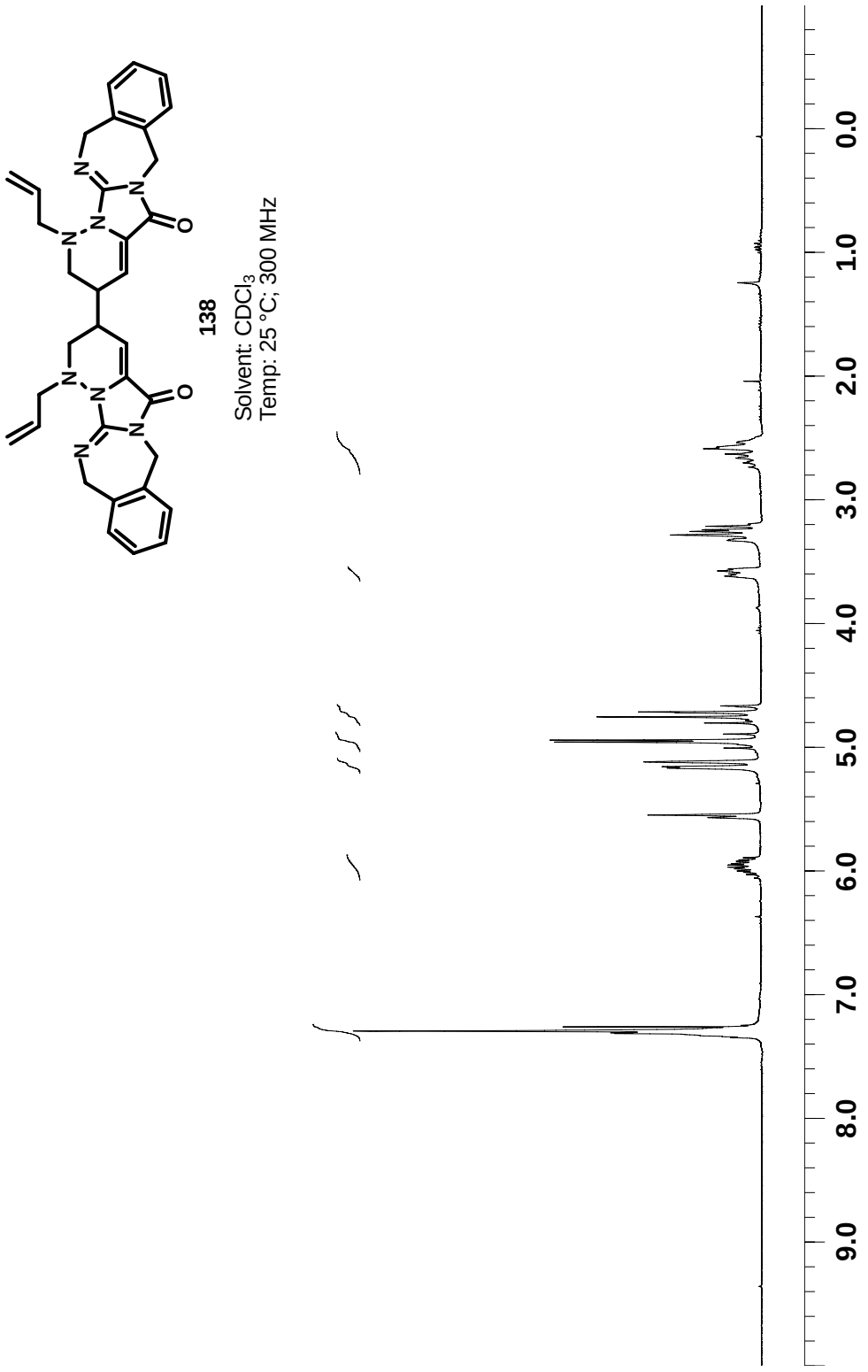
138
Solvent: CDCl3
Temp: 25 °C; 300 MHz
9.0
8.0
7.0
6.0
5.0
4.0
3.0
2.0
1.0
0.0

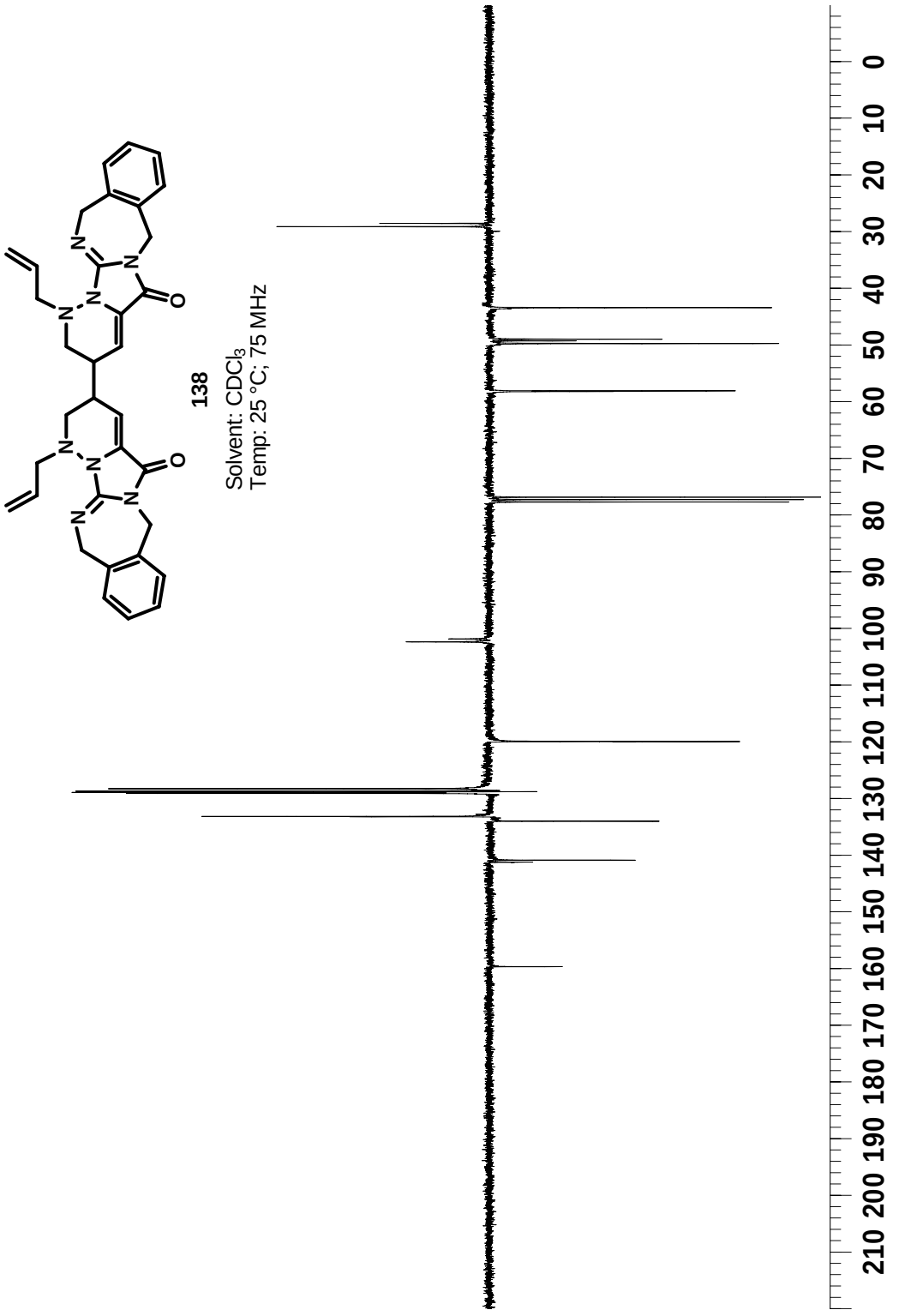
138
Solvent: CDCl3
Temp: 25 °C; 75 MHz
0
10
20
30
40
50
60
70
80
90
100
110
120
130
140
150
160
170
180
190
200
210

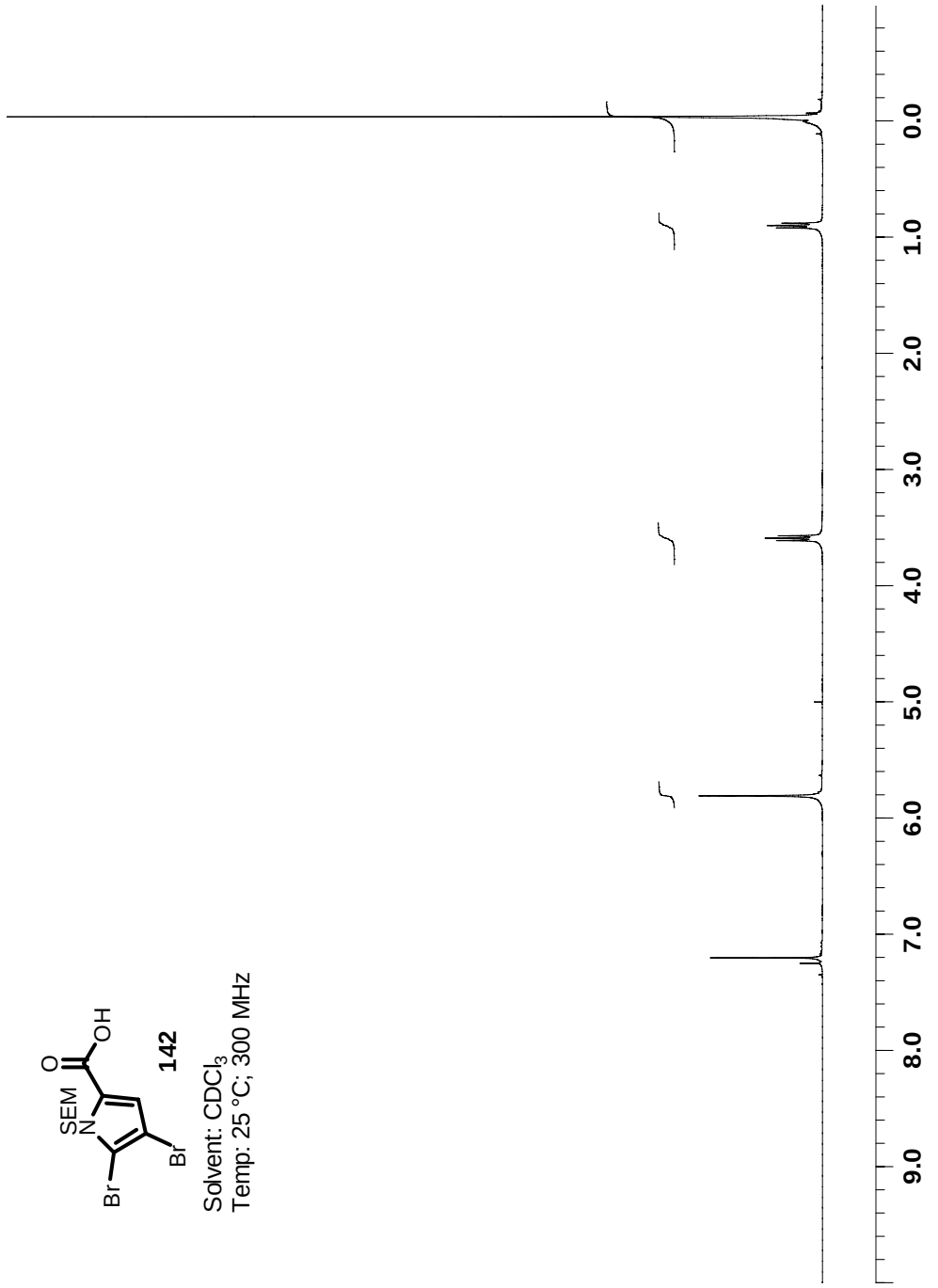
SEM
N
O
OH
Br
Br
142
Solvent: CDCl3
Temp: 25 °C; 300 MHz
9.0
8.0
7.0
6.0
5.0
4.0
3.0
2.0
1.0
0.0

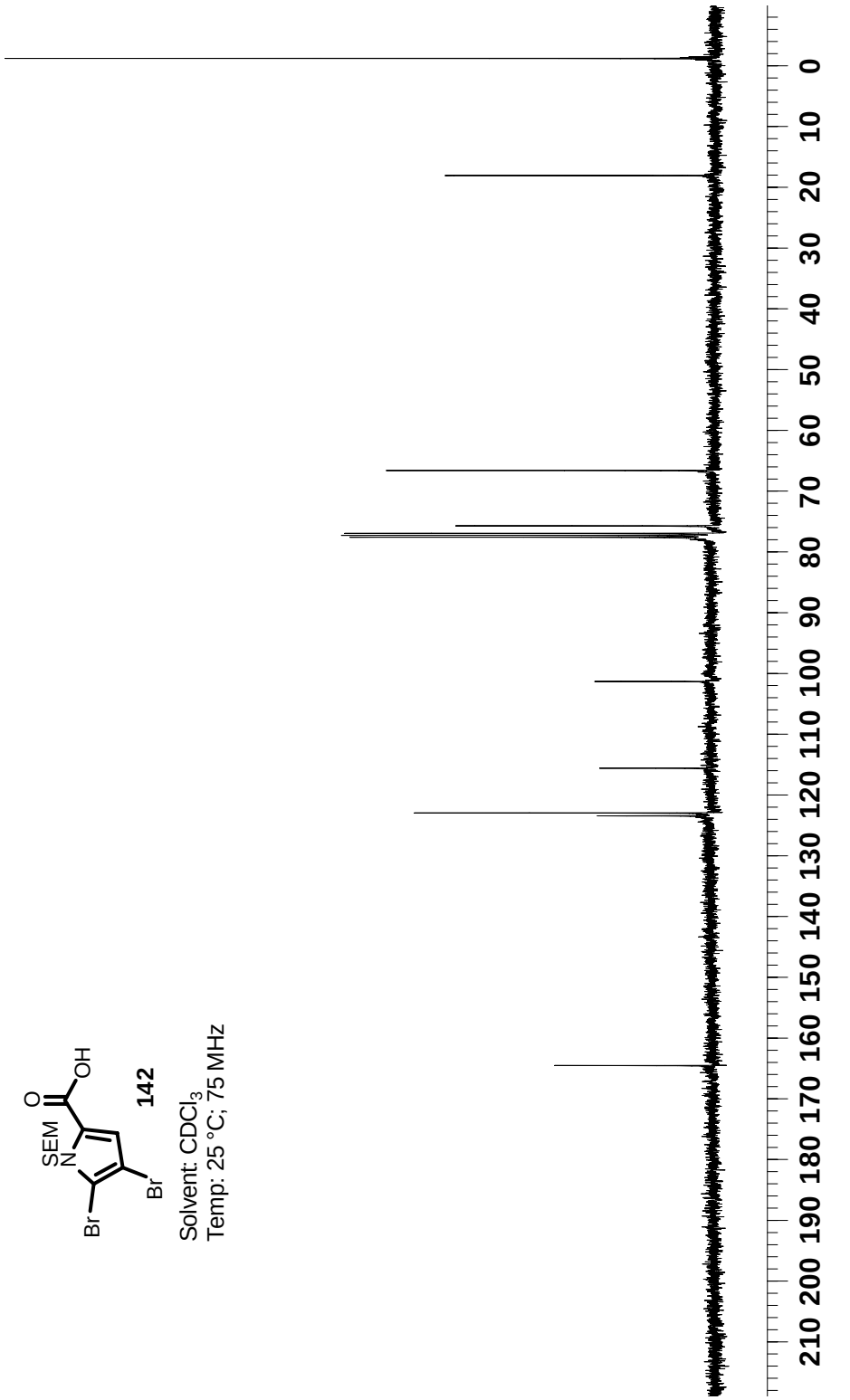
O
OH
SEM
N
Br
Br
142
Solvent: CDCl3
Temp: 25 °C; 75 MHz
210 200 190 180 170 160 150 140 130 120 110 100 90 80 70 60 50 40 30 20 10 0

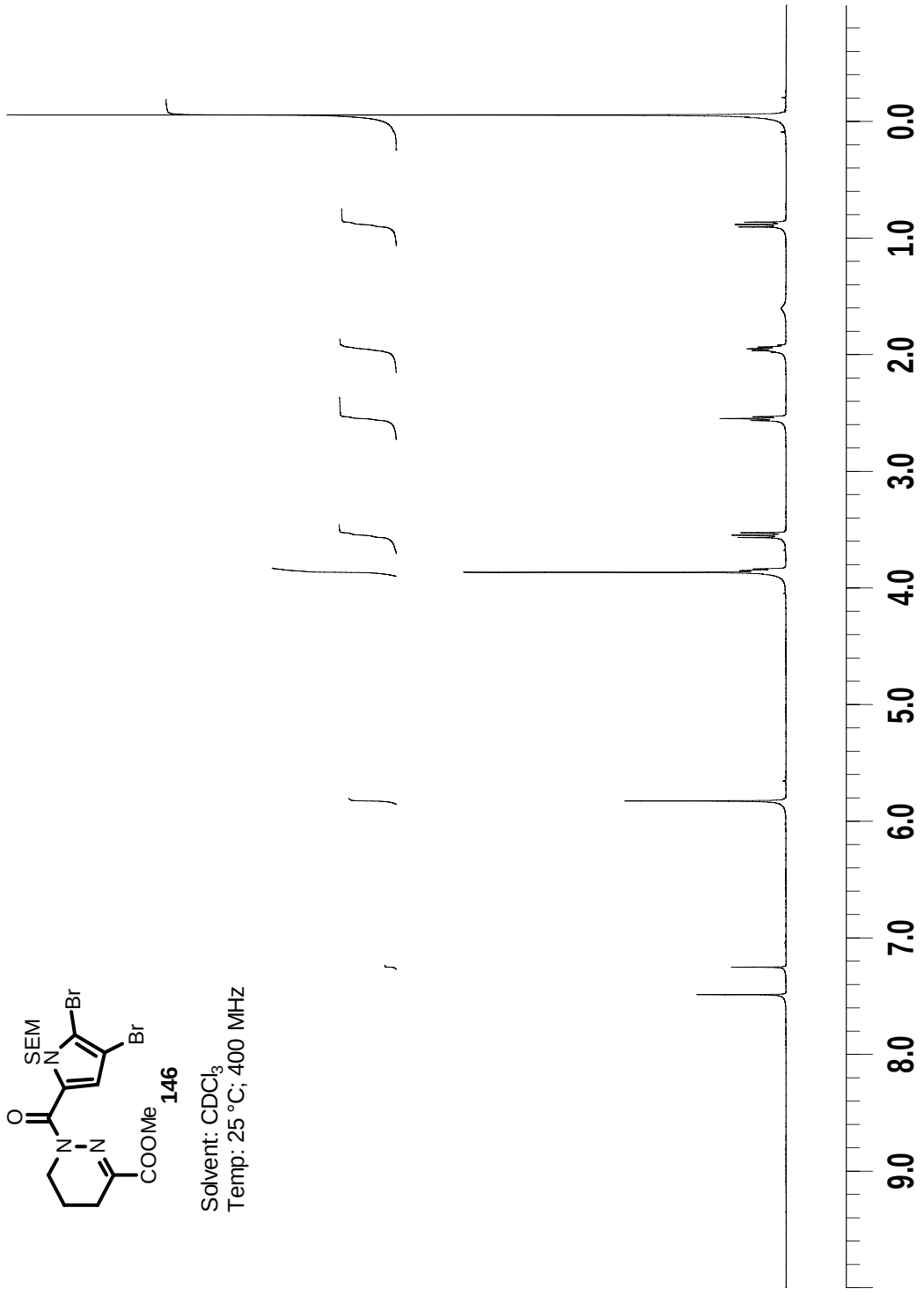
SEM
N
Br
Br
O
N
N
COOMe
146
Solvent: CDCl3
Temp: 25 °C; 400 MHz
9.0
8.0
7.0
6.0
5.0
4.0
3.0
2.0
1.0
0.0

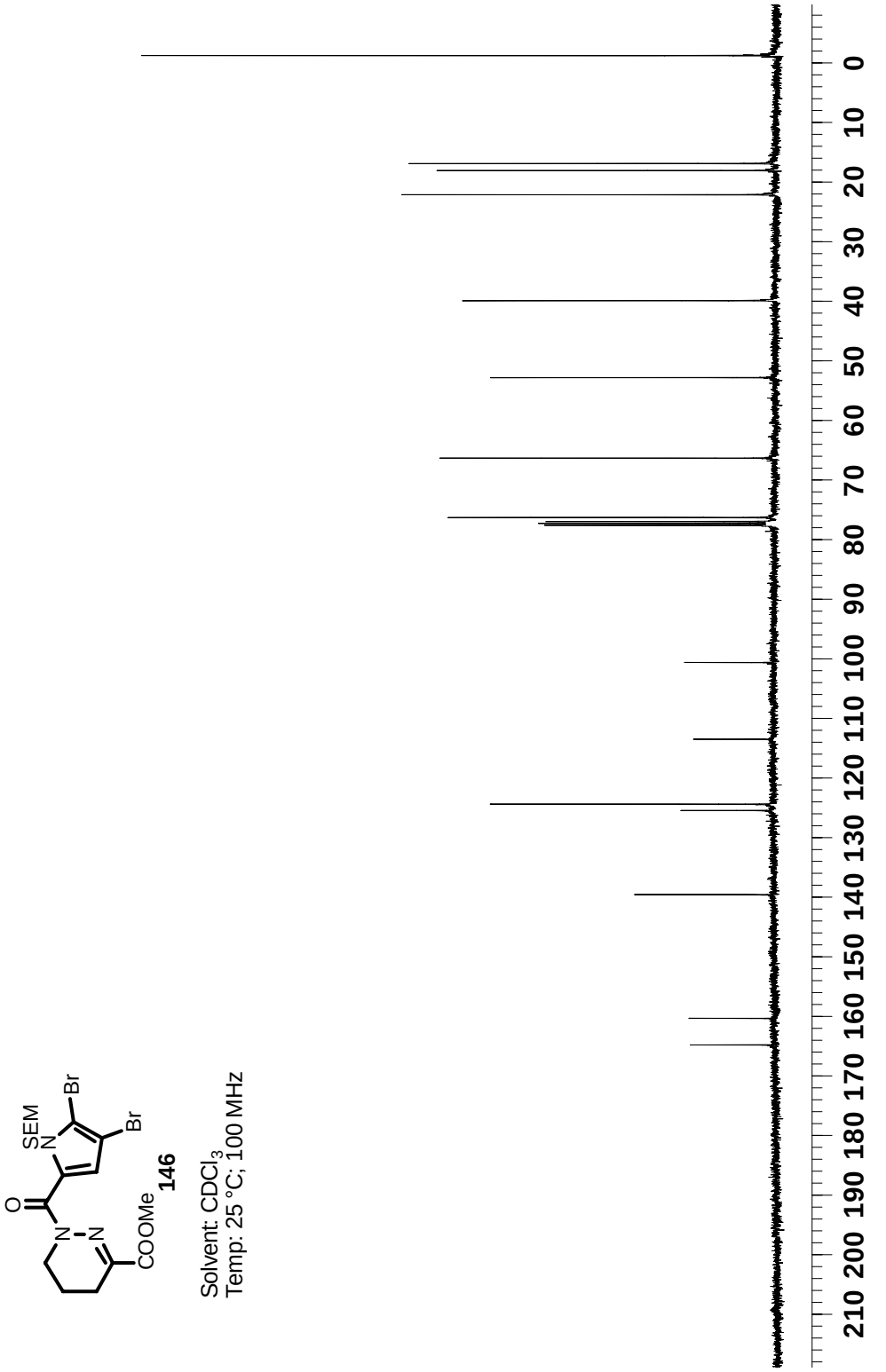
SEM
N
Br
Br
O
N
N
COOMe
146
Solvent: CDCl3
Temp: 25 °C; 100 MHz
210 200 190 180 170 160 150 140 130 120 110 100 90 80 70 60 50 40 30 20 10 0

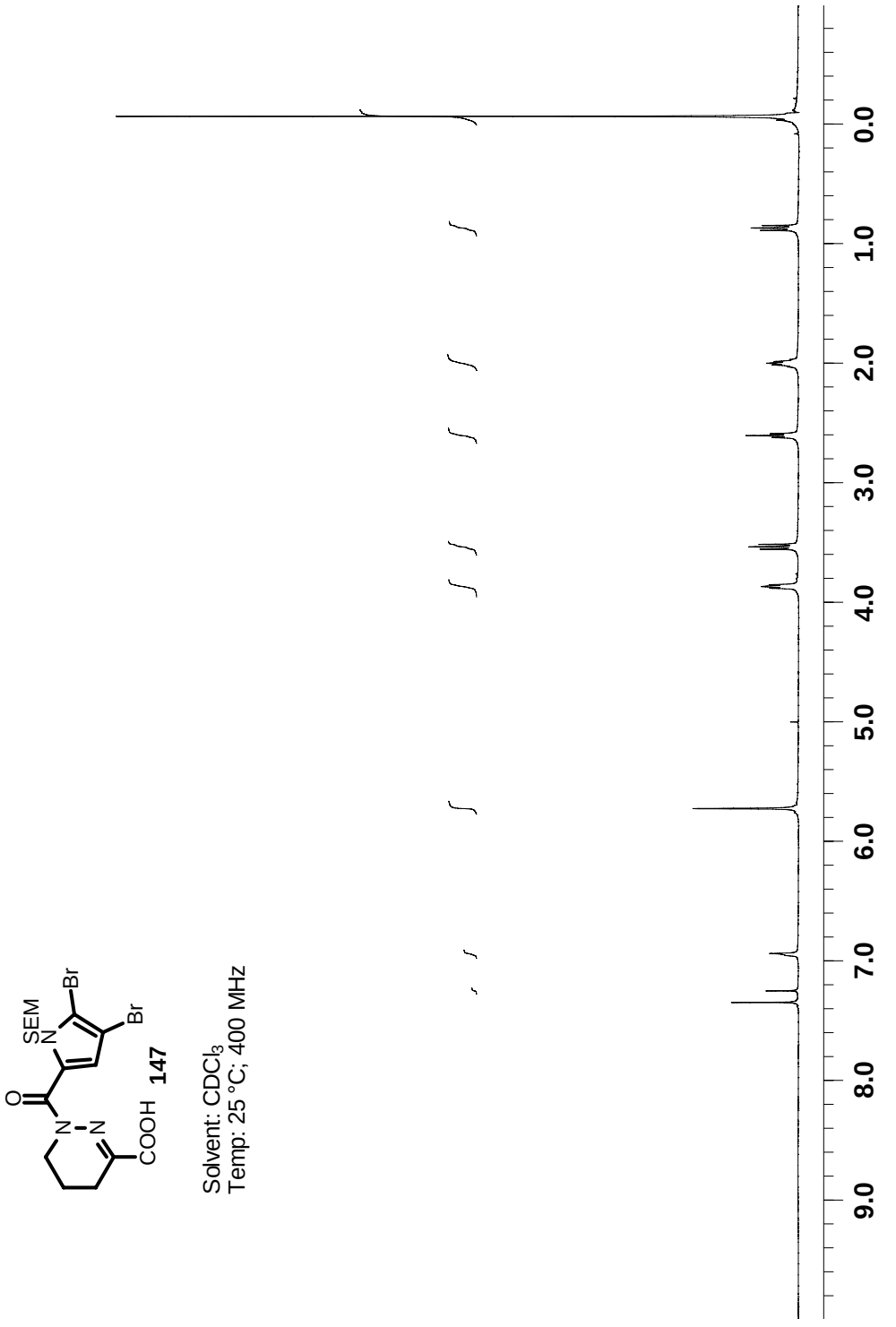
SEM
Br
Br
O
N
N
COOH
147
Solvent: CDCl3
Temp: 25 °C; 400 MHz
9.0
8.0
7.0
6.0
5.0
4.0
3.0
2.0
1.0
0.0

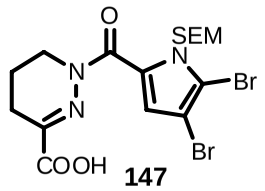

147

Solvent: $CDCl_3$
Temp: 25 °C; 100 MHz

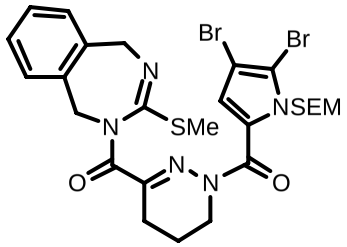

146

Solvent: $CDCl_3$
Temp: 25 °C; 400 MHz

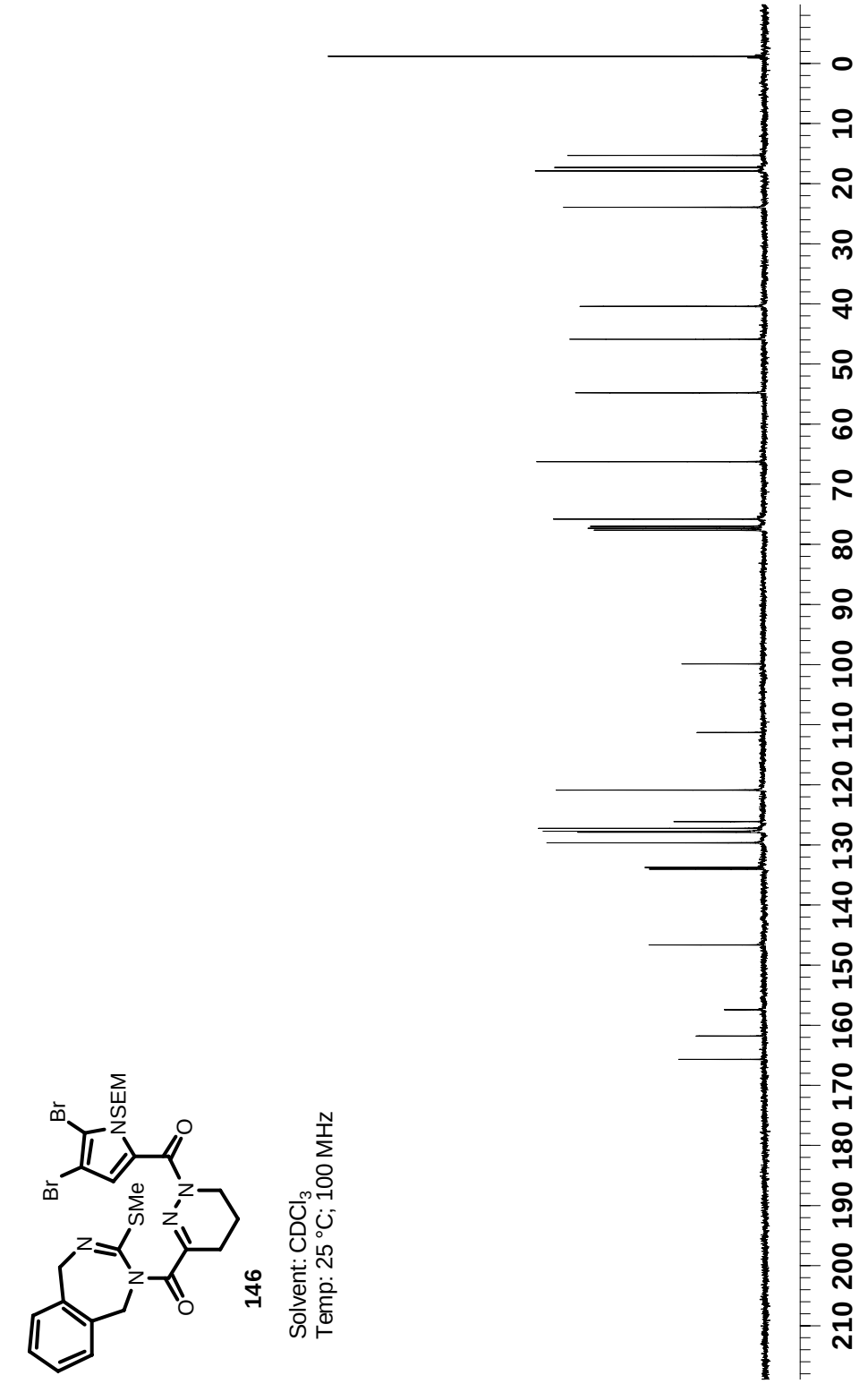
Br
Br
NSEM
SMe
N
N
N
O
O
146
Solvent: CDCl3
Temp: 25 °C; 100 MHz
210 200 190 180 170 160 150 140 130 120 110 100 90 80 70 60 50 40 30 20 10 0

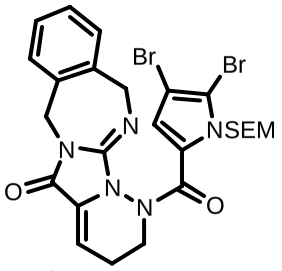

150

Solvent: CD_3CN
Temp: 70 °C; 400 MHz

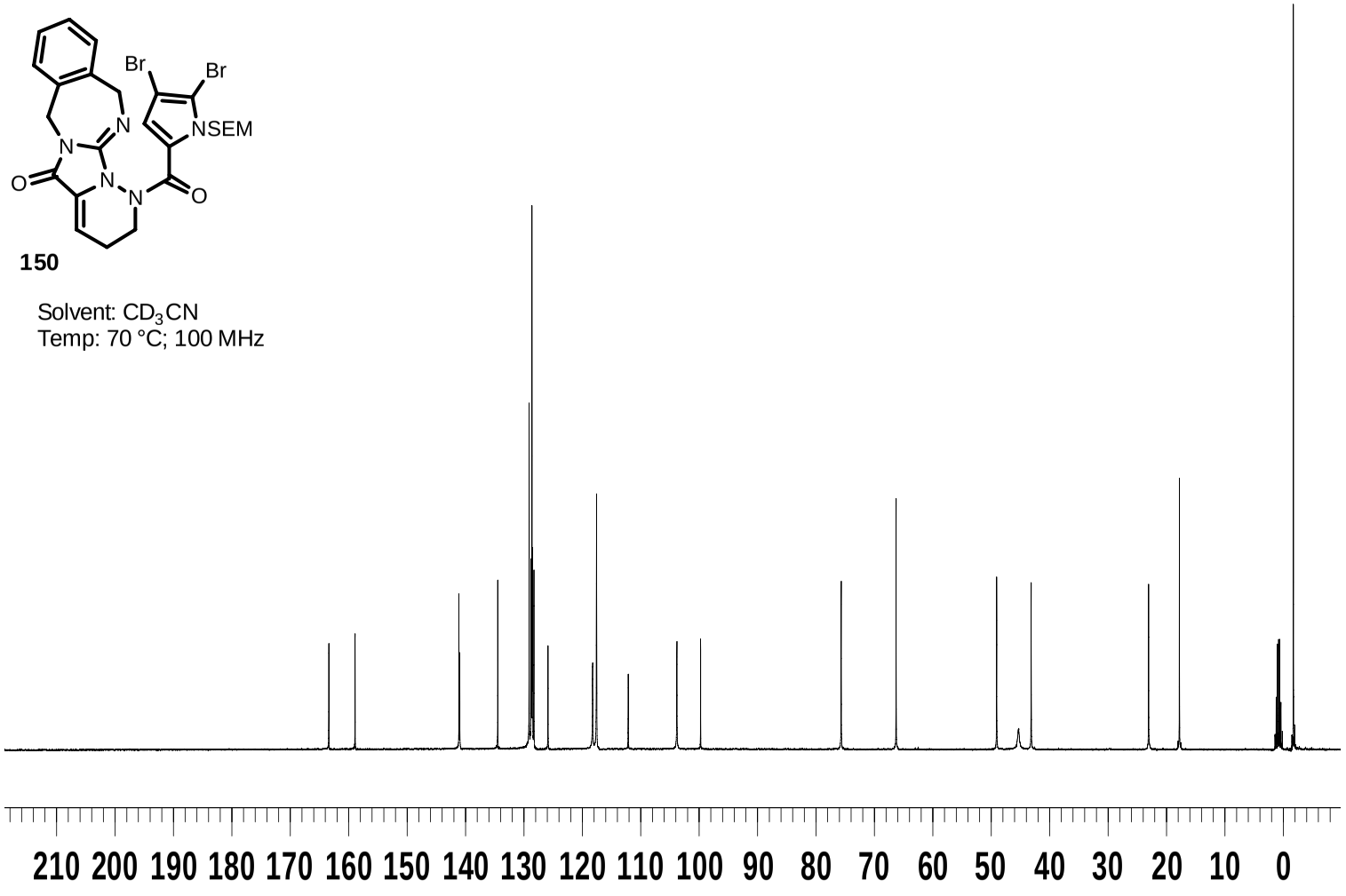
Br
Br
N
NSEM
N
N
N
O
O
150
Solvent: CD3CN
Temp: 70 °C; 100 MHz
210 200 190 180 170 160 150 140 130 120 110 100 90 80 70 60 50 40 30 20 10 0

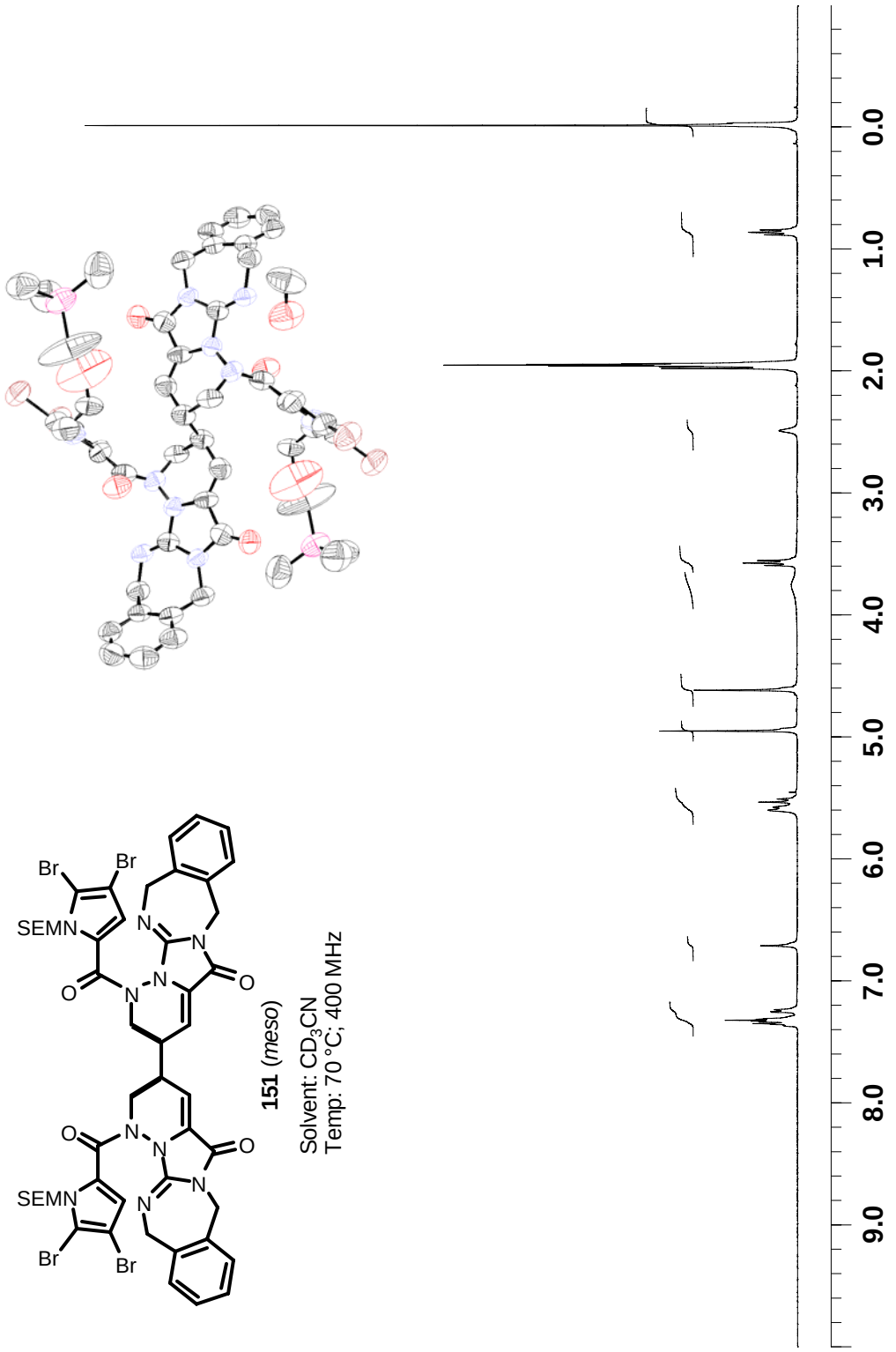
Br
Br
SEMN
N
N
N
N
O
O
O
N
N
N
N
O
SEMN
Br
Br
151 (meso)
Solvent: CD3CN
Temp: 70 °C; 400 MHz
0.0
1.0
2.0
3.0
4.0
5.0
6.0
7.0
8.0
9.0

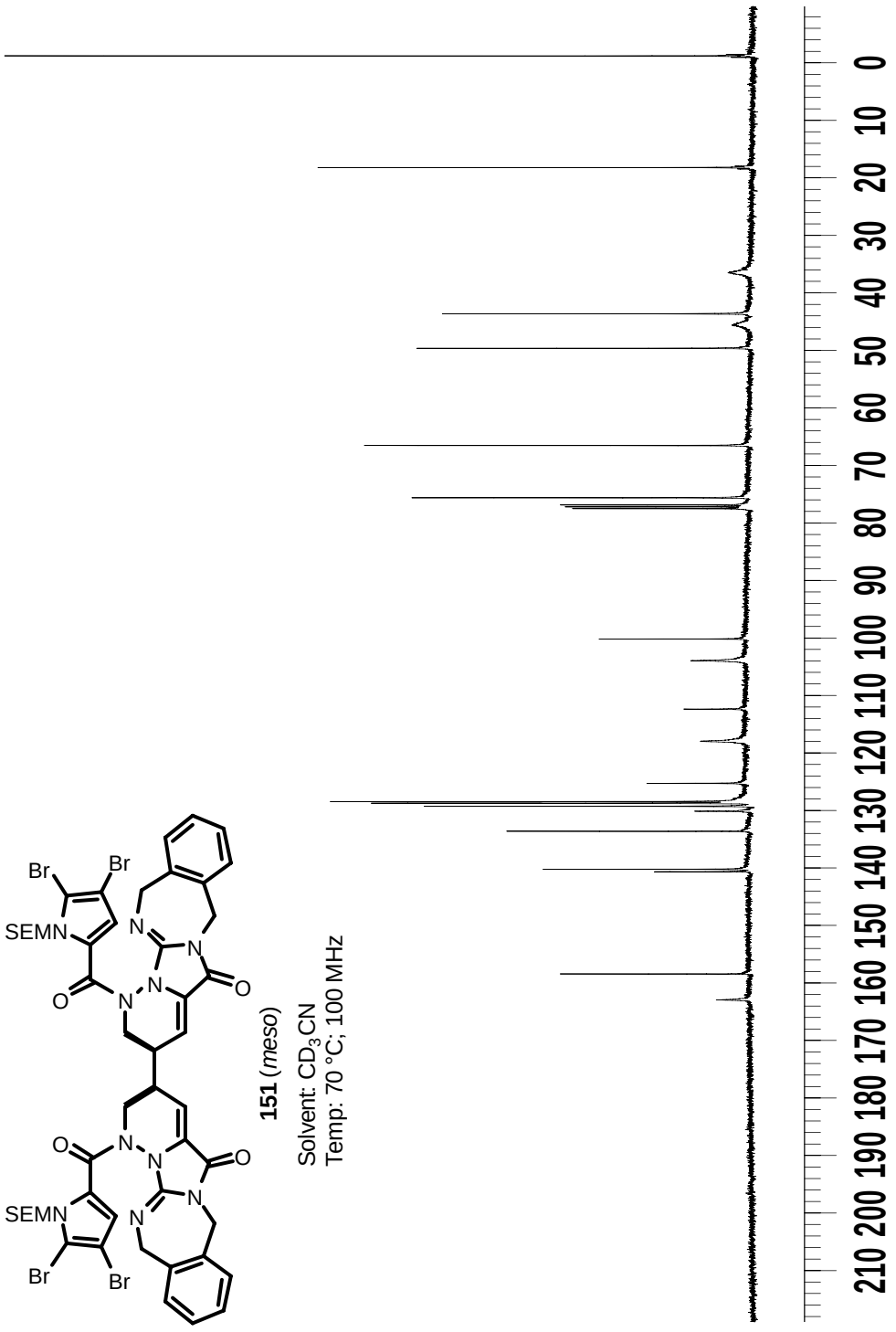
Br
Br
SEMN
O
N
N
N
N
O
O
N
N
O
SEMN
Br
Br
151 (meso)
Solvent: CD3CN
Temp: 70 °C; 100 MHz
0
10
20
30
40
50
60
70
80
90
100
110
120
130
140
150
160
170
180
190
200
210

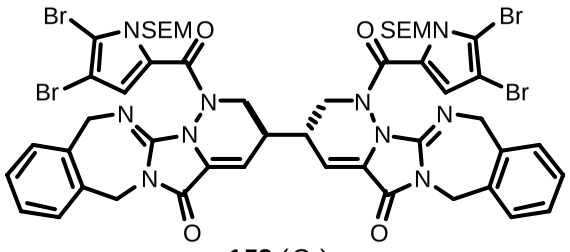

152 (C_2)

Solvent: CD_3CN
Temp: 70 °C; 400 MHz

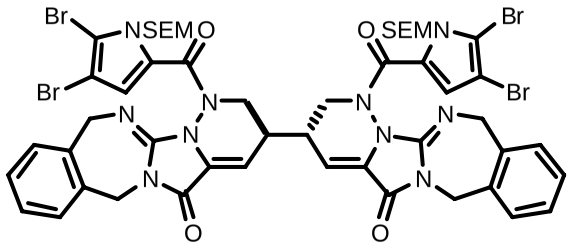

152 (C_2)

Solvent: CD_3CN
Temp: 70 °C; 100 MHz

APPENDIX B
X-ray Crystallographic Data for 136

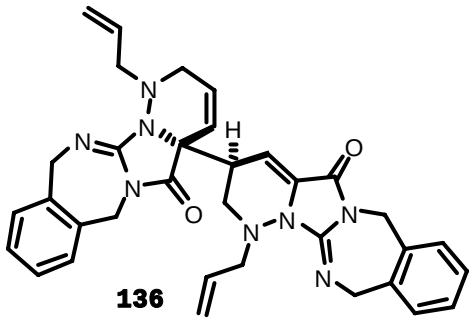

136

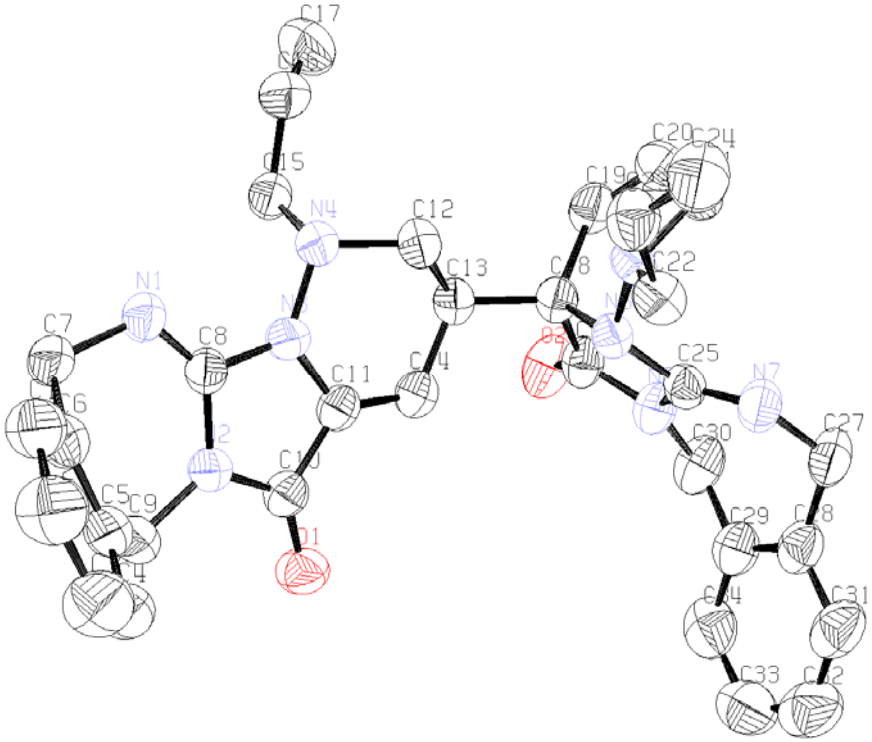

Table 1. Crystal data and structure refinement for 136

Empirical formula	C34 H34 N8 O2
Formula weight	586.70
Wavelength	0.71073 A
Crystal system, space group	Triclinic, P -1
Unit cell dimensions	a = 10.5970(4) Å alpha = 101.7740(18)°
	b = 11.4680(5) Å beta = 101.7910(16)°
	c = 13.4690(7) Å gamma = 97.4190(19)°
Volume	1543.47(12) A^3
Z, Calculated density	2, 1.262 Mg/m^3
Absorption coefficient	0.082 mm^-1

Intensity Measurements

Diffractometer	Enraf-Nonius
Detector	Kappa CCD
Radiation	RMoKa (l=0.71069A)
Temperature	293(2) K
Scan-Type	w-2theta
Theta range for data collection	2.91 to 25.81 deg.
Reflections collected / unique	5686 / 5686 [R(int) = 0.0900]

Structure Solution and Refinement

Refinement method	Full-matrix least-squares on F^2
Data / restraints / parameters	5686 / 0 / 533
Goodness-of-fit on F^2	0.992
Final R indices [I>2sigma(I)]	R1 = 0.0524, wR2 = 0.1257
R indices (all data)	R1 = 0.0851, wR2 = 0.1432
Largest diff. peak and hole	0.178 and -0.255 e.A^-3

Table 2. Atomic coordinates (x 10^4) and equivalent isotropic displacement parameters (Å^2 x 10^3) for qingyi6. U(eq) is defined as one third of the trace of the orthogonalized Uij tensor.

	x	y	z	U(eq)
C(1)	2543(3)	8596(3)	4703(2)	63(1)
C(2)	1572(3)	7623(3)	4592(3)	76(1)
C(3)	676(3)	7139(3)	3651(3)	78(1)
C(4)	747(3)	7662(3)	2810(2)	64(1)
C(5)	1713(2)	8635(2)	2912(2)	51(1)
C(6)	2623(3)	9113(2)	3868(2)	52(1)

C(7)	3693(3)	10165(2)	3959(2)	54(1)
C(8)	4318(2)	9391(2)	2403(2)	43(1)
C(9)	1824(3)	9195(3)	2008(2)	52(1)
C(10)	3133(3)	8669(2)	696(2)	45(1)
C(11)	4535(2)	8680(2)	726(2)	43(1)
C(12)	6991(3)	8332(3)	1416(2)	49(1)
C(13)	6587(3)	8384(2)	262(2)	45(1)
C(14)	5139(3)	8314(2)	-26(2)	46(1)
C(15)	7192(3)	10494(2)	2253(2)	51(1)
C(16)	8581(3)	10686(3)	2838(2)	66(1)
C(17)	9569(4)	11246(4)	2564(4)	95(1)
O(1)	2204(2)	8394(2)	-62(1)	59(1)
N(1)	4684(2)	9847(2)	3375(2)	48(1)
N(2)	3069(2)	9057(2)	1711(2)	44(1)
N(3)	5171(2)	9125(2)	1767(2)	49(1)
N(4)	6543(2)	9238(2)	2138(2)	47(1)
C(18)	7072(2)	7433(2)	-481(2)	44(1)
C(19)	8554(3)	7646(3)	-339(2)	55(1)
C(20)	9252(3)	6805(3)	-166(2)	60(1)
C(21)	8691(3)	5660(3)	61(3)	56(1)
C(22)	6810(3)	4773(3)	653(2)	54(1)

C(23)	7467(3)	4839(3)	1758(2)	61(1)
C(24)	8010(4)	3985(3)	2076(3)	79(1)
C(25)	6291(2)	5461(2)	-1516(2)	44(1)
C(26)	6513(3)	7436(2)	-1617(2)	52(1)
C(27)	5910(4)	3660(3)	-2838(2)	66(1)
C(28)	4645(3)	3797(2)	-3498(2)	59(1)
C(29)	4503(3)	4915(2)	-3719(2)	60(1)
C(30)	5626(4)	5967(3)	-3314(2)	66(1)
C(31)	3610(4)	2829(3)	-3888(2)	75(1)
C(32)	2459(4)	2956(5)	-4500(3)	90(1)
C(33)	2309(4)	4059(5)	-4730(3)	90(1)
C(34)	3334(4)	5048(4)	-4333(2)	79(1)
O(2)	6492(2)	8328(2)	-1977(1)	73(1)
N(5)	7434(2)	5795(2)	313(2)	45(1)
N(6)	6593(2)	6174(2)	-483(2)	42(1)
N(7)	6212(2)	4329(2)	-1742(2)	56(1)
N(8)	6089(2)	6272(2)	-2167(2)	51(1)

Table 3. Bond lengths [Å] for qingyi6. Estimated standard deviations in the least significant figures are given in parentheses.

C(1)-C(2)	1.379(4)	C(13)-C(14)	1.492(4)
C(1)-C(6)	1.386(4)	C(13)-C(18)	1.537(3)
C(2)-C(3)	1.378(5)	C(15)-N(4)	1.477(3)
C(3)-C(4)	1.396(4)	C(15)-C(16)	1.485(4)
C(4)-C(5)	1.377(4)	C(16)-C(17)	1.314(5)
C(5)-C(6)	1.400(3)	N(3)-N(4)	1.417(3)
C(5)-C(9)	1.505(4)	C(18)-N(6)	1.467(3)
C(6)-C(7)	1.512(4)	C(18)-C(19)	1.523(4)
C(7)-N(1)	1.474(3)	C(18)-C(26)	1.524(3)
C(8)-N(1)	1.265(3)	C(19)-C(20)	1.318(4)
C(8)-N(3)	1.388(3)	C(20)-C(21)	1.486(4)
C(8)-N(2)	1.409(3)	C(21)-N(5)	1.459(3)
C(9)-N(2)	1.473(3)	C(22)-N(5)	1.470(3)
C(10)-O(1)	1.220(3)	C(22)-C(23)	1.492(4)
C(10)-N(2)	1.367(3)	C(23)-C(24)	1.300(4)
C(10)-C(11)	1.476(4)	C(25)-N(7)	1.259(3)
C(11)-C(14)	1.331(3)	C(25)-N(8)	1.409(3)
C(11)-N(3)	1.383(3)	C(25)-N(6)	1.411(3)
C(12)-N(4)	1.467(3)	C(26)-O(2)	1.220(3)
C(12)-C(13)	1.542(4)	C(26)-N(8)	1.356(3)

C(27)-N(7)	1.467(3)	C(30)-N(8)	1.476(3)
C(27)-C(28)	1.495(4)	C(31)-C(32)	1.369(5)
C(28)-C(31)	1.386(4)	C(32)-C(33)	1.383(5)
C(28)-C(29)	1.394(4)	C(33)-C(34)	1.396(5)
C(29)-C(34)	1.386(4)	N(5)-N(6)	1.426(3)
C(29)-C(30)	1.505(4)		

Table 4. Bond Angles [°] for qingyi6. Estimated standard deviations in the least significant figures are given in parentheses.

C(2)-C(1)-C(6)	120.2(3)	N(1)-C(7)-C(6)	113.9(2)
C(3)-C(2)-C(1)	120.8(3)	N(1)-C(8)-N(3)	123.8(2)
C(2)-C(3)-C(4)	119.1(3)	N(1)-C(8)-N(2)	132.1(2)
C(5)-C(4)-C(3)	120.5(3)	N(3)-C(8)-N(2)	104.0(2)
C(4)-C(5)-C(6)	119.8(3)	N(2)-C(9)-C(5)	110.7(2)
C(4)-C(5)-C(9)	121.4(2)	O(1)-C(10)-N(2)	125.7(2)
C(6)-C(5)-C(9)	118.8(2)	O(1)-C(10)-C(11)	128.5(2)
C(1)-C(6)-C(5)	119.4(3)	N(2)-C(10)-C(11)	105.7(2)
C(1)-C(6)-C(7)	121.5(3)	C(14)-C(11)-N(3)	123.9(2)
C(5)-C(6)-C(7)	119.1(2)	C(14)-C(11)-C(10)	131.1(2)

N(3)-C(11)-C(10) 105.0(2)
N(4)-C(12)-C(13) 114.3(2)
C(14)-C(13)-C(18) 113.1(2)
C(14)-C(13)-C(12) 108.2(2)
C(18)-C(13)-C(12) 113.6(2)
C(11)-C(14)-C(13) 118.6(2)
N(4)-C(15)-C(16) 110.4(2)
C(17)-C(16)-C(15) 124.2(4)
C(8)-N(1)-C(7) 119.0(2)
C(10)-N(2)-C(8) 112.4(2)
C(10)-N(2)-C(9) 122.3(2)
C(8)-N(2)-C(9) 125.1(2)
C(11)-N(3)-C(8) 112.8(2)
C(11)-N(3)-N(4) 122.9(2)
C(8)-N(3)-N(4) 124.1(2)
N(3)-N(4)-C(12) 107.6(2)
N(3)-N(4)-C(15) 109.9(2)
C(12)-N(4)-C(15) 113.9(2)
N(6)-C(18)-C(19) 110.0(2)
N(6)-C(18)-C(26) 100.8(2)
C(19)-C(18)-C(26) 105.4(2)
N(6)-C(18)-C(13) 114.6(2)
C(19)-C(18)-C(13) 113.8(2)
C(26)-C(18)-C(13) 111.0(2)
C(20)-C(19)-C(18) 122.1(3)
C(19)-C(20)-C(21) 122.5(3)
N(5)-C(21)-C(20) 108.4(2)
N(5)-C(22)-C(23) 109.4(2)
C(24)-C(23)-C(22) 124.6(3)
N(7)-C(25)-N(8) 130.4(2)
N(7)-C(25)-N(6) 123.7(2)
N(8)-C(25)-N(6) 105.8(2)
O(2)-C(26)-N(8) 125.8(2)
O(2)-C(26)-C(18) 125.9(2)
N(8)-C(26)-C(18) 108.2(2)
N(7)-C(27)-C(28) 115.4(2)
C(31)-C(28)-C(29) 119.6(3)
C(31)-C(28)-C(27) 120.9(3)
C(29)-C(28)-C(27) 119.5(3)
C(34)-C(29)-C(28) 119.8(3)
C(34)-C(29)-C(30) 120.1(3)
C(28)-C(29)-C(30) 120.1(3)

N(8)-C(30)-C(29) 113.0(2)

C(32)-C(31)-C(28) 120.7(4)

C(31)-C(32)-C(33) 120.2(4)

C(32)-C(33)-C(34) 119.9(4)

C(29)-C(34)-C(33) 119.8(4)

N(6)-N(5)-C(21) 111.3(2)

N(6)-N(5)-C(22) 114.4(2)

C(21)-N(5)-C(22) 114.9(2)

C(25)-N(6)-N(5) 118.6(2)

C(25)-N(6)-C(18) 109.1(2)

N(5)-N(6)-C(18) 110.6(2)

C(25)-N(7)-C(27) 120.1(2)

C(26)-N(8)-C(25) 111.2(2)

C(26)-N(8)-C(30) 121.2(2)

C(25)-N(8)-C(30) 127.3(2)

Table 5. Anisotropic displacement parameters ($Å^2$ x 10^3) for 136. The anisotropic displacement factor exponent takes the form: -2 pi^2 [h^2 a*2 U11 + ... + 2 h k a* b* U12]

	U11	U22	U33	U23	U13	U12
C(1)	59(2)	83(2)	49(2)	15(2)	21(2)	6(2)
C(2)	76(2)	96(2)	62(2)	30(2)	28(2)	4(2)
C(3)	73(2)	85(2)	77(2)	19(2)	33(2)	-9(2)
C(4)	55(2)	75(2)	60(2)	10(2)	20(2)	0(2)
C(5)	45(2)	59(2)	50(2)	8(1)	18(1)	8(1)
C(6)	50(2)	58(2)	50(2)	8(1)	20(1)	9(1)
C(7)	53(2)	60(2)	45(2)	1(1)	15(1)	7(1)
C(8)	44(2)	39(1)	45(2)	7(1)	14(1)	7(1)
C(9)	44(2)	61(2)	52(2)	11(1)	15(1)	11(1)
C(10)	48(2)	43(1)	42(2)	10(1)	11(1)	6(1)
C(11)	49(2)	34(1)	44(2)	9(1)	11(1)	4(1)
C(12)	52(2)	49(2)	51(2)	11(1)	17(1)	16(1)
C(13)	50(2)	42(1)	46(2)	9(1)	17(1)	10(1)
C(14)	55(2)	41(1)	44(2)	10(1)	14(1)	7(1)
C(15)	49(2)	48(2)	51(2)	2(1)	15(1)	5(1)

C(16)	50(2)	72(2)	65(2)	1(2)	9(2)	6(2)
C(17)	57(2)	97(3)	123(4)	1(2)	26(2)	14(2)
O(1)	50(1)	76(1)	45(1)	10(1)	7(1)	6(1)
N(1)	49(1)	50(1)	44(1)	3(1)	16(1)	7(1)
N(2)	41(1)	48(1)	42(1)	7(1)	10(1)	8(1)
N(3)	40(1)	59(1)	43(1)	2(1)	9(1)	7(1)
N(4)	42(1)	47(1)	48(1)	5(1)	12(1)	8(1)
C(18)	47(2)	41(1)	47(2)	10(1)	19(1)	5(1)
C(19)	54(2)	46(2)	63(2)	5(1)	26(1)	-6(2)
C(20)	44(2)	68(2)	67(2)	4(1)	25(1)	4(2)
C(21)	46(2)	57(2)	63(2)	6(2)	17(2)	12(1)
C(22)	53(2)	53(2)	61(2)	21(1)	16(1)	11(1)
C(23)	74(2)	61(2)	51(2)	14(2)	20(2)	19(2)
C(24)	105(3)	75(2)	57(2)	20(2)	8(2)	34(2)
C(25)	43(2)	45(2)	47(2)	10(1)	19(1)	9(1)
C(26)	65(2)	46(2)	52(2)	11(1)	27(1)	10(1)
C(27)	85(2)	49(2)	60(2)	-3(1)	18(2)	17(2)
C(28)	68(2)	56(2)	47(2)	1(1)	19(1)	8(2)
C(29)	73(2)	66(2)	41(2)	5(1)	20(2)	13(2)
C(30)	93(3)	64(2)	43(2)	13(1)	22(2)	8(2)
C(31)	87(3)	72(2)	55(2)	-5(2)	21(2)	0(2)

C(32)	81(3)	110(3)	63(2)	-4(2)	19(2)	-3(3)
C(33)	70(3)	136(4)	54(2)	1(2)	12(2)	24(3)
C(34)	95(3)	96(3)	48(2)	13(2)	18(2)	32(2)
O(2)	114(2)	48(1)	62(1)	20(1)	29(1)	8(1)
N(5)	36(1)	50(1)	53(1)	15(1)	15(1)	12(1)
N(6)	43(1)	39(1)	45(1)	11(1)	15(1)	9(1)
N(7)	65(2)	47(1)	55(1)	4(1)	15(1)	14(1)
N(8)	66(2)	46(1)	45(1)	11(1)	20(1)	9(1)

Table 6. Hydrogen coordinates (x 10^4) and isotropic displacement parameters (A^2 x 10^3) for 136

	x	y	z	U(eq)
H(1)	3180(30)	8920(30)	5390(30)	82(9)
H(2)	1510(30)	7270(30)	5180(30)	90(10)
H(3)	-30(30)	6470(30)	3590(20)	98(11)
H(4)	70(30)	7300(20)	2090(20)	74(8)
H(71)	4190(20)	10503(19)	4709(19)	42(6)
H(72)	3270(30)	10870(20)	3722(19)	64(8)

H(91)	1810(30)	10120(30)	2160(20)	67(8)
H(92)	1020(30)	8760(20)	1350(20)	64(8)
H(121)	6650(20)	7570(20)	1510(17)	49(7)
H(122)	7980(30)	8460(20)	1675(19)	61(8)
H(13)	7010(20)	9170(20)	189(19)	63(8)
H(14)	4590(20)	8002(19)	-739(19)	44(6)
H(151)	6720(20)	11020(20)	2660(20)	56(7)
H(152)	7170(20)	10730(20)	1580(20)	58(7)
H(16)	8780(30)	10260(20)	3450(20)	67(8)
H(171)	10500(40)	11430(30)	2980(20)	90(10)
H(172)	9440(60)	11490(50)	1830(50)	200(30)
H(19)	8940(20)	8420(20)	-453(17)	50(7)
H(20)	10160(30)	6950(20)	-160(20)	69(8)
H(211)	8610(20)	4960(20)	-544(18)	47(6)
H(212)	9320(30)	5540(20)	710(20)	63(8)
H(221)	5870(30)	4930(20)	627(19)	64(8)
H(222)	6850(30)	3960(30)	180(20)	65(8)
H(23)	7420(30)	5530(30)	2250(30)	95(11)
H(241)	8400(30)	4060(30)	2810(30)	91(10)
H(242)	8070(30)	3200(30)	1530(30)	104(11)
H(271)	5900(30)	2830(30)	-2820(20)	80(9)

H(272)	6620(30)	3940(30)	-3170(30)	99(12)
H(301)	6400(30)	5800(30)	-3570(20)	81(10)
H(302)	5390(30)	6740(30)	-3540(20)	79(9)
H(31)	3670(30)	2000(30)	-3720(20)	95(11)
H(32)	1680(40)	2290(40)	-4810(30)	125(14)
H(33)	1510(40)	4230(30)	-5160(30)	133(15)
H(34)	3290(30)	5850(30)	-4490(20)	78(10)

APPENDIX C
X-ray Crystallographic Data for 137

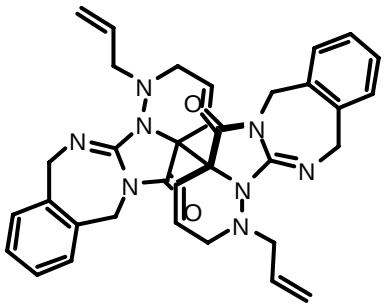

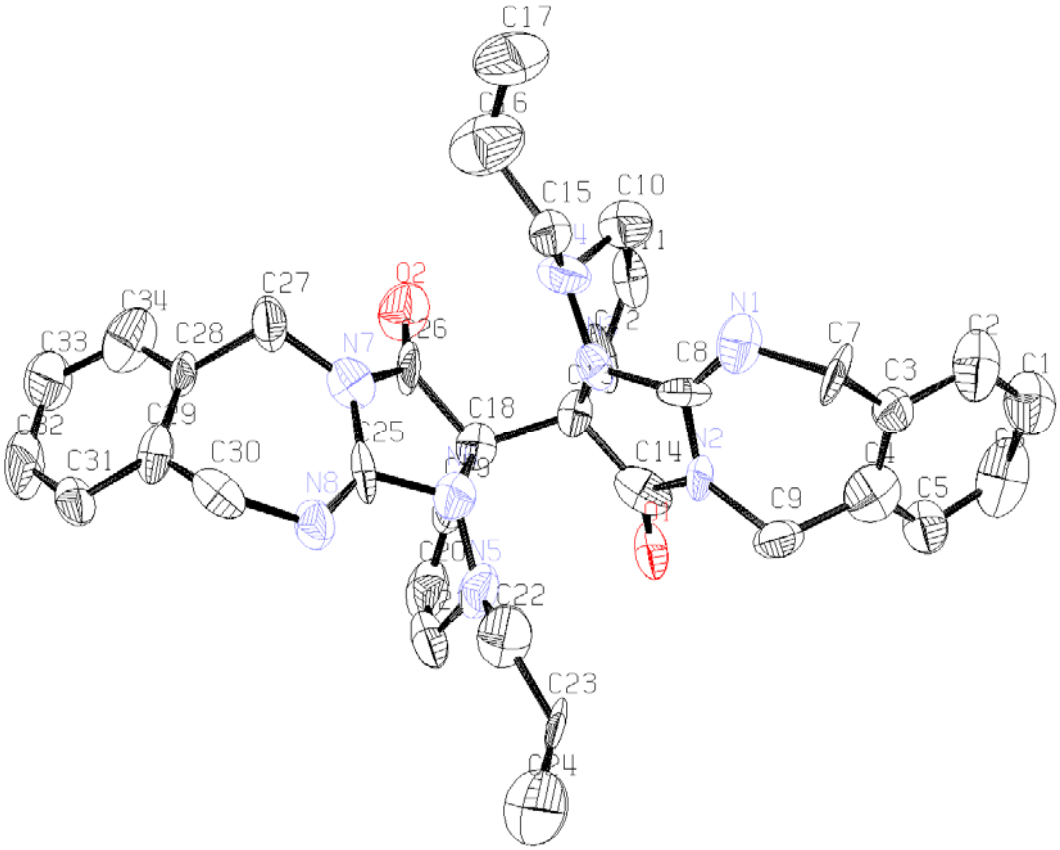

Table 1. Crystal data and structure refinement for 137

Empirical formula	C34 H32 N8 O2
Formula weight	584.68
Wavelength	0.71073 A
Crystal system, space group	Monoclinic, C c
Unit cell dimensions	a = 12.1990(10) A
	b = 11.3930(10) A beta = 90.771(3)°
	c = 21.935(3) A
Volume	3048.3(5) A^3
Z, Calculated density	4, 1.274 Mg/m^3
Absorption coefficient	0.083 mm^-1

Intensity Measurements

Diffractometer	Enraf-Nonius
Detector	Kappa CCD
Radiation	RMoKa (l=0.71069A)
Temperature	293(2) K
Scan-Type	w-2theta
Theta range for data collection	3.06 to 25.81 deg.
Reflections collected / unique	2782 / 2782 [R(int) = 0.0600]

Structure Solution and Refinement

Refinement method	Full-matrix least-squares on F^2
Data / restraints / parameters	2782 / 2 / 501
Goodness-of-fit on F^2	0.989
Final R indices [I>2sigma(I)]	R1 = 0.0501, wR2 = 0.1144
R indices (all data)	R1 = 0.0822, wR2 = 0.1375
Largest diff. peak and hole	0.171 and -0.170 e.A^-3

Table 2. Atomic coordinates (x 10^4) and equivalent isotropic displacement parameters (Å^2 x 10^3) for 137. U(eq) is defined as one third of the trace of the orthogonalize Uij tensor.

	x	y	z	U(eq)
C(1)	9538(16)	6617(17)	4198(9)	70(5)
C(2)	8676(15)	7417(15)	4238(10)	75(6)
C(3)	8186(13)	7645(16)	4803(8)	54(5)
C(4)	8629(15)	7049(14)	5310(9)	64(5)
C(5)	9465(14)	6192(15)	5265(8)	55(5)
C(6)	9880(15)	6026(12)	4686(11)	77(7)
C(7)	7342(11)	8598(16)	4861(9)	57(5)

C(8)	6100(12)	7445(14)	5497(7)	46(4)
C(9)	8037(12)	7306(15)	5917(8)	50(4)
C(10)	4364(17)	6276(17)	4791(9)	69(5)
C(11)	4792(14)	5074(14)	5030(9)	55(5)
C(12)	5102(13)	4888(12)	5592(9)	54(5)
C(13)	5234(12)	5978(15)	6020(7)	51(4)
C(14)	6463(14)	6040(13)	6177(7)	51(4)
C(15)	3747(13)	8149(18)	5179(8)	60(5)
C(16)	2541(17)	8060(17)	4951(11)	93(7)
C(17)	2210(20)	8570(30)	4438(11)	111(8)
C(18)	4506(11)	5952(12)	6591(7)	42(4)
C(19)	4697(14)	5010(20)	7034(12)	66(6)
C(20)	5068(14)	5080(20)	7605(11)	73(6)
C(21)	5440(14)	6181(17)	7834(9)	57(5)
C(22)	6089(17)	8192(16)	7457(10)	73(6)
C(23)	7181(12)	8040(20)	7730(9)	94(8)
C(24)	7520(20)	8680(30)	8204(15)	142(12)
C(25)	3641(12)	7484(12)	7145(7)	42(4)
C(26)	3271(12)	5981(16)	6425(7)	53(4)
C(27)	1690(14)	7283(17)	6714(8)	55(5)
C(28)	1201(10)	7045(13)	7317(6)	39(4)

C(29)	1553(12)	7657(13)	7836(8)	46(4)
C(30)	2478(14)	8548(13)	7766(7)	51(5)
C(31)	1105(13)	7417(14)	8403(7)	50(5)
C(32)	280(16)	6605(19)	8443(10)	80(6)
C(33)	-157(15)	6060(20)	7916(9)	90(7)
C(34)	367(15)	6284(16)	7368(10)	73(6)
N(1)	6256(11)	8124(12)	5047(7)	54(4)
N(2)	6878(9)	6951(12)	5890(6)	46(4)
N(3)	5083(10)	7059(9)	5696(5)	38(3)
N(4)	4141(11)	7022(12)	5319(6)	52(3)
N(5)	5557(10)	7000(12)	7350(7)	56(4)
N(6)	4665(10)	7053(11)	6935(6)	53(4)
N(7)	2867(10)	6977(10)	6722(6)	47(3)
N(8)	3557(10)	8156(12)	7586(6)	47(4)
O(1)	7014(8)	5292(10)	6481(5)	58(3)
O(2)	2785(9)	5312(10)	6132(5)	68(4)

Table 3. Bond lengths [Å] for 137. Estimated standard deviations in the least significant figures are given in parentheses.

C(1)-C(6)	1.33(3)	C(14)-O(1)	1.27(1)
C(1)-C(2)	1.40(3)	C(14)-N(2)	1.31(1)
C(2)-C(3)	1.41(2)	C(15)-N(4)	1.40(2)
C(3)-C(4)	1.41(2)	C(15)-C(16)	1.55(3)
C(3)-C(7)	1.50(2)	C(16)-C(17)	1.32(3)
C(4)-C(5)	1.42(2)	C(18)-N(6)	1.47(1)
C(4)-C(9)	1.55(2)	C(18)-C(19)	1.46(3)
C(5)-C(6)	1.39(3)	C(18)-C(26)	1.55(2)
C(7)-N(1)	1.49(2)	C(19)-C(20)	1.33(3)
C(8)-N(1)	1.27(1)	C(20)-C(21)	1.42(3)
C(8)-N(3)	1.39(2)	C(21)-N(5)	1.42(2)
C(8)-N(2)	1.39(1)	C(22)-C(23)	1.46(3)
C(9)-N(2)	1.47(1)	C(22)-N(5)	1.52(2)
C(10)-N(4)	1.47(2)	C(23)-C(24)	1.33(4)
C(10)-C(11)	1.55(2)	C(25)-N(8)	1.24(1)
C(11)-C(12)	1.30(2)	C(25)-N(7)	1.44(2)
C(12)-C(13)	1.57(2)	C(25)-N(6)	1.42(2)
C(13)-N(3)	1.43(2)	C(26)-O(2)	1.15(2)
C(13)-C(18)	1.54(9)	C(26)-N(7)	1.40(2)
C(13)-C(14)	1.54(2)	C(27)-N(7)	1.48(2)

C(27)-C(28)	1.48(2)	C(31)-C(32)	1.37(3)
C(28)-C(29)	1.40(2)	C(32)-C(33)	1.41(3)
C(28)-C(34)	1.34(2)	C(33)-C(34)	1.39(3)
C(29)-C(31)	1.39(2)	N(3)-N(4)	1.40(2)
C(29)-C(30)	1.53(2)	N(5)-N(6)	1.41(2)
C(30)-N(8)	1.45(2)		

Table 4. Bond Angles [°] for 137. Estimated standard deviations in the least significant figures are given in parentheses.

C(6)-C(1)-C(2)	120.6(18)	N(1)-C(8)-N(3)	125.4(14)
C(3)-C(2)-C(1)	120.3(18)	N(1)-C(8)-N(2)	128.2(14)
C(2)-C(3)-C(4)	116.4(16)	N(3)-C(8)-N(2)	106.4(13)
C(2)-C(3)-C(7)	120.5(16)	N(2)-C(9)-C(4)	111.9(13)
C(4)-C(3)-C(7)	122.5(15)	N(4)-C(10)-C(11)	108.1(15)
C(5)-C(4)-C(3)	123.1(17)	C(12)-C(11)-C(10)	123.7(15)
C(5)-C(4)-C(9)	122.4(17)	C(11)-C(12)-C(13)	117.8(14)
C(3)-C(4)-C(9)	114.2(15)	N(3)-C(13)-C(12)	111.8(14)
C(4)-C(5)-C(6)	115.5(17)	N(3)-C(13)-C(18)	110.3(14)
C(1)-C(6)-C(5)	123.7(16)	C(12)-C(13)-C(18)	114.6(14)
N(1)-C(7)-C(3)	111.9(13)	N(3)-C(13)-C(14)	100.9(12)

C(12)-C(13)-C(14) 105.3(12)
C(18)-C(13)-C(14) 113.0(10)
O(1)-C(14)-N(2) 125.1(16)
O(1)-C(14)-C(13) 126.5(15)
N(2)-C(14)-C(13) 108.0(14)
N(4)-C(15)-C(16) 109.3(15)
C(17)-C(16)-C(15) 122.0(20)
N(6)-C(18)-C(19) 105.4(16)
N(6)-C(18)-C(13) 108.9(13)
C(19)-C(18)-C(13) 117.6(14)
N(6)-C(18)-C(26) 102.9(12)
C(19)-C(18)-C(26) 108.6(13)
C(13)-C(18)-C(26) 112.1(9)
C(20)-C(19)-C(18) 129.0(20)
C(19)-C(20)-C(21) 119.2(18)
C(20)-C(21)-N(5) 110.4(16)
C(23)-C(22)-N(5) 110.1(17)
C(24)-C(23)-C(22) 122.0(20)
N(8)-C(25)-N(7) 133.8(13)
N(8)-C(25)-N(6) 123.2(15)
N(7)-C(25)-N(6) 103.0(13)
O(2)-C(26)-N(7) 127.8(14)
O(2)-C(26)-C(18) 127.4(14)
N(7)-C(26)-C(18) 104.8(14)
N(7)-C(27)-C(28) 110.4(13)
C(29)-C(28)-C(34) 118.6(15)
C(29)-C(28)-C(27) 120.8(13)
C(34)-C(28)-C(27) 120.4(16)
C(28)-C(29)-C(31) 120.6(14)
C(28)-C(29)-C(30) 118.0(13)
C(31)-C(29)-C(30) 121.3(16)
N(8)-C(30)-C(29) 119.8(12)
C(32)-C(31)-C(29) 119.2(17)
C(33)-C(32)-C(31) 120.9(16)
C(34)-C(33)-C(32) 117.1(17)
C(33)-C(34)-C(28) 123.1(19)
C(8)-N(1)-C(7) 125.1(15)
C(14)-N(2)-C(8) 110.5(13)
C(14)-N(2)-C(9) 124.9(14)
C(8)-N(2)-C(9) 124.1(13)
C(8)-N(3)-N(4) 123.4(12)
C(8)-N(3)-C(13) 108.5(13)

N(4)-N(3)-C(13) 111.4(11)

N(3)-N(4)-C(15) 112.1(12)

N(3)-N(4)-C(10) 108.8(13)

C(15)-N(4)-C(10) 115.1(13)

N(6)-N(5)-C(21) 115.2(13)

N(6)-N(5)-C(22) 112.6(14)

C(21)-N(5)-C(22) 121.1(16)

N(5)-N(6)-C(25) 118.6(13)

N(5)-N(6)-C(18) 112.8(12)

C(25)-N(6)-C(18) 110.4(12)

C(26)-N(7)-C(25) 113.2(12)

C(26)-N(7)-C(27) 122.2(13)

C(25)-N(7)-C(27) 122.9(12)

C(25)-N(8)-C(30) 119.2(14)

Table 5. Anisotropic displacement parameters ($Å^2$ x 10^3) for 137. The anisotropic displacement factor exponent takes the form: -2 pi^2 [h^2 a*^2 U11 + ... + 2 h k a* b* U12]

	U11	U22	U33	U23	U13	U12
C(1)	74(14)	54(12)	81(13)	23(11)	17(10)	6(10)
C(2)	64(11)	65(11)	96(16)	13(11)	31(10)	7(10)
C(3)	41(9)	83(12)	39(12)	-16(10)	6(8)	-7(8)
C(4)	74(13)	40(10)	79(14)	-13(9)	0(11)	-38(9)
C(5)	55(12)	52(10)	56(13)	8(9)	11(9)	7(9)
C(6)	75(12)	17(7)	140(20)	-13(10)	34(13)	-10(7)
C(7)	14(8)	69(12)	89(12)	19(10)	17(8)	-9(8)
C(8)	50(11)	56(10)	33(9)	2(8)	-22(8)	-2(9)
C(9)	41(10)	62(12)	47(12)	14(9)	-15(8)	-14(9)
C(10)	63(13)	87(14)	57(13)	-2(11)	-6(9)	-10(10)
C(11)	62(10)	47(10)	57(14)	-3(9)	31(9)	-7(8)
C(12)	83(11)	18(7)	62(13)	-11(8)	52(9)	0(7)
C(13)	32(9)	73(12)	49(11)	-1(10)	11(8)	-4(8)
C(14)	89(12)	25(8)	40(10)	-11(8)	-2(9)	12(8)

C(15)	40(9)	98(15)	41(10)	-10(10)	4(8)	-1(9)
C(16)	88(13)	79(12)	111(17)	-18(12)	-23(11)	26(11)
C(17)	91(16)	148(19)	93(17)	21(14)	-27(13)	42(15)
C(18)	42(9)	33(9)	50(10)	5(9)	7(8)	2(7)
C(19)	32(9)	83(14)	82(17)	-7(13)	12(9)	10(9)
C(20)	48(10)	91(15)	81(17)	36(12)	17(10)	29(10)
C(21)	63(12)	64(13)	44(11)	8(10)	26(9)	11(10)
C(22)	66(13)	70(12)	85(15)	-51(11)	12(11)	-24(9)
C(23)	16(8)	200(20)	64(11)	-47(12)	24(7)	-18(10)
C(24)	92(19)	220(40)	110(20)	10(20)	16(17)	-40(20)
C(25)	49(10)	29(8)	49(10)	5(8)	38(8)	4(7)
C(26)	29(9)	76(12)	53(10)	-25(9)	25(7)	5(8)
C(27)	46(11)	71(13)	49(11)	2(10)	23(8)	2(10)
C(28)	19(7)	59(10)	39(10)	-11(8)	12(6)	-13(7)
C(29)	39(9)	30(9)	70(13)	-7(9)	19(8)	20(7)
C(30)	78(13)	43(9)	31(9)	-1(8)	4(8)	1(9)
C(31)	55(11)	63(10)	33(10)	19(8)	11(8)	29(9)
C(32)	62(12)	105(14)	75(14)	45(12)	43(11)	8(11)
C(33)	49(11)	150(18)	72(15)	4(12)	19(11)	-43(11)
C(34)	56(13)	56(11)	109(17)	-12(11)	7(10)	-3(10)
N(1)	47(9)	46(9)	71(11)	2(8)	14(7)	4(6)

N(2)	26(8)	72(9)	39(9)	1(7)	14(6)	-18(7)
N(3)	47(9)	33(7)	33(8)	5(6)	12(6)	-11(6)
N(4)	61(9)	60(9)	36(8)	-8(7)	-11(7)	10(7)
N(5)	35(7)	65(9)	68(10)	-13(8)	11(7)	9(6)
N(6)	41(8)	68(9)	50(9)	-4(8)	6(7)	-9(7)
N(7)	63(10)	31(6)	47(9)	-8(7)	6(6)	-3(7)
N(8)	45(8)	53(9)	43(9)	-3(7)	10(6)	15(6)
O(1)	54(7)	70(8)	52(8)	7(6)	28(6)	-3(6)
O(2)	56(7)	67(8)	82(9)	-27(7)	5(7)	-22(6)

Table 6. Hydrogen coordinates (x 10^4) and isotropic displacement parameters (A^2 x 10^3) for 137.

	x	y	z	U(eq)
H(1)	7330(40)	9330(50)	4540(30)	0(16)
H(2)	2600(50)	8950(50)	8270(30)	14(18)
H(3)	8090(40)	8260(50)	6050(30)	0(14)
H(4)	4620(70)	4500(70)	6900(40)	0(30)
H(5)	6230(60)	6310(60)	8060(30)	10(19)

H(6) 5480(40) 3990(50) 5810(30) 8(17)

H(7) 4050(110) 8660(110) 4880(60) 70(40)

H(8) 3650(80) 8610(80) 5660(50) 50(30)

H(9) 3700(100) 5770(100) 4590(50) 100(40)

H(10) 1300(70) 6590(70) 6440(40) 40(30)

H(11) 5530(100) 8500(100) 7740(50) 50(30)

H(12) 5260(130) 6590(130) 8160(70) 120(60)

H(13) 220(50) 5730(60) 7070(30) 0(18)

H(14) 8400(40) 7830(50) 3850(30) 0(16)

H(15) 9980(90) 5950(90) 5680(50) 90(40)

H(16) 5700(200) 8700(200) 6980(120) 240(120)

H(17) 4700(40) 4280(50) 4740(30) 13(15)

H(18) 7660(50) 9220(50) 5150(30) 0(16)

H(19) 5030(80) 6400(80) 4520(50) 40(30)

H(20) 8360(80) 8500(80) 8390(40) 80(30)

H(21) 40(50) 6360(50) 8840(30) 3(14)

H(23) -610(90) 5530(80) 8020(40) 40(30)

H(24) 8260(80) 6910(80) 6220(40) 30(30)

H(25) 2660(80) 9250(100) 4360(50) 70(40)

H(26) 2000(40) 7320(50) 5120(30) 3(15)

APPENDIX D
X-ray Crystallographic Data for 151

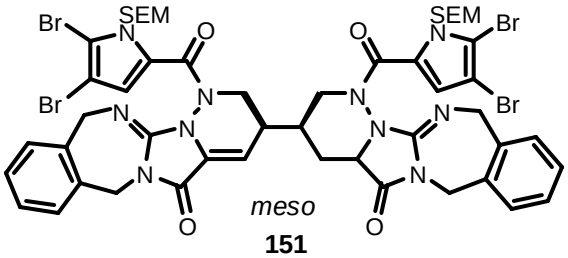

151

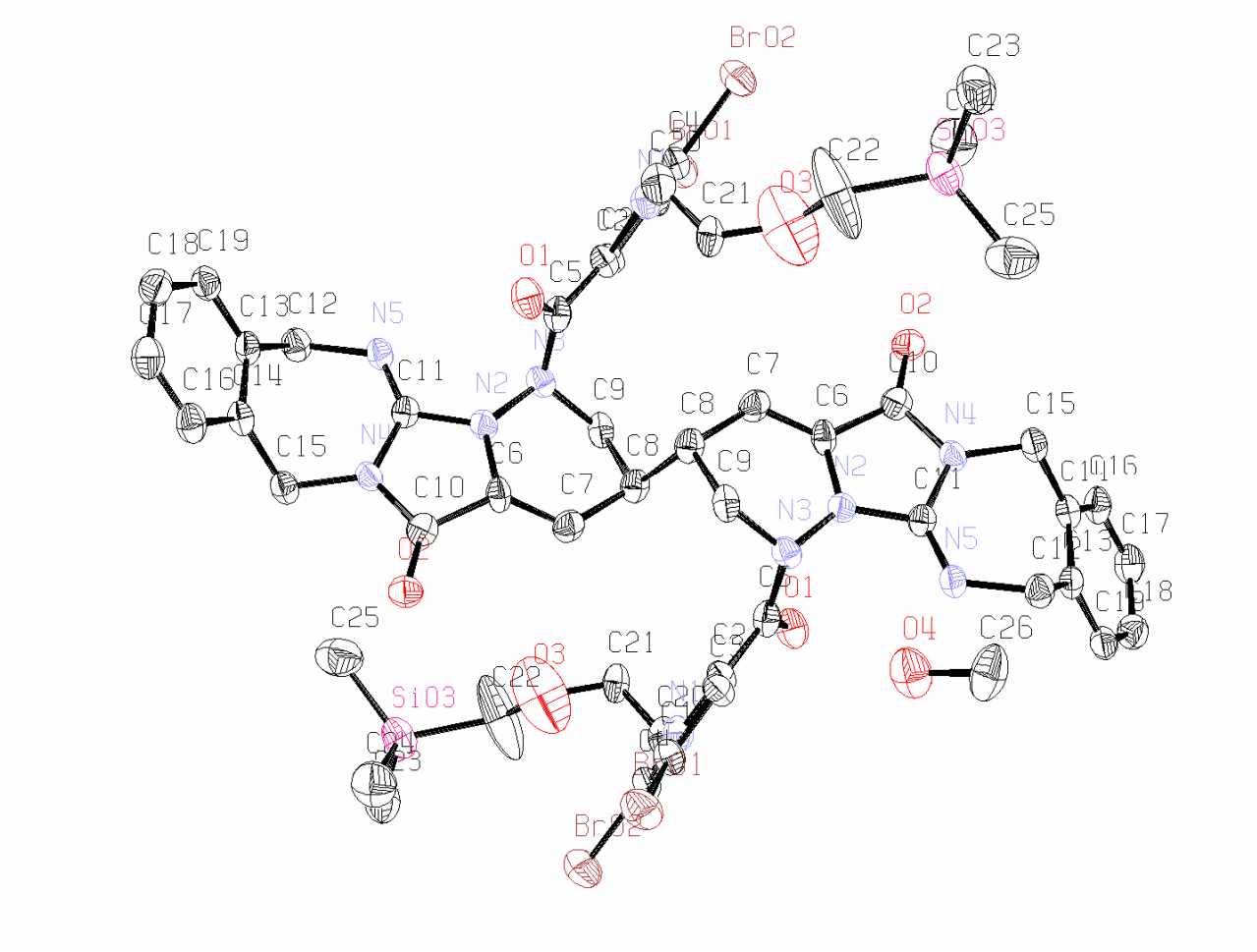

Table 1. Crystal data and structure refinement for 151.

Empirical formula	C52 H62 Br4 N10 O8 Si2
Formula weight	1330.90
Wavelength	0.71073 Å
Crystal system, space group	Triclinic, P-1
Unit cell dimensions	a = 9.8570(14) Å alpha = 83.814(4)°
	b = 10.3480(13) Å beta = 84.734(4)°
	c = 14.654(2) Å gamma = 77.178(6)°
Volume	1445.4(4) $Å^3$
Z, Calculated density	1, 1.520 Mg/m^3
Absorption coefficient	2.886 mm^{-1}

Intensity Measurement

Diffractometer	Enraf-Nonius
Detector	Kappa CCD
Radiation	MoKa (l=0.71069A)
Temperature	293(2) K
Scan-Type	w-2theta
Reflections collected / unique	2853 / 2853 [R(int) = 0.0600]
Completeness to theta = 20.82	94.3 %
Absorption correction	Empirical

Max. and min. transmission	0.82 and 0.66

Structure Solution and Refinement

Refinement method	Full-matrix least-squares on F^2
Data / restraints / parameters	2853 / 0 / 364
Goodness-of-fit on F^2	1.058
Final R indices [I>2sigma(I)]	R1 = 0.0617, wR2 = 0.1517
R indices (all data)	R1 = 0.1087, wR2 = 0.1784
Largest diff. peak and hole	0.352 and -0.328 $e.A^{-3}$

Table 2. Atomic coordinates (x 10^4) and equivalent isotropic displacement parameters (Å^2 x 10^3) for 151. U(eq) is defined as one third of the trace of the orthogonalizedUij tensor.

	x	y	z	U(eq)
Br1	2806(1)	3924(1)	3143(1)	107(1)
Br2	5724(1)	5482(1)	3020(1)	115(1)
Si3	5895(3)	10234(3)	1826(2)	102(1)
C(1)	3001(10)	5210(9)	3887(6)	74(3)
C(2)	2685(9)	6632(8)	4979(6)	66(2)

C(3)	2097(11)	5727(9)	4610(6)	73(3)
C(4)	4151(10)	5759(10)	3835(6)	79(3)
C(5)	2145(12)	7373(9)	5780(7)	76(3)
C(6)	-572(9)	9219(9)	6914(6)	67(2)
C(7)	-982(10)	10084(10)	6206(7)	75(3)
C(8)	-619(10)	9707(8)	5236(6)	72(2)
C(9)	-301(9)	8156(8)	5273(6)	72(2)
C(10)	-1007(9)	9288(10)	7906(7)	72(2)
C(11)	280(9)	7159(9)	7653(6)	63(2)
C(12)	913(9)	5185(8)	8635(6)	74(2)
C(13)	1446(10)	5755(8)	9384(6)	65(2)
C(14)	688(9)	6946(9)	9708(6)	66(2)
C(15)	-660(9)	7627(8)	9291(6)	73(3)
C(16)	1175(13)	7470(9)	10421(7)	83(3)
C(17)	2369(13)	6832(12)	10817(7)	90(3)
C(18)	3107(10)	5657(12)	10496(8)	92(3)
C(19)	2664(11)	5121(9)	9779(7)	78(3)
C(20)	4878(11)	7531(12)	4657(8)	103(3)
C(21)	4382(10)	8832(9)	4334(7)	73(3)
C(22)	5540(30)	9790(20)	3074(11)	278(15)
C(23)	7725(11)	10406(12)	1688(8)	127(4)

C(24)	5651(15)	8882(11)	1168(9)	147(5)
C(25)	4837(13)	11815(13)	1364(10)	153(5)
C(26)	500(30)	3002(14)	7051(11)	136(6)
O(1)	2874(7)	7701(6)	6299(5)	92(2)
O(2)	-1683(7)	10194(6)	8318(4)	87(2)
N(1)	3955(8)	6660(7)	4511(5)	75(2)
N(2)	239(7)	7964(7)	6823(5)	70(2)
N(3)	691(8)	7524(6)	5965(5)	66(2)
N(4)	-479(7)	8003(7)	8300(5)	66(2)
N(5)	896(7)	5952(7)	7719(5)	66(2)
O(3)	4580(20)	9180(20)	3426(13)	317(9)
O(4)	955(9)	3894(8)	6410(6)	134(3)

Table 3. Bond lengths [Å] for 151. Estimated standard deviations in the least significant figures are given in parentheses.

Br(01)-C(1)	1.860(9)	Si(03)-C(24)	1.851(11)
Br(02)-C(4)	1.857(9)	Si(03)-C(22)	1.858(16)
Si(03)-C(25)	1.833(12)	C(1)-C(4)	1.369(12)
Si(03)-C(23)	1.842(11)	C(1)-C(3)	1.392(12)

C(2)-N(1)	1.375(10)	C(12)-N(5)	1.483(10)
C(2)-C(3)	1.384(12)	C(12)-C(13)	1.488(11)
C(2)-C(5)	1.465(12)	C(13)-C(19)	1.379(12)
C(4)-N(1)	1.404(11)	C(13)-C(14)	1.397(11)
C(5)-O(1)	1.215(10)	C(14)-C(16)	1.395(12)
C(5)-N(3)	1.411(11)	C(14)-C(15)	1.509(11)
C(6)-C(7)	1.326(11)	C(15)-N(4)	1.468(10)
C(6)-N(2)	1.379(10)	C(16)-C(17)	1.363(12)
C(6)-C(10)	1.483(12)	C(17)-C(18)	1.377(13)
C(7)-C(8)	1.504(12)	C(18)-C(19)	1.386(13)
C(8)-C(8)#1	1.556(16)	C(20)-C(21)	1.374(12)
C(8)-C(9)	1.561(11)	C(20)-N(1)	1.459(12)
C(9)-N(3)	1.473(10)	C(21)-O(3)	1.349(18)
C(10)-O(2)	1.207(10)	C(22)-O(3)	1.291(18)
C(10)-N(4)	1.398(10)	C(26)-O(4)	1.363(17)
C(11)-N(5)	1.259(9)	N(2)-N(3)	1.384(9)
C(11)-N(2)	1.397(10)		
C(11)-N(4)	1.407(10)		

Symmetry transformations used to generate equivalent atoms: #1 -x,-y+2,-z+1

Table 4. Bond Angles [°] for 151. Estimated standard deviations in the least significant figures are given in parentheses.

C(25)-Si(03)-C(23)	106.9(6)	N(3)-C(5)-C(2)	113.2(9)
C(25)-Si(03)-C(24)	109.1(6)	C(7)-C(6)-N(2)	123.6(8)
C(23)-Si(03)-C(24)	110.6(6)	C(7)-C(6)-C(10)	129.2(9)
C(25)-Si(03)-C(22)	114.9(10)	N(2)-C(6)-C(10)	106.7(8)
C(23)-Si(03)-C(22)	105.8(8)	C(6)-C(7)-C(8)	120.5(9)
C(24)-Si(03)-C(22)	109.4(7)	C(7)-C(8)-C(8)#1	112.1(9)
C(4)-C(1)-C(3)	107.9(9)	C(7)-C(8)-C(9)	107.7(7)
C(4)-C(1)-Br(01)	123.8(8)	C(8)#1-C(8)-C(9)	112.0(9)
C(3)-C(1)-Br(01)	128.1(8)	N(3)-C(9)-C(8)	112.3(7)
N(1)-C(2)-C(3)	108.5(8)	O(2)-C(10)-N(4)	125.3(9)
N(1)-C(2)-C(5)	123.9(9)	O(2)-C(10)-C(6)	130.8(9)
C(3)-C(2)-C(5)	127.4(9)	N(4)-C(10)-C(6)	103.9(8)
C(2)-C(3)-C(1)	107.9(9)	N(5)-C(11)-N(2)	122.9(8)
C(1)-C(4)-N(1)	108.3(8)	N(5)-C(11)-N(4)	132.7(8)
C(1)-C(4)-Br(02)	129.1(8)	N(2)-C(11)-N(4)	104.5(7)
N(1)-C(4)-Br(02)	122.6(8)	N(5)-C(12)-C(13)	116.5(7)
O(1)-C(5)-N(3)	122.2(9)	C(19)-C(13)-C(14)	119.1(8)
O(1)-C(5)-C(2)	124.1(10)	C(19)-C(13)-C(12)	121.3(9)

C(14)-C(13)-C(12)	119.5(9)	C(10)-N(4)-C(11)	112.7(7)
C(16)-C(14)-C(13)	119.6(9)	C(10)-N(4)-C(15)	122.3(7)
C(16)-C(14)-C(15)	121.1(9)	C(11)-N(4)-C(15)	124.9(7)
C(13)-C(14)-C(15)	119.2(8)	C(11)-N(5)-C(12)	119.0(7)
N(4)-C(15)-C(14)	113.1(7)	C(22)-O(3)-C(21)	123.7(17)
C(17)-C(16)-C(14)	121.1(9)		
C(16)-C(17)-C(18)	118.9(10)		
C(17)-C(18)-C(19)	121.4(10)		
C(13)-C(19)-C(18)	119.8(9)		
C(21)-C(20)-N(1)	112.8(8)		
O(3)-C(21)-C(20)	118.3(13)		
O(3)-C(22)-Si(03)	125.3(15)		
C(2)-N(1)-C(4)	107.4(7)		
C(2)-N(1)-C(20)	125.9(9)		
C(4)-N(1)-C(20)	126.7(9)		
N(3)-N(2)-C(6)	121.3(7)		
N(3)-N(2)-C(11)	125.4(7)		
C(6)-N(2)-C(11)	112.0(7)		
N(2)-N(3)-C(5)	112.6(7)		
N(2)-N(3)-C(9)	111.2(7)		
C(5)-N(3)-C(9)	121.9(7)		

Symmetry transformations used to generate equivalent atoms: #1 -x,-y+2,-z+1

Table 5. Anisotropic displacement parameters ($Å^2$ x 10^3) for 151. The anisotropic displacement factor exponent takes the form: -2 pi^2 [h^2 a*2 U11 + ... + 2 h k a* b* U12]

	U11	U22	U33	U23	U13	U12
Br(01)	128(1)	103(1)	97(1)	-40(1)	10(1)	-29(1)
Br(02)	100(1)	131(1)	106(1)	-8(1)	31(1)	-24(1)
Si(03)	113(2)	119(2)	89(2)	-21(2)	12(2)	-62(2)
C(1)	78(6)	83(6)	66(7)	-8(5)	0(5)	-30(5)
C(2)	80(7)	64(5)	59(6)	-12(5)	9(5)	-26(5)
C(3)	76(7)	75(6)	67(7)	-13(5)	11(6)	-19(6)
C(4)	82(7)	93(7)	56(6)	0(5)	8(5)	-15(6)
C(5)	97(9)	72(6)	63(7)	7(5)	-7(6)	-30(6)
C(6)	96(7)	69(7)	42(6)	-5(5)	-5(5)	-31(5)
C(7)	94(7)	49(6)	80(8)	-4(6)	-6(6)	-13(5)
C(8)	92(7)	57(6)	71(7)	-1(5)	-8(6)	-29(5)
C(9)	82(6)	91(7)	53(6)	4(5)	-7(5)	-40(5)

C(10)	78(6)	64(7)	79(8)	-4(6)	-7(6)	-24(5)
C(11)	75(6)	59(6)	59(7)	-3(6)	-8(5)	-23(5)
C(12)	93(7)	61(5)	70(7)	-3(5)	0(5)	-23(5)
C(13)	92(7)	57(6)	47(6)	0(5)	1(5)	-23(5)
C(14)	81(6)	73(6)	49(6)	-2(5)	1(5)	-32(5)
C(15)	91(7)	71(6)	58(7)	-3(5)	9(5)	-26(5)
C(16)	120(9)	70(6)	64(7)	-1(5)	1(6)	-38(6)
C(17)	110(8)	98(8)	72(7)	-2(7)	-13(7)	-46(7)
C(18)	84(7)	109(9)	82(8)	9(7)	-14(6)	-24(7)
C(19)	90(7)	76(6)	64(7)	3(5)	8(6)	-21(6)
C(20)	95(8)	136(10)	87(8)	2(8)	-13(6)	-48(8)
C(21)	86(6)	78(7)	71(7)	16(5)	-13(5)	-59(5)
C(22)	410(30)	430(30)	118(13)	-74(16)	85(16)	-370(30)
C(23)	126(9)	152(11)	115(10)	12(8)	-7(8)	-65(8)
C(24)	199(13)	115(9)	138(12)	-41(8)	-8(10)	-40(9)
C(25)	140(11)	153(12)	163(13)	-54(10)	-8(10)	-6(9)
C(26)	217(19)	110(9)	98(11)	10(8)	-54(12)	-64(11)
O(1)	111(5)	105(5)	73(5)	-13(4)	-4(4)	-46(4)
O(2)	107(5)	63(4)	82(5)	-15(3)	4(4)	-1(4)
N(1)	80(5)	80(5)	70(5)	2(4)	-1(5)	-33(4)
N(2)	91(5)	56(5)	57(5)	-9(4)	6(4)	-5(4)

N(3)	86(6)	57(4)	60(5)	-18(4)	8(5)	-22(4)
N(4)	80(5)	64(5)	51(5)	-11(4)	7(4)	-13(4)
N(5)	81(5)	64(5)	56(5)	-2(4)	5(4)	-25(4)
O(3)	370(20)	420(30)	223(18)	-71(18)	44(16)	-220(20)
O(4)	189(8)	119(6)	107(6)	-28(5)	12(6)	-61(6)

Table 6. Hydrogen coordinates (x 10^4) and isotropic displacement parameters (A^2 x 10^3) for 151.

	x	y	z	U(eq)
H(9A)	-1165	7851	5415	87
H(9B)	81	7884	4672	87
H(12A)	1479	4301	8569	89
H(12B)	-30	5087	8825	89
H(15A)	-1309	7036	9395	88
H(15B)	-1066	8420	9601	88
H(16)	676	8269	10629	99
H(17)	2680	7184	11297	108
H(18)	3920	5215	10766	111

H(19)	3187	4335	9564	93
H(20A)	4996	7490	5310	123
H(20B)	5787	7211	4350	123
H(21A)	3387	9049	4499	88
H(21B)	4806	9388	4662	88
H(22A)	6407	9266	3292	333
H(22B)	5362	10621	3362	333
H(23A)	8317	9593	1920	191
H(23B)	7828	11121	2025	191
H(23C)	7983	10596	1048	191
H(24A)	6196	8049	1411	221
H(24B)	5948	9055	532	221
H(24C)	4684	8840	1218	221
H(25A)	3873	11760	1414	230
H(25B)	5131	11994	729	230
H(25C)	4952	12519	1706	230
H(4)	921	4589	6641	200
H(3)	1170	5500	4760	36
H(8)	-1520	10200	4820	90
H(7)	-1600	10930	6280	50
H(26A)	-500	2990	7260	270

H(26B)	1030	2820	7620	210

CHAPTER FOUR

BASE INDUCED N-N BOND CLEAVAGE AND AN ALTERNATIVE APPROACH FOR SPIROCYCLIZATION

4.1 Initial Strategy to Cleave N-N Bond in 151

In order to pursue the construction of the "all-syn" stereochemistry of palau'amine **11**, our retrosynthetic analysis requires the use constrained bisalkylidene type structure as starting material for the electrophilic chlorination reaction, such as **154** (Figure 4.1). As was shown in previous chapter, titanocene dichloride mediated oxidative dimerization of SEM-pyrrole monomer **150** provided good selectivity for dimer **151** when $Cu(OTf)_2$ was used as the oxidant. Compound **154** can be obtained from the symmetric dimer **151** by an N-N bond cleavage.

Figure 4.1

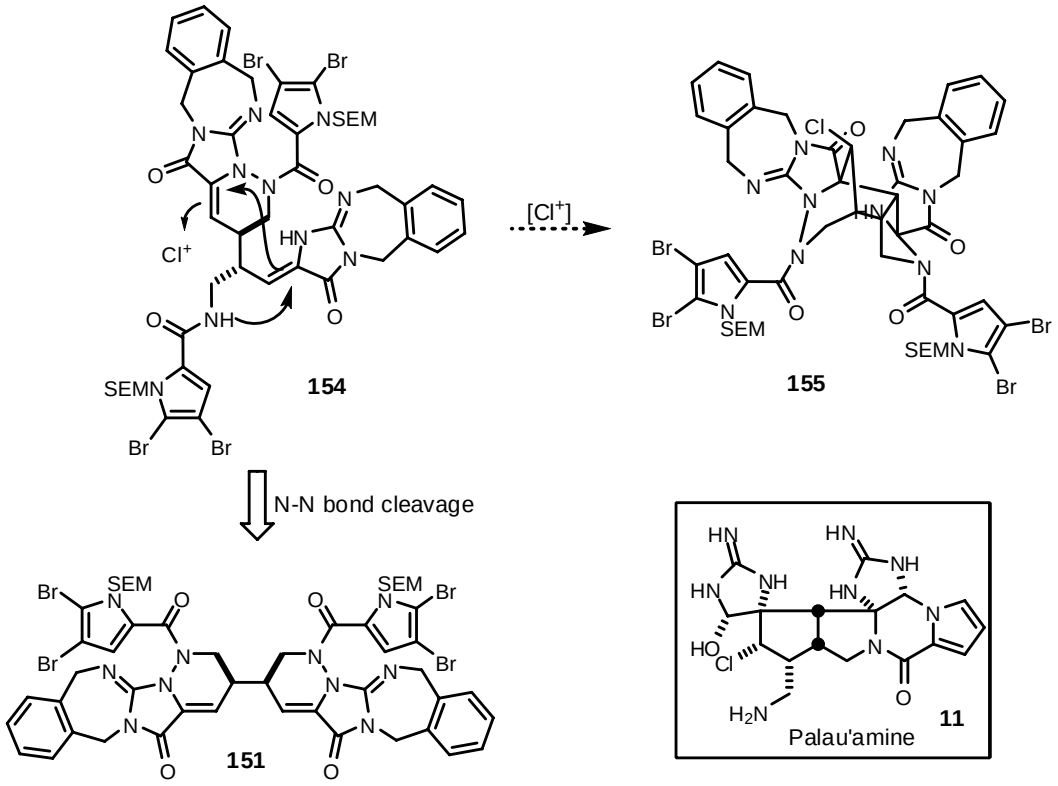

In context of compound **151**, the enamide and the pyrrole-bromide are easier to be reduced than the N-N bond. Then we pursued an indirect approach. We planned to use some type of metal hydride species to perform a conjugate reduction to generate the corresponding metal ketene aminal **156** (Scheme 4.1). The fragmentation of **156** will lead to intermediate **157**. Followed by tautomerization, the N-N bond cleaved product **154** can be potentially obtained in one step. We were fully aware that the orbitals of the donor and the acceptor overlap very poorly in this planned fragmentation process. Traditional concerted fragmentation reactions had strict stereochemical requirements[1], but we were

hoping to provoke other mechanisms such as photo-initiation or single electron transfer[2].

Scheme 4.1

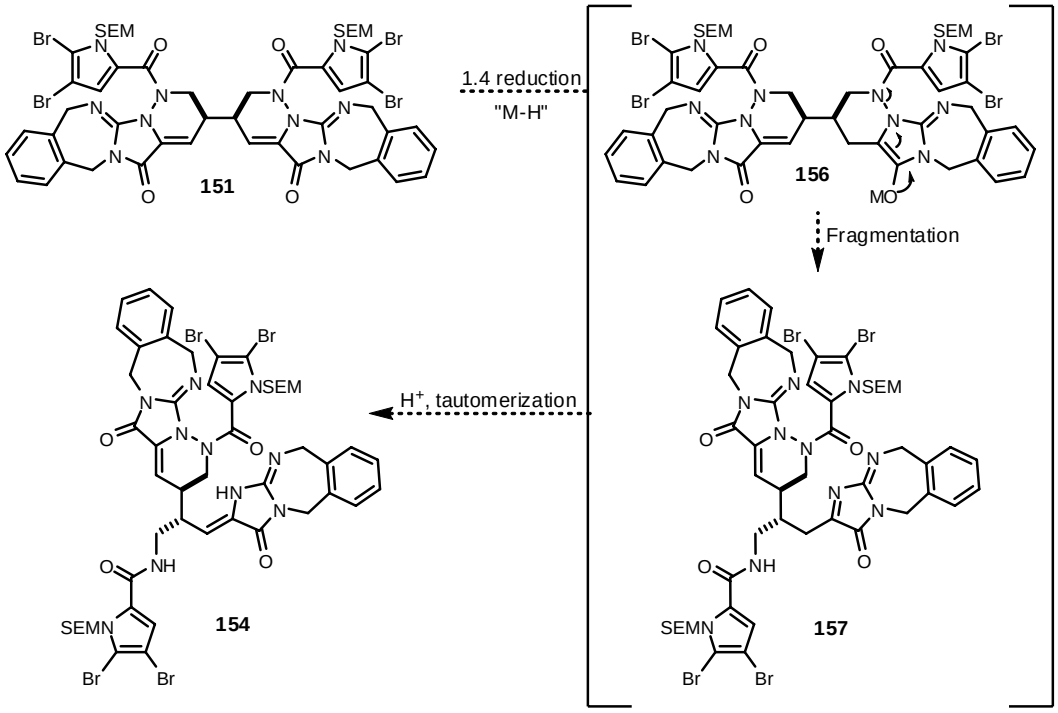

4.2 Conjugated Reduction via Rh(I) Catalyzed Hydrosilylation

The reported conjugate reduction methodologies were examined thoroughly[3] (Scheme 4.2). Unfortunately, none of them delivered the desired results. More disappointingly, the majority of methods failed to delivery any reactions at all, possibly due to the basicity of compound **151**.

Scheme 4.2

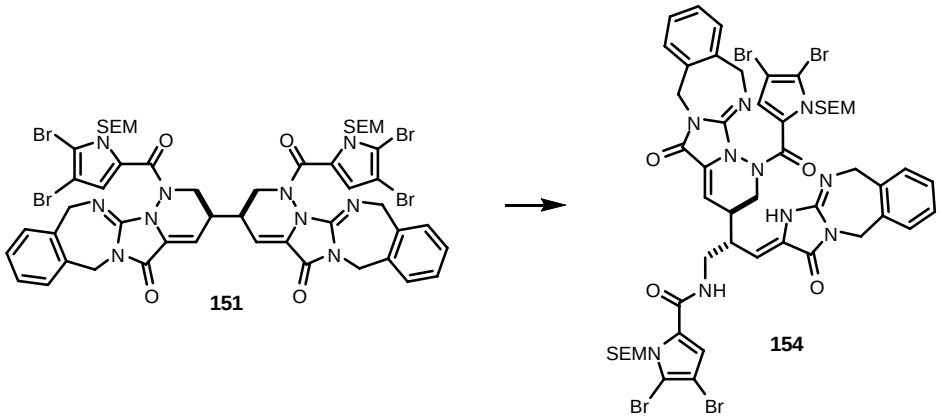

Conditions	Results
Speier's catalyst (H_2PtCl_6•$6H_2O$)	No reaction
Karstedt catalyst $Pt_2\{[(CH_2=CH)Me_2Si]_2O\}_3$	No reaction
$Mn(dpm)_3$/HSiMe2Ph/*i*-PrOH	No reaction
Stryker's reagent $[Ph_3PCuH]_6$ with and without TMSCl	No reaction
$Mo(CO)_6/H_3SiPh$	No reaction
$[RhCl(C_2H_4)_2]_2$/$(Ar)_3$-P/$HSiMe_2Ph$	No reaction
$Cu(OAc)_2$/polymethyl hydrosilane (PMHS)	No reaction
L-selectide	messy reaction
CuF_2, H_3SiPh, Josiphos, PMHS	No reaction
SmI_2	Messy reaction
Borane reagents: $(Ipc)_2BH$, catechlorborance	messy reaction
$Co(acac)_2$, DIBAL	No reaction

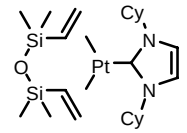

Karstedt's catalyst

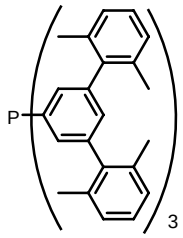

$(Ar)_3$-P

More promising results were obtained when a hydrosilylation reaction catalysed by Wilkinson's catalyst was used to perform the conjugate reduction. This methodology was developed by the Ojima group[4]. At the end of this reaction, mono-saturated product **159** was isolated in 10% yield together with unreacted starting material **151** (Scheme 4.3). The silyl ketene aminal **158** is believed to be the intermediate of the reaction. Compound **158** is hygroscopic and

hydrolyzed in situ or during work up to afford the product **159**[5]. Even though the turn over of the catalyst was very low, we were encouraged by this result due to the possibility of inducing the fragmentation by treating silyl intermediated **158** with fluoride sources.

Scheme 4.3

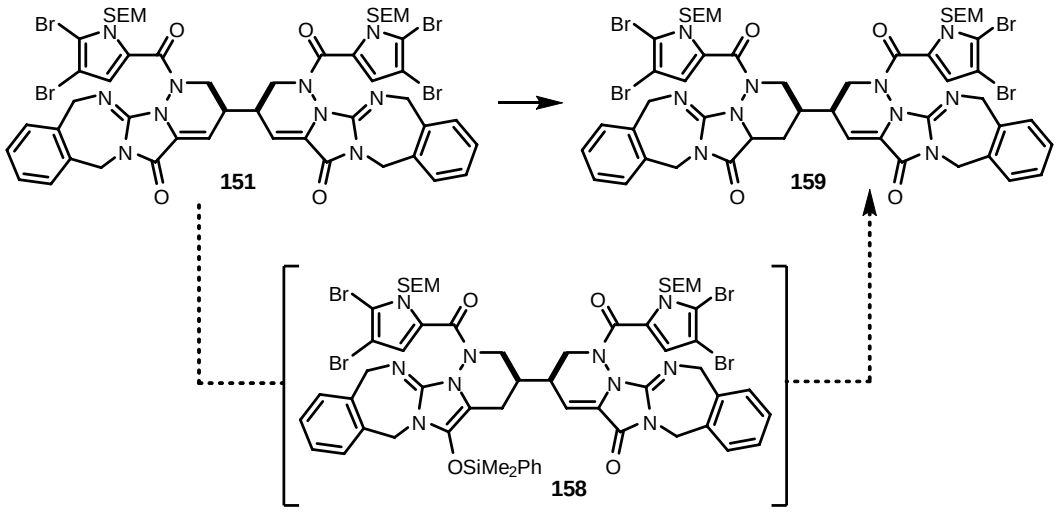

Conditions: $RhCl(PPh_3)_3$ (10%), $HSiMe_2Ph$, CH_2Cl_2, 50 °C, 12 h, (10%).

Then optimizations of reaction conditions were taken place to increase the yield of this conjugate hydrosilylation reaction. Halogened solvents and relatively non-coordinating ones are suitable solvents, such as: CH_2Cl_2 and DCE. $HSiMe_2Ph$ was proven to be the superior silane. The reaction was performed at 50 °C in sealed tubes. Increasing the temperature further or heating time did not lead to better results. However, even under the best conditions, the yield is only 15%.

As no significant improvement was achieved by varying the above factors, we turned our attention to the catalyst itself. Complex **160** seemed like a good

catalyst candidate, even though no literature was reported about it being used as the catalyst in hydrosilylation reactions (Figure 4.2). Comparing to traditional phosphine ligands, N-heterocyclic carbenes (NHC) are more electron donating, thus the complex's metal centre is more stablized[6]. During the catalysis, the COD ligand will be hydrosilylated and eventually fall off the metal center. This would provide us the opportunity to add external ligands to further tune the activity of the metal center.

Figure 4.2

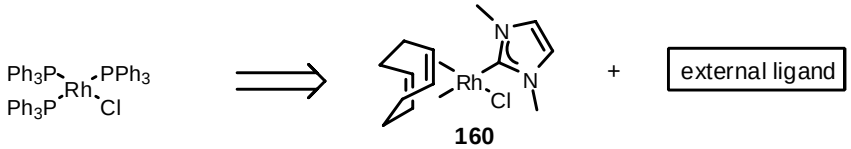

Wilkinson's catalyst **160** Rh(COD)(NHC-Me)Cl

At the same time we were working on solving this problem, the Crabtree group published a new method using imidazolium carboxylate as NHC transfer agents to synthesize a variety of transition metal complexes[7]. Compound **160** was synthesized following their procedures (Scheme 4.4). Unlike other organometallic compounds, it is stable enough to be purified by column chromatography using 1% MeOH/CH_2Cl_2. The bright yellow crystalline compound **160** was stored in freezer for months without losing its activity. No special caution is needed during handling the compound.

Scheme 4.4

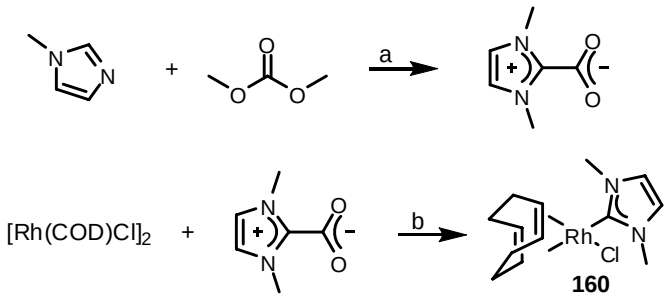

Conditions: a). neat, 120 °C, 24h, (65%). b). CH_3CN, 75 °C, 15 min, (90%)

When 10 mol% catalyst **160** was employed in the hydrosilylation reaction of **151** without any additives, almost no reaction was detected. Then we started to look at adding external ligands. Davephos **161**[8], invented by Buchwald group performed the best of all the ligands (Scheme 4.5). When the HPF_6 salt form of the starting material **151** was employed, the reaction catalyzed by complex **160** with Davephos as the external ligand worked a slightly better than Wilkinson's catalyst (Scheme 4.5, entry 7).

Scheme 4.5

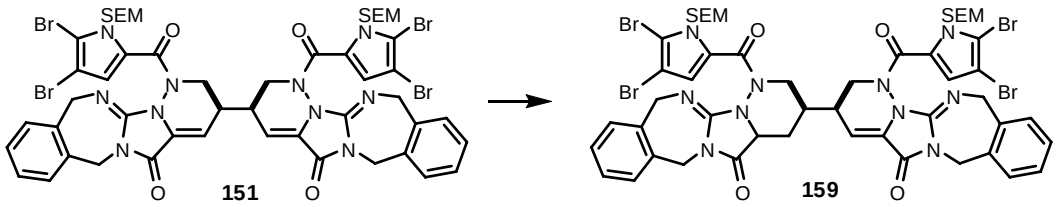

Entry	Starting Material	Phosphine Ligands	Solvent	Results
1	Free amine	None	CH_2Cl_2	no reaction
2	Free amine	Cy_3P	CH_2Cl_2	5% conversion
3	Free amine	PPh2 PPh2	CH_2Cl_2	no reacton
4	Free amine	PPh2 PPh2	CH_2Cl_2	no reaction
5	Free amine	Me_2N, PCy_2 **161**	CH_2Cl_2	10% conversion
6	Free amine	Me_2N, PCy_2 **161**	PhH	5% conversion
7	HPF6 salt	Me_2N, PCy_2 **161**	CH_2Cl_2	20% conversion,

Conditions: **160** (10mol%), liganids (10mol%), 50^{o}C, 18h

Even though the conversion of the hydrosilylation reaction was still low, it was encouraging to see that the efficiency of the catalyst was improved. Next we turned our attention to Lewis acids. Using the salt form of the starting material resulted in the direct hydrolysis of silyl ketene aminal intermediate **158**. As our goal is to achieve N-N bond cleavage in a one-pot operation, Lewis acids seemed

like a better alternative. Of all the Lewis acids we had screened, most of them did not improve the reaction or some of them caused a lot decomposition of the dimer **151**. However, $MgBr_2 \bullet Et_2O$ gave the most interesting results.

When the $MgBr_2 \bullet Et_2O$ was used as an additive, the conversion of this hydrosilylation reaction is excellent. Besides the mono-reduced compound **159** isolated in 30% yield, the TLC of the crude reaction showed another non-polar spot, which was isolated in 40% yield. The structure of this compound was assigned as **162**, based on NMR analysis[9] (Scheme 4.6). The two SEM groups on the pyrroles in **162** were deprotected by BF_3 etherate treatment to afford compound **163**. The structure of the compound **162** was further verified by X-ray crystal structure of compound **163**.

Scheme 4.6

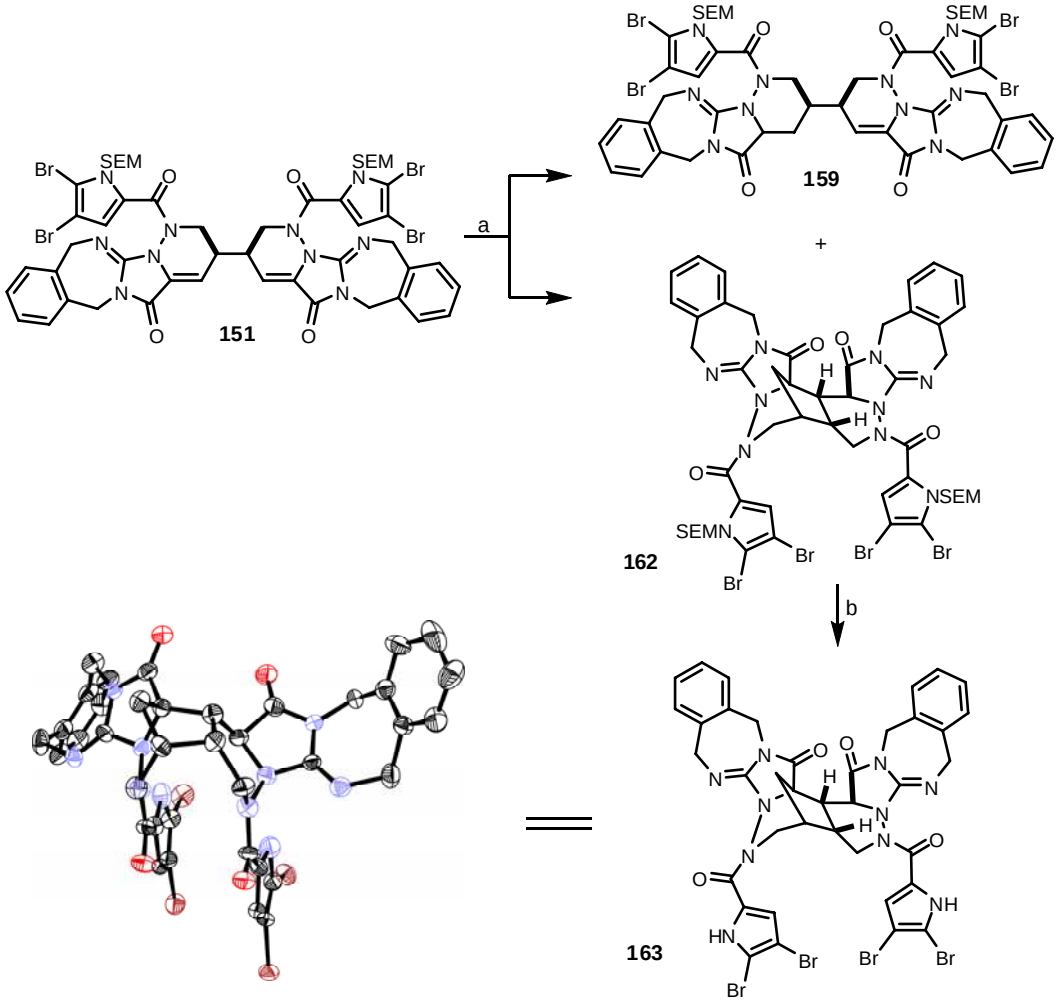

Conditions: (a) **160** (10mol%), davephos **161** (10mol%), $MgBr_2 \bullet OEt_2$ (1.5 eq), $HSiMe_2Ph$ (1.1 eq), CH_2Cl_2, 15 h, **162** (45%), **159** (30%); (b) $BF_3 \bullet OEt_2$ (4 eq), CH_2Cl_2, rt, 3 h, (70%)

4.3 From Mukaiyama-Michael Adduct to Des-chloropalau'amine Synthesis.

The formation of the polycyclic compound **162** was not anticipated, but it can be rationalized by the silyl ketene aminal **158** undergoing an internal Mukaiyama-Michael addition[10] (Scheme 4.7). We are very excited by this

discovery because the new bond formed by this reaction is the 5→6' bond in our retrosynthetic analysis. Just in this case, there is no chlorine incorporated (Chapter 1, section 1.5).

Scheme 4.7

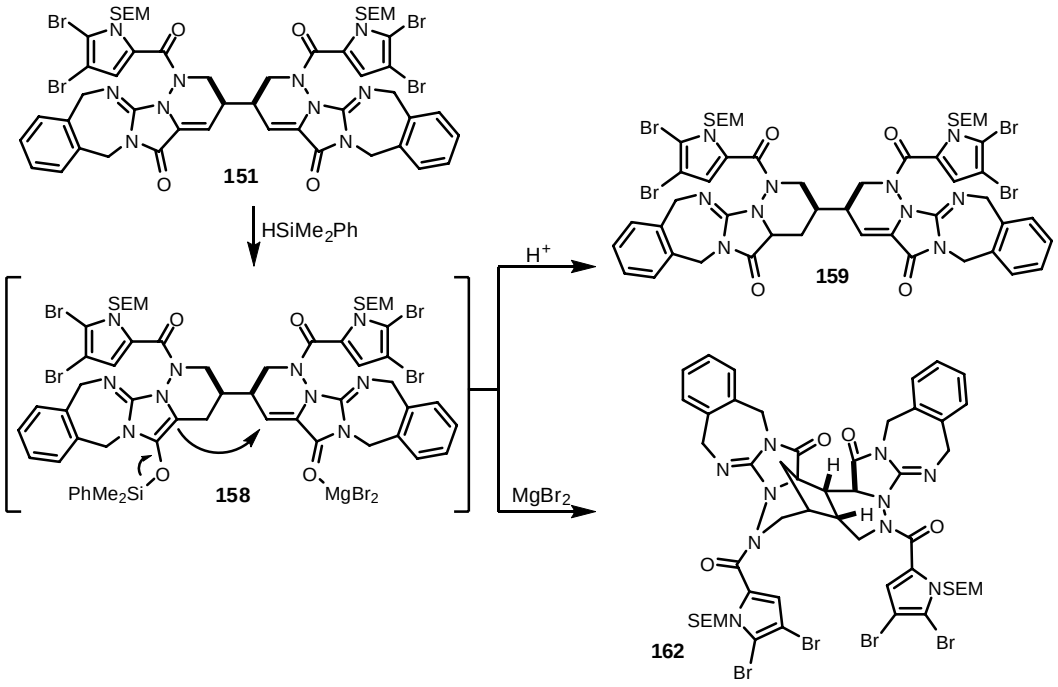

Compound **162** already has the central five membered ring formed and what makes it even more exciting is that: the stereochemistry around the ring is the same as the originally proposed structure except that lacks the chlorine at the C17 position (Figure 4.3). This opened up an opportunity for us to synthesize des-chloropalau'amine, which could potentially be helpful for exploring the unknown mechanism of the natural product's biological activities.

Figure 4.3

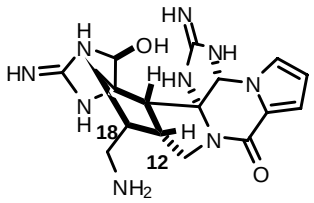

Palau'amine **11**

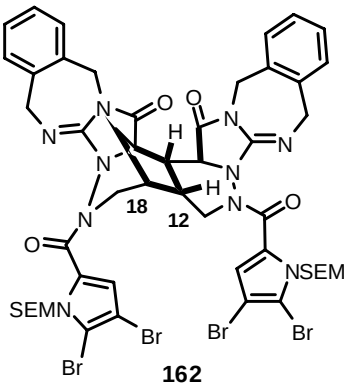

162

On the path to the synthesis of des-chloropalau'amine from compound **162**, the next step was to cleave both N-N bonds. SmI_2 was the chosen reagent. It was prepared freshly right before the reaction from samarium powder and iodoform[13]. The reaction was carried under strict air-excluded argon atmosphere. The progression of the reduction is indicated by the persistence of the dark blue color of SmI_2.

As indicated by the mass analysis, the major product isolated from the reaction was a two electron reduction product. Interestingly, it was converted to a new highly fluorescent spot by TLC analysis when it was left on the bench top overnight. The structure of the fluorescent spot was identified as **165**. Presumably, its formation went through the intermediate **164** (Scheme 4.8). Then intermediate **164** was oxidated, presumably by air, to generate the thermodynamically favored conjugated tetrasubstituted enamide.

Scheme 4.8

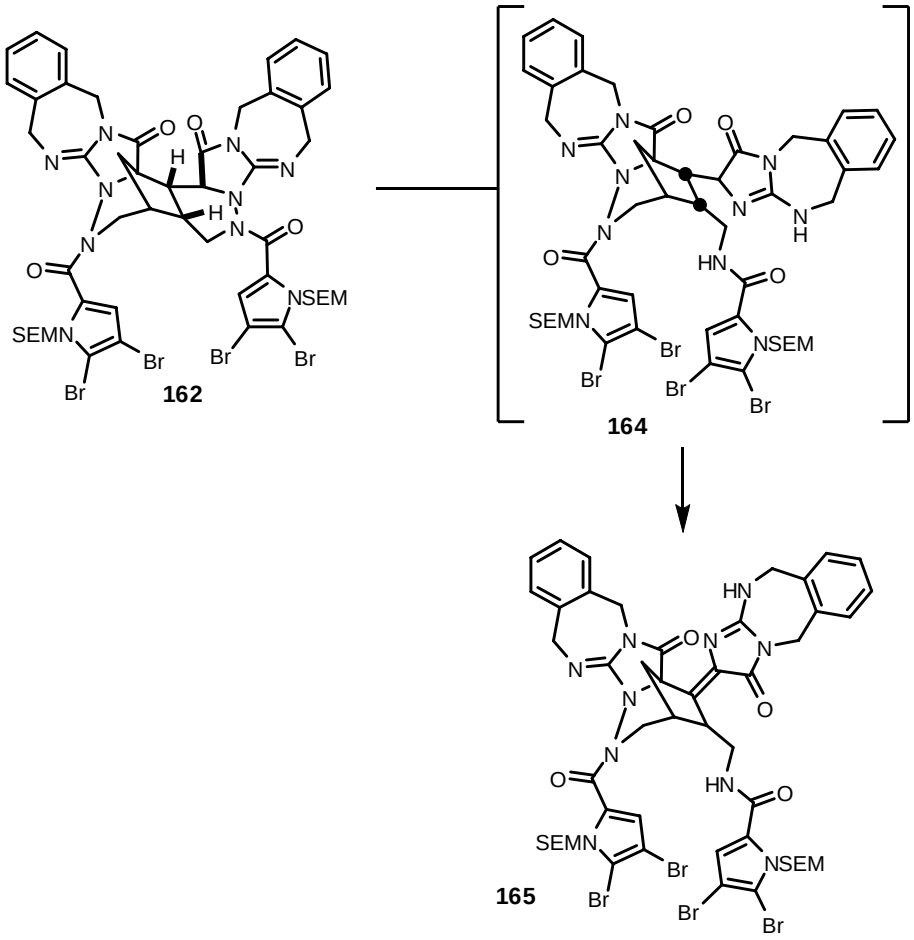

Conditions: SmI_2, MeOH/THF(1:4), –78 °C, 30 min, work up, rt, overnite, (40%)

In order to confirm the structure of compound **165**, Mukaiyama-Michael adduct **162** was treated with KHMDS[12]. The α methine proton was deprotonated (Scheme 4.9). The resultant potassium enolate fragments to afford the N-N bond cleaved product **165**, which is identical to the fluorescent spot isolated from SmI_2 reaction by TLC and NMR analysis.

The close relationship between compound **165** and des-chloropalau'amine is quite apparent. The pursuit of the synthesis of des-chloropalau'amine from compound **162** and **165** was carried out by other group members in the lab.

Scheme 4.9

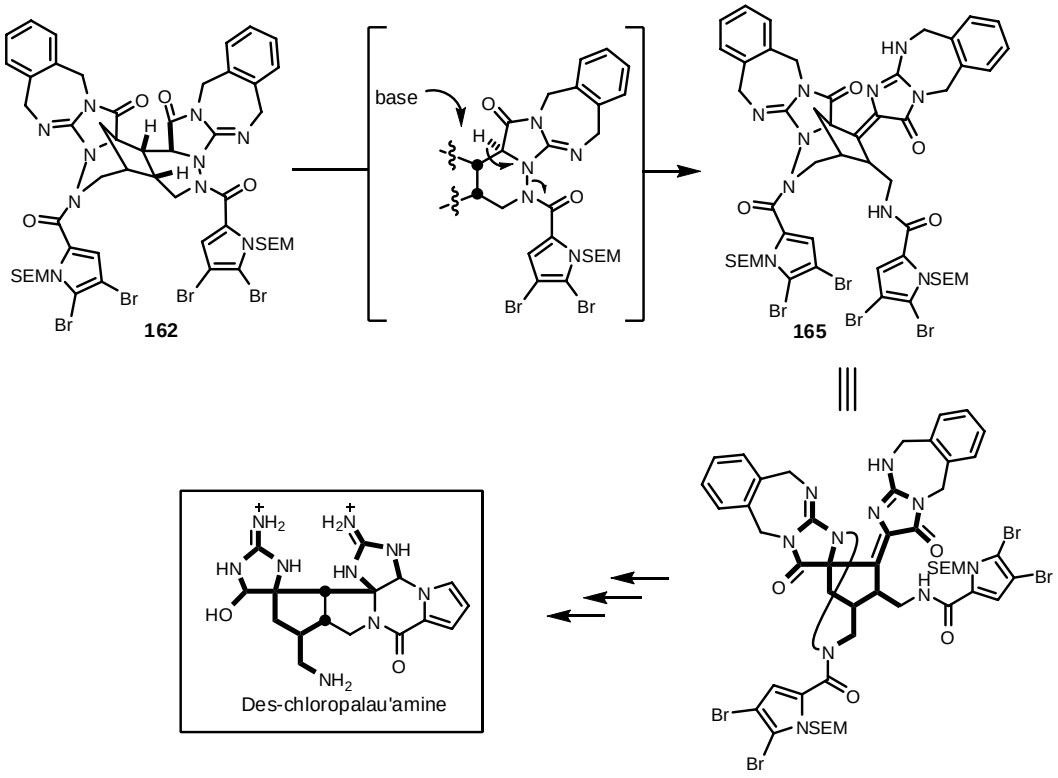

Conditions: KHMDS (2.2 eq), THF, –78 °C to rt, 15min, (70%).

4.4 A Two-Step Pathway to Achieve N-N Bond Cleavage

As discussed in section 4.2, the use of $MgBr_2$ as an additive was essential for facilitating the turn over in rhodium catalysis. However, it also induced the intramolecular Mukaiyama-Michael process at the same time, which obstructs the

one-pot N-N bond cleavage pathway (Figure 4.4). Therefore, an alternative was required.

Figure 4.4

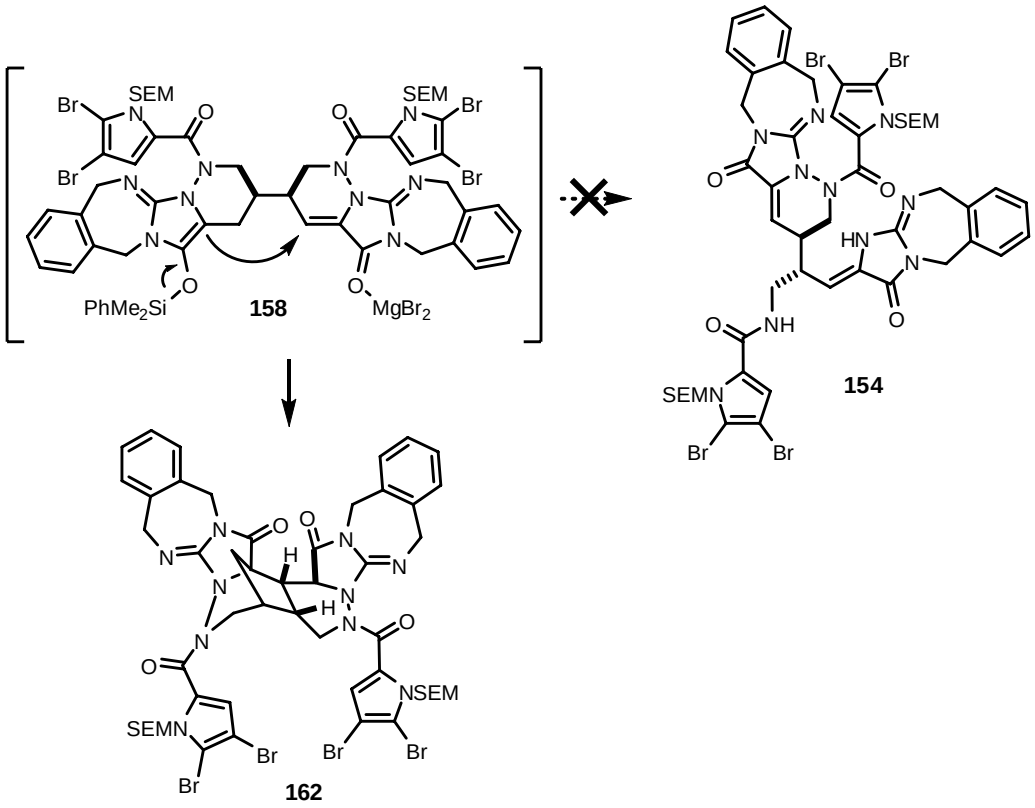

A useful observation is the successful N-N bond cleavage of compound **162** when it was treated with KHMDS (Scheme 4.9). So instead of pursuing the one-pot approach, we turned to a two-step path. The strategy is to isolate the mono-reduced dimer **159** from the hydrosilylation reaction. Then it will be subjected to basic conditions to regenerate intermediate **156** (Scheme 4.10). If the fragmentation process occurs, it should provide desired compound **154**.

Scheme 4.10

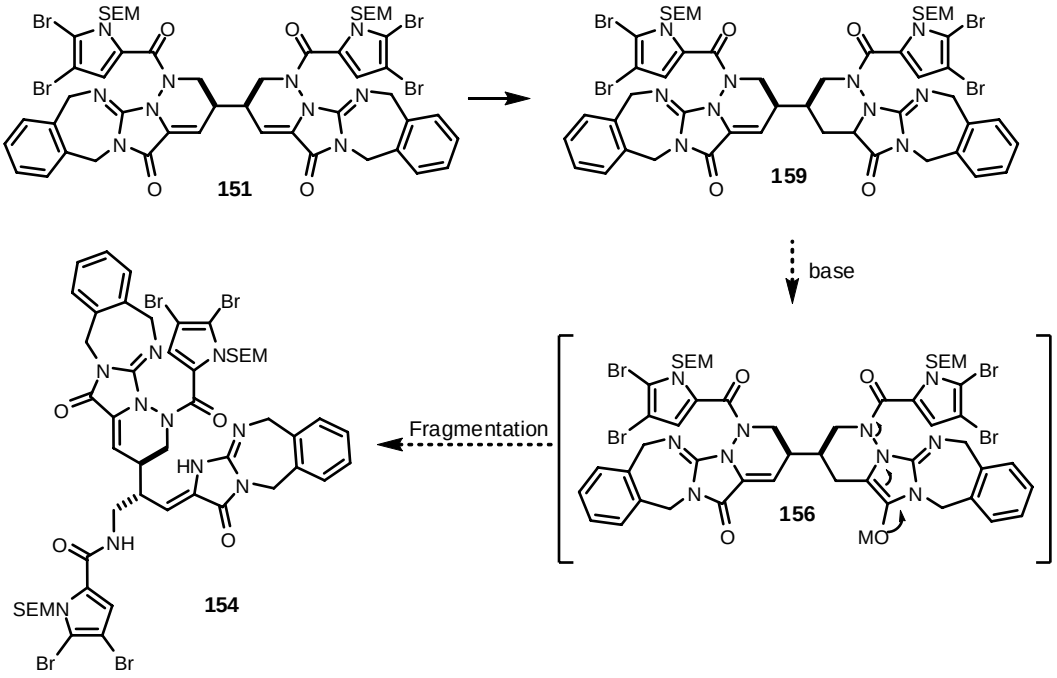

First, we needed to optimize the hydrosilylation reaction condition to favor the formation of compound **159** and minimize the formation of **162**. The salt form of the starting material was employed to facilitate the in situ hydrolysis of silyl ketene aminal **158**. It was found that the presence of $MgBr_2$, which was required to assist the turnover of catalyst, induced the formation of compound **162**. Therefore we started to look for other Lewis acids that would not induce the Mukaiyama-Michael process but keep the catalyst active at the same time. The use of MgI_2 turned out to be the answer. Not only was there an absence of the conjugate addition process but its addition also made the catalyst more active. In this case, the double- reduction became the main side reaction. By carefully

controlling the amount of acid and silane used in the reaction, the mono-reduced dimer **159** can be isolated in modest yield.

Scheme 4.11

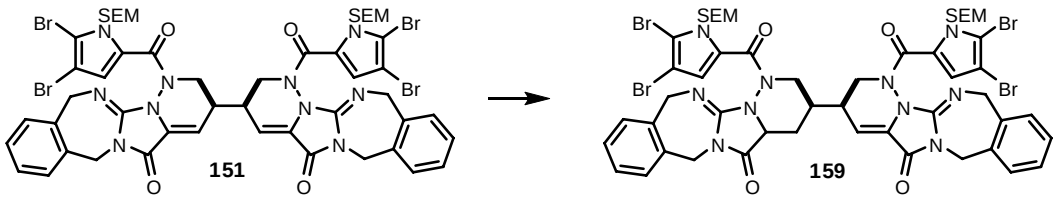

Conditions: **160** (5mol%), davephose **161** (5mol%), NH_4PF_6 (1.1 eq), MgI_2 (0.8 eq), $HSiMe_2Ph$ (1.1 eq), CH_2Cl_2, 24 h, **159** (60%).

With sufficient amount of compound **159** in hands; we were ready to try the base induced fragmentation. Massive decomposition was observed when KHMDS was employed. Then we switched to DBU. To the DMF solution of **159**, DBU and LiCl stock solution was added. The mixture was heated up to 50 °C. The use of TLC analysis showed that the starting material converted to a bright yellow spot with time. The structure of the yellow compound **166** was established by NMR analysis. One of N-N bonds did get cleaved but exclusively on the more oxidized side. In this case, the γ proton on the conjugated side was deprotonated and generated an extended conjugated enolate, which fragmented to afford compound **166**.

Scheme 4.12

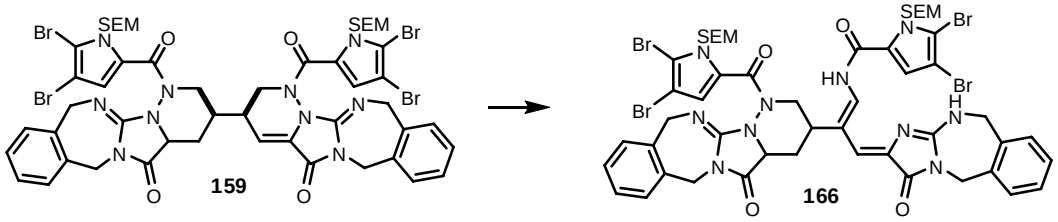

Conditions: DBU (1.3 eq), LiCl (1.2 eq), DMF, 52 °C, 6 h, (70%)

4.5 New Strategy: Chlorine Incorporation Before N-N bond Cleavage

As shown in the previous section, due to the acidity of the γ proton on the conjugated side in **159,** the DBU/LiCl treatment of compound **159** affords exclusively the product with the N-N bond cleavage on the wrong side. In order to decrease the acidity of the γ proton, **159** was treated with t-BuOCl in methanol[14]. A chlorine atom was incorporated and the resulting iminium ion was trapped with methanol to provide compound **167** (Scheme 4.13). In the context of compound **167**, the γ proton on the side of chlorine incorporation is no longer acidic enough to compete for the deprotonation. When **167** was treated with KHMDS, α proton to carbonyl was deprotoned, followed by fragmentation to afford **168**.

Scheme 4.13

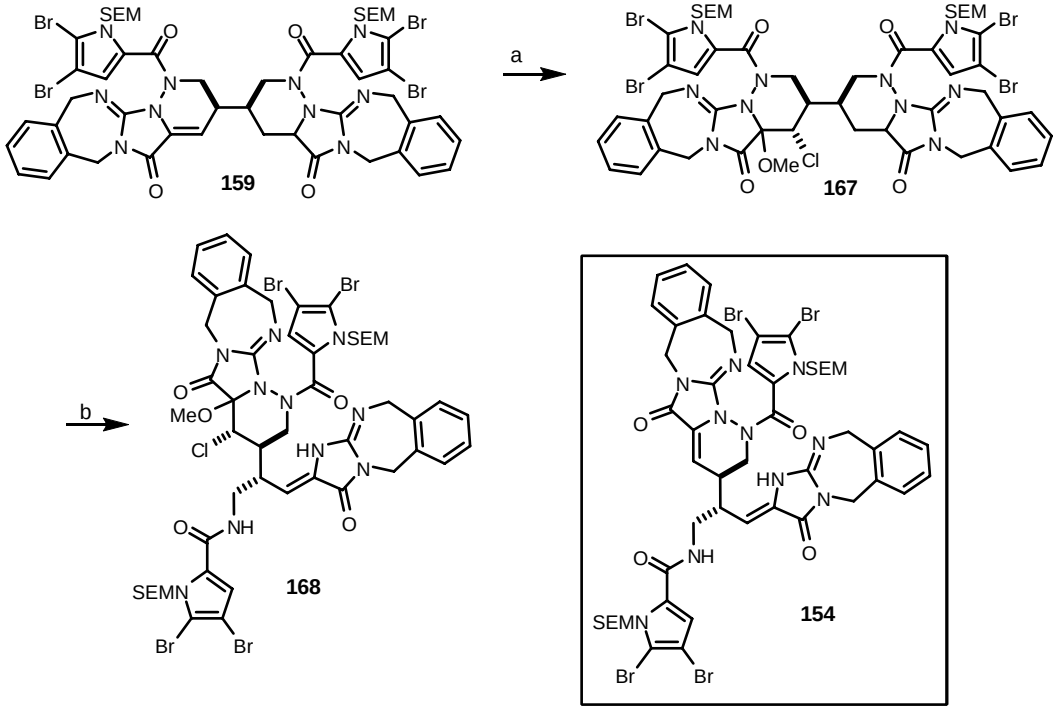

Conditions: a). *t*-BuOCl (1.05 eq), MeOH/THF, –78 °C, 2h, rt, 1.5h. (>95%); b). KHMDS (2.05 eq), THF, –78 °C, 2h, (50%)

Compound **168** is a more advanced intermediate compared to the asymmetric bisalkylidene **154** since it already has chlorine incorporated (Scheme 4.13). The next step is to force compound **168** to expel the methoxy group and generate the imnium ion **169**, the similar intermediate that was proposed in the original plan (chapter 1, section 1.5). Without interference of the external nucleophile, it was expected that the "enamine" would act as an internal nucleophile to give the desired product **155**. Many conditions had been carried out, including many Lewis acids and different bronstead acids under thermal conditions. However none of them succeeded.

Scheme 4.14

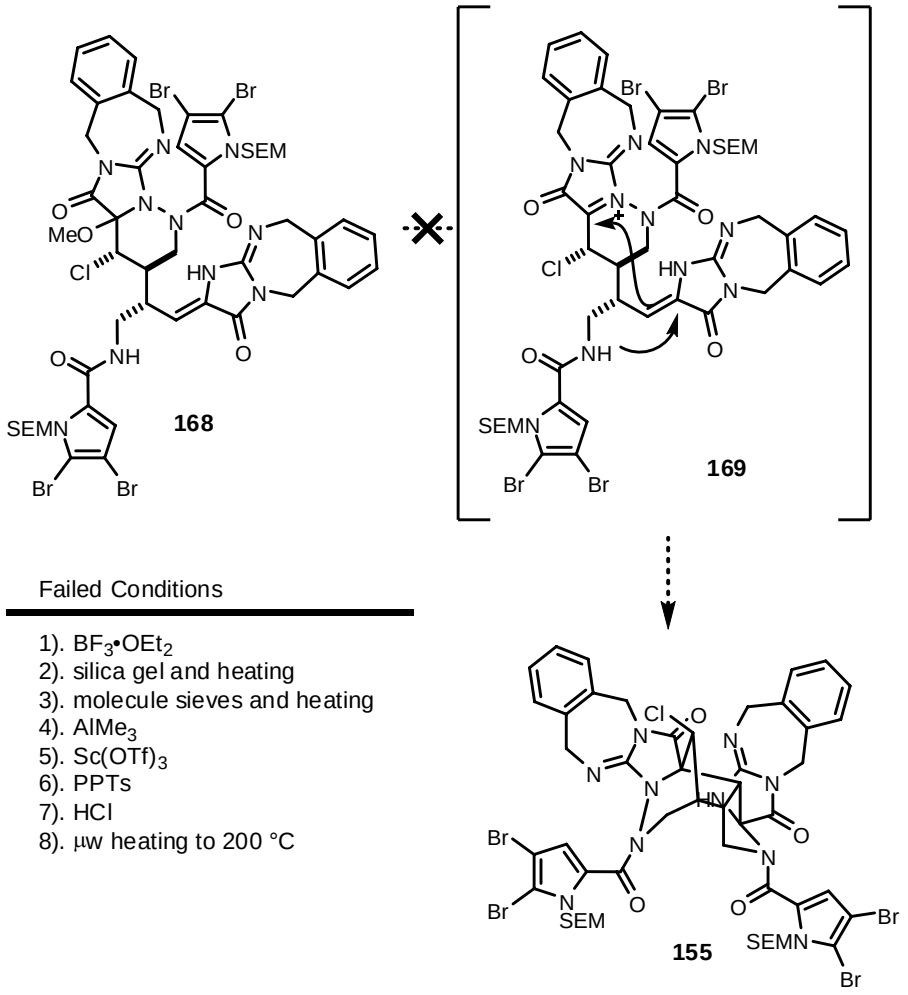

Under all the conditions we tried, there is no indication of the intermediate **169**'s formation. Since methanol had been proven to be a poor leaving group, we started to look at other potential nucleophiles. Acetic acid[15], formic acid, TFE and even chlorine gas were studied but failed to provide any success.

4.6 Experimental Section

4.6.1 Materials and Methods

Unless stated otherwise, reactions were performed under an argon atmosphere in flame-dried glassware. Tetrahydrofuran (THF), dichloromethane (CH_2Cl_2), diethyl ether (Et_2O), toluene (C_7H_8), benzene (C_6H_6) and acetonitrile (CH_3CN) were passed through Glass Contour solvent drying systems prior to use. Fine chemical reagents were obtained from commercial sources and used without further purification. Column chromatography was performed on E. Merck silica gel 60 (240-400 mesh). Thin layer chromatography and preparative layer chromatography utilized pre-coated plates from E. Merck (silica gel 60 PF254, 0.25mm or 0.5mm). Nuclear Magnetic Resonance (NMR) spectra were recorded on either a Varian Inova-600, Inova-400 or Mercury-300 magnetic resonance spectrometer. ^1H NMR chemical shifts are given in parts per million (δ) relative to a residual solvent signal. Infrared spectra were recorded on a Perkin-Elmer FT-IR spectrum 1000 using samples prepared as thin films between salt plates. Electrospray-ionization mass spectra (LRMS) were measured on a Shimadzu LCMS-2010 single quadrupole.

4.6.2 Preparative Procedures

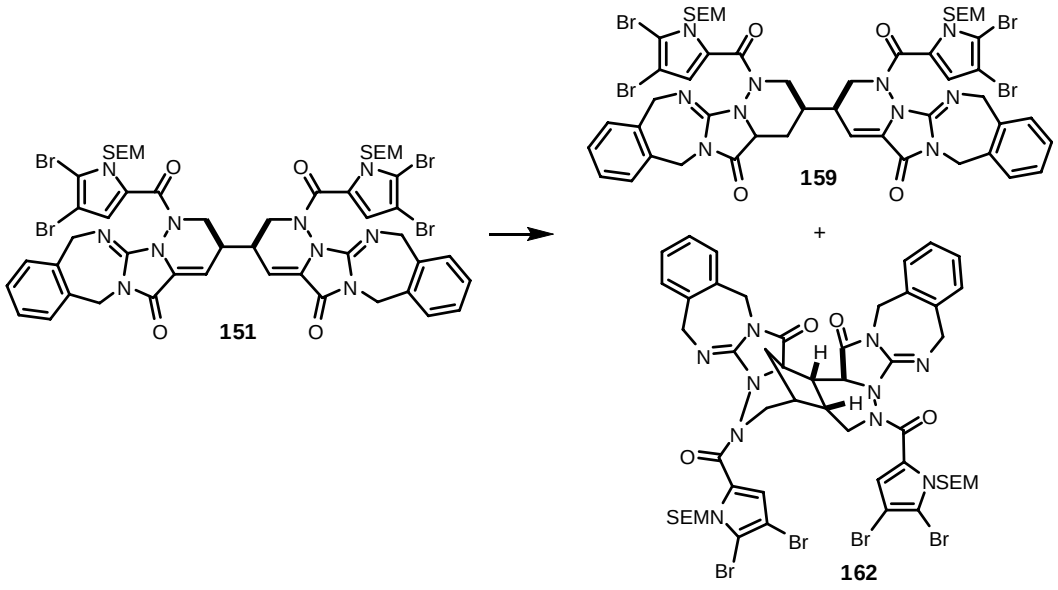

Compound 159 and 162: A solution of *meso* **21** (40 mg, 0.032 mmol) and MgBr2•Et2O (12 mg, 0.047 mmol) in THF (0.3 mL) was stirred at rt for 10 min before evaporation of the solvent. The residue was re-dissolved in a stock solution of Rh(I) catalyst **160** (1 mg), 2-dicyclohexylphosphino-2'-(N,N-dimethylamino)biphenyl **161** (1.2 mg) and $HSiMe_2Ph$ (5.5 μL, 0.035 mmol) in CH_2Cl_2 (0.16 mL). The resulting mixture was heated at 40 °C for 15 h. The reaction mixture was diluted with EtOAc, washed with saturated $NaHCO_3$, water and brine. The organic layer was dried over Na_2SO_4, filtered and concentrated *in vacuo*. Purification by silica gel chromatography (1:4 EtOAc/CH_2Cl_2) afforded polycycle **162** (18 mg, 45%) and mono reduction product **159** (12 mg, 30%).

162: white film; R_f = 0.9 (1:9 $CH_3CN/CHCl_3$); IR (film): 3430, 2950, 1751, 1695, 1684, 1448, 1418, 1409, 1247, 1091, 858, 835, 756, 700 cm-1; ^{1}H NMR (400

MHz, CD_3CN): δ 7.24-7.42 (m, 8H), 6.70 (s, 1H), 6.60 (s, 1H), 5.63 (dd, 2H, *J* = 2.8, 10.5Hz), 5.47 (m, 2H), 4.90-5.18 (m, 4H), 4.55-4.68 (m 3H), 4.40 (dd, 1H, *J* = 7.1, 13.1), 4.26 (d, 1H, *J* = 11.2Hz), 4.13 (d, 1H, *J* = 13.6Hz), 3.46-3.74 (m, 6H), 3.38 (m, 1H), 3.26 (m, 1H), 2.98 (m, 1H), 2.88, (t, 1H, *J* = 11.6Hz), 2.58 (t, 1H, *J* = 12.8Hz), 2.52 (m, 1H), 1.42 (d, 1H, *J* = 11.8Hz), 0.87 (m, 4H), -0.02 (s, 9H), -0.06 (s, 9H). ^{13}C NMR (75 MHz, $CDCl_3$): δ 168.6, 167.8, 163.8, 159.4, 146.3, 142.4, 140.2, 134.4, 133.1, 128.8, 128.7, 128.5, 128.4, 128.0, 127.9, 127.8, 124.6, 118.4, 113.7, 111.3, 108.4, 100.8, 99.6, 75.5, 75.1, 67.7, 66.1, 53.2, 49.9, 49.3, 48.8, 44.0, 43.4, 40.8, 40.4, 33.6, 33.5, 31.5, 17.9, 17.8, -1.4, -1.4. MS (positive electrospray) calc'd for $(C50H58Br4N10O6Si2+H)^+$: 1271.08, found 1270.94. Treatment of **162** with excess BF3 etherate provided derivative **163**. Crystals of **29** (PTLC purified) suitable for X-ray diffraction were grown from CH_3CN (slow evaporation).

159: white foam; R_f = 0.65 (1:4 CH_3CN:$CHCl_3$); IR (film): 2951, 2873, 1749, 1630, 1403, 1248, 1092, 836, 667 cm-1; ^1H NMR (400 MHz, CD_3CN): δ 7.30-7.40 (m, 7H), 7.24 (m, 1H), 6.76 (s, 1H), 6.69 (s, 1H), 5.81 (m, 1H), 5.60 (m, 3H), 5.44 (m, 1H), 4.56-5.00 (m, 8H), 4.44 (ddd, 1H, *J*=1.8, 3.1, 12.9Hz), 3.70 (dd, 1H, *J*=11.6Hz), 3.63 (t, 4H, *J* =8.1Hz), 3.46 (m, 1H), 2.54 (dd, 1H, *J* =11.6, 12.8Hz), 2.36 (dt, 1H, *J* =5.2, 10.4Hz), 2.12 (m, 1H), 1.70 (m, 1H), 1.35 (q, 1H, *J*=12.3Hz), 0.76-0.93 (m, 4H), 0.02 (s, 9H), -.0.03 (s, 9H). MS (positive electrospray) calc'd for $(C50H58Br4N10O6Si2+H)^+$: 1271.08, found 1271.04.

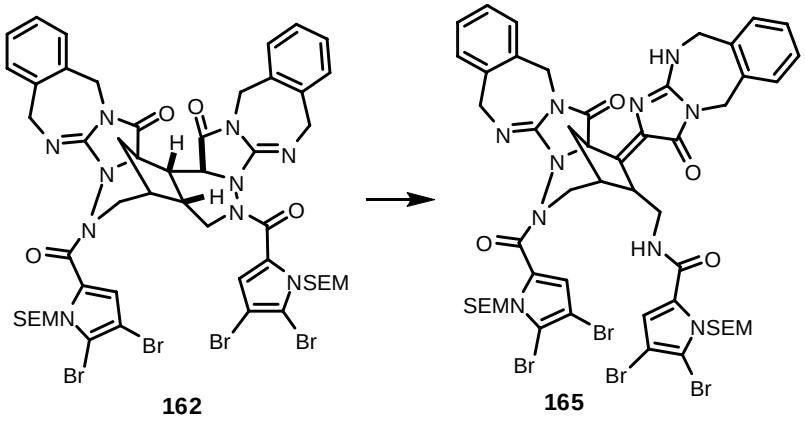

162 **165**

Compound (165). KHMDS (70 μL, 0.5 M in toluene) was added to a solution of **162** (22 mg, 0.017 mmol) in THF (100 μL) at −78 °C. The dark pink solution was stirred at −78 °C for 30 min and then warmed to rt. After stirring at rt for 30 min, 10 μL AcOH was added and the solution diluted with CH_2Cl_2. The organics were washed with saturated aq $NaHCO_3$, water and brine, dried over Na_2SO_4, and concentrated *in vacuo*. Purification by preparative thin layer chromatography (3:7 $CH_3CN/CHCl_3$) afforded **165** as white film (18 mg, 80%).

165: R_f = 0.6 (3:7 $CH_3CN/CHCl_3$); ^1H NMR (400 MHz, CD_3CN): δ 9.27 (app d, 1H, *J*=7.4Hz), 7.30-7,45 (m, 7H), 7.21 (m, 1H), 6.74 (s, 1H), 6.61 (s, 1H), 5.87 (d, 1H, *J* =10.8Hz), 5.82 (d, 1H, *J*=10.8Hz), 5.66 (d, 1H, *J*=10.8Hz), 5.39 (d, 1H, *J* =10.8Hz), 4.93 (m, 4H), 4.64 (m, 2H), 4.39 (m, 2H), 3.71 (m, 1H), 3.54 (m, 2H), 3.40 (m, 2H), 3.23 (m, 1H), 2.95 (m, 2H), 2.57 (m, 1H), 1.64 (d, 1H, *J*=11.8Hz), 0.60-0.90 (m, 4H), -0.04 (s, 9H), -0.29 (s, 9H); MS (positive electrospray) calc'd for $(C50H58Br4N10O6Si2+H)^+$: 1271.08, found 1270.94.

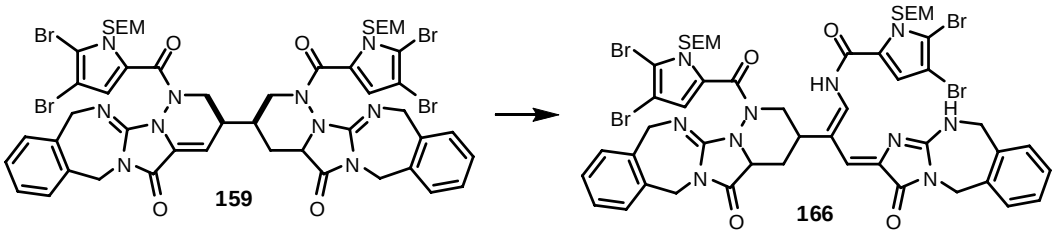

Compound 166: Reduction product **159** (20 mg, 0.016 mmol) was dissolved in a stock solution of LiCl (0.8 mg, 0.019 mmol) and DBU (3 μL, 0.021 mmol) in DMF (100 μL- argon sparged). After heating at 52 °C for 3 h, the reaction mixture was quenched with acetic acid (5 μL) and diluted with CH_2Cl_2. The resulting solution was washed with saturated $NaHCO_3$, water and brine. The organic layer was dried over Na_2SO_4, filtered and concentrated *in vacuo*. The residue was purified by preparative thin layer chromatography (1:4 $CH_3CN/CHCl_3$) to afford **166** as bright yellow solid (14 mg, 70%).

166: Rf = 0.8 (2:9 $CH_3CN/CHCl_3$); 1H NMR (400 MHz, CD_3CN/D_2O): δ 7.20-7,45 (m, 8H), 6.87 (s, 1H), 6.82 (s, 1H), 6.75 (s, 1H), 5.92 (s, 1H), 5,79 (s, 2H), 5,64 (d, 1H, *J* = 10.8Hz), 5.46 (d, 1H, *J* = 10.7Hz), 4.88(m, 5H), 4.50(m, 3H), 4.31 (d, 1H, *J* = 12.4Hz), 3.85 (dd, 1H, *J* = 4.6, 11.4Hz), 3.50-3.57(m, 4H), 2.75(m, 1H), 2.53(tt, 1H, *J* = 3.0, 11.8Hz), 2.17(m,1H), 1.62 (m, 1H), 0.77-0.90 (m, 4H), -0.04 (s, 9H), -0.02 (s, 9H). MS (positive electrospray) calc'd for $(C50H58Br4N10O6Si2+H)^+$: 1271.08, found 1271.45.

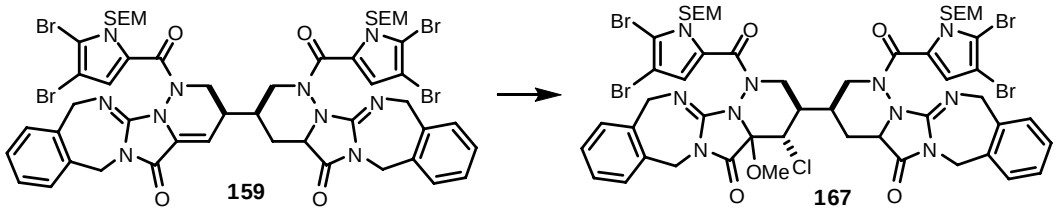

Compound 167: Compound **159** (60 mg, 0.047 mmol) was dissolved in THF (0.75 mL) and MeOH (1.2 mL). The solution was cooled down to −78 °C, followed by the addition of stock solution of *t*-BuOCl (5.7 μL, 0.05mmol) in CH_2Cl_2 (50 μL). The reaction mixture was stirred at −78 °C for 2 hours and rt for another 2 hours. The solvent was removed and the resulting residue was PTLC (CH_3CN:$CHCl_3$ = 2:8) to afford diastereoisomers mixture (58 mg, 97%).

167 (diastereoisomer 1) white solid; R_f = 0.7 (EtOAc:CH_2Cl_2= 1:9); IR (film, cm^{-1}): 2951, 1760, 1694, 1526, 1401, 1298, 1149, 1089, 923, 858, 836; ^{1}H NMR (400 MHz,CD_3CN): 7.28-7.45 (m, 8H,), 6.88 (s, 1H), 6.83 (s, 1H), 5.84 (d, 1H, *J* = 10.3 Hz), 5.84 (d, 1H, *J* = 10.3 Hz), 5.56 (d, 1H, *J* = 10.6 Hz), 5.47 (d, 1H, *J* = 10.6 Hz), 5.31 (d, 1H, *J* = 10.7 Hz), 4.46-5.14 (m, 11H), 3.96 (dd, 1H, *J* = 4.7 Hz and 11.6 Hz), 3.43-3.59 (m, 5H), 2.96 (dd, 1H, *J* = 3.1 and 14.2 Hz), 2.87 (s, 3H), 2.54 (m, 1H), 2.32 (m, 1H), 2.10 (m, 1H), 1.60 (ddd, 1H, *J* = 4.4, 11.7, 14.8 Hz), 0.82 (m, 4H), 0.00 (s, 9H), -0.02 (s, 9H); MS (positive electrospray) calc'd for $(C_{51}H_{61}Br_4ClN_{10}O_7Si_2+H)^+$: 1337.05, found 1337.05.

167 (diastereoisomer 2) white solid; R_f = 0.6 (EtOAc:CH_2Cl_2= 1:9); IR (film, cm^{-1}): 2951, 1759, 1693, 1402, 1210, 1091, 836; ^{1}H NMR (400 MHz,CD_3CN): 7.26-

7.43 (m, 8H,), 6.99 (s, 1H), 6.77 (s, 1H), 5.82 (d, 1H, *J* = 10.3 Hz), 5.64 (d, 1H, *J* = 10.5 Hz), 5.46 (d, 1H, *J* = 10.5 Hz), 5.38 (d, 1H, *J* = 10.3 Hz), 5.31 (d, 1H, *J* = 10.7 Hz), 4.19-5.04 (m, 11H), 3.79 (dd, 1H, *J* = 4.9 Hz and 11.6 Hz), 3.43-3.59 (m, 4H), 2.98 (dd, 1H, *J* = 11.4 and 13.3 Hz), 2.87 (s, 3H), 2.43 (m, 1H), 2.30 (m, 1H), 2.10 (m, 1H), 1.76 (m, 1H), 0.81-1.00 (m, 4H), 0.00 (s, 18H). MS (positive electrospray) calc'd for $(C_{51}H_{61}Br_4ClN_{10}O_7Si_2+H)^+$: 1337.05, found 1337.06.

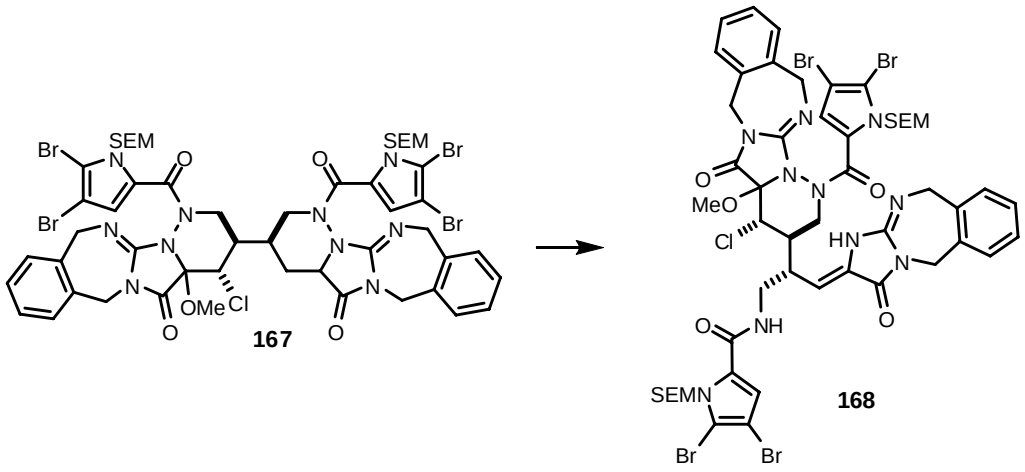

Compound 168: KHMDS (125 μL, 0.5M) was added to the THF (0.3 mL) solution of 139 (36 mg, 0.028mmol) at −78 °C. After stirred at −78 °C for 15 minutes, the reaction was allowed to warm up to room temperature. Acetic acid (5 μL) was used to quench the reaction. The reaction mixture was taken up with CH_2Cl_2 and washed with sat.$NaHCO_3$, water, brine and dried over Na_2SO_4. After the solvent removal in vacuo the residue was purified by PTLC (CH_3CN:$CHCl_3$ = 2:8) to afford diastereoisomers mixture (18 mg, 50%)

168: white solid; R_f = 0.7 (CH_3CN : $CHCl_3$ = 2:8); IR (film, cm^{-1}): 2951, 1700, 1607, 1544, 1410, 1312, 1248, 1092, 836, 752; ^1H NMR (400 MHz, CD_3CN): 7.30-7.49 (m, 8H,), 6.86 (s, 1H), 6.74 (s, 1H), 5.85 (d, 1H, *J* = 10.3 Hz), 5.77 (q, 1H, *J* = 10.5 Hz), 5.58 (d, 1H, *J* = 9.1 Hz), 5.38 (d, 1H, *J* = 10.4 Hz), 4.86-5.04 (m, 5H), 4.50-4.64 (m, 4H), 4.14 (d, 1H, *J* = 11.6 Hz), 3.44-3.74 (m, 5H), 3.03 (m, 1H), 0.77-1.02 (m, 4H), 0.00 (s, 9H), -0.02 (s, 9H). MS (positive electrospray) calc'd for $(C_{51}H_{61}Br_4ClN_{10}O_7Si_2+H)^+$: 1337.05, found 1337.05.

4.7 Notes and References

(1) Grob, C. A.; *Angew. Chem. Int. Ed.* **1967**, 6, 1.

(2) Wender, P. A.; Manly, C. J. *J. Am. Chem. Soc*. **1990**, 112, 8579-8581.

(3) (a) Sperier, J. L.; Webster, J. A.; Barnes, G. H. *J. Am. Chem. Soc*. **1957**. 79, 974-979. (b) Chandra, G.; Lo, P. Y.; Hitchcock, P. B.; Lappert, M. F. *Organometallics*, **1987**, 191-192. (c) Markò, I, E.; Stèrin, S.; Buisine, O.; Mignani, G.; Branlard, P.; Tinant, B.; Declercq, J. Science, 2002, 298, 204-206.(d) Magnus, P.; Payne, A. H.; Waring, M. J.; Scott, D. A. Lynch, V. *Tetrahedron Lett*, **2000**, 41, 9725-9730. (e) Mahoney, W.; Stryker, J. M. *J. Am. Chem. Soc*. **1989**, 111, 8818-8823. (f) Keinan, E.; Perez, D. *J. Org. Chem.* **1987**, 52, 2576-2580. (g) Niyomura, O.; Iwasawa, T.; Sawada, N, Tokunaga, M.; Obora, Y.; Tsuji, Y. *Organimetallics*, **2005**, 24, 3468-3475. (h) Ikeno, T.; Kimura, T.; Ohtsuka, Y.; Yamada, T. *Synlett*, **1999**, 96-98.

(4) Ojima, I.; Kogure, T. *Organometallics*, **1982**, 1390-1399.

(5) Manthorpe, J. M.; Gleason, J. L. *J. Am. Chem. Soc*. **2001**, 123, 2091-2092.

(6) (a) Irikura, K. K.; Goddard, W. A.; Beauchamp, J. L. *J. Am. Chem. Soc.* **1992**, 114, 48-51. (b) Arduenga, A. J.; Dias, H. V. R.; Harlow, R. L.; Kline, M. *J. Am. Chem. Soc.* **1992**, 114, 5530-5534.

(7) Voutchkova, A. M.; Appelhans, L. N.; Chianese, A. R.; Crabtree, R. H. *J. Am. Chem. Soc.* **2005**, 127, 17624-17625.

(8) K.W. Anderson, S.L. Buchwald *Angew. Chem. Int. Ed*. **2005**, 44, 6173-6177.

(9) Its proton spectrum in CD_3CN has a doublet at 4.2pppm. It gradually diminished over one day, when D_2O was added to the sample. Base on exchangeable rate and coupling pattern, it was assigned as the methine proton next to carbonyl.

(10) Mukaiyama, T. *Angew. Chem. Int. Ed*. **2003**, 16, 817-826.

(11) Concellón, J. M.; Rodrīguez-Solla, H.; Bardales, E.; Huerta, M. *Eur. J. Org. Chem.* **2003**, 1775-1778.

(12) Gong, Y.; Bausch, M. J.; Wang, L. *Tetrahedron Lett*, **2001**, 42, 1-4.

(13) Concellón, J. M.; Rodriguez-Solla, H.; Barfales, E.; Huerta, M. *Eur. J. Org.* **2003**, 1775-1778.

(14) Mittendorf, J.; Hiemstra, H.; Speckamp, W. N. Tetrahedron, 1990, 46, 4049-4062.

(15) Nagasaka, T., Abe, Masako, Ozawa, N.; Kosugi, Y.; Hamaguchi, F. *Heterocycles*, **1983**, 20, 985-990.

APPENDIX E
Spectra of Compounds Appearing In Chapter 4

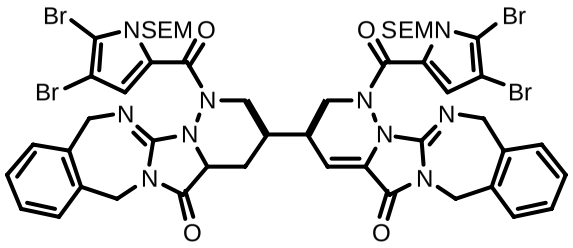

159
one isomer
unknown stereochemisty

Solvent: CD_3CN
Temp: 70 °C; 400 MHz

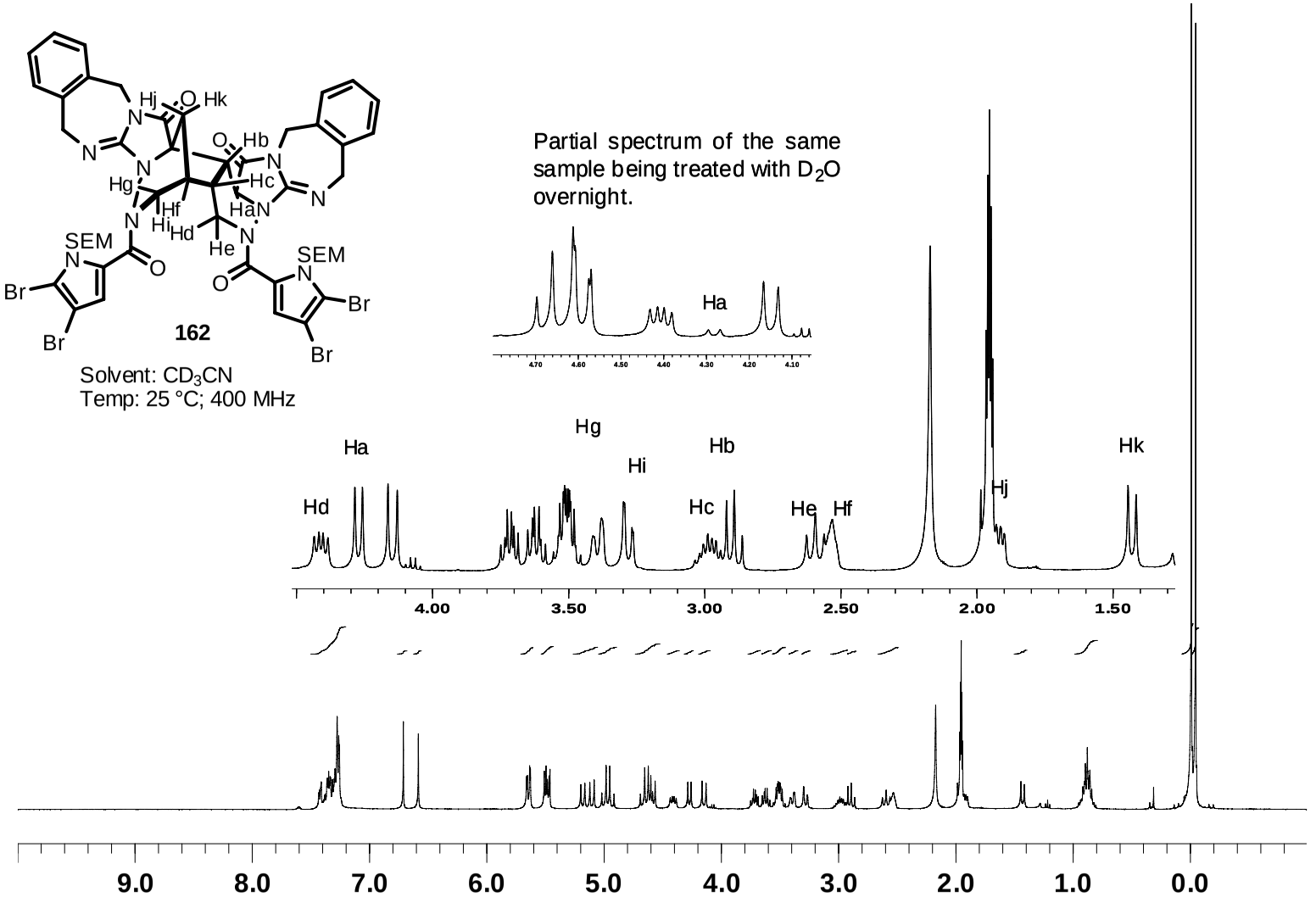
Hj
O
Hk
O
Hb
N
N
N
N
Hg
Hc
N
Hf
HaN
N
Hi
Hd
He
N
SEM
N
O
O
SEM
N
Br
Br
Br
Br
162
Solvent: CD3CN
Temp: 25 °C; 400 MHz
Partial spectrum of the same sample being treated with D2O overnight.
Ha
Hg
Ha
Hb
Hi
Hk
Hd
Hc
He
Hf
Hj
4.00
3.50
3.00
2.50
2.00
1.50
9.0
8.0
7.0
6.0
5.0
4.0
3.0
2.0
1.0
0.0

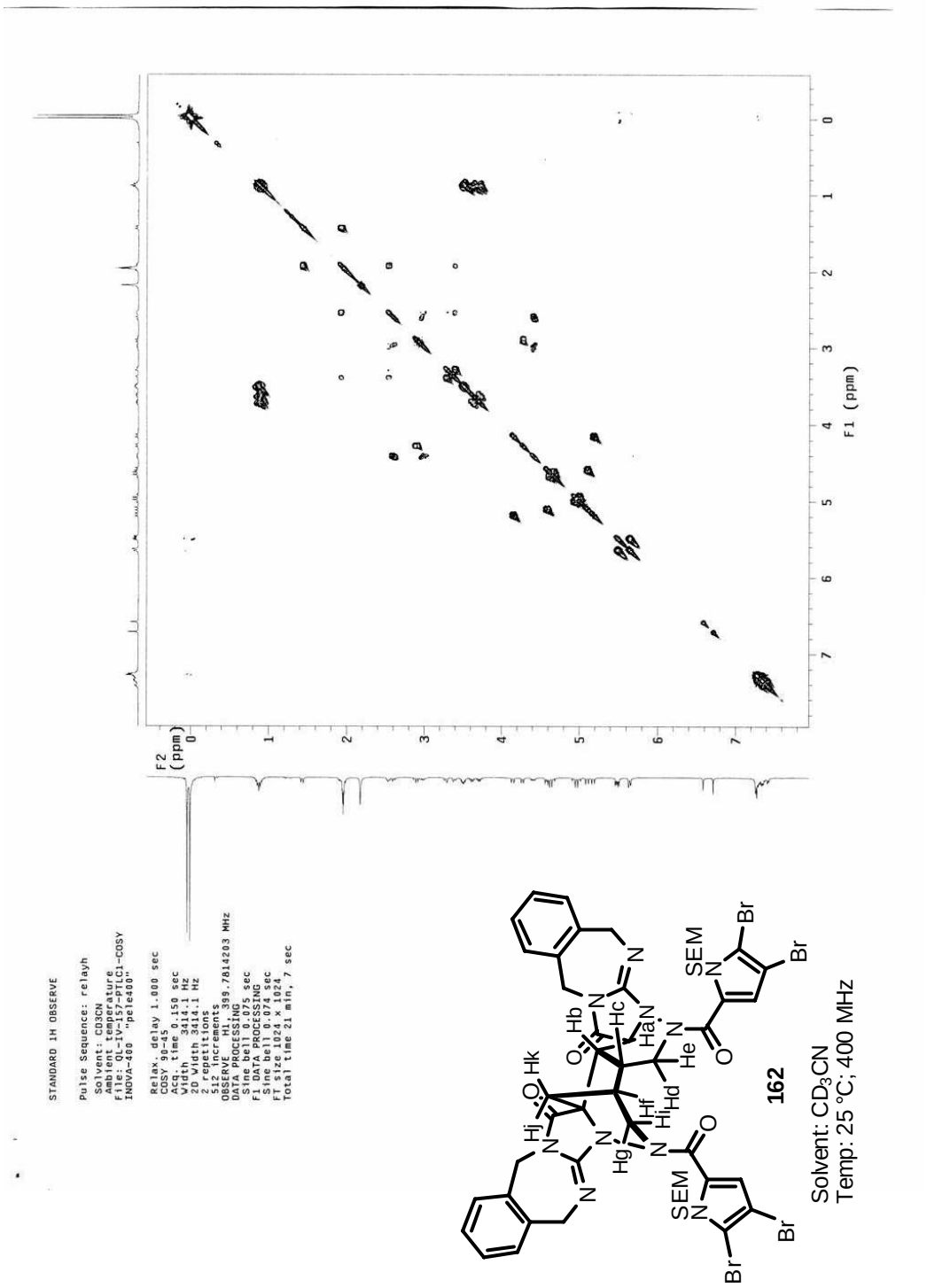
STANDARD 1H OBSERVE
Pulse Sequence: relayh
Solvent: CD3CN
Ambient temperature
File: d:\varian\ft\...\COSY
INOVA-400 "pele400"
Relax. delay 1.000 sec
COSY 90-45
Acq. time 0.150 sec
Width 3414.1 Hz
2D Width 3414.1 Hz
2 repetitions
512 increments
OBSERVE H1, 399.7814203 MHz
DATA PROCESSING
Sine bell 0.075 sec
FT DATA PROCESSING
Sine bell 0.075 sec
FT size 1024 x 1024
Total time 21 min, 7 sec
F2 (ppm)
F1 (ppm)
Ha
Hb
Hc
Hd
He
Hf
Hg
Hi
Hj
Hk
SEM
Br
162
Solvent: CD3CN
Temp: 25 °C; 400 MHz

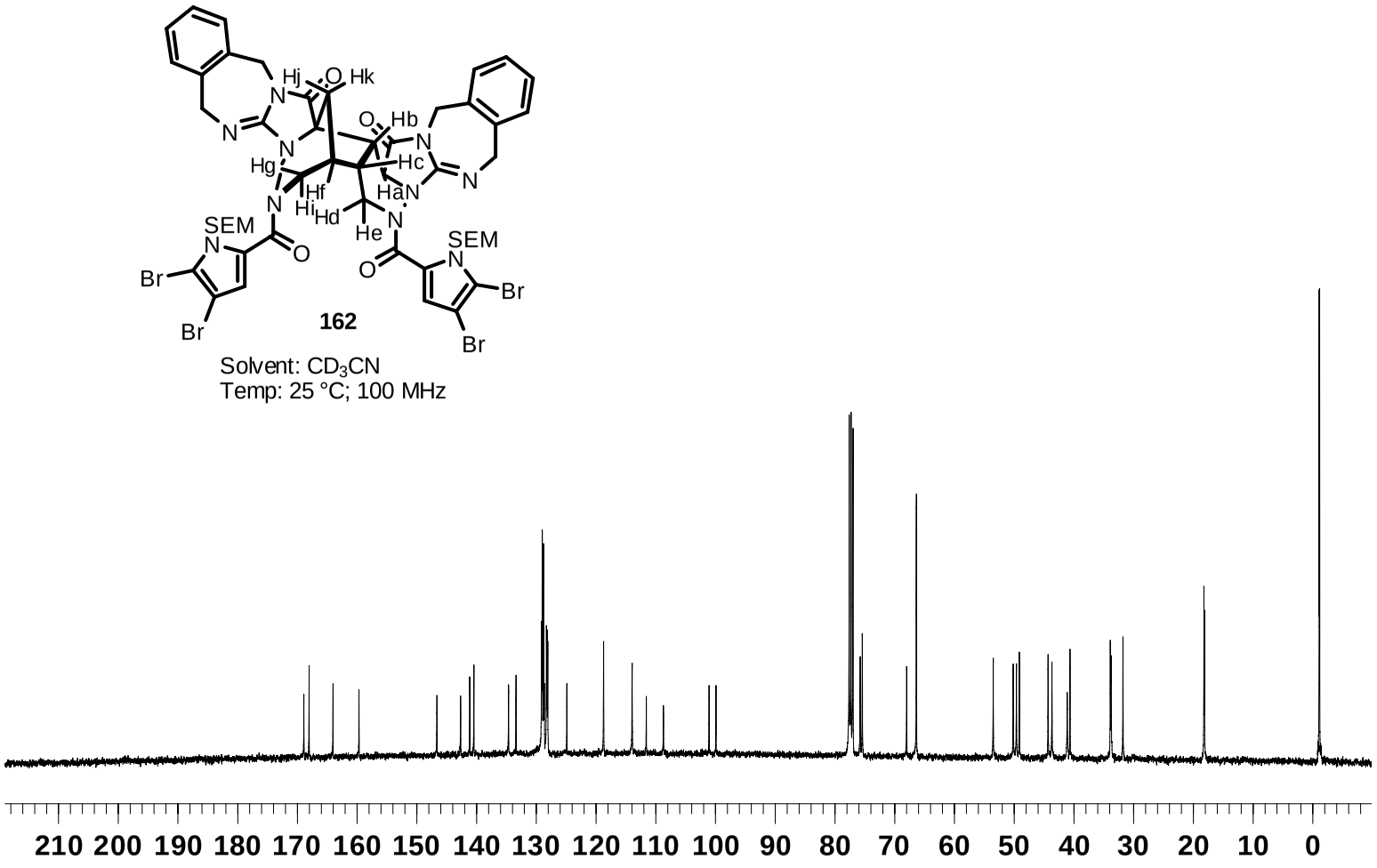
Hj
O
Hk
Hb
Hc
Hg
Hf
Hi
Hd
He
Ha
SEM
SEM
Br
Br
Br
Br
162
Solvent: CD3CN
Temp: 25 °C; 100 MHz
210 200 190 180 170 160 150 140 130 120 110 100 90 80 70 60 50 40 30 20 10 0

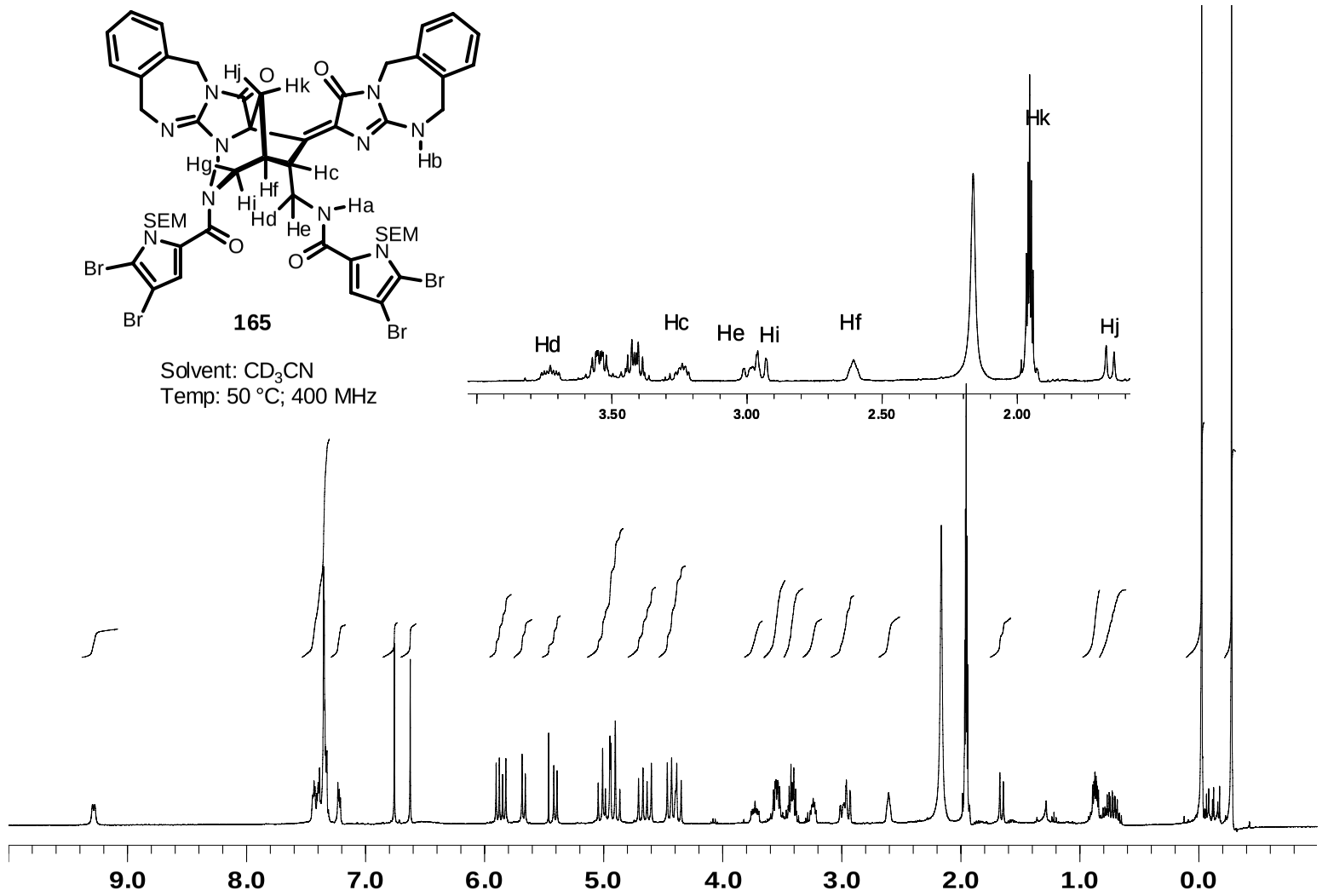
Hj
O
Hk
O
N
N
N
N
N
N
Hb
Hg
Hc
Hf
Hi
Hd
He
N
Ha
SEM
N
O
O
SEM
N
Br
Br
Br
Br
165
Solvent: CD3CN
Temp: 50 °C; 400 MHz
Hk
Hd
Hc
He
Hi
Hf
Hj
3.50
3.00
2.50
2.00
9.0
8.0
7.0
6.0
5.0
4.0
3.0
2.0
1.0
0.0

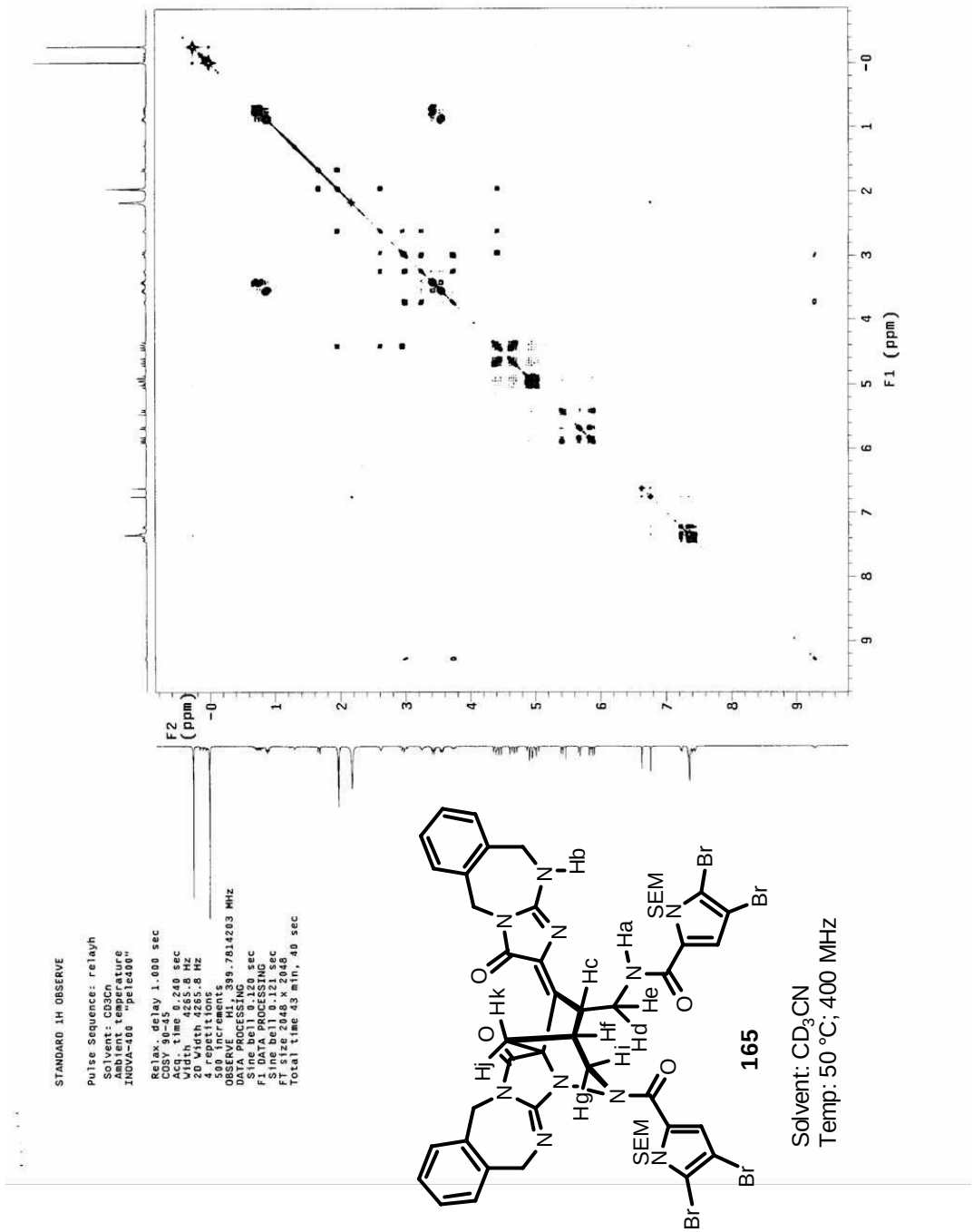
STANDARD 1H OBSERVE
Pulse Sequence: relayh
Solvent: CD3Cn
Ambient temperature
INOVA-400 "pele400"
Relax. delay 1.000 sec
COSY 90-45
Acq. time 0.240 sec
Width 4255.8 Hz
2D Width 4255.8 Hz
4 repetitions
500 increments
OBSERVE H1, 399.7814203 MHz
DATA PROCESSING
Sine bell 0.120 sec
FT of F2 DATA
Sine bell 0.121 sec
FT size 2048 x 2048
Total time 43 min, 40 sec
F2 (ppm)
F1 (ppm)
Hb
Hc
Ha
He
Hd
Hf
Hi
Hg
Hj
Hk
SEM
Br
165
Solvent: CD3CN
Temp: 50 °C; 400 MHz

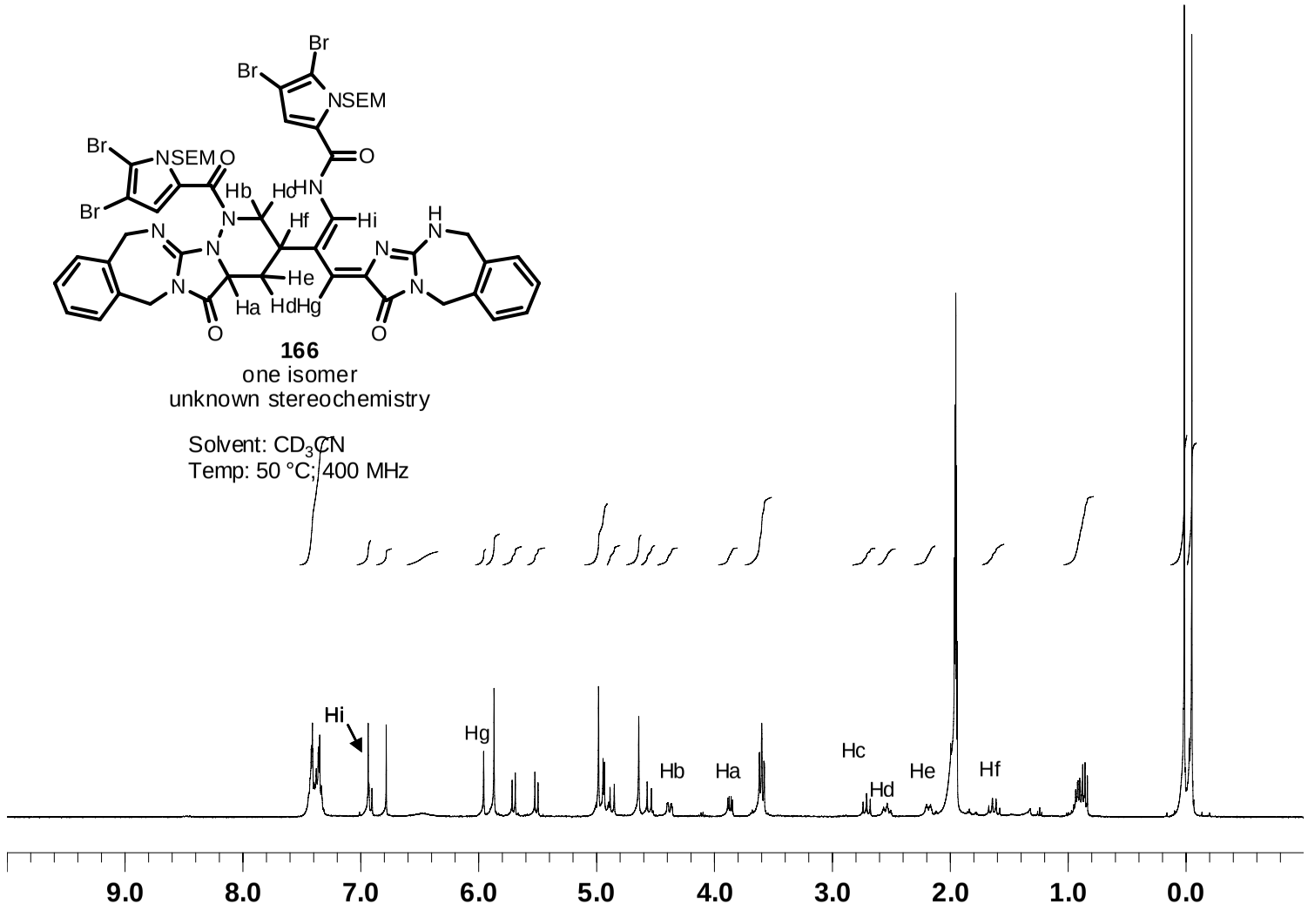
Br
Br
NSEM
Br
NSEM
O
O
Hb
Hd
HN
Br
N
Hf
Hi
H
N
N
N
N
N
He
N
Ha
HdHg
O
O
166
one isomer
unknown stereochemistry
Solvent: CD3CN
Temp: 50 °C; 400 MHz
Hi
Hg
Hb
Ha
Hc
Hd
He
Hf
9.0
8.0
7.0
6.0
5.0
4.0
3.0
2.0
1.0
0.0

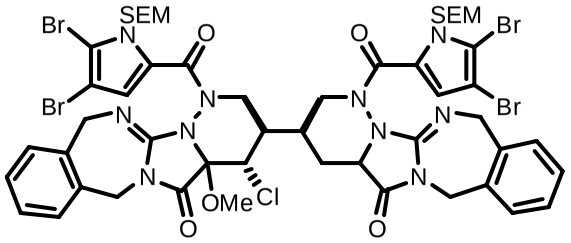

167, diastereoisomer 1

Solvent: CD_3CN
Temp: 50 °C; 400 MHz

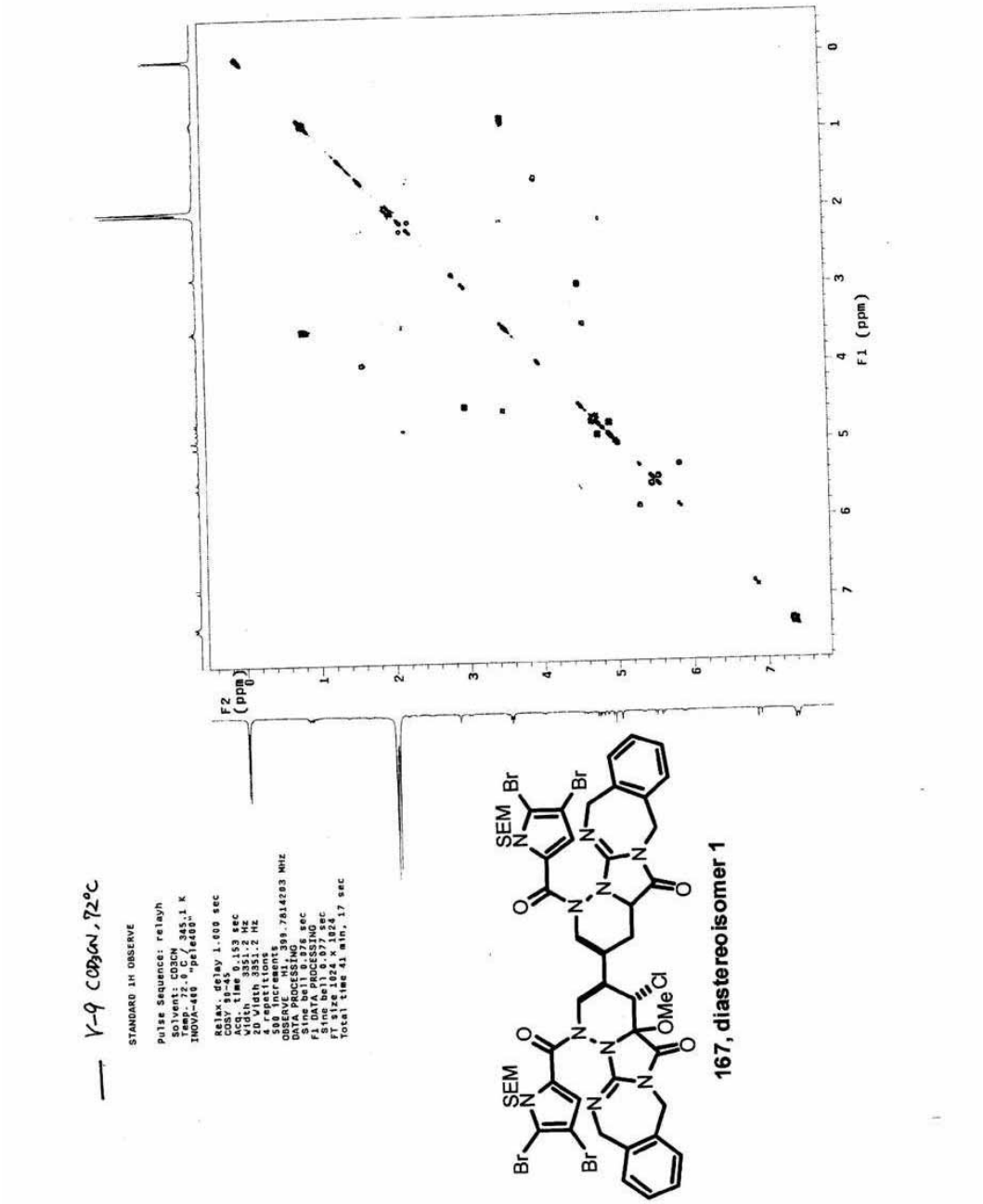
— V-9 COSGN, 22°C
STANDARD 1H OBSERVE
Pulse Sequence: relayh
Solvent: CDCN 345.1 K
Temp 72.0 C / 345.1 K
INOVA-400 "pe1e400"
Relax. delay 1.000 sec
COSY 90-45
Acq. time 0.153 sec
Width 3351.2 Hz
2D Width 3351.2 Hz
4 repetitions
512 increments
OBSERVE H1, 399.7814203 MHz
DATA PROCESSING
Sine bell 0.077 sec
FT size 1024 x 1024
Total time 41 min, 17 sec
F2 (ppm)
F1 (ppm)
SEM
Br
OMe
Cl
167, diastereoisomer 1

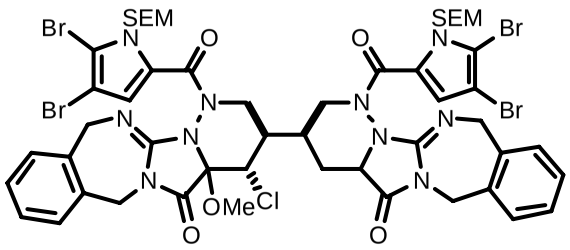

167, diastereoisomer 2

Solvent: CD_3CN
Temp: 50 °C; 400 MHz

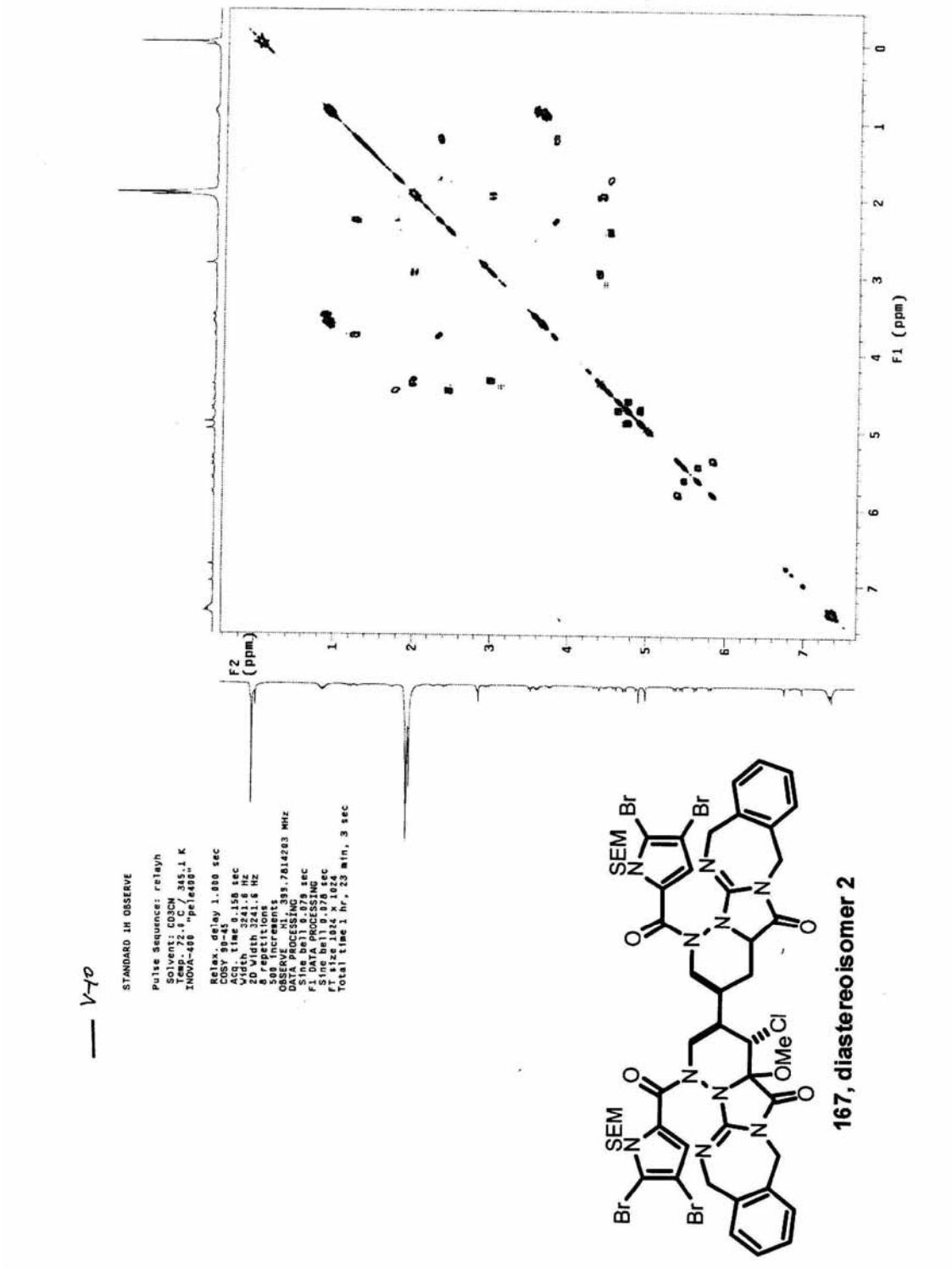
V-40
STANDARD 1H OBSERVE
Pulse Sequence: relayh
Solvent: CD3CN
Temp. 72.0 C / 345.1 K
INOVA-400 "pele400"
Relax. delay 1.000 sec
Pulse 45.0 degrees
Acq. time 0.158 sec
Width 3241.6 Hz
2D Width 3241.6 Hz
8 repetitions
508 increments
OBSERVE H1, 399.7814203 MHz
DATA PROCESSING
Sine bell 0.079 sec
F1 DATA PROCESSING
Sine bell 0.076 sec
FT size 1024 x 1024
Total time 1 hr, 23 min, 3 sec
F2 (ppm)
F1 (ppm)
SEM
Br
OMe
Cl
167, diastereoisomer 2

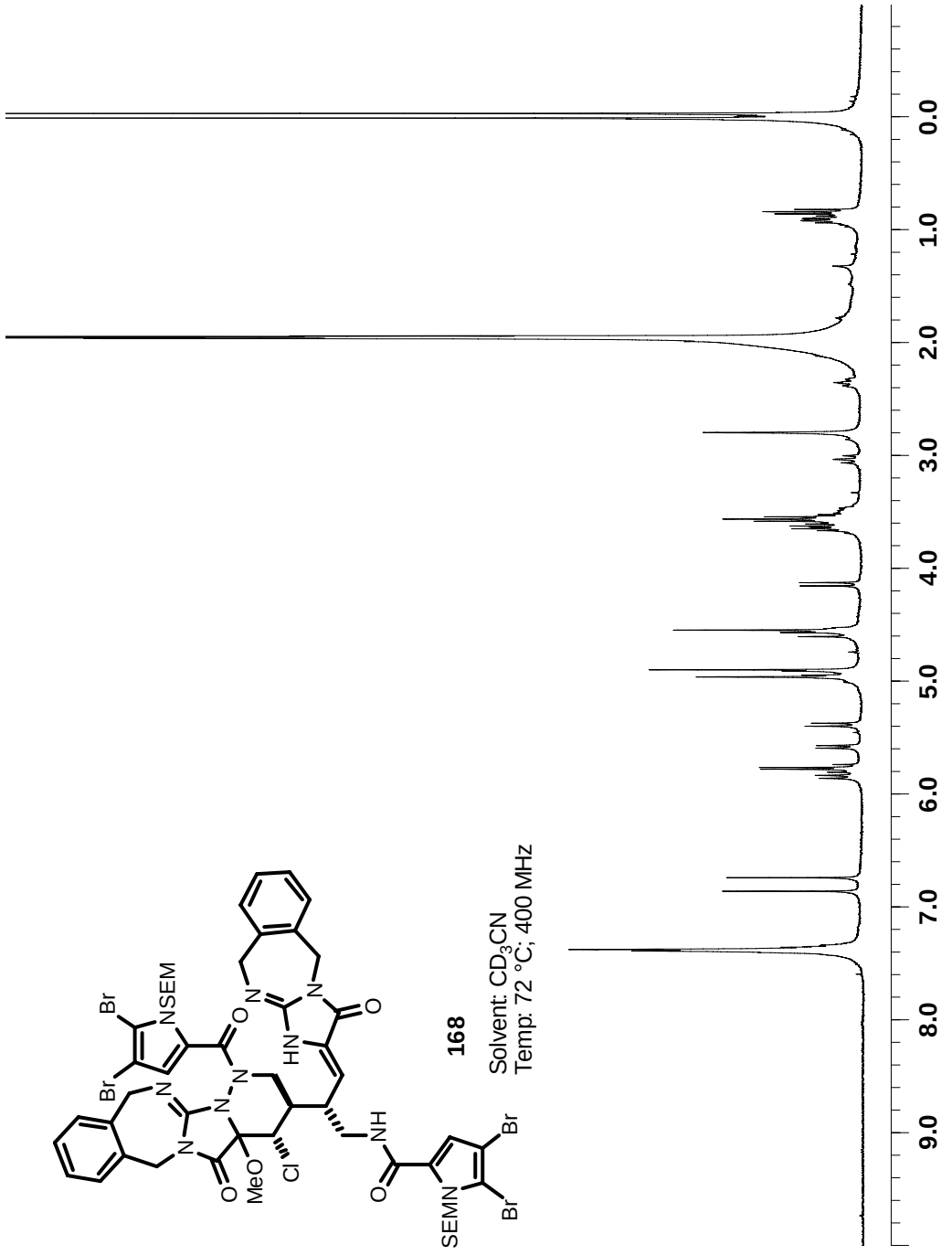
Br
NSEM
Br
N
N
N
N
N
O
O
MeO
Cl
HN
O
NH
O
SEMN
Br
Br
168
Solvent: CD3CN
Temp: 72 °C; 400 MHz
9.0
8.0
7.0
6.0
5.0
4.0
3.0
2.0
1.0
0.0

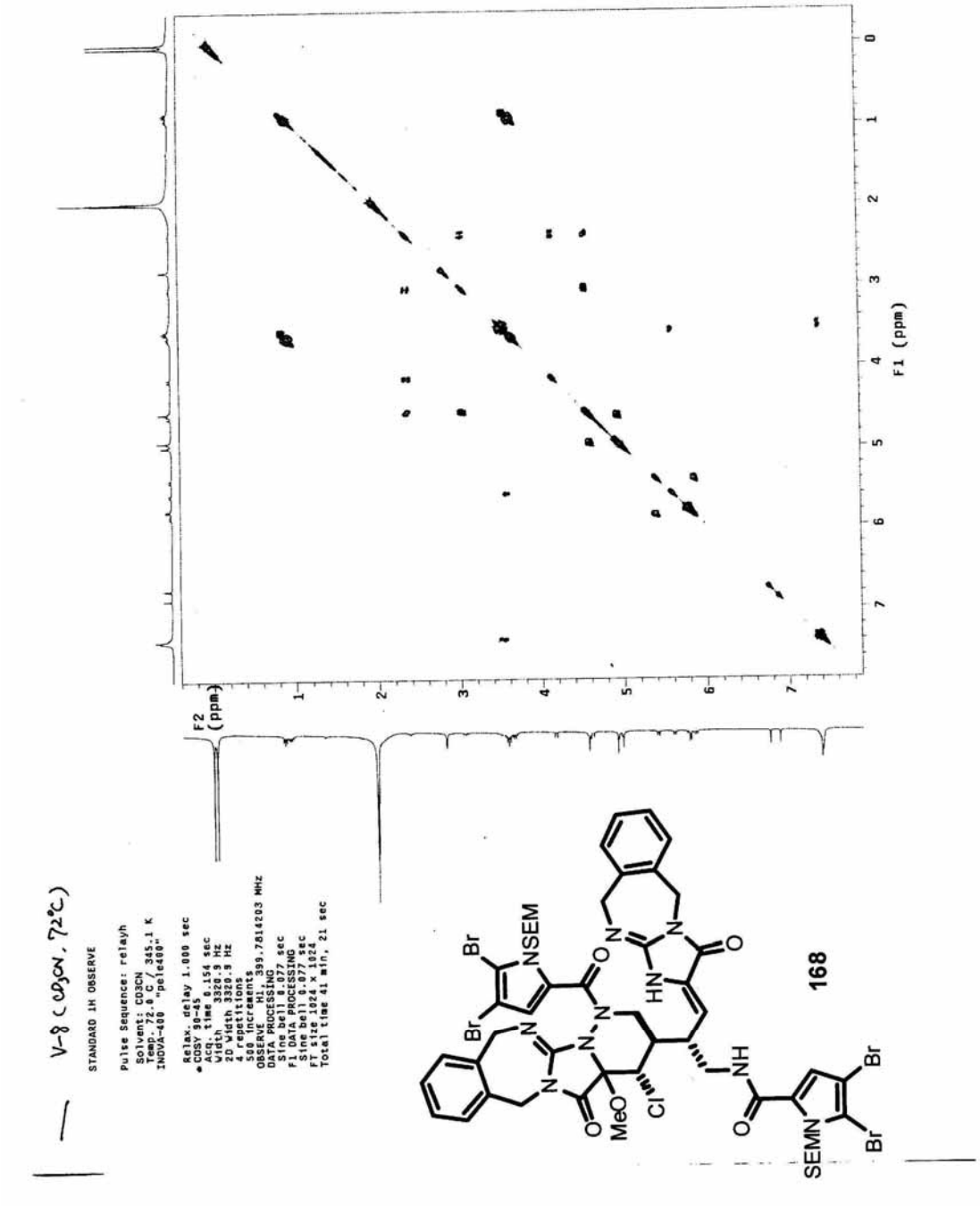
V-8 (CDCN, 72°C)
STANDARD 1H OBSERVE
Pulse Sequence: relayh
Solvent: CD3CN
Temp. 72.0 C / 345.1 K
INOVA-400 "pele400"
Relax. delay 1.000 sec
COSY 90-45
Acq. time 0.154 sec
Width 3320.9 Hz
2D Width 3320.9 Hz
4 repetitions
500 increments
OBSERVE H1, 399.7814203 MHz
DATA PROCESSING
FT mode 1777 sec
FI DATA PROCESSING
Sine bell 0.077 sec
FT size 1024 x 1024
Total time 41 min, 21 sec
F2 (ppm)
F1 (ppm)
Br
NSEM
Br
HN
MeO
Cl
NH
SEMN
Br
Br
168

APPENDIX F
X-ray Crystallographic Data for 163

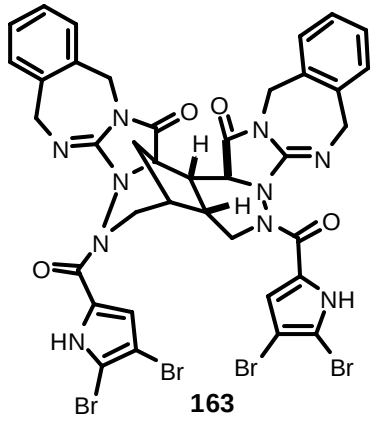

163

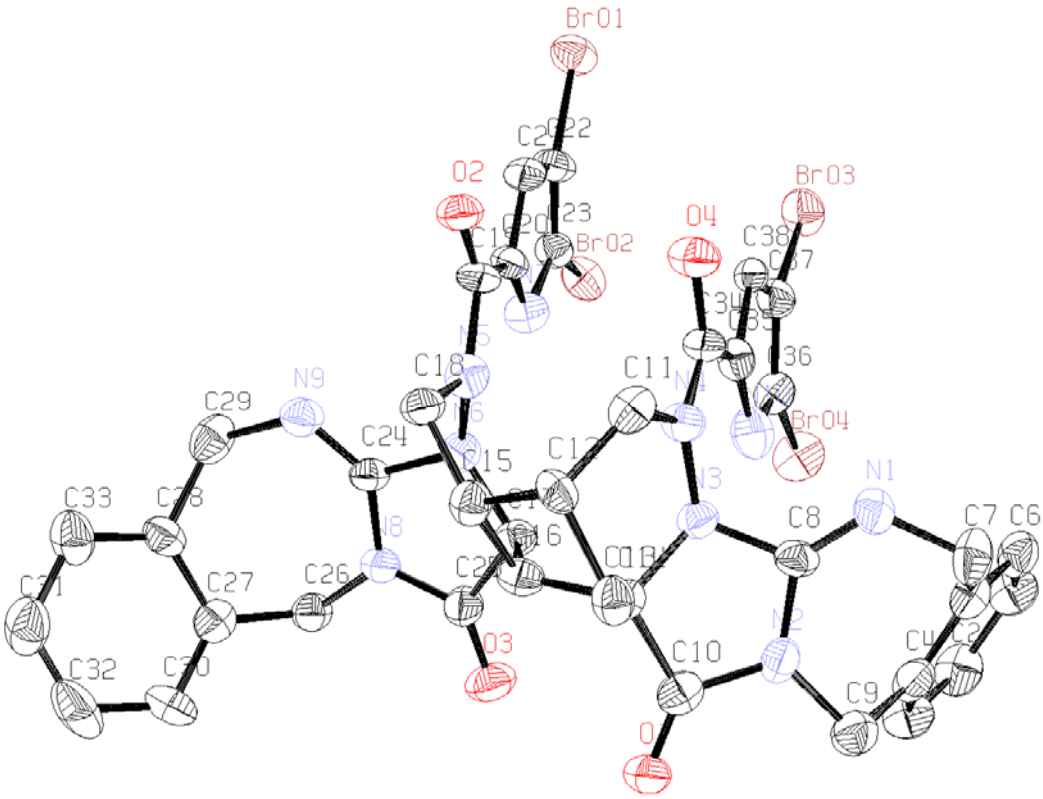

Table 1. Crystal data and structure refinement for 163.

Empirical formula	C38 H30 Br4 N10 O4
Formula weight	1010.36
Wavelength	0.71073 A
Crystal system, space group	Tetragonal, I 41/a
Unit cell dimensions	a = 27.7840(18) Å
	b = 27.7840(18) Å
	c = 21.9750(13) Å
Volume	16963.6(19) $Å^3$
Z, Calculated density	16, 1.582 Mg/m^3
Absorption coefficient	3.847 mm^{-1}

Intensity Measurements

Diffractometer	Enraf-Nonius
Detector	Kappa CCD
Radiation	MoKa (l=0.71069A)
Temperature	293(2) K
Scan-Type	w-2theta
Theta range for data collection	2.78 to 20.81 deg.
Limiting indices	0<=h<=27, -19<=k<=19, 0<=l<=21
Reflections collected / unique	4418 / 4418 [R(int) = 0.0000]

Completeness to theta = 20.81	99.2 %
Absorption correction	Empirical
Max. and min. transmission	0.79 and 0.52

Structure Solution and Refinement

Refinement method	Full-matrix least-squares on F^2
Data / restraints / parameters	4418 / 0 / 516
Goodness-of-fit on F^2	1.062
Final R indices [I>2sigma(I)]	R1 = 0.0899, wR2 = 0.2017
R indices (all data)	R1 = 0.1336, wR2 = 0.2214
Extinction coefficient	0.00066(15)
Largest diff. peak and hole	1.833 and -0.369 $e.A^{-3}$

Table 2. Atomic coordinates (x 10^4) and equivalent isotropic displacement parameters ($Å^2$ x 10^3) for 163. U(eq) is defined as one third of the trace of the orthogonalized Uij tensor.

	x	y	z	U(eq)
Br1	6154(1)	3492(1)	295(1)	99(1)
Br2	7149(1)	2743(1)	778(1)	102(1)

Br3	6374(1)	3137(1)	2085(1)	106(1)
Br4	7054(1)	2079(1)	2576(1)	121(1)
C(1)	6656(8)	1545(8)	4173(8)	103(5)
C(2)	6942(7)	1150(10)	4004(8)	116(6)
C(3)	6740(7)	743(7)	3749(8)	101(5)
C(4)	6254(8)	752(6)	3665(6)	95(5)
C(5)	5955(7)	1148(7)	3826(7)	98(5)
C(6)	6189(8)	1551(6)	4070(6)	96(5)
C(7)	5411(6)	1120(7)	3709(6)	105(6)
N(1)	5308(4)	1142(5)	3054(5)	81(3)
C(8)	5474(5)	856(6)	2703(7)	74(4)
N(2)	5748(5)	440(5)	2803(5)	84(4)
C(9)	6004(7)	298(6)	3384(7)	103(5)
N(3)	5465(4)	884(4)	2064(5)	70(3)
N(4)	5135(4)	1196(4)	1799(5)	75(3)
C(10)	5799(6)	141(7)	2291(7)	83(4)
O(1)	6007(4)	-230(4)	2255(4)	91(3)
C(11)	4704(5)	984(6)	1507(6)	83(4)
C(12)	4799(5)	521(5)	1246(6)	74(4)
C(13)	5005(5)	182(5)	1746(6)	82(4)
C(14)	5500(5)	396(5)	1806(6)	71(4)

C(15)	5207(5)	497(5)	762(6)	79(4)
C(16)	5680(5)	405(6)	1153(7)	79(4)
C(17)	6111(6)	754(5)	1016(7)	74(4)
N(5)	5562(4)	1268(5)	438(5)	82(4)
N(6)	6039(4)	1072(4)	514(5)	77(3)
C(18)	5208(6)	890(5)	294(6)	80(4)
C(19)	5479(7)	1751(5)	304(7)	86(5)
O(2)	5096(4)	1867(3)	108(4)	83(3)
C(20)	5874(5)	2073(5)	407(6)	65(3)
C(21)	5783(6)	2530(6)	314(6)	67(4)
C(22)	6159(7)	2829(6)	426(7)	88(5)
C(23)	6528(5)	2546(5)	580(6)	73(4)
N(7)	6352(6)	2065(6)	567(6)	108(4)
C(24)	6277(5)	896(5)	-10(7)	67(4)
N(8)	6616(4)	579(4)	215(5)	80(3)
C(25)	6548(6)	485(6)	813(7)	81(4)
O(3)	6786(5)	227(4)	1122(5)	114(4)
C(26)	6992(5)	351(5)	-148(6)	82(4)
C(27)	6802(5)	78(7)	-687(7)	85(4)
C(28)	6530(6)	329(5)	-1139(7)	85(4)
C(29)	6460(6)	884(7)	-1069(7)	105(5)

N(9)	6170(5)	1037(4)	-532(6)	86(3)
C(30)	6872(7)	-398(7)	-765(9)	111(6)
C(31)	6464(9)	-365(10)	-1715(9)	127(8)
C(32)	6709(10)	-617(8)	-1282(13)	147(9)
C(33)	6363(7)	113(8)	-1640(8)	109(6)
C(34)	5250(6)	1676(6)	1768(6)	78(4)
O(4)	4943(4)	1949(4)	1550(5)	95(3)
C(35)	5693(5)	1865(6)	1976(6)	69(4)
N(10)	6118(6)	1702(6)	2219(6)	109(4)
C(36)	6422(5)	2096(6)	2279(6)	80(4)
C(37)	6165(7)	2494(5)	2093(7)	88(5)
C(38)	5742(5)	2361(5)	1898(5)	54(3)

Table 3. Bond lengths [Å] for 163. Estimated standard deviations in the least significant figures are given in parentheses.

Br1-C(22)	1.86(1)	C(1)-C(6)	1.32(2)
Br2-C(23)	1.86(1)	C(1)-C(2)	1.40(2)
Br3-C(37)	1.88(1)	C(2)-C(3)	1.38(3)
Br4-C(36)	1.87(1)	C(3)-C(4)	1.36(2)

C(4)-C(5)	1.42(2)	C(15)-C(18)	1.50(2)
C(4)-C(9)	1.57(2)	C(15)-C(16)	1.59(2)
C(5)-C(6)	1.40(2)	C(16)-C(17)	1.57(2)
C(5)-C(7)	1.54(2)	C(17)-N(6)	1.42(2)
C(7)-N(1)	1.47(2)	C(17)-C(25)	1.50(2)
N(1)-C(8)	1.20(2)	N(5)-C(19)	1.39(2)
C(8)-N(2)	1.40(2)	N(5)-N(6)	1.44(2)
C(8)-N(3)	1.40(2)	N(5)-C(18)	1.47(1)
N(2)-C(10)	1.40(2)	N(6)-C(24)	1.41(1)
N(2)-C(9)	1.51(2)	C(19)-O(2)	1.19(1)
N(3)-N(4)	1.39(2)	C(19)-C(20)	1.43(2)
N(3)-C(14)	1.47(2)	C(20)-C(21)	1.31(2)
N(4)-C(34)	1.37(2)	C(20)-N(7)	1.37(1)
N(4)-C(11)	1.48(2)	C(21)-C(22)	1.36(2)
C(10)-O(1)	1.18(2)	C(22)-C(23)	1.33(2)
C(10)-C(14)	1.52(2)	C(23)-N(7)	1.42(1)
C(11)-C(12)	1.43(2)	C(24)-N(9)	1.24(1)
C(12)-C(13)	1.56(2)	C(24)-N(8)	1.38(1)
C(12)-C(15)	1.55(2)	N(8)-C(25)	1.35(1)
C(13)-C(14)	1.51(2)	N(8)-C(26)	1.46(1)
C(14)-C(16)	1.52(2)	C(25)-O(3)	1.18(1)

C(26)-C(27)	1.50(2)	C(31)-C(32)	1.36(3)
C(27)-C(30)	1.35(2)	C(34)-O(4)	1.23(1)
C(27)-C(28)	1.43(2)	C(34)-C(35)	1.41(2)
C(28)-C(33)	1.34(2)	C(35)-N(10)	1.37(1)
C(28)-C(29)	1.56(2)	C(35)-C(38)	1.39(1)
C(29)-N(9)	1.48(1)	N(10)-C(36)	1.38(1)
C(30)-C(32)	1.37(3)	C(36)-C(37)	1.38(2)
C(31)-C(33)	1.37(3)	C(37)-C(38)	1.30(2)

Table 4. Bond Angles [°] for 163. Estimated standard deviations in the least significant figures are given in parenthes

C(6)-C(1)-C(2)	121.4(18)
C(3)-C(2)-C(1)	121.3(17)
C(4)-C(3)-C(2)	116.2(18)
C(3)-C(4)-C(5)	124.0(17)
C(3)-C(4)-C(9)	118.5(19)
C(5)-C(4)-C(9)	117.5(18)
C(6)-C(5)-C(4)	116.3(18)
C(6)-C(5)-C(7)	124.1(18)

C(4)-C(5)-C(7)	119.6(17)
C(1)-C(6)-C(5)	120.8(19)
N(1)-C(7)-C(5)	110.6(12)
C(8)-N(1)-C(7)	121.8(14)
N(1)-C(8)-N(2)	130.9(15)
N(1)-C(8)-N(3)	126.7(14)
N(2)-C(8)-N(3)	102.3(12)
C(8)-N(2)-C(10)	114.6(12)
C(8)-N(2)-C(9)	127.0(13)
C(10)-N(2)-C(9)	118.3(13)
N(2)-C(9)-C(4)	109.3(13)
N(4)-N(3)-C(8)	117.7(11)
N(4)-N(3)-C(14)	117.2(10)
C(8)-N(3)-C(14)	109.4(11)
C(34)-N(4)-N(3)	118.3(11)
C(34)-N(4)-C(11)	123.6(12)
N(3)-N(4)-C(11)	117.8(11)
O(1)-C(10)-N(2)	128.0(14)
O(1)-C(10)-C(14)	128.7(15)
N(2)-C(10)-C(14)	103.3(14)
C(12)-C(11)-N(4)	112.5(12)

C(11)-C(12)-C(13) 109.3(11)

C(11)-C(12)-C(15) 116.5(12)

C(13)-C(12)-C(15) 100.8(11)

C(14)-C(13)-C(12) 99.1(11)

N(3)-C(14)-C(13) 109.7(11)

N(3)-C(14)-C(10) 101.3(11)

C(13)-C(14)-C(10) 112.0(12)

N(3)-C(14)-C(16) 111.8(12)

C(13)-C(14)-C(16) 102.9(11)

C(10)-C(14)-C(16) 119.2(12)

C(18)-C(15)-C(12) 116.1(13)

C(18)-C(15)-C(16) 119.0(12)

C(12)-C(15)-C(16) 103.9(11)

C(14)-C(16)-C(17) 116.2(13)

C(14)-C(16)-C(15) 103.8(11)

C(17)-C(16)-C(15) 115.3(12)

N(6)-C(17)-C(25) 101.1(12)

N(6)-C(17)-C(16) 115.0(12)

C(25)-C(17)-C(16) 111.6(12)

C(19)-N(5)-N(6) 122.7(13)

C(19)-N(5)-C(18) 122.0(13)

N(6)-N(5)-C(18)	111.7(12)
C(24)-N(6)-C(17)	110.5(11)
C(24)-N(6)-N(5)	117.9(10)
C(17)-N(6)-N(5)	116.8(11)
N(5)-C(18)-C(15)	111.8(11)
O(2)-C(19)-N(5)	119.0(16)
O(2)-C(19)-C(20)	124.8(13)
N(5)-C(19)-C(20)	116.3(16)
C(21)-C(20)-N(7)	104.1(14)
C(21)-C(20)-C(19)	115.7(14)
N(7)-C(20)-C(19)	140.2(15)
C(20)-C(21)-C(22)	114.6(14)
C(23)-C(22)-C(21)	106.0(14)
C(23)-C(22)-Br(01)	128.9(15)
C(21)-C(22)-Br(01)	124.8(14)
C(22)-C(23)-N(7)	106.6(13)
C(22)-C(23)-Br(02)	126.7(13)
N(7)-C(23)-Br(02)	126.7(12)
C(20)-N(7)-C(23)	108.7(13)
N(9)-C(24)-N(8)	133.6(13)
N(9)-C(24)-N(6)	121.9(13)

N(8)-C(24)-N(6) 104.4(11)

C(25)-N(8)-C(24) 112.1(12)

C(25)-N(8)-C(26) 123.1(12)

C(24)-N(8)-C(26) 124.8(11)

O(3)-C(25)-N(8) 126.5(14)

O(3)-C(25)-C(17) 125.7(14)

N(8)-C(25)-C(17) 107.8(13)

N(8)-C(26)-C(27) 113.4(12)

C(30)-C(27)-C(28) 117.9(16)

C(30)-C(27)-C(26) 122.9(16)

C(28)-C(27)-C(26) 119.2(15)

C(33)-C(28)-C(27) 122.4(16)

C(33)-C(28)-C(29) 118.7(17)

C(27)-C(28)-C(29) 118.7(15)

N(9)-C(29)-C(28) 115.2(13)

C(24)-N(9)-C(29) 120.7(13)

C(27)-C(30)-C(32) 120(2)

C(33)-C(31)-C(32) 121.0(19)

C(31)-C(32)-C(30) 121(2)

C(28)-C(33)-C(31) 118(2)

O(4)-C(34)-N(4) 117.0(15)

O(4)-C(34)-C(35)	119.9(15)
N(4)-C(34)-C(35)	123.1(13)
N(10)-C(35)-C(38)	106.7(13)
N(10)-C(35)-C(34)	139.0(15)
C(38)-C(35)-C(34)	114.3(14)
C(35)-N(10)-C(36)	107.6(14)
C(37)-C(36)-N(10)	106.7(13)
C(37)-C(36)-Br(04)	127.6(13)
N(10)-C(36)-Br(04)	125.7(13)
C(38)-C(37)-C(36)	109.6(13)
C(38)-C(37)-Br(03)	123.2(13)
C(36)-C(37)-Br(03)	127.2(15)
C(37)-C(38)-C(35)	109.2(12)

Table 5. Anisotropic displacement parameters ($Å^2$ x 10^3) for 163. The anisotropic displacement factor exponent takes the form: -2 pi^2 [h^2 a*2 U11 + ... + 2 h k a* b* U12]

	U11	U22	U33	U23	U13	U12
Br1	102(1)	76(1)	120(1)	10(1)	20(1)	3(1)
Br2	79(1)	103(1)	124(1)	-15(1)	8(1)	-3(1)
Br3	130(2)	83(1)	105(1)	-7(1)	15(1)	-23(1)
Br4	90(1)	136(2)	137(2)	8(1)	-19(1)	-24(1)
C(1)	95(15)	109(15)	104(12)	10(10)	-29(11)	-17(13)
C(2)	76(13)	160(20)	111(13)	-1(13)	-27(10)	-3(15)
C(3)	75(13)	110(15)	118(13)	11(11)	-27(10)	-9(11)
C(4)	134(17)	83(12)	69(9)	11(8)	-15(10)	-19(12)
C(5)	125(16)	103(14)	65(9)	10(9)	-4(9)	6(13)
C(6)	120(17)	98(13)	71(9)	-6(9)	-17(9)	-15(12)
C(7)	85(13)	160(18)	71(10)	-7(10)	13(8)	0(11)
N(1)	57(8)	109(10)	77(8)	-5(7)	6(6)	15(7)
C(8)	62(9)	71(11)	90(12)	8(9)	7(8)	16(8)
N(2)	106(10)	86(9)	60(7)	2(7)	-3(6)	-19(8)
C(9)	128(15)	87(12)	92(11)	6(9)	-8(10)	-8(11)

N(3)	72(8)	66(8)	71(8)	5(6)	-11(6)	1(6)
N(4)	73(8)	67(9)	85(7)	-5(6)	-16(6)	0(7)
C(10)	71(10)	91(13)	87(11)	17(10)	5(8)	-8(9)
O(1)	101(8)	73(7)	99(7)	8(6)	2(6)	17(6)
C(11)	62(9)	104(13)	82(9)	10(9)	-8(7)	-10(9)
C(12)	74(10)	65(10)	84(9)	-21(8)	-4(8)	-1(7)
C(13)	86(11)	83(11)	78(9)	-11(8)	5(8)	-19(9)
C(14)	77(10)	73(10)	63(8)	2(7)	-1(7)	2(8)
C(15)	83(11)	79(10)	76(9)	-4(8)	0(8)	-11(8)
C(16)	65(10)	68(11)	105(11)	2(8)	-5(8)	8(8)
C(17)	80(11)	59(9)	82(9)	9(8)	-2(8)	-4(9)
N(5)	62(8)	95(11)	90(8)	-6(7)	-8(6)	-4(7)
N(6)	76(9)	81(9)	74(7)	-6(7)	-12(6)	5(7)
C(18)	89(11)	67(10)	83(9)	6(8)	-19(8)	5(8)
C(19)	121(16)	44(10)	92(10)	8(7)	-9(10)	20(11)
O(2)	84(7)	71(7)	95(7)	7(5)	-21(6)	15(6)
C(20)	68(11)	52(10)	76(8)	-7(7)	-10(7)	10(8)
C(21)	36(9)	78(13)	87(10)	4(8)	-14(7)	14(9)
C(22)	97(13)	67(10)	99(10)	15(8)	23(9)	27(11)
C(23)	78(11)	60(10)	81(9)	1(7)	-3(7)	-7(9)
N(7)	116(13)	108(13)	100(9)	3(8)	-12(8)	26(10)

C(24) 64(9) 62(9) 76(10) 10(8) 3(8) 9(7)

N(8) 91(9) 69(8) 79(9) 6(6) 5(7) 17(7)

C(25) 75(11) 92(12) 75(11) 0(9) -4(8) 15(9)

O(3) 117(10) 116(9) 109(8) 32(7) -6(7) 39(8)

C(26) 83(11) 82(10) 80(9) 10(8) 14(8) 10(9)

C(27) 74(11) 99(14) 83(10) 7(10) 7(8) 0(9)

C(28) 96(12) 62(10) 96(11) -6(9) 16(9) -3(9)

C(29) 90(12) 144(17) 82(10) 18(10) 10(9) 1(11)

N(9) 84(9) 84(9) 91(9) 6(7) 5(7) 10(7)

C(30) 116(15) 66(12) 150(17) -15(11) 5(12) 18(10)

C(31) 170(20) 120(20) 98(14) -10(13) -11(13) -58(16)

C(32) 190(20) 88(16) 170(20) -54(17) 33(19) -44(16)

C(33) 122(15) 102(16) 104(13) -19(11) 7(11) -41(12)

C(34) 84(12) 71(12) 80(9) 7(8) -4(8) 29(10)

O(4) 88(8) 77(7) 121(8) 0(6) -19(6) 10(6)

C(35) 57(10) 82(12) 69(8) -12(7) -6(7) -7(8)

N(10) 108(12) 118(12) 100(9) -24(8) 0(9) -14(11)

C(36) 69(10) 90(12) 81(9) -2(8) -17(7) -22(10)

C(37) 117(15) 67(11) 80(9) 1(8) 15(9) 2(11)

C(38) 55(9) 54(10) 55(7) -5(6) -14(6) -5(7)

Table 6. Hydrogen coordinates (x 10^4) and isotropic displacement parameters (A^2 x 10^3) for 163.

	x	y	z	U(eq)
H(1)	6800	1808	4360	123
H(2)	7273	1162	4065	140
H(3)	6925	477	3642	122
H(6)	6012	1826	4161	115
H(7A)	5285	821	3875	126
H(7B)	5251	1385	3914	126
H(9A)	6243	53	3297	123
H(9B)	5774	166	3671	123
H(11A)	4450	953	1807	99
H(11B)	4591	1199	1190	99
H(12)	4501	386	1079	89
H(13A)	4824	203	2122	99
H(13B)	5016	-151	1611	99
H(15)	5151	199	536	95
H(18A)	5282	754	-102	96
H(18B)	4889	1033	271	96

H(7)	6518	1811	647	129
H(26A)	7172	131	110	98
H(26B)	7213	597	-289	98
H(29A)	6774	1034	-1042	127
H(29B)	6305	1005	-1434	127
H(30)	7031	-576	-469	133
H(31)	6364	-520	-2068	153
H(32)	6765	-943	-1339	177
H(33)	6185	282	-1927	131
H(10)	6184	1410	2316	131
H(161)	5790	70	1100	30
H(17)	6270	980	1290	90
H(21)	5590	2611	257	0
H(38)	5513	2452	1654	60

CHAPTER FIVE

CHLORINATION STUDY OF SYMMETRIC BISALKYLIDENE AND FUTURE WORK

5.1 The Synthesis of Symmetric Bisalkylidene 171.

As describes in chapter four, our efforts to construct the stereochemistry of palau'amine **11** had met a huge resistance. At the same time the stereochemistry revisions appeared in the literature. The most convincing way to prove the correct stereochemistry is by synthetically constructing each version. As the first step towards this goal, we decided to test feasibility of our key idea, the chlorination induced cascade reaction, on the readily available starting material.

Direct generation of symmetric bisalkylidene **171** from double reduced *meso* dimer **170** via double elimination seemed viable (Scheme 5.1). Compound **171** was a good candidate to test the chlorination reaction. The results of the chlorination reaction performed on **171** would allow us to gain some insights about the stereochemical outcomes.

Scheme 5.1

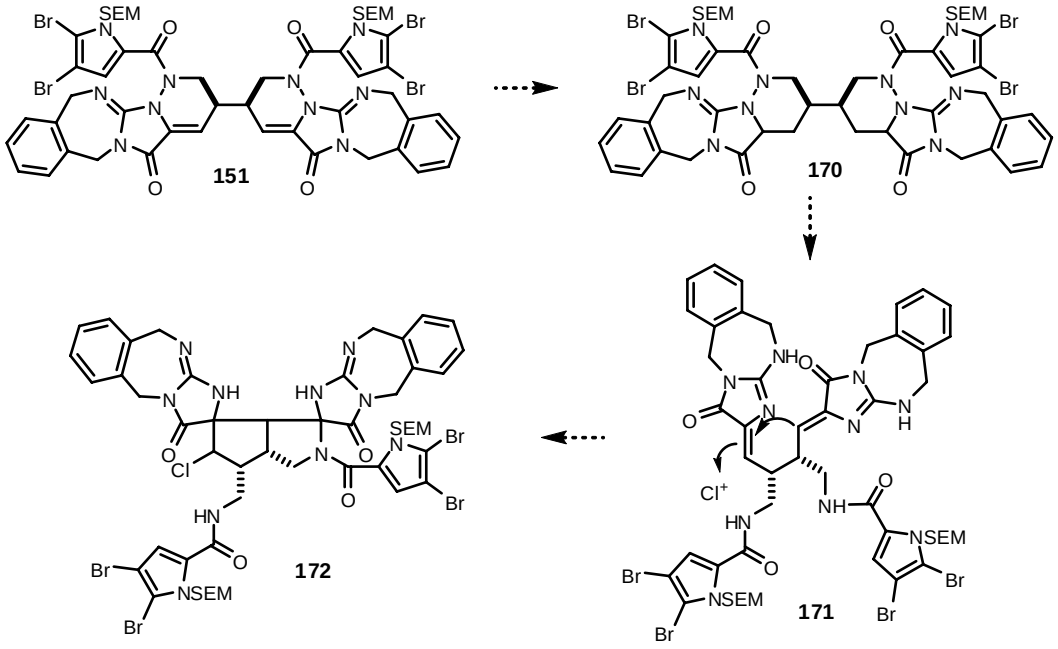

As was mentioned in chapter 4 (section 4.4), when MgI_2 was used as the additive for the Rh(I) catalyzed hydrosilylation methodology we developed, the double reduced dimers **170** were formed as side products. Following this line of logic, under the same reaction conditions, the inconsequential diastereoisomeric mixture of **170** was isolated in good yield by using two equivalents of $HSiMe_2Ph$ in the reaction (Scheme 5.2).

Scheme 5.2

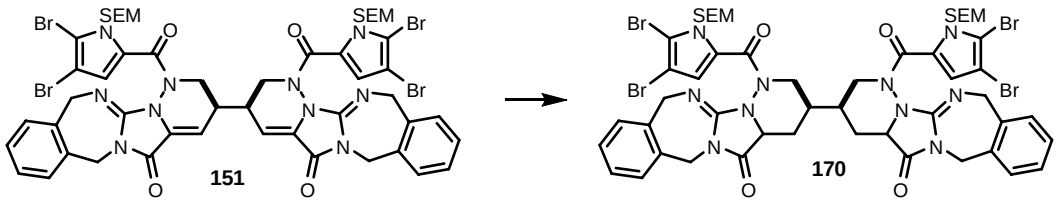

Conditions: **160** (5 mol%), davephose **161** (5 mol%), MgI_2 (0.5 eq), NH_4PF_6 (2 eq), $HSiMe_2Ph$(2.1 eq), CH_2Cl_2, 15 h, 83%

One thing worthy of mentioning is that the reaction did not require a stoichiometric amount of MgI_2 to achieve a high turnover of catalyst. This observation challenged the original hypothesis that MgI_2 acted as a Lewis acid to neutralize the basic sites of the starting material or product to prevent the Rh(I) complex **160** from being poisoned. So could it be a counter-ion effect? It was possible that a Rh-I species was generated from a transmetallation step between the catalyst and MgI_2, which was actually the true catalyst. This hypothesis was not hard to test since the corresponding Rh-I complex **176** was known[2]. It was synthesized according to the literature (Scheme 5.3).

Scheme 5.3

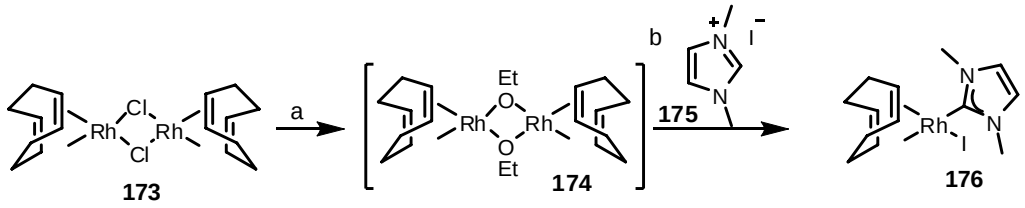

Conditions: a). NaH (4 eq), EtOH, rt, 30 min; b). **145** (2.2 eq), rt, 24 h, (71%).

With the complex **176** in hand, the hypothesis was quickly tested. Two reactions were carried side by side under identical reaction conditions, except that one reaction had Rh-Cl **160** as the catalyst, while the other had Rh-I **176** instead (Scheme 5.4). As the one with Rh-I **176** went to completion, the one with Rh-Cl **130** had no reaction. These experiments strongly support the counterion effect hypothesis.

Scheme 5.4

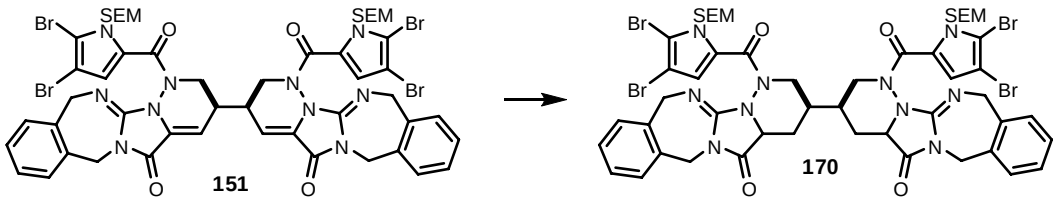

entry	Catalyst	NH_4PF_6	$HSiMe_2Ph$	Yield
1	**160**, [COD]RhCl(NHC-Me)	2	2.1	0%
2	**176,** [COD]RhI(NHC-Me)	2	2.1	80%

Conditions: catalyst (10 mol%), CH_2Cl_2, 50 °C.

5.2 Double Elimination

With the double reduction problem solved, the next transformation we needed to achieve was the double elimination to cleave the N-N bond and form the exocyclic double bond. We still planned on using the base induced fragmentation methodology[4]; however in this case we would generate an intermediate that has four negative charges. The potential instability of this intermediate was our major concern initially.

While the KHMDS treatment of **170** did afford symmetric bisalkylidene **171**, the reaction was very demanding in terms of technique and also limited by the reaction scale. The maximum reaction scale was 10 mg, otherwise only decomposition was observed. In order to increase the efficacy of the reaction, Boron lewis acids were premixed with **170** before the addition of the base to facilitate the deprotonation and the following fragmentation.

Dicyclohexyllboron triflate[5] was the optimal lewis acid. Compound **171** could be isolated in 50% yield, when the reaction was carefully executed as follows: the THF solution of **170** was precooled to −78 °C. To it was added a THF solution of dicyclohexylboron triflate. The mixture was stirred at −78 °C for another 10 minutes before KHMDS was added rapidly in one portion. The cooling bath was immediately taken off after the addition and the reaction was allowed to warm up to rt. Acetic acid was used to quench the reaction. After a routine work up, the solution was dried over anhydrous K_2CO_3. The reaction can be scaled up to 60 mg without diminishing the yield.

Scheme 5.5

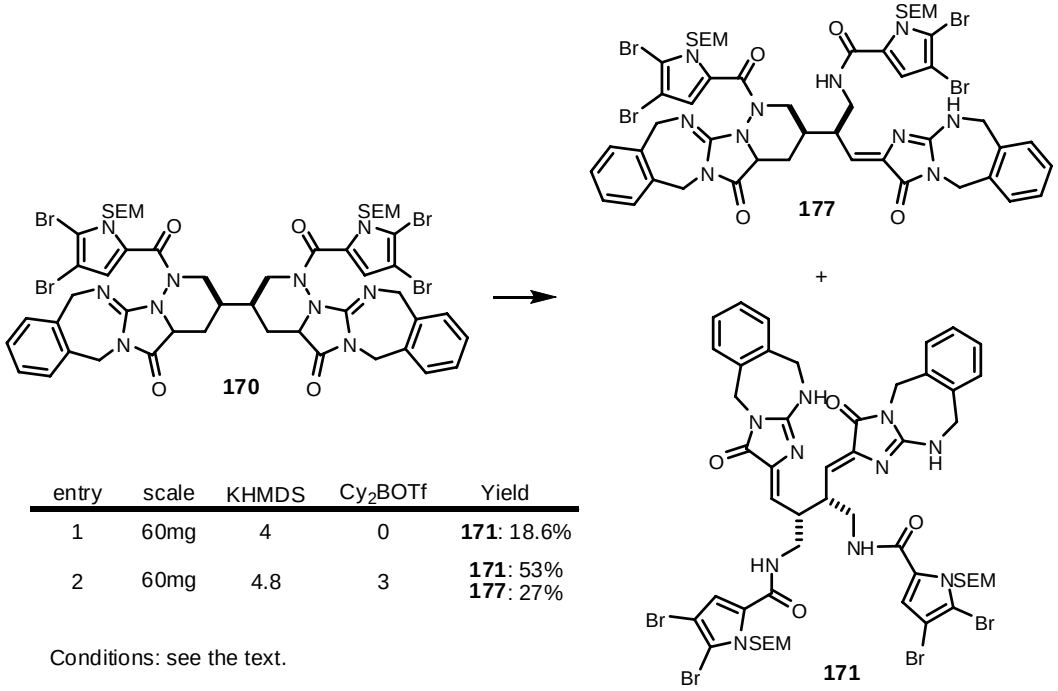

entry	scale	KHMDS	Cy_2BOTf	Yield
1	60mg	4	0	**171**: 18.6%
2	60mg	4.8	3	**171**: 53% **177**: 27%

Conditions: see the text.

The compound **171** can be purified by crystallization from acetonitrile. However, a single crystal that was suitable for X-ray crystallography was not obtained even after extensive effort. The geometry of the double bond is tentatively assigned as *Z* based on the literature precedence[6].

5.3 Chlorination Reaction Study

Compound **171** was a suitable substrate to test the chlorination idea. Quite discouragingly, when the THF solution of **171** was treated with *t*-BuOCl, many products were formed. Since this was the reaction has the most significance in the whole study, much effort had been invested in isolation and purification of the products. Four major products were isolated eventually. They formed two isomeric pairs: **178**/**179** and **180/181**. Fortunately, the central cyclopetane ring was formed in all four products, presumably through the intermediate **182**. The formation of diastereoisomeric pair **180**/**181** was possible due to tautomerization of the iminium ion **182**. The unusual formation of the N-N bond in pair **178**/**179** could be due to the addition of adjacent guanidine to iminium ion at its N-terminal in intermediate **182** due to the space proximity.

Scheme 5.6

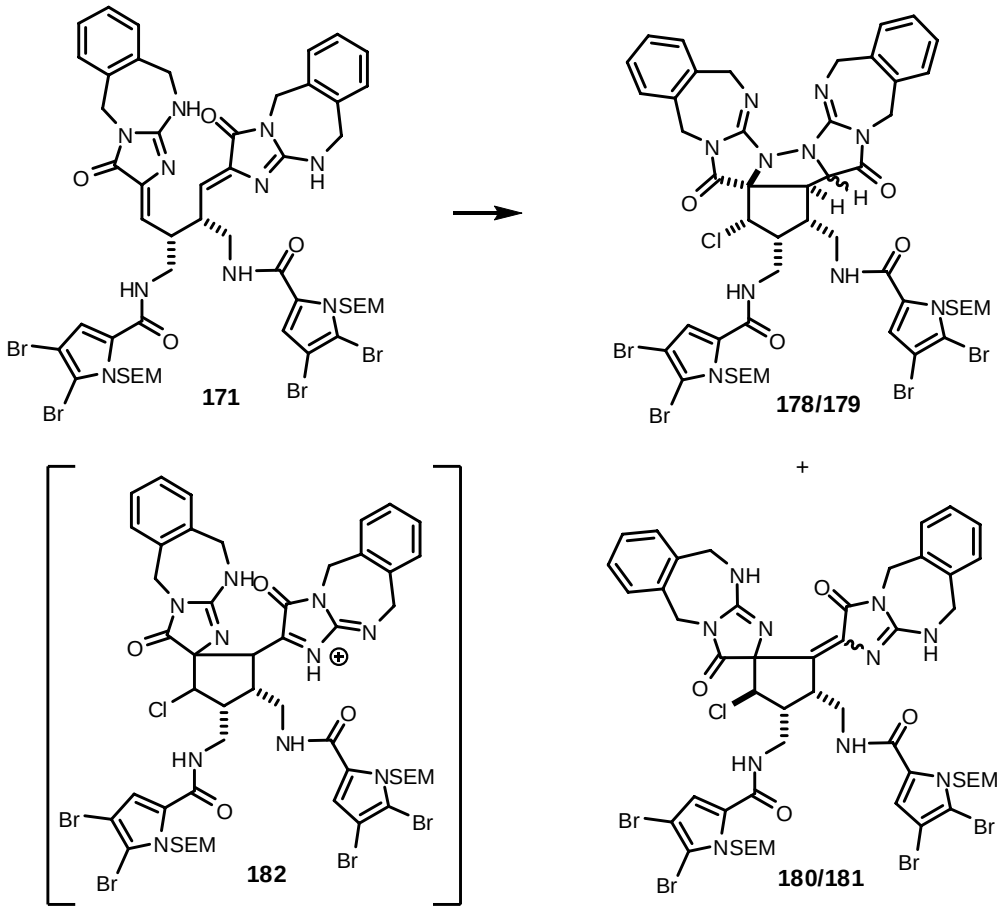

Conditions: *t*-BuOCl (1.05 eq), THF, -78^{o}C, 0.5h, rt, 3h, **178/179** (13%),**180/182**(20%)

The structures of compounds **178-181** were established by NMR analysis. Take compound **178** for example; there were one dd at 7.8 ppm and one triplet at 7.5 ppm which readily exchange with D_2O in the ^{1}H NIMR spectrum. They were identified as the protons of the two amides. Started form this information, combined COSY data (Figure 5.1), the connectivity of protoned carbons were established. The structure of the molecule was further established by HMBC data.

The N-N bond formation was indirectly supported by the fact that all the protons were carbon bounded based on the HMQC, except the two amide protons.

The relative stereochemistry of H18 and H12 should be *cis* based on the fact compound **178** was derived from *meso* dimer **151**. The coupling constant between H17 and H18 is 3.9 Hz, which supports a *cis* stereochemistry. H10 is correlated to H12 and H18 in the NOSEY, indicating they are on the same face of the diazabicyclo[3.3.0]octane ring. The small coupling constant between H11 and H10 (J < 1 Hz) indicates a *trans* relationships[7]. The stereochemistry of C16 was assigned as shown in Figure 5.1 to minimize the strain of the molecule. The structures of Compound **179-181** were assigned accordingly. The coupling constants of H17 and H18 in **180**/**181** are 12.8 and 12.1 Hz, so the relative stereochemistry is assigned as *trans*.

Figure 5.1

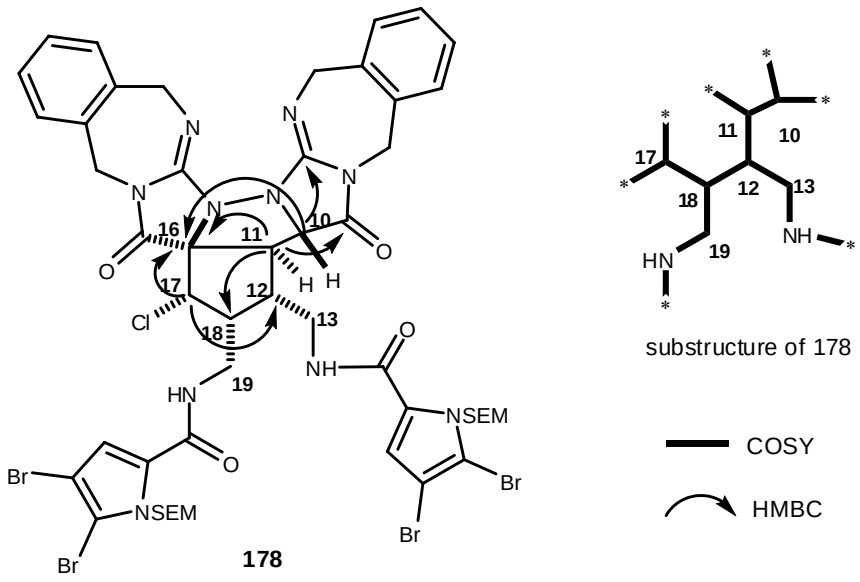

Next, we were curious to see if metal ions had effects on this fascinating reaction. $ZnCl_2$ caused the severe decomposition of the starting material, while other metal salts, such as, LiCl and $CaCl_2$ did not have any effect on the reaction.

Magnesium salts had been proven once more to be special for our series of compounds. When the starting material was mixed with $MgCl_2$ before the addition of *t*-BuOCl, the diastereisomer pair **178**/**179** was formed in better yield and the formation of other pair is greatly diminished. However the reaction can not go to completion. Then we switched to $MgBr_2 \bullet Et_2O$ complex, which has better solubility than $MgCl_2$. In this case, the **183**/**184** was isolated in 70% yield. Initially, compounds **183**/**184** was thought to be the same compounds **178**/**179** based on the TLC and NMR analysis. However, the mass data showed that instead of a chlorine atom, it was a bromine atom that was incorporated into the molecules **183**/**184**. What most likely happened was that an electrophilic bromine source was generated prior to the cyclization reaction. This discovery enables us to have the potential of generating bromo-palau'amine. Efforts on obtaining crystallography information of compounds **178**/**179, 183**/**184** and their derivatives are still on going.

Even though the amide failed to add to the iminium ion **182** to form the bicyclo[3,3,0]-azaoctane ring system, it can be potentially achieved by other transformations through these products from the chlorination reaction. At this

point, the study of *meso* series has proven our central tenet to be valid and the desired oxidative spiroannulation[8] was demonstrated.

Scheme 5.7

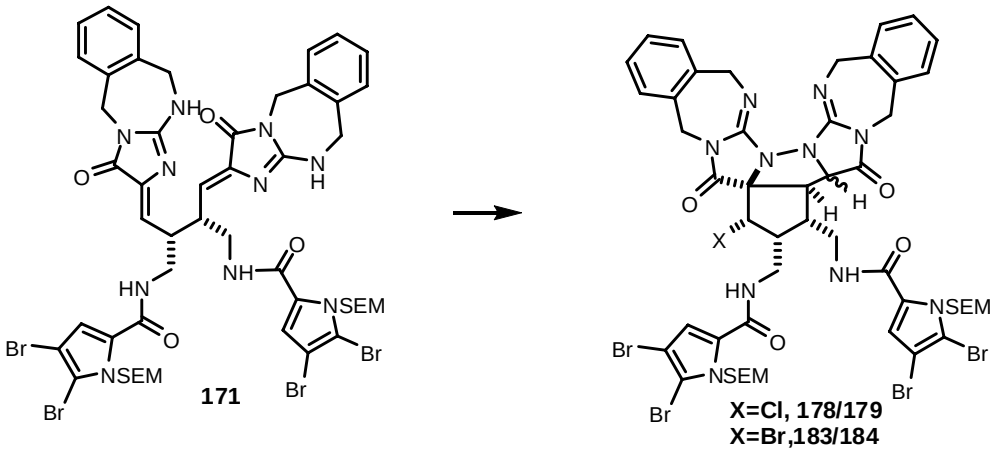

entry	Lewis acid	X	Yield
1	$MgCl_2$	Cl	**180/181**: 7% **178/179**: 30% **171**: 30%
2	$MgBr_2$	Br	**185/186**: <5% **183/184**: 70%

Conditions: *t*-BuOCl (1.05 eq), THF,–78 °C, 0.5 h, rt, 3 h.

5.4 Future Study

The benzodiazepine protecting group we chose for the guanidine motif worked very well for our purposes; however no deprotection method has been invented even after our extensive efforts. This has become our major concern for the synthetic pathway we are currently pursuing.

I would like to propose an alternative pathway to synthesize the bisalkylidene construct, which has the advantage of not having to use protecting groups or using easy removal protecting groups.

Acylation of the commercially available δ-valerolactam **187** with compound **145** should provide compound **188**. Traditional selenium chemistry[9] or other methodology[10] will be employed to install the unsaturation. Our oxidative dimerization will be employed to form the C-C bond at the γ position. Analogous to our present pathway, the *meso* **192** and C_2 **190** diastereoisomers are expected from the reaction and thus give us opportunities to explore the synthesis of both proposed structures of palau'amine.

Scheme 5.8

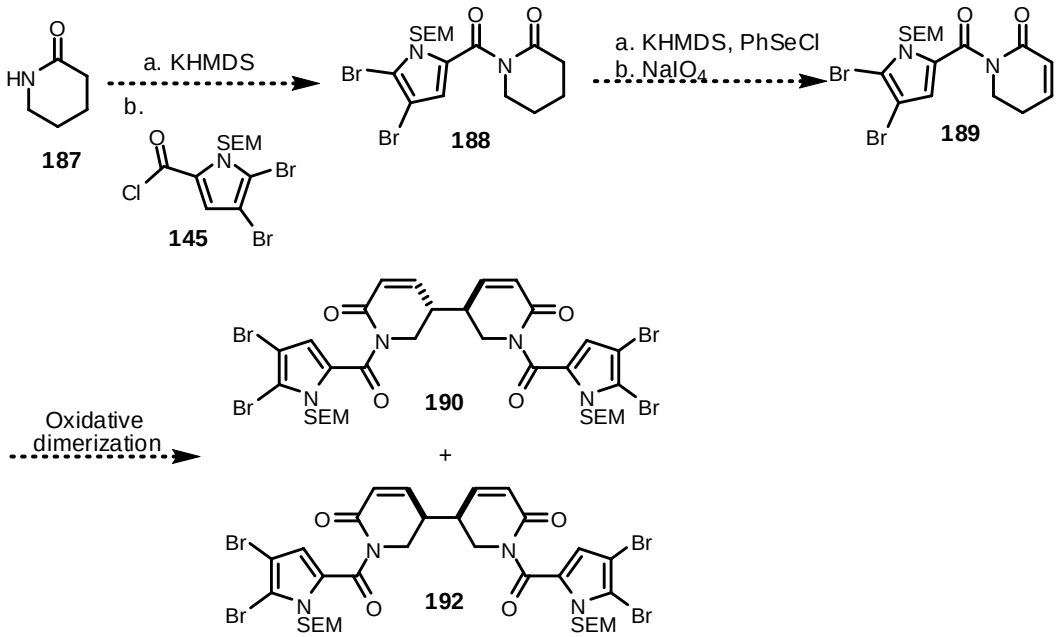

Take *meso* dimer **192** for example and the same chemisty can be also

applied to the C_2 dimer **191**. The next transformation is converting compound **192** to **193**. There are potentially two ways. One is to oxidize the double bond to the epoxide[11] **194** followed by an acid promoted rearrangement to obtain **193**. If the acid step fails, we could try another approach. Enamide**192** can be reduced using our Rh(I) NHC complexes, the α-hydroxy functionality can be installed by either Davis oxaziridine chemisty[12] or MoOPH reagent[13]. An oxidation can follow to afford the compound **193**.

Scheme 5.9

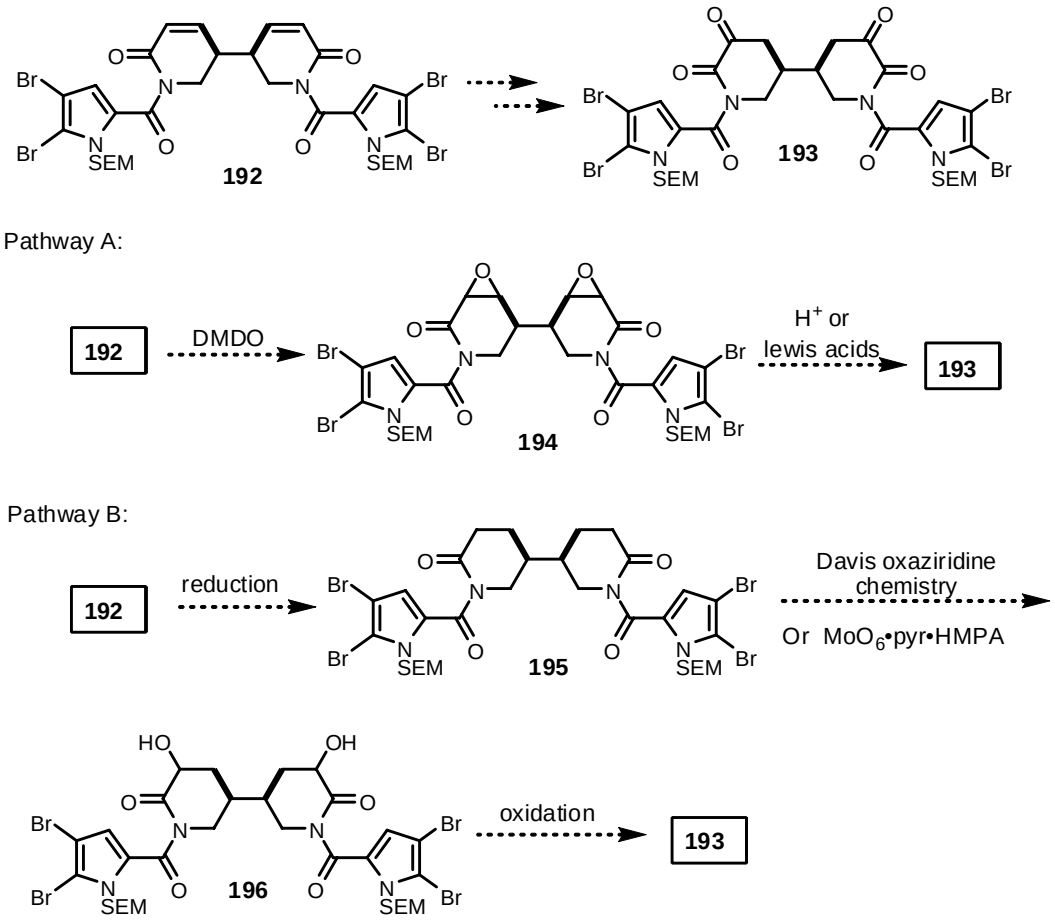

Next, compound **193** can be condensed with guanidine to afford bisalkylidene **198**[14]. At this point, solubility could be a big issue because the bisguanidine moieties. Since we believe our approach is biosynthetically relevant, the chlorination reaction can be executed in conditions that mimic nature. For example, using H_2O as the solvent to solubilize intermediated **198** or using different salt forms of **198**. Otherwise the protected guanidine will be employed for this condensation. If this synthetic sequence is successfully achieved in the lab, the bisalkylidene **198-200** will be synthesized in 9-10 steps. Depending on the chlorination reaction results, the palau'amine family of alkaloids can be potentially synthesized in under 20 steps.

Scheme 5.10

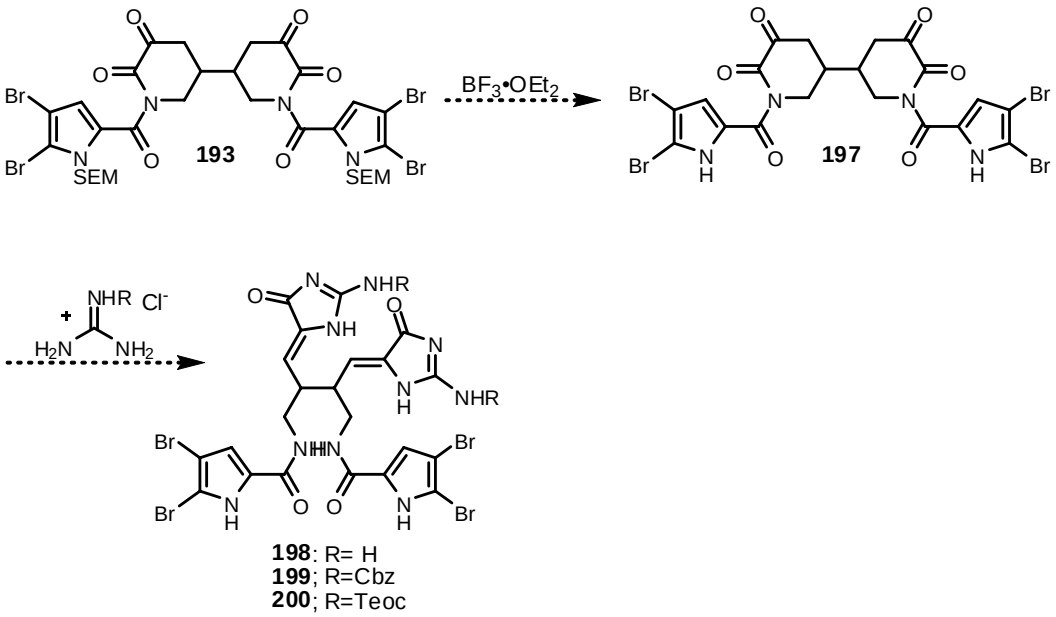

5.5 Experimental Section

5.5.1 Materials and Methods

Unless stated otherwise, reactions were performed under an argon atmosphere in flame-dried glassware. Tetrahydrofuran (THF), dichloromethane (CH_2Cl_2), diethyl ether (Et_2O), toluene (C_7H_8), benzene (C_6H_6) and acetonitrile (CH_3CN) were passed through Glass Contour solvent drying systems prior to use. Fine chemical reagents were obtained from commercial sources and used without further purification. Column chromatography was performed on E. Merck silica gel 60 (240-400 mesh). Thin layer chromatography and preparative layer chromatography utilized pre-coated plates from E. Merck (silica gel 60 PF254, 0.25mm or 0.5mm). Nuclear Magnetic Resonance (NMR) spectra were recorded on either a Varian Inova-600, Inova-400 or Mercury-300 magnetic resonance spectrometer. ^1H NMR chemical shifts are given in parts per million (δ) relative to a residual solvent signal. Infrared spectra were recorded on a Perkin-Elmer FT-IR spectrum 1000 using samples prepared as thin films between salt plates. Electrospray-ionization mass spectra (LRMS) were measured on a Shimadzu LCMS-2010 single quadrupole.

5.5.2 Preparative Procedures

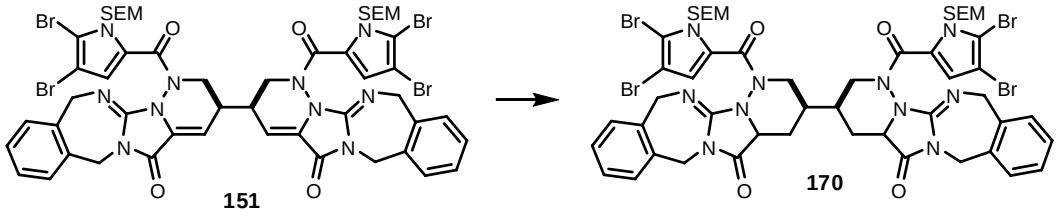

Doubly Reduced meso-dimer (170). The THF (3 mL) solution of dimer **151** (460 mg, 0.364 mmol), MgI_2 (50 mg, 0.18 mmol), and NH_4PF_6 (120 mg, 0.74 mmol) was stirred at rt for 15 minutes before the solvent was removed in vacuo. The resultant solid was taken up with the CH_2Cl_2 (2.45 mL) stock solution of Rh(I) (5.75 mg, 5 mol%), davephose (6.5 mg, 5.5 mol%) and $HSiMe_2Ph$ (170 μL, 1.10 mmol). The reaction mixture was heated at 55 °C for 1.5 days. The reaction mixture was taken up in CH_2Cl_2 and washed with sat. $NaHCO_3$, water, brine and dried over Na_2SO_4. After the solvent removal in vacuo the residue was purified by silica gel column chromatography (EtOAc: CH_2Cl_2= 1:9 to 1:4) to afford **162** as white film (23 mg, 4.5%), **170** (diastereoisomer 1) (345 mg, 66%) and **170** (diastereoisomer 2) (85 mg, 16%).

170 (diastereoisomer 1): white solid; R_f = 0.45 (CH_3CN:$CHCl_3$=2:8); IR (film, cm^{-1}): 3422, 2950, 1753, 1704, 1651, 1403, 1248, 1067, 836, 740. 610; ^1H NMR (400 MHz,CD_3CN): δ= 7.31-7.39 (m, 8H), 6.77 (s, 2H), 5.67 (d, 2H, *J* =10.6Hz), 5.48 (d, 2H, *J*=10.6Hz), 4.92 (s, 4H), 4.78 (d, 2H, *J*=14.4Hz), 4.58 (d, 2H, *J* =14.4Hz), 4.40 (m, 2H), 3.78 (dd, 2H, *J* = 4.9, 11.6Hz), 3.56 (t, 4H, *J* =7.9Hz), 2.49 (dd, 2H, *J* =11.2, 12.8Hz), 2.21(m, 2H), 1.59 (m, 2H), 1.29 (m, 2H), 0.87 (m,

4H), 0.00 (s, 18H). ^{13}C NMR (125 MHz, $CDCl_3$): δ=169.56, 164.16, 145.60, 140.39, 133.37, 129.61, 128.90, 128.75, 117.66, 111.35, 99.77, 75.44, 66.45, 56.47, 49.56, 43.61, 43.43, 35.05, 30.50, 18.23, -1.07. MS (positive electrospray) calc'd for $(C_{50}H_{60}Br_4N_{10}O_6Si_2+H)^+$: 1273.09, found 1273.1.

170 (diastereoisomer 2): A solution of *meso* **151** (460 mg, 0.364 mmol), MgI_2 (50 mg, 0.18 mmol), and NH_4PF_6 (120 mg, 0.74 mmol) in THF (3 mL) was stirred at rt for 15 minutes and then the solvent was removed *in vacuo*. The residue was suspended in a stock solution of Rh(I) catalyst **160** (5.75 mg, 5 mol%), 2-dicyclohexylphosphino-2'-(N,N-dimethylamino)biphenyl (6.5 mg, 5.5 mol%) **161** and $HSiMe_2Ph$ (170 μL, 1.10 mmol) in CH_2Cl_2 (2.45 mL). The reaction mixture was heated at 55 °C for 36 h and then diluted with CH_2Cl_2, washed with saturated $NaHCO_3$, water and brine. The organic layer was dried over Na_2SO_4, filtered and concentrated *in vacuo*. The residue was purified by silica gel chromatography (gradient from 1:9 → 1:4 EtOAc/CH_2Cl_2) to afford **162** as white film (23 mg, 4.5%), **170** diastereoisomer 1(395 mg, 66%) followed by **170** diastereoisomer 2 (85 mg, 16%).

170 (diastereoisomer 1): white solid; R_f = 0.45 (1:4 $CH_3CN/CHCl_3$); IR (film): 3422, 2950, 1753, 1704, 1651, 1403, 1248, 1067, 836, 740. 610 cm^{-1}; ^1H NMR (400 MHz, CD_3CN): δ 7.31-7.39 (m, 8H), 6.77 (s, 2H), 5.67 (d, 2H, *J* =10.6Hz), 5.48 (d, 2H, *J*=10.6Hz), 4.92 (s, 4H), 4.78 (d, 2H, *J*=14.4Hz), 4.58 (d, 2H, *J*=14.4Hz), 4.40 (m, 2H), 3.78 (dd, 2H, *J* = 4.9, 11.6Hz), 3.56 (t, 4H, *J* =7.9Hz),

2.49 (dd, 2H, *J* =11.2, 12.8Hz), 2.21(m, 2H), 1.59 (m, 2H), 1.29 (m, 2H), 0.87 (m, 4H), 0.00 (s, 18H). ^{13}C NMR (125 MHz, $CDCl_3$): δ 169.6, 164.2, 145.6, 140.4, 133.4, 129.6, 128.9, 128.8, 117.7, 111.4, 99.8, 75.4, 66.5, 56.5, 49.6, 43.6, 43.4, 35.1, 30.5, 18.2, -1.1. MS (positive electrospray) calc'd for $(C50H60Br4N10O6Si2+H)^+$: 1273.09, found 1273.1. Crystals suitable for X-ray diffraction were grown from CH3CN (slow evaporation).

170 (diastereoisomer 2): brown foam; R_f = 0.2 (CH_3CN:$CHCl_3$=2:8); IR (film, cm^{-1}): 2952, 1754, 1693, 1403, 1299, 1248, 1155, 1092, 941; ^{1}H NMR (400 MHz,CD_3CN): δ= 7.28-7.38 (m, 8H), 6.77 (s, 1H), 6.76 (s, 1H), 5.55-5.67 (m, 4H), 4.57-5.00 (m, 8H), 4.40(m, 1H), 4.07 (m, 2H), 3.79 (dd, 1H, *J* = 4.9, 11.6Hz) 3.52 (dd, 4H, *J* = 8.4, 16.9Hz), 3.15 (dd, 1H, *J* = 4.9, 13.1Hz), 2.32 (dd, 1H, *J* = 11.7, 12.6Hz), 2.24 (m, 1H), 2.00 (m, 1H), 1.76 (m, 1H), 1.10 (m, 1H), 0.85 (m, 4H), -0.01 (s, 9H), -0.04 (s, 9H). ^{13}C NMR (125 MHz, $CDCl_3$): δ=170.33, 169.60, 163.67, 146.93, 145.32, 140.50, 140.08, 133.64, 133.59, 129.53, 129.46, 128.79, 128.69, 128.61, 128.53, 125.74, 125.67, 117.41, 117.38, 111.23, 110.87, 99.69, 99.58, 75.56, 75.31, 60.61, 56.48, 56.31, 49.58, 49.39, 43.87, 43.67, 43.52, 43.05, 32.95, 32.68, 30.78, 26.95, 21.28, 18.144, 17.98, 14.44, -1.06, -1.19. MS (positive electrospray) calc'd for $(C50H60Br4N10O6Si2+H)^+$: 1273.09, found 1272.8.

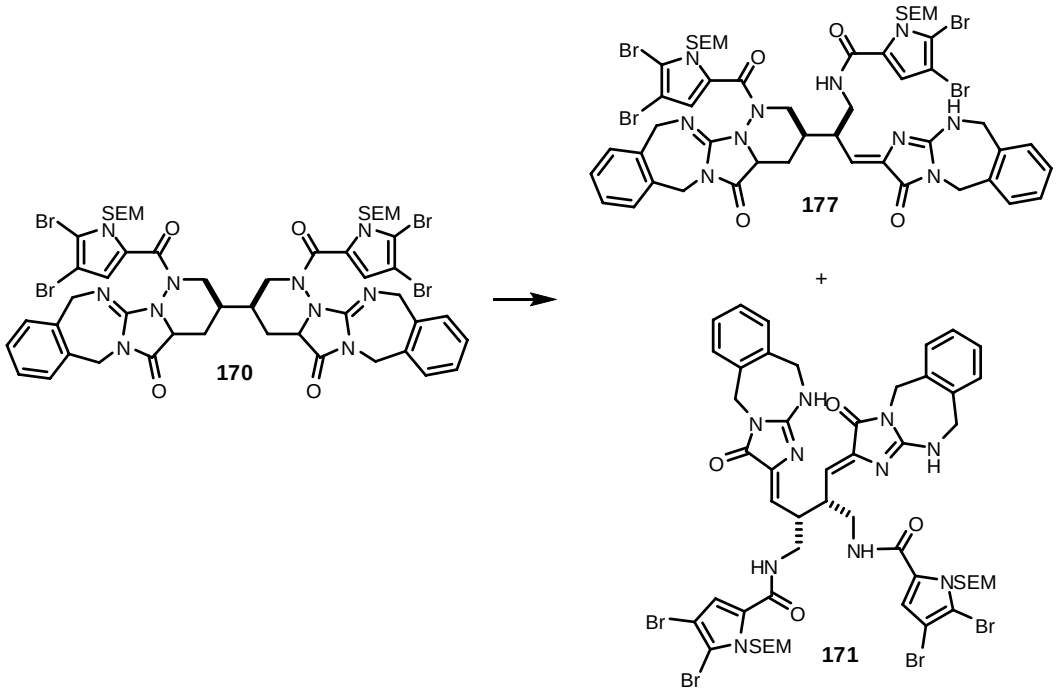

Bisalklydiene 171: A solution of Cy_2BOTf (47 mg, 0.144 mmol) in THF (0.48 mL) was cooled to −78 °C and added rapidly to a solution of **170** (60 mg, 0.047 mmol) in THF (1.5 mL) at −78 °C. KHMDS (0.5M in toluene, 470 μL) was then added and the cooling bath immediately removed. The red solution was warmed to rt and quenched with 20 μL AcOH. The reaction was diluted with CH_2Cl_2 and washed with saturated NaHCO3, water and brine. The organic layer was dried over Na_2SO_4, filtered and solvent was removed *in vacuo*. The residue was purified by silica gel column chromatography (1:49 MeOH/CH_2Cl_2) to afford **171** as light yellow solid (32 mg, 53%) along with mono alkylidene **177** (16 mg, 27%). Analytically pure **177** was obtained as a white powder following trituration with CH_3CN.

171: R_f = 0.5 (1:19 MeOH/CH_2Cl_2); IR (film): 1668, 1606, 1425, 1317, 1245, 1091, 836 cm-1; ^{1}H NMR (500 MHz, DMSO-*d6*): δ 8.30 (bs, 2H), 8.01 (bs, 2H), 7.31-7.38 (m, 8H), 6.76 (s, 2H), 5.71 (d, 4H, *J* =10.5), 5.64(d, 2H, *J* = 10.5), 5.56(d, 2H, *J* = 7.2Hz), 4.87 (s, 4H), 4.45 (s, 4H), 3.41 (t, 6H, *J* = 7.8Hz), 3.07 (m, 4H), 0.71 (t, 4H, *J* = 7.8Hz), -0.13 (s, 18H); 13C NMR (125MHz, DMSO-*d6*): δ 167.0, 159.4, 157.5, 142.1, 138.8, 135.1, 128.7, 128.6, 128.3, 128.2, 117.1, 114.8, 110.1, 98.8, 94.3, 74.3, 65.1, 43.3, 42.5, 41.8, 40.0, 17.0, -1.5; MS (positive electrospray) calc'd for $(C50H60Br4N10O6Si2+H)^+$: 1273.09, found 1272.8.

177: off-white solid; R_f = 0.75 (1:19 MeOH/CH_2Cl_2); IR (film): 3400, 2952, 1644, 1418, 1247, 1068, 835 cm^{-1}; ^{1}H NMR (500 MHz, DMSO-*d6*): δ 7.33 (m, 8H), 6.72 (s, 1H), 6.67 (s, 1H), 5.69 (m, 3H), 5.60 (d, 1H, *J* = 9.6 Hz), 5.47 (m, 1H), 4.69 (m, 8H), 4.34 (m, 1H), 3.78 (dd, 1H, *J* = 11.6, 4.9 Hz), 3.52 (m, 5H), 3.31 (m, 1H), 2.76 (ddd, 1H, *J* = 4.1, 8.9, 13.4 Hz), 2.44 (m, 1H), 2.27 (m, 1H), 1.90 (m, 1H), 1.28 (m, 1H), 0.83 (m, 4H), -0.03 (s, 9H), -0.06 (s, 9H). 13C NMR (125MHz, CDCl3): δ 169.8, 166.8, 164.4, 160.3, 157.9, 145.8, 141.5, 140.6, 137.4, 134.5, 133.2, 129.6, 129.5, 129.1, 128.8, 128.7, 128.6, 128.6, 128.5, 125.5, 117.6, 116.5, 115.6, 111.2, 110.9, 99.7, 75.5, 75.1, 70.8, 70.5, 66.4, 66.3, 56.8, 49.4, 45.3, 44.2, 43.7, 43.4, 41.5, 40.2, 35.8, 34.6, 31.3, 30.4, 25.7, 24.4, 18.2, 18.0, -1.1, -1.2. MS (positive electrospray) calc'd for $(C50H60Br4N10O6Si2+H)^+$: 1273.09, found 1272.8.

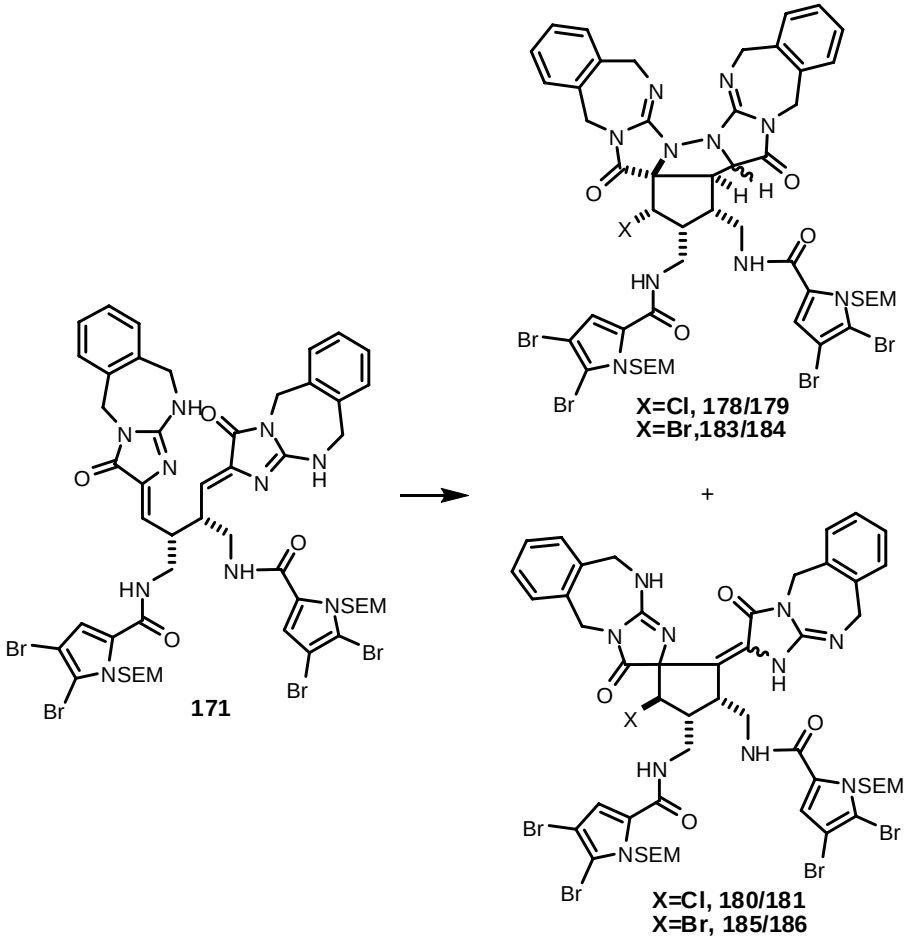

Procedure A. no additive

Bisalkylidene **171** (40 mg, 0.031 mmol) was dissolved in 1 mL THF and the resulting mixture was cooled to −78 °C. A solution of freshly prepared *t*-BuOCl (see *Organic Syntheses*, Coll. Vol. 5, p.184 (1973) - 4.2 μL, 0.038 mmol) in CH_2Cl_2 (50 μL) was added and the reaction was stirred at -78 °C for 2h and rt for another 2h. The solvent was removed *in vacuo* and the residue was purified by preparative thin layer chromatography (CH_3OH:CH_2Cl_2 = 1:19). This affords one

impure diastereomer of **178** followed by a pure second diastereomer **179** and impure alkylidene **180**.

179: (4 mg, 10% yield): white film; R_f = 0.7 (MeOH:CH_2Cl_2= 5:95); IR (film, cm-1): 2923, 1750, 1650, 1513, 1455, 1404, 1247, 1092, 948, 836; ^{1}H NMR (500 MHz,CD_3CN): 7.85 (dd, 1H, *J* = 4.5, 7.3 Hz), 7.57 (t, 1H, *J* = 5.6 Hz), 7.27 (m, 8H), 7.07 (s, 1H), 6.89 (s, 1H), 5.80 (m, 4H), 4.74 (d, 1H, *J* = 2.9 Hz), 4.63 (m, 3H), 4.53 (d, 1H, J = 3.9 Hz), 4.30 (m, 2H), 4.20 (m, 2H), 3.82 (m, 3H), 3.62 (ddd, 1H, *J* = 1.9, 5.7, 14.2 Hz), 3.51 (m, 4H), 3.41 (ddd, 1H, *J* = 4.5, 9.8, 14.0 Hz), 3.17 (m, 1H), 2.59 (td, 1H, *J* = 5.4, 9.4 Hz), 2.16 (1H, overlapped with H2O peak), 0.80 (m, 4H), -0.09 (s, 9H), -0.11 (s, 9H). ^{13}C NMR (125 MHz, $CDCl_3$): 170.0, 162.7, 161.2, 160.5, 148.4, 140.0, 133.5, 129.7, 129.6, 128.9, 128.8, 128.7, 128.4, 127.8, 127.5, 117.0, 116.4, 112.2, 111.6, 100.3, 100.0, 88.0, 77.5, 75.7, 75.3, 66.7, 66.2, 65.8, 58.0, 56.6, 49.0, 43.7, 43.4, 41.0, 38.6, 37.0, 35.9, 18.1, -1.2, -1.2. MS (positive electrospray) calc'd for $(C50H59Br4ClN10O6Si2+H)^+$: 1307.0539, found 1307.3955.

178: impure material was subjected to a second preparative thin layer chromatography, eluting with 10% $CH_3CN/CHCl_3$, to afford **178** (~1 mg) as a white film. R_f = 0.8 (MeOH:CH_2Cl_2 = 5:95); IR (film): 2852, 1737, 1681, 1543, 1456, 1397, 1248, 1093, 949 cm^{-1}; ^{1}H NMR (400 MHz, CD3CN): δ 7.57 (t, 1H, *J* = 5.0 Hz), 7.45 (t, 1H, *J* = 5.4 Hz), 7.30 (m, 8H), 7.06 (s, 1H), 6.90 (s, 1H), 5.78 (m, 4H), 5.25 (d, 1H, *J* = 4.0 Hz), 4.80 (m, 7H), 4.50 (m, 1H), 4.29 (d, 1H, *J* = 5.5

Hz), 4.16 (m, 1H), 3.63 (ddd, 1H, *J* = 3.5, 5.8, 14.9 Hz), 3.52 (m, 6H), 3.30 (m, 1H), 2.57 (tt, 1H, *J* = 5.7, 11.3 Hz), 2,28 (m, 1H), 0.86 (m, 2H), 0.66 (m, 2H), -0.05 (s, 9H), -0.12 (s, 9H). MS (positive electrospray) calc'd for $(C_{50}H_{59}Br_4ClN_{10}O_6Si_2+H)^+$: 1307.05, found 1306.90.

180: impure material was subjected to a second preparative thin layer chromatography, eluting with 10% CH_3OH/CH_2Cl_2) to afford **180** as a white film (8 mg, 20% yield). **180**: R_f = 0.4 (MeOH:CH_2Cl_2= 1:9); IR (film): 2945, 1681, 1601, 1547, 1418, 1312, 1248, 1092, 857 cm-1; 1H NMR (400 MHz,CD3CN): δ 8.52 (appr s, 1H), 7.36 (m, 8H), 7.03 (m, 1H), 6.85 (s, 1H), 6.72 (s, 1H), 5,87 (dd, 1H, *J* = 10.5, 12 Hz), 5.72 (t, 1H, *J* = 10.0 Hz), 4.68 (m, 7H), 4.30 (d, 1H, *J* = 14.8 Hz), 4.26 (d, 1H, *J* = 12.7 Hz), 3.76 (td, 1H, *J* =

3.9, 12.4 Hz), 3.53 (m, 7H), 3.24 (dt, 1H, *J* = 3.9, 12.5 Hz), 2.89 (m, 1H), 0.84 (m, 1H), -0.07 (s, 18H). MS (MALDI) calc'd for $(C50H59Br4ClN10O6Si2+H)^+$: 1307.05, found 1307.50.

Procedure B. MgCl2 additive

Bisalkylidene **171** (10 mg, 0.0075 mmol) and $MgCl_2$ (1.5 mg, 0.016mmol) were dissolved in THF (0.25 mL) and the mixture was cooled to −78 °C. A solution of freshly prepared *t*-BuOCl (1 μL, 0.0075 mmol) in CH_2Cl_2 (50 μL) was added and the reaction mixture was stirred at -78 °C for 2 h and at rt for another 2 h. The solvent was removed *in vacuo* and the residue purified by preparative thin layer

chromatography (CH_3OH:CH_2Cl_2 = 1:19) to afford **179** (2.8 mg, 26%), **178**(< 1 mg) and recovered **171** (3 mg, 30%).

Procedure C. $MgBr_2$•Et_2O additive

Bisalkylidene **171** (60 mg, 0.047 mmol) and $MgBr_2$•Et_2O (15 mg, 0.058mmol) were dissolved in 0.8 mL THF and the mixture cooled to -78 °C. A solution of freshly prepared *t*-BuOCl (6 μL, 0.054 mmol) in CH_2Cl_2 (100 μL) was added and the reaction stirred at -78 °C for 2 h and at rt for another 2 h. The solvent was evaporated and the residue was purified by preparative thin layer chromatography (CH_3OH:CH_2Cl2 = 1:19) to afford two diastereomers of **180+181** as light yellow solid (45 mg, 75%). These materials have 1H NMR spectra that are identical to **179+178**. They are distinguished only by mass: MS (MALDI) calc'd for C50H59Br45N10O6Si2(M+H)+: 1351.0, found 1350.8.

5.6 Notes and References

(1) (a) Buchanan, M. S.; Carroll, A. R.; Addepalli, R.; Avery, V. M.; Hooper, J. N. A.; Quinn, R. J. *J. Org. Chem.* **200**7, 2309-2317; (b) Kobayashi, H.; Kitamura, K.; Nagai, K.; Nakao, Y.; Fusetani, N.; Soest, R. W. M.; Matsunaga, S. *Tetrahedron Lett*. **2007**, 48, 2127-2129; (c) Köck, M.; Grube, A.; Seiple, I. B.; Baran, P. S. *Angew. Chem. Int. Ed*. **2007**, 46, 6586-6594.

(2) Herrmann, W. A.; Schütz, J.; Frey, G. D.; Herdtweck, E. *Organometallics*, **2006**, 25, 2437-2448.

(3) Baker, M. V.; brayshaw, S. K.; Skelton, B. W.; White, A. H. *Inorg. Chim. Acta,* **2004**, 357, 2841-2849.

(4) Gong, Y.; Bausch, M. J.; Wang, L. *Tetrahedron Lett*, **2001**, 42, 1-4

(5) Brown, H. C.; Ganesan, K.; Dhar, R. K. *J. Org. Chem.* **1993**, *58*, 147-153.

(6) Guella, G.; Mancini, I.; Zibrowius, H.; Pietra, F. *Helv. Chim. Acta.* **1989**, 72, 1444-1450.

(7) (a). Maehe, H.; Leach, M.; Williams, T. H.; Blount, J. F. *Can. J. Chem.* **1980**, *58*, 501-526. (b) Nishimura, S.; Matsunaga, S.; Shibazaki, M.; Suzuki, K.; Furihata, Soest, R. W. M.; Fusetani, N. *Org. Lett.* **2003**, 5, 2255-2257.

(8) Moldvai, I.; Szántay, C.; Tárkányi, G. *Tetrahedron*, **1995**, 51, 9103-9118.

(9) Casamitjana, N.; López, V.; Jorge, A.; Bosch, J.; Molins, E.; Roig, A. *Tetrahedron*, **2000**, 56, 4027-4042.

(10) Matsuo, J.; Aizawa, Y. *Tetrahedron Lett*, **2005**, 46, 407-410.

(11) De Macėdo, P, Marrano, C.; Keillor, J. W. *Bioorg. Med. Chem*, **2002**, 10, 355-360.

(12) Davis, F. A.; Chen, B. *Chem. Rev*, **1992**, 92, 919-934.

(13) Jansen, B. J. M.; Sengers, H.; Bos, H.; de Goot. *J. Org. Chem*. **1988**, 53, 855-859.

(14) Li, C.; Danishefsky, S. J. *Tetrahedron Lett*, **2006**, 47, 385-387.

APPENDIX G
Spectra of Compounds Appearing In Chapter 5

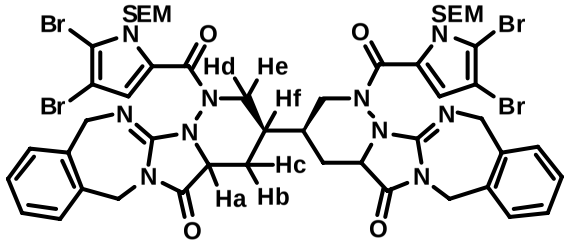

170

Solvent: CD_3CN
Temp: 50 °C; 400 MHz

Note: Spectral data appears to indicate one isomer. However, TLC and PTLC suggest a mixture of two closely related species.

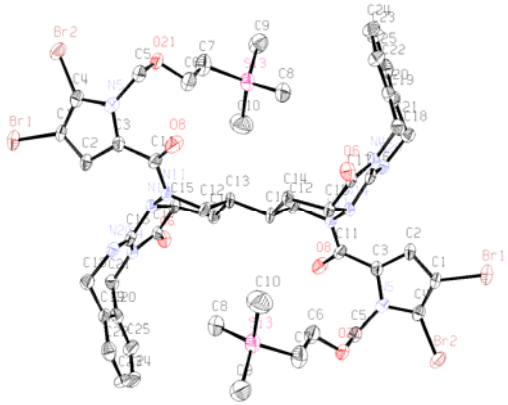

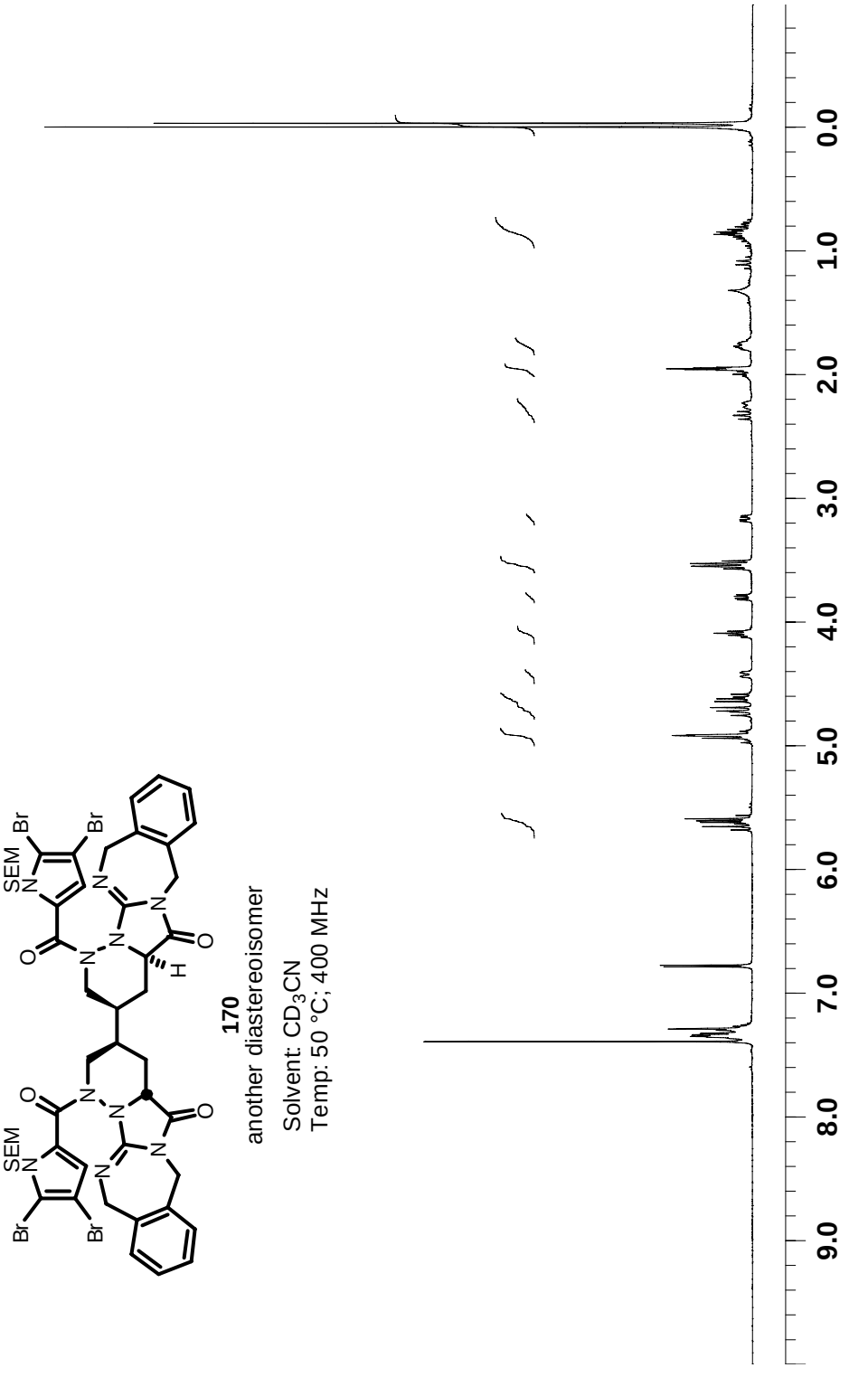

170
another diastereoisomer
Solvent: CD_3CN
Temp: 50 °C; 400 MHz

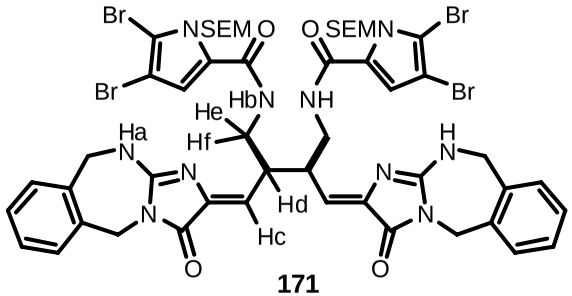

171

Solvent: DMSO-d_6
Temp: 50 °C; 500 MHz
* high concentration

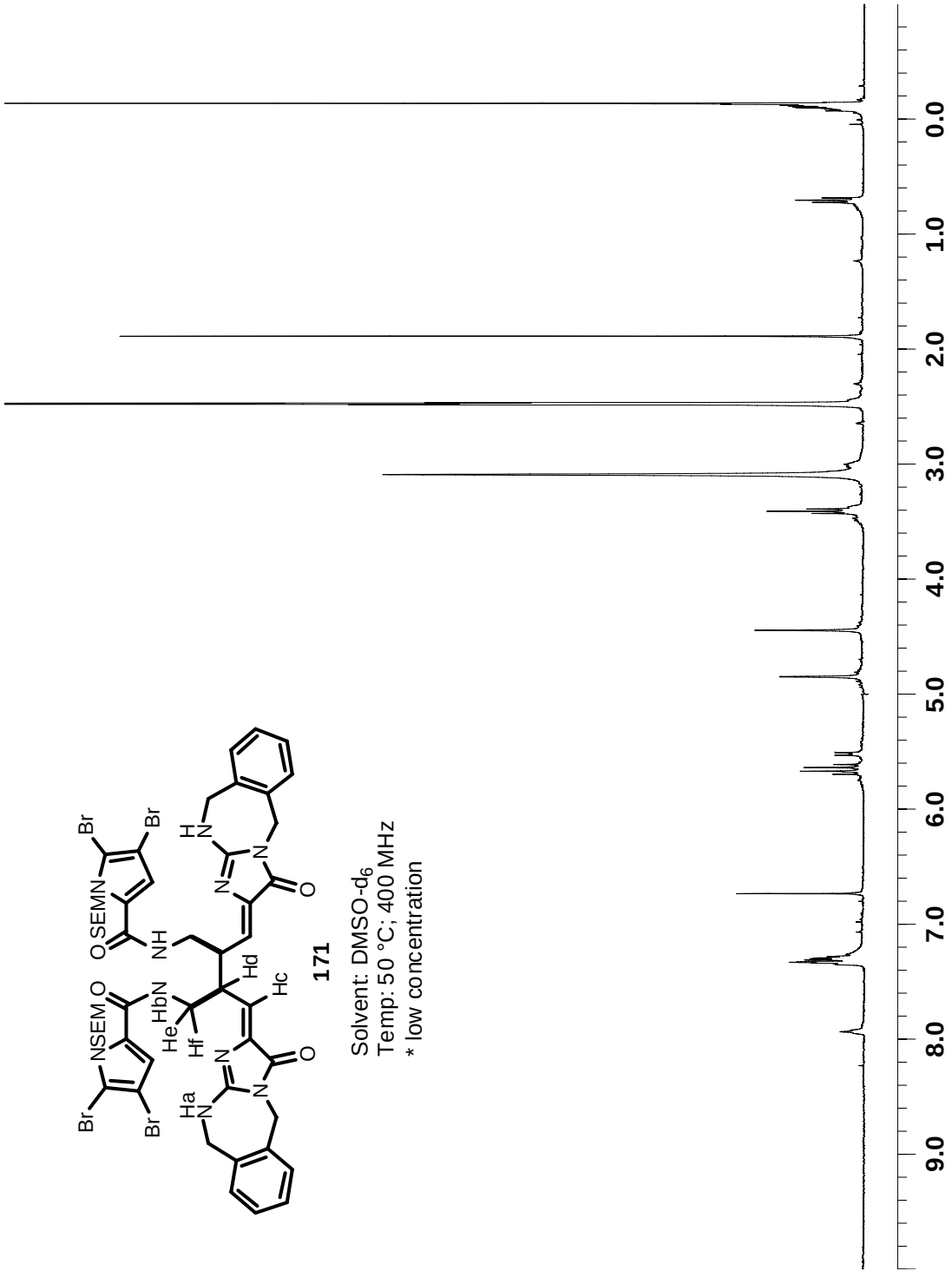
Br
Br
O
SEMN
NH
HbN
He
Hf
Hd
Hc
Ha
H
N
N
N
N
O
O
Br
Br
NSEM
O
171
Solvent: DMSO-d6
Temp: 50 °C; 400 MHz
* low concentration
9.0
8.0
7.0
6.0
5.0
4.0
3.0
2.0
1.0
0.0

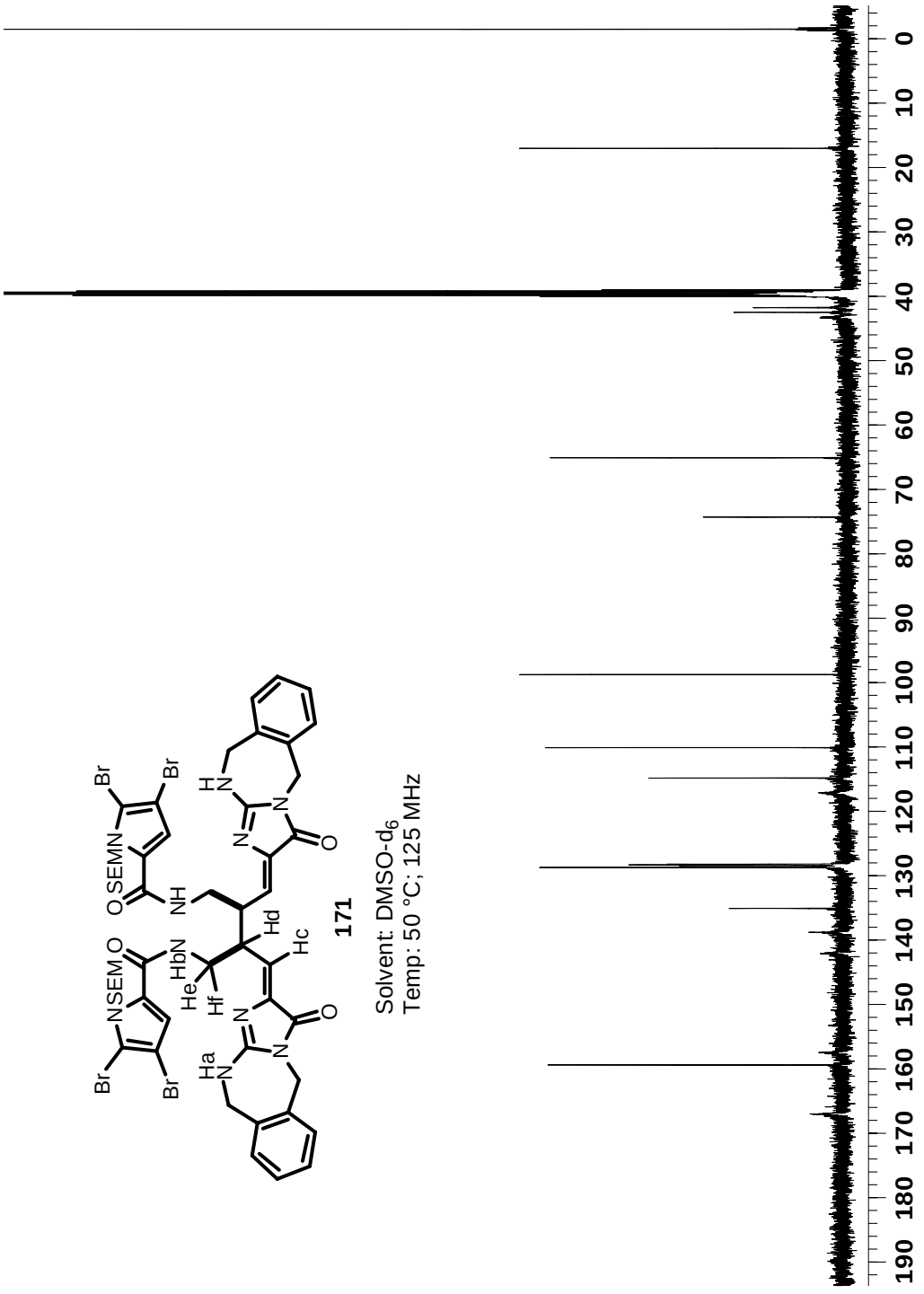
Br
Br
O SEMN
NH
HbN
He
Hf
Hd
Hc
Ha
N
H
O
171
Solvent: DMSO-d6
Temp: 50 °C; 125 MHz
0
10
20
30
40
50
60
70
80
90
100
110
120
130
140
150
160
170
180
190

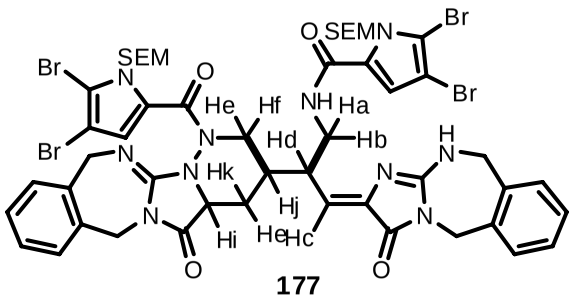

177

Solvent: CD_3CN
Temp: 50 °C; 400 MHz

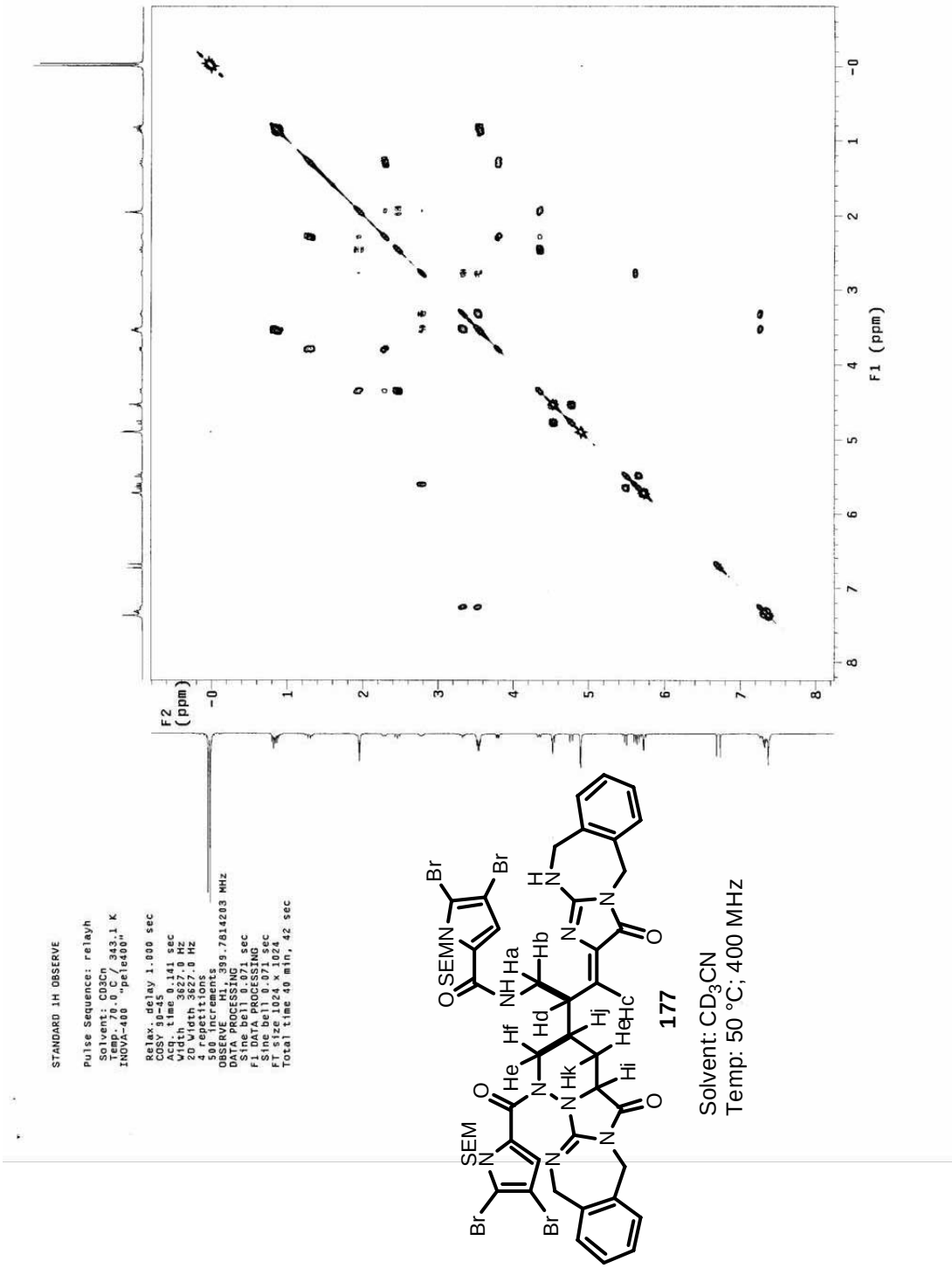
STANDARD 1H OBSERVE
Pulse Sequence: relayh
Solvent: CD3Cn
Temp. 70.0 C / 343.1 K
INOVA-400 "pele400"
Relax. delay 1.000 sec
COSY 90-45
Acq. time 0.141 sec
Width 3627.0 Hz
2D Width 3627.0 HZ
4 repetitions
500 increments
OBSERVE H1, 399.7814203 MHz
DATA PROCESSING
Sine bell 0.071 sec
FT DATA PROCESSING
Sine bell 0.071 sec
FT size 1024 x 1024
Total time 40 min, 42 sec
F2 (ppm)
F1 (ppm)
SEMN
NH
Ha
Hb
Hc
Hd
He
Hf
Hi
Hj
Hk
SEM
Br
177
Solvent: CD3CN
Temp: 50 °C; 400 MHz

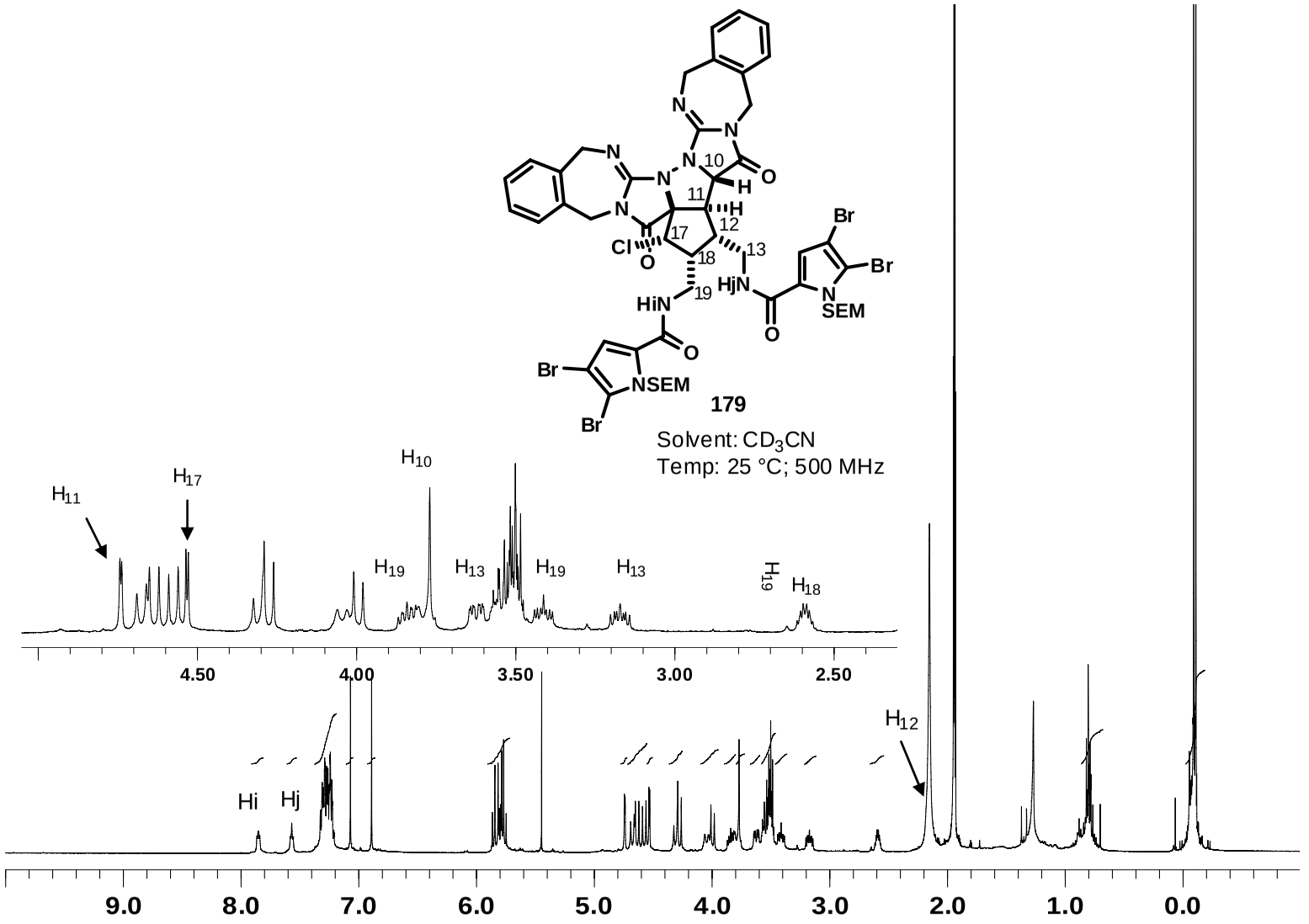
179
Solvent: CD3CN
Temp: 25 °C; 500 MHz
H11
H17
H10
H19
H13
H19
H13
H19
H18
Hi
Hj
H12
9.0
8.0
7.0
6.0
5.0
4.0
3.0
2.0
1.0
0.0
4.50
4.00
3.50
3.00
2.50

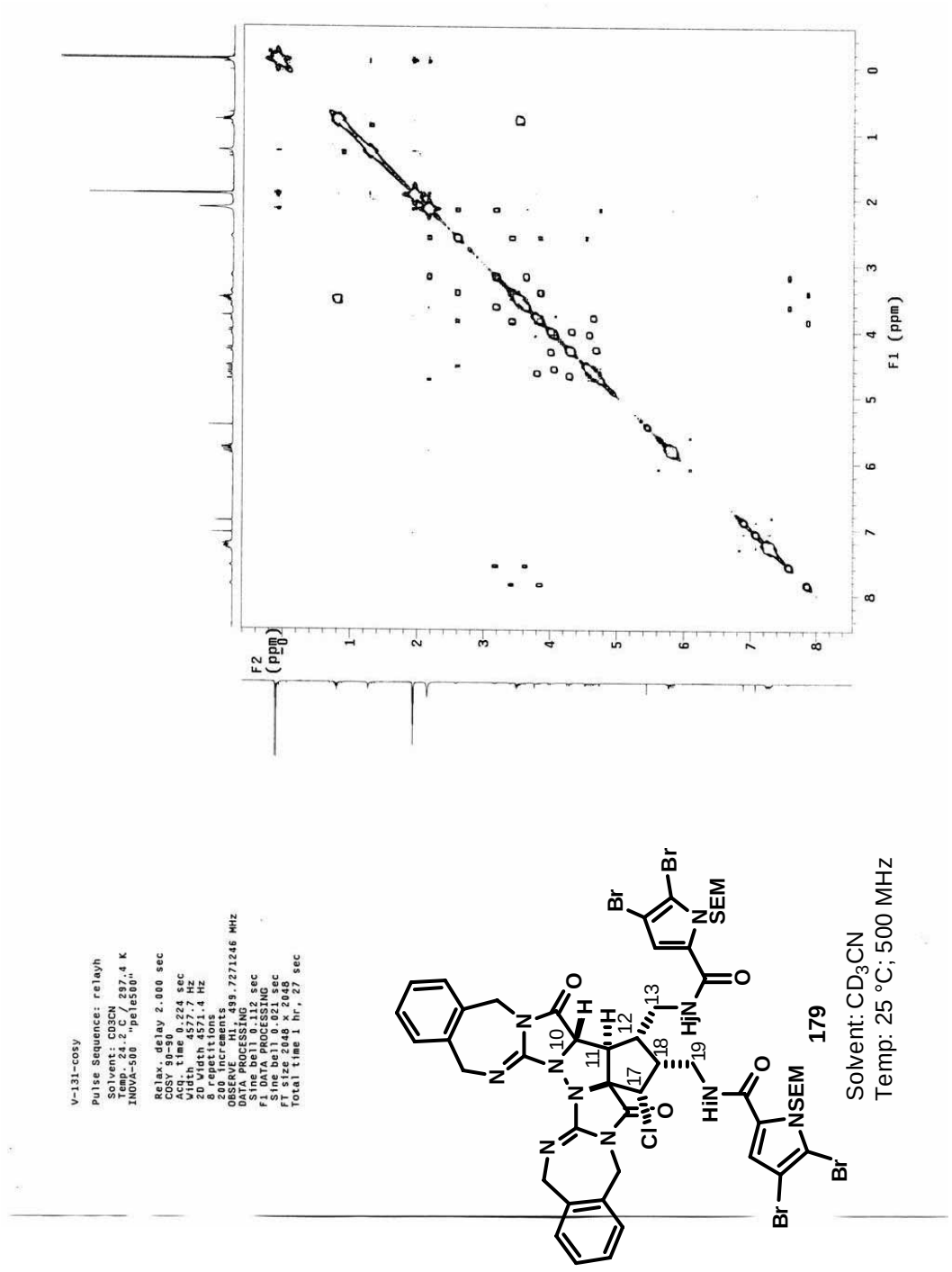
V-131-cosy
Pulse Sequence: relayh
Solvent: CD3CN
Temp. 24.2 C / 297.4 K
INOVA-500 "pele500"
Relax. delay 2.000 sec
COSY 90-90
Acq. time 0.224 sec
Width 4572.7 Hz
2D Width 4571.4 Hz
8 repetitions
200 increments
OBSERVE H1, 499.7271246 MHz
DATA PROCESSING
FT size 2048 x 2048
Total time 1 hr, 27 sec
F2 (ppm)
F1 (ppm)
Br
Br
SEM
N
O
HjN
H
H
10
11
12
13
17
18
19
Cl
O
HiN
O
NSEM
Br
Br
179
Solvent: CD3CN
Temp: 25 °C; 500 MHz

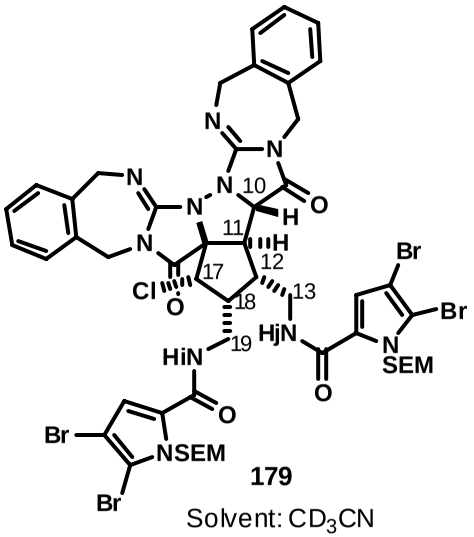

179

Solvent: CD_3CN
Temp: 25 °C; 800 MHz
Pulse sequence: noesy

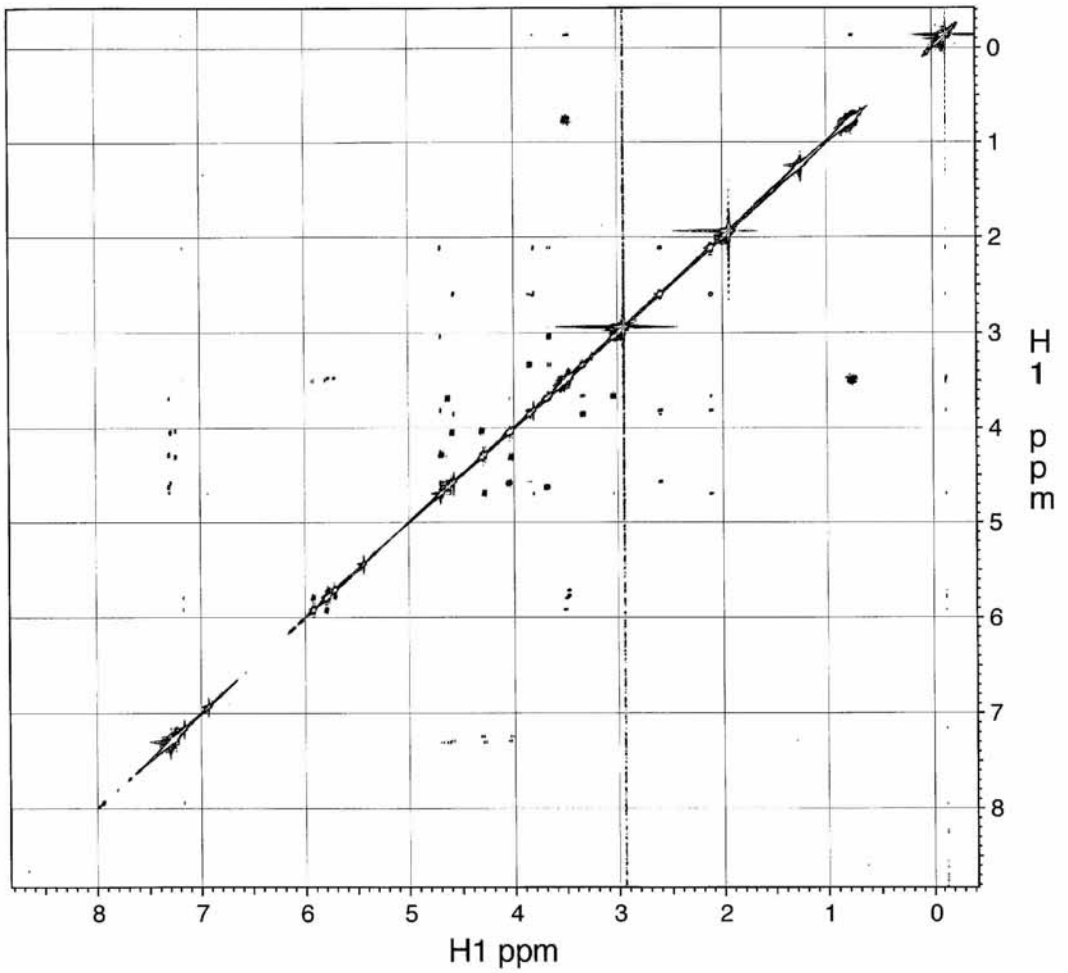

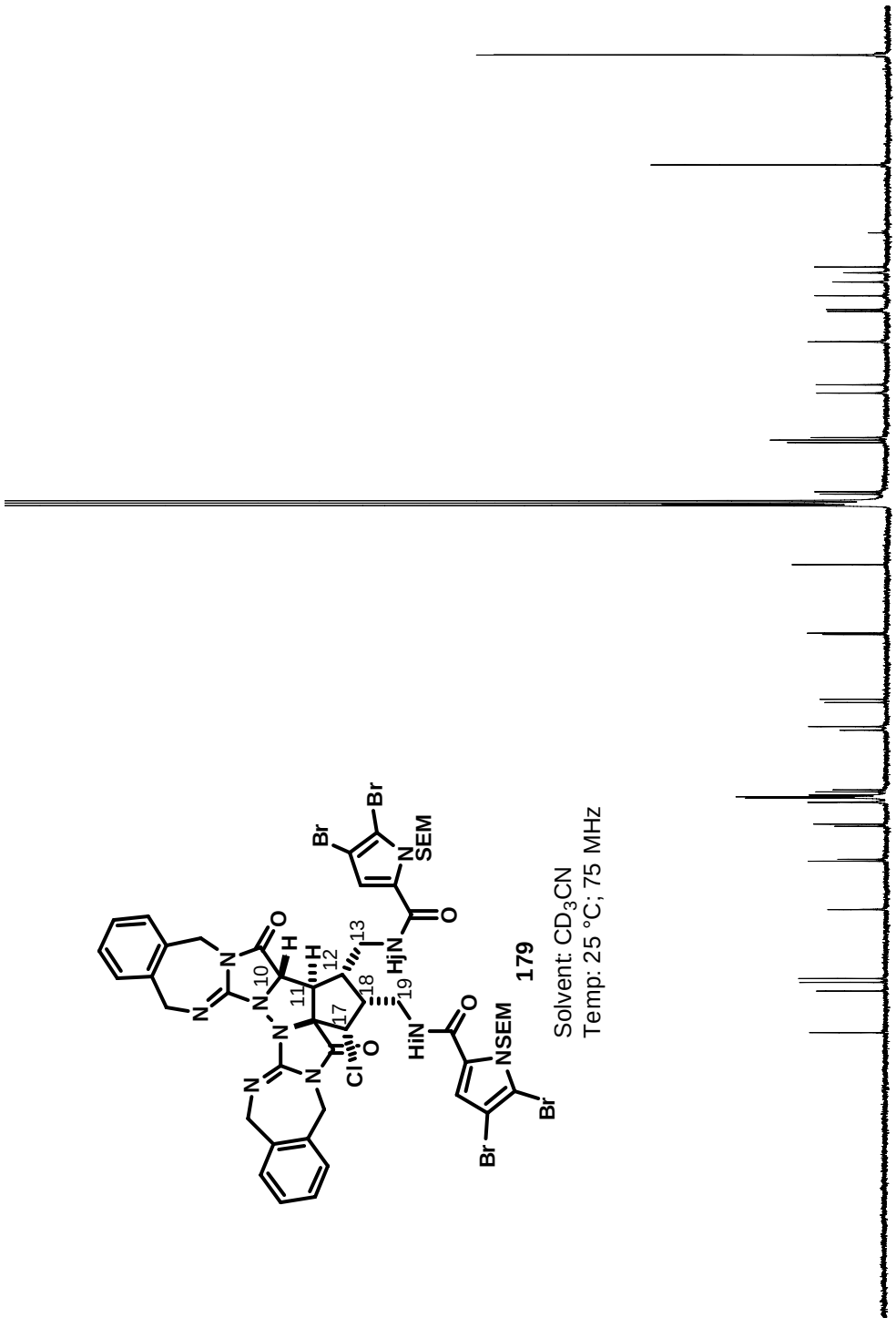
179
Solvent: CD3CN
Temp: 25 °C; 75 MHz
0 10 20 30 40 50 60 70 80 90 100 110 120 130 140 150 160 170 180 190 200 210

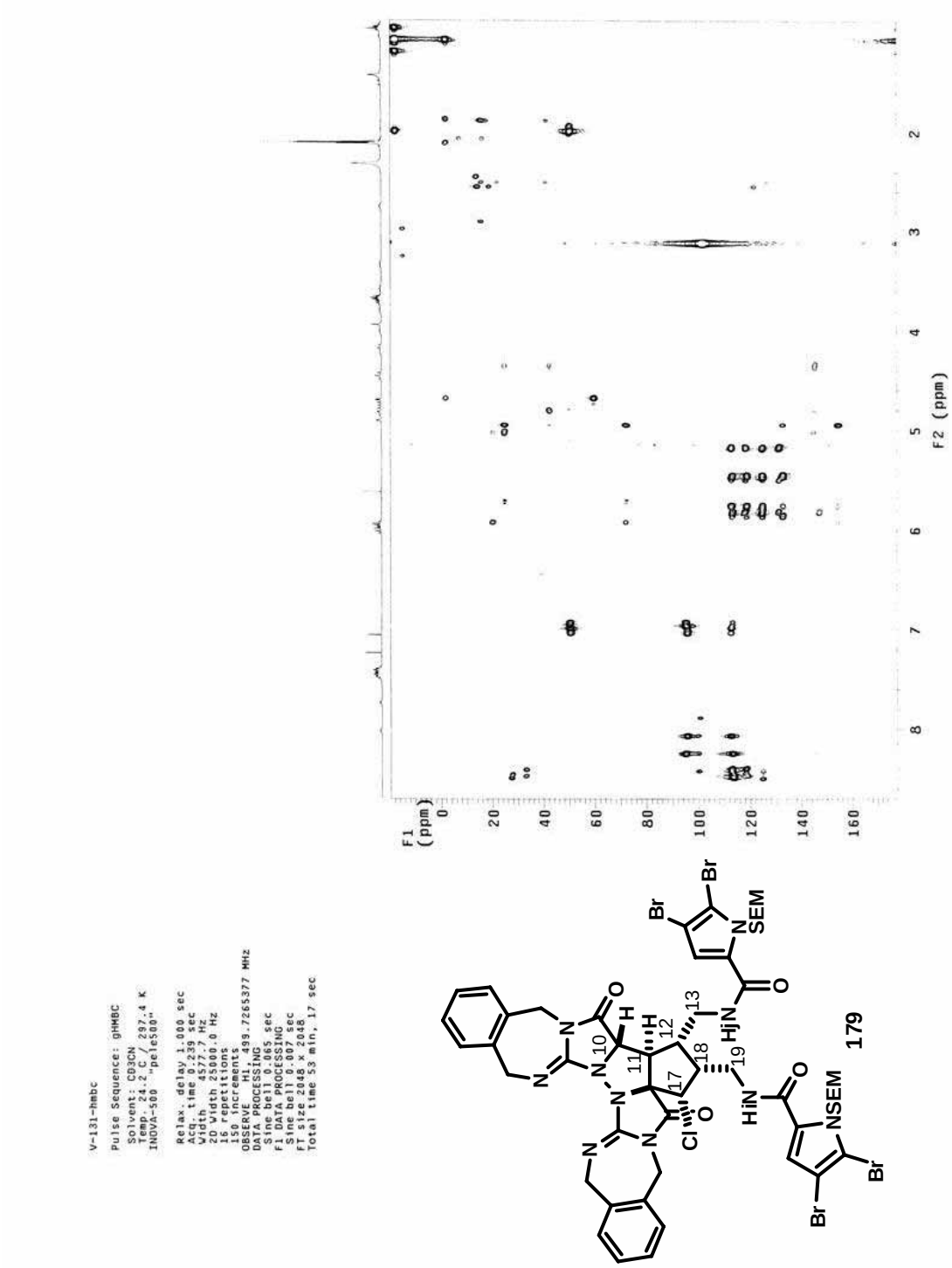
V-131-hmbc
Pulse Sequence: gHMBC
Solvent: CD3CN
Temp. 24.2 C / 297.4 K
INOVA-500 "pele500"
Relax. delay 1.000 sec
Acq. time 0.239 sec
Width 4577.7 Hz
2D Width 25000.0 Hz
16 repetitions
150 increments
OBSERVE H1, 499.7265377 MHz
DATA PROCESSING
Sine bell 0.065 sec
FT 2D PROCESSING
Sine bell 0.037 sec
FT size 2048 x 2048
Total time 53 min, 17 sec
F1 (ppm)
F2 (ppm)
Br
SEM
HjN
HiN
NSEM
Cl
179

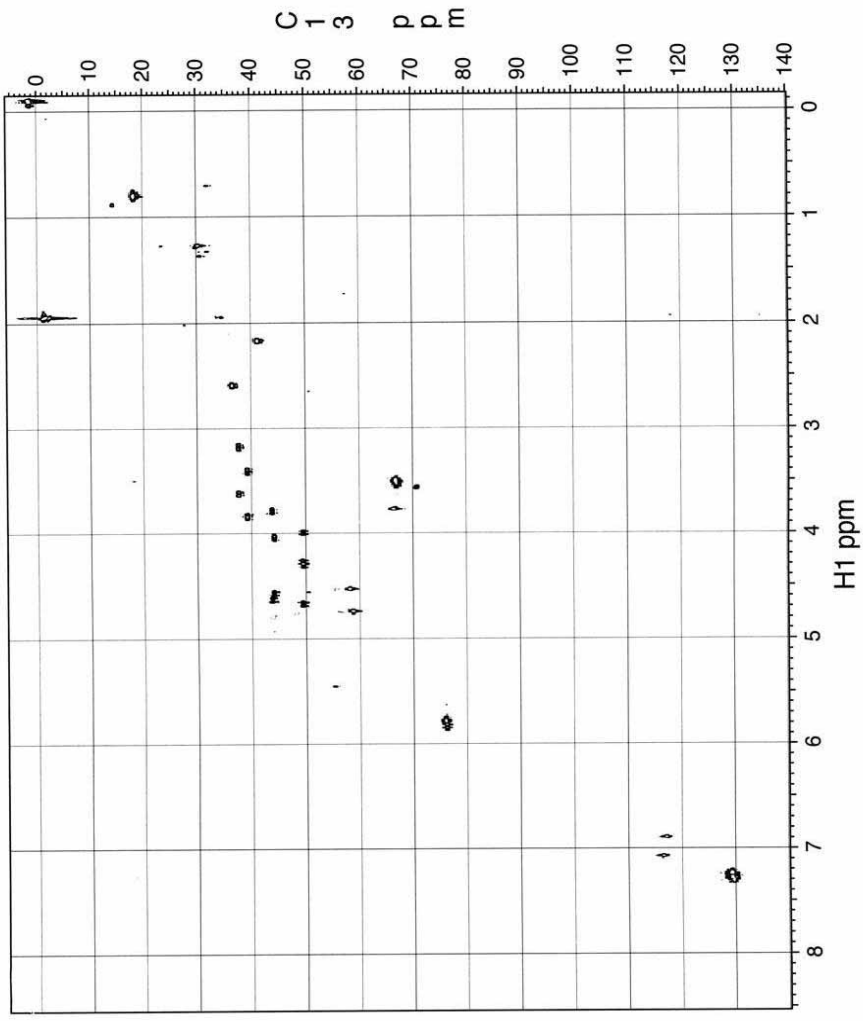

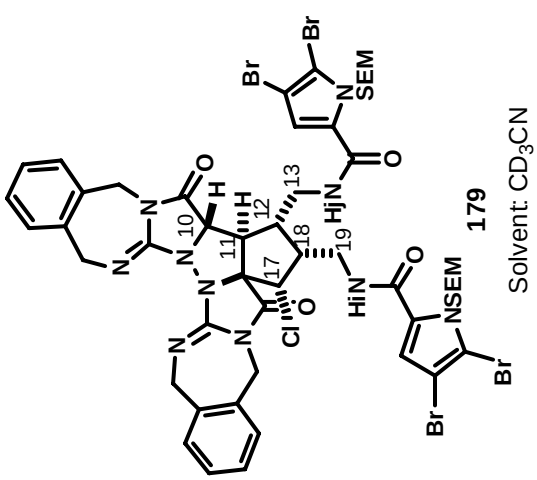

179

Solvent: CD_3CN
Temp: 25 °C; 800 MHz
Pulse sequence: gChsqc

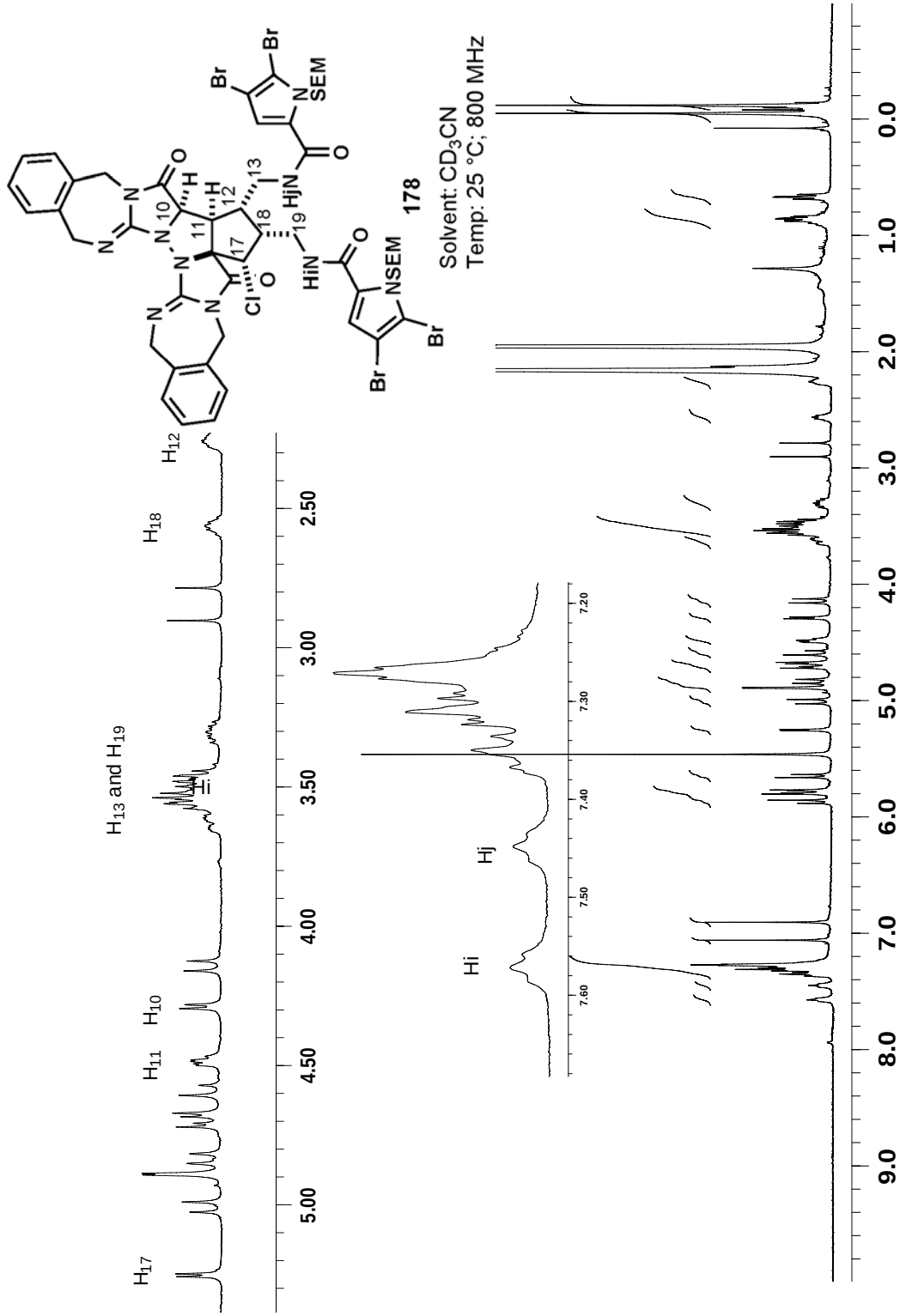
Br
Br
SEM
N
O
HjN
H
H
13
12
10
11
18
19
17
O
Cl
HiN
NSEM
O
Br
Br
178
Solvent: CD3CN
Temp: 25 °C; 800 MHz
H17
H11
H10
H13 and H19
H18
H12
Hi
Hj
5.00
4.50
4.00
3.50
3.00
2.50
7.60
7.50
7.40
7.30
7.20
9.0
8.0
7.0
6.0
5.0
4.0
3.0
2.0
1.0
0.0

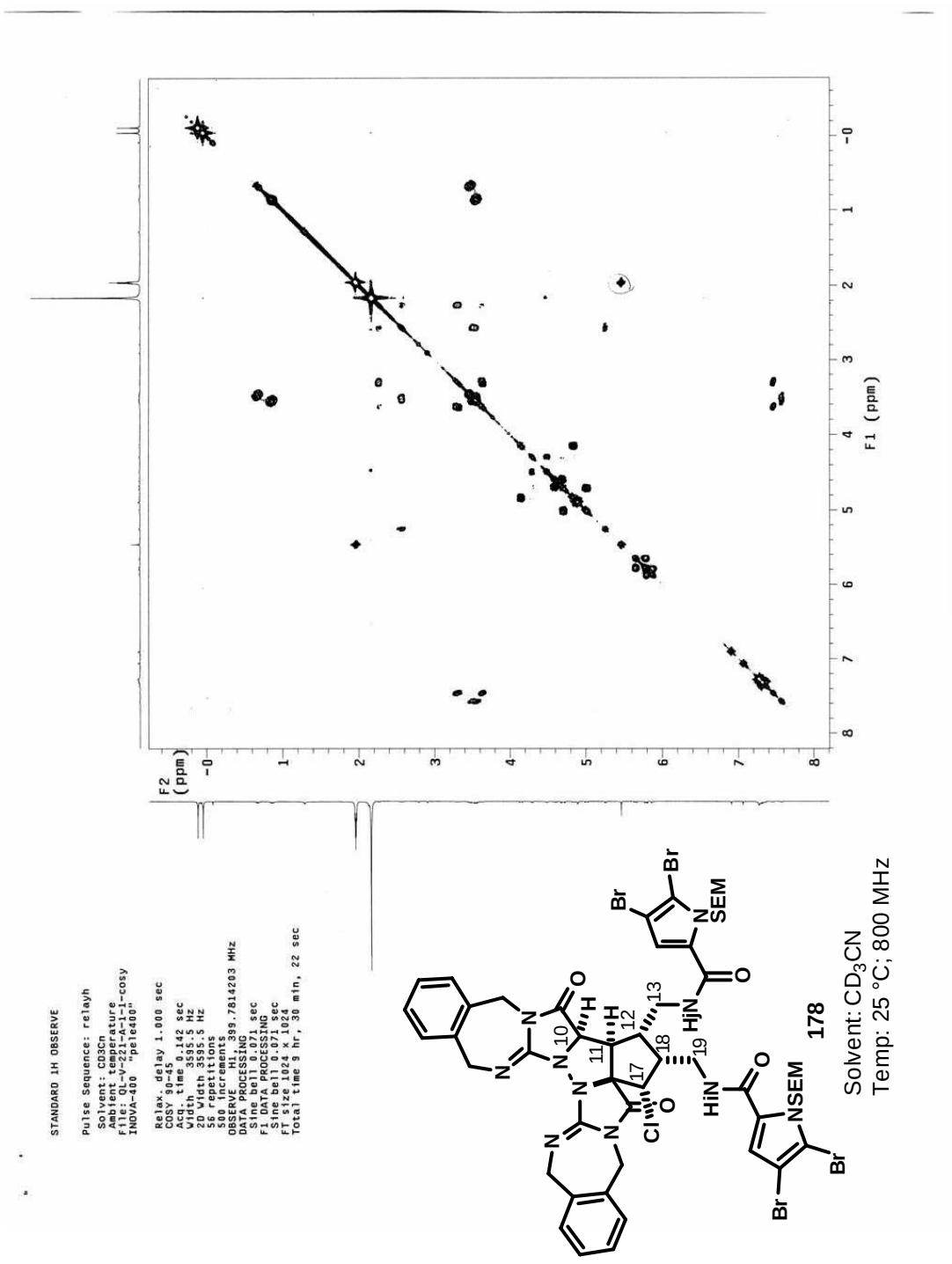
STANDARD 1H OBSERVE
Pulse Sequence: relayh
Solvent: CD3Cn
Ambient temperature
File: QL-V-221-A-1-1-cosy
INOVA-400 "pele400"
Relax. delay 1.000 sec
COSY 90-45
Acq. time 0.142 sec
Width 3595.5 Hz
2D Width 3595.5 Hz
56 repetitions
500 increments
OBSERVE H1, 399.7814203 MHz
DATA PROCESSING
Sine bell 0.071 sec
FT DATA PROCESSING
Sine bell 0.071 sec
FT size 1024 x 1024
Total time 9 hr, 30 min, 22 sec
F2 (ppm)
F1 (ppm)
Br
Br
SEM
N
O
HjN
13
12
H
10
11
17
18
19
Cl
HiN
NSEM
Br
Br
178
Solvent: CD3CN
Temp: 25 °C; 800 MHz

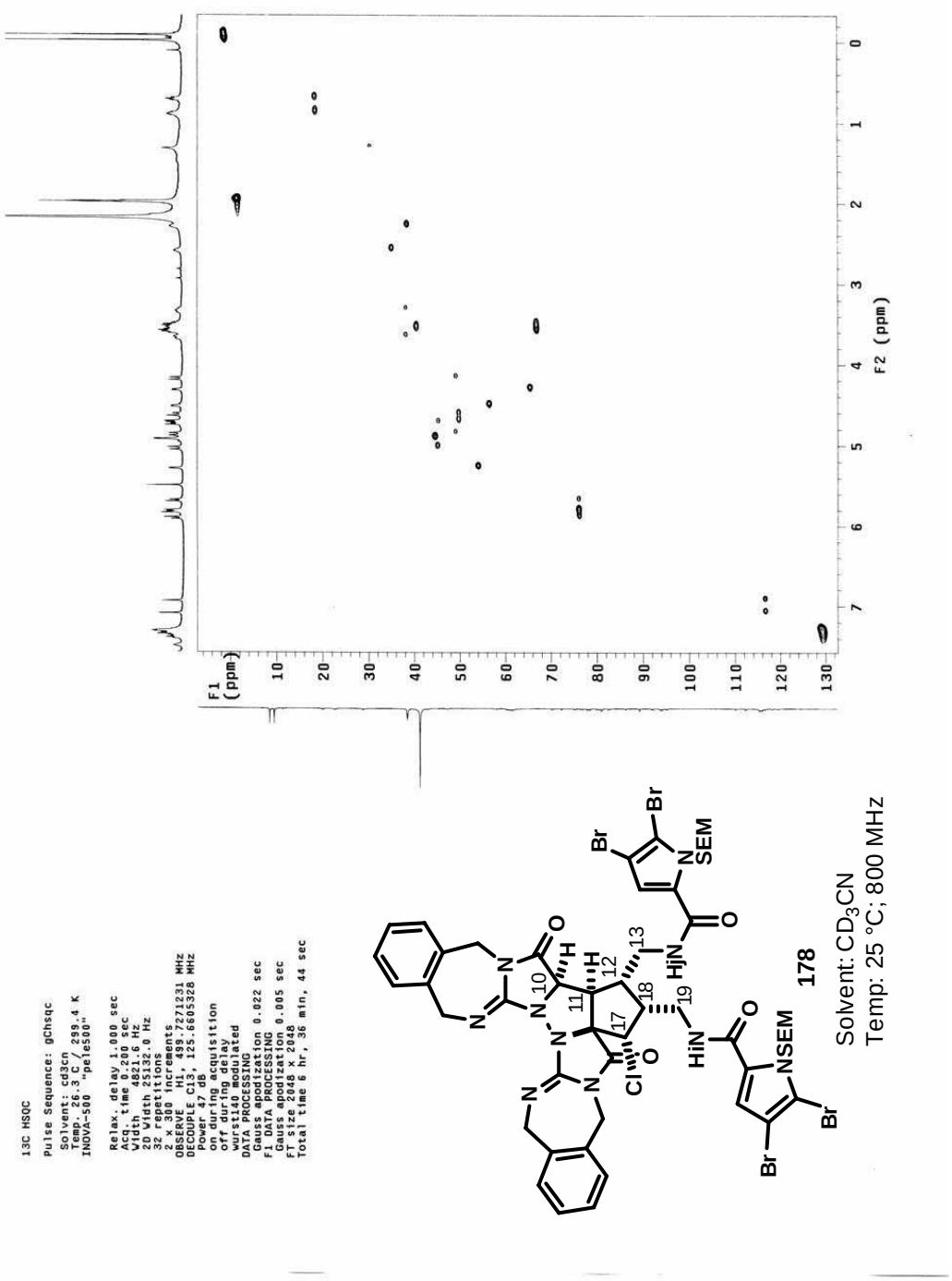
13C HSQC
Pulse Sequence: gChsqc
Solvent: cd3cn
Temp: 26.3 C / 299.4 K
INOVA-500 "pele500"
Relax. delay 1.000 sec
Acq. time 0.200 sec
Width 4821.6 Hz
F1 Width 25132.0 Hz
32 repetitions
2 x 300 increments
OBSERVE H1, 499.7271231 MHz
DECOUPLE C13, 125.6605328 MHz
Power 47 dB
on during acquisition
Off during delay
wurst140 Modulated
DATA PROCESSING
Gauss apodization 0.022 sec
F1 DATA PROCESSING
Gauss apodization 0.005 sec
FT size 2048 x 2048
Total time 6 hr, 36 min, 44 sec
F1 (ppm)
F2 (ppm)
178
Solvent: CD3CN
Temp: 25 °C; 800 MHz

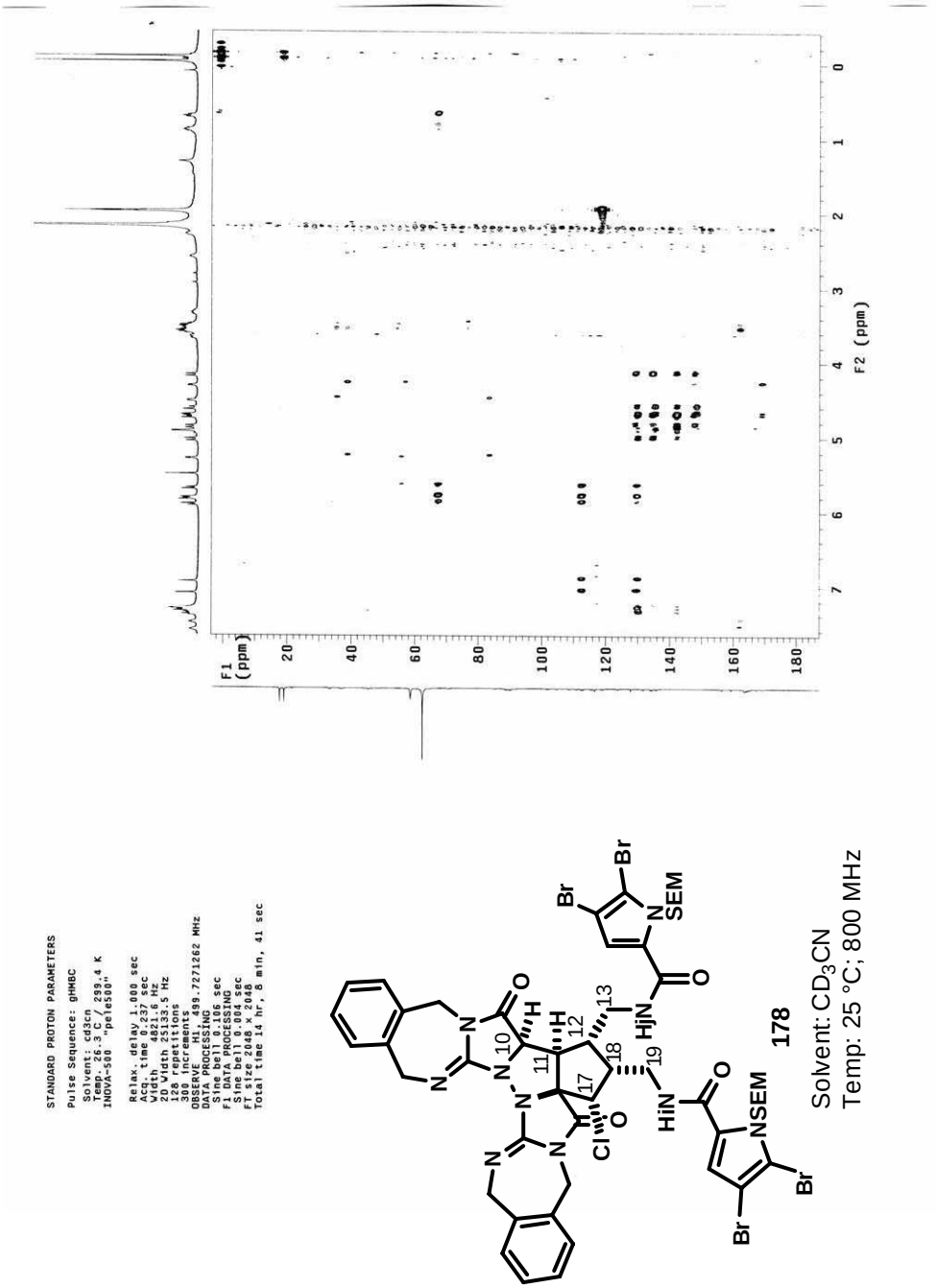
STANDARD PROTON PARAMETERS
Pulse Sequence: gHMBC
Solvent: cd3cn
Temp: 25.0 C / 289.4 K
INOVA-500 "pfg500"
Relax. delay 1.000 sec
Acq. time 0.237 sec
Width 4821.6 Hz
20 Width 2253.5 Hz
128 repetitions
300 increments
OBSERVE H1, 499.7271262 MHz
DATA PROCESSING
Sine bell 0.116 sec
FI DATA PROCESSING
Sine bell 0.004 sec
FT size 2048 x 2048
Total time 14 hr, 8 min, 41 sec
F1 (ppm)
F2 (ppm)
Br
Br
SEM
N
O
HjN
H
H
O
Cl
HiN
NSEM
Br
Br
178
Solvent: CD3CN
Temp: 25 °C; 800 MHz

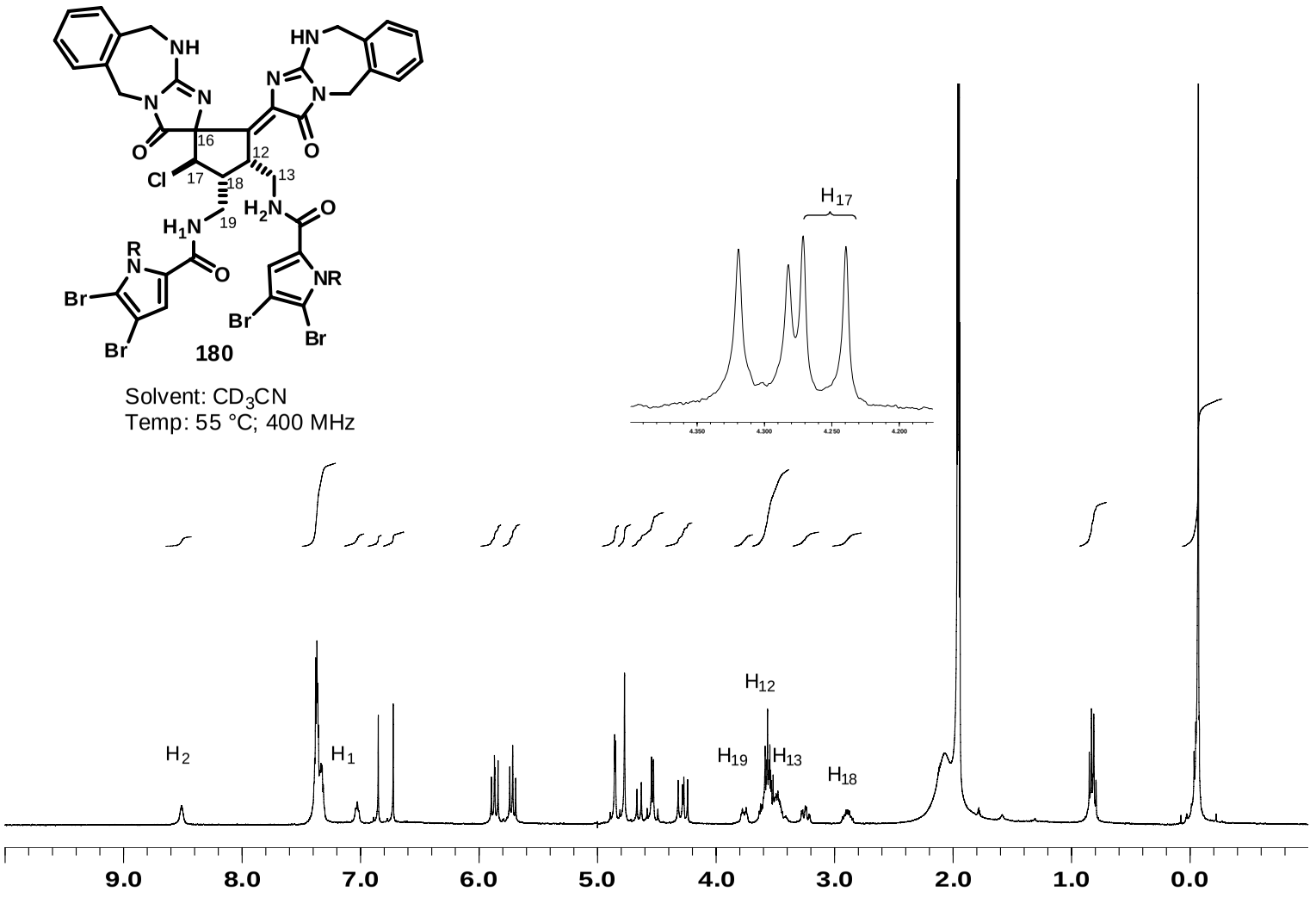
NH
HN
N
N
N
N
O
O
16
12
13
Cl
17
18
19
H_1N
H_2N
O
R
N
O
NR
Br
Br
Br
Br
180
Solvent: CD_3CN
Temp: 55 °C; 400 MHz
H_{17}
H_2
H_1
H_{12}
H_{19}
H_{13}
H_{18}
9.0
8.0
7.0
6.0
5.0
4.0
3.0
2.0
1.0
0.0

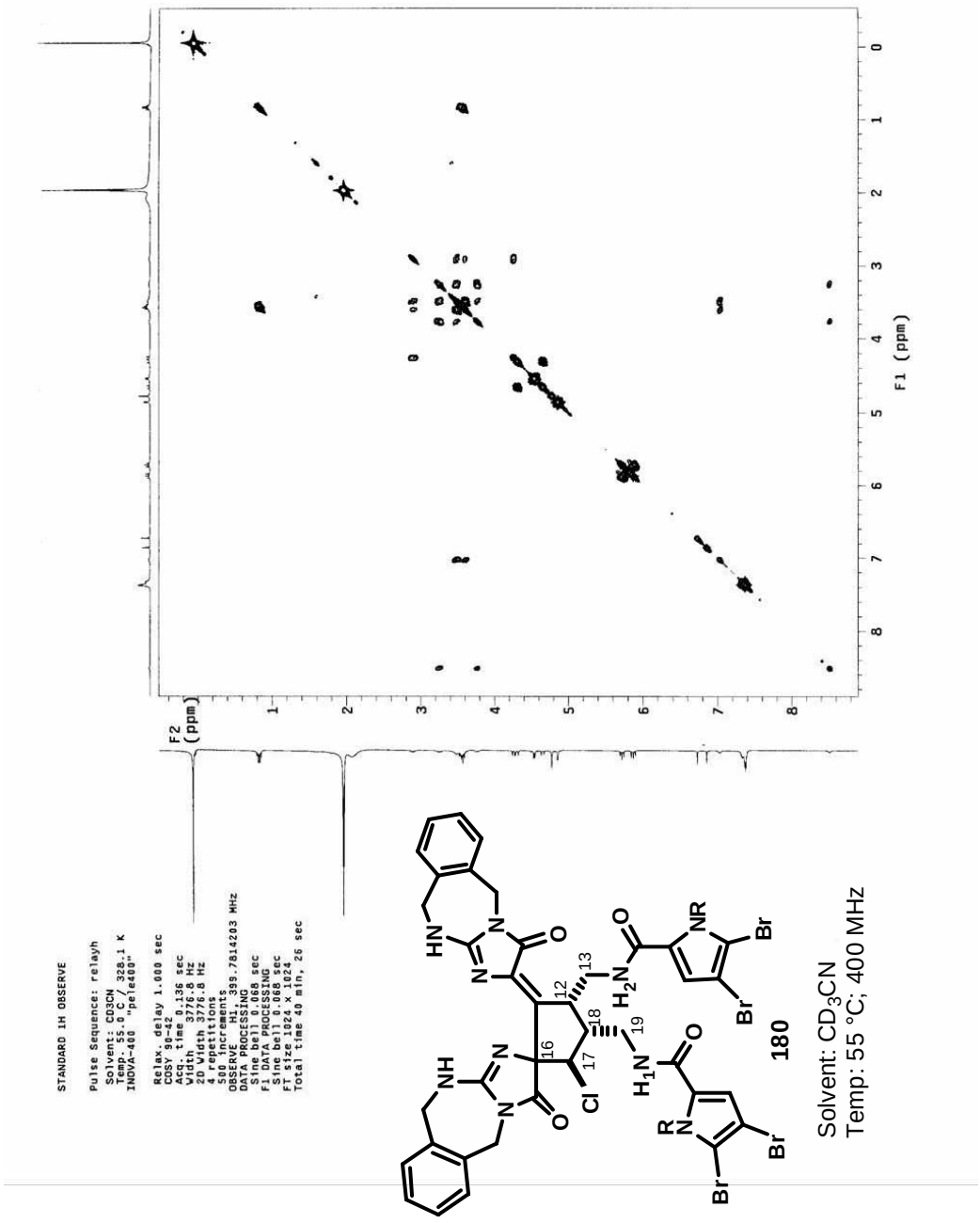
STANDARD 1H OBSERVE
Pulse Sequence: relayh
Solvent: CD3CN
Temp. 55.0 C / 328.1 K
INOVA-400 "pele400"
Relax. delay 1.000 sec
COSY 90-62
Acq. time 0.136 sec
Width 3776.8 HZ
2D Width 3776.8 HZ
4 repetitions
500 increments
OBSERVE H1, 399.7814203 MHz
Data processing
Sine bell 0.068 sec
F1 DATA PROCESSING
Sine bell 0.068 sec
FT size 1024 x 1024
Total time 40 min, 26 sec
F2 (ppm)
F1 (ppm)
Solvent: CD3CN
Temp: 55 °C; 400 MHz
180

VITAE

Qingyi Li was born in Zhengzhou, Henan in China, on June 1st, 1977, the daughter of Yuen-Feng Wang and En-Jiang Li. After completing her work at Zhengzhou No.1 High School, Henan, in 1995, she entered Zhengzhou University at the same year. She received the degree of Bachelor of Science 1999. At the beginning of 2000, she entered the Graduate School of chemistry department at the University of Texas at El Paso. She was awarded the degree of Master of Sciene in Augest, 2003. At the same year, she began graduate studies in organic synthesis in the laboratory of Patrick G. Harran at University of Texas Southwestern Medical Center at Dallas. She then obtained her Doctorate of Philosophy from U.T. Southwestern in May 2008.

Permanent Address: 23 western Building, unit 12
Zhengzhou University
Zhengzhou , Henan, 450052
P. R. China